A GEOMETRIC AND MICRORADIOGRAPHIC STUDY OF FUNCTIONAL ADAPTATION IN THE HUMAN SKELETON

By

RICHARD ALLAN LAZENBY, M.A.

A Thesis
Submitted to the School of Graduate Studies
in Partial Fulfillment of the Requirements
for the Degree
Doctor of Philosophy

McMaster University
June, 1992

HUMAN SKELETAL FUNCTIONAL ADAPTATION

DOCTOR OF PHILOSOPHY (1992) McMASTER UNIVERSITY
(Anthropology) Hamilton, Ontario

TITLE: A Geometric and Microradiographic Study of Functional Adaptation in the Human Skeleton

AUTHOR: Richard Allan Lazenby, B. A. (Simon Fraser University)

M. A. (Simon Fraser University)

SUPERVISOR: Professor Shelley R. Saunders

NUMBER OF PAGES: ix, 210

ABSTRACT

Continuing Periosteal Apposition (CPA) refers to recent lamellar bone formation on the external surface of the mature skeleton. CPA is most often viewed as mechanical compensation, a form of functional adaptation in the event of overstrain pursuant either to high levels of physical activity, or to prior endosteal bone resorption and increased endocortical porosity. The theoretical basis for this expectation derives primarily from Frost's Mechanostat, describing the relationship of bone surfaces and bone cellular activity in response to changes in the functional strain environment.

An objective of the study was to ascertain how CPA might be associated with structural (geometric) properties characterizing entire cross-sections (areas and moments of area), as well as with proximate histological variables, such as intracortical porosity and mean bone age. The latter variable is derived from a mathematical model developed in this study, which provides an index of intracortical remodelling 'history'.

Left and right second metacarpals, and the left second metatarsal, obtained from medical school cadavers (n = 89 bones) and a small EuroCanadian historic cemetery (n = 21 bones) comprised the sample for this study; the majority were male, and over 50 years of age. Cross-sectional geometric properties indicative of structural strength were measured from three sections prepared from each element, one at midshaft and two from the distal diaphysis; a subsample was microradiographed for histological evaluation at four locations within each cross-section.

Although not without exception, the directional asymmetries identified between the various structural and histological variables: (1) tend to reflect presumed functional strain inequities pertaining to side (e.g., right > left), gender (male > female), age (young > old). The presumed inequity for 'lifestyle' (historic > cadaver) was not supported. (2) support the conclusion that CPA constitutes a component of functional adaptation in the skeleton and may act as mechanical compensation; and (3) support the Mechanostat as an interpretive framework for skeletal biological analyses.

ACKNOWLEDGEMENTS

Beyond the meritorious support of my supervisory committee, Drs. Shelley Saunders (McMaster University), Susan Pfeiffer (University of Guelph) and Emöke Szathmary (University of Western Ontario), the following individuals and institutions have contributed intellectually, materially and/or financially towards completion of this dissertation, and I thank them all.

My fellow graduate students, Rebecca Southern and Anne Keenleyside (McMaster University); Chris Dudar and Peter Berti (University of Guelph). McMaster University, Department of Anthropology (Chairs: Dr. E.J.E. Szathmary; Dr. D.R. Counts); McMaster University, School of Graduate Studies (Dr. W. Slater); University of Guelph, School of Human Biology (Dr. M. Mahaney; Ms. Connie Tavres), and Department of Pathology, Ontario Ministry of Agriculture and Food (Ms. Pat Weir, technician); the Ontario Graduate Scholarship program (1989, 1990); McMaster University, the Ontario Heritage Foundation and the Waterloo Regional Heritage Foundation funded the historic cemetery excavation. Dr. Mark Skinner, Simon Fraser University; Dr. Nancy Ossenberg, Queen's University; and the various Heads and Technicians from the Departments of Anatomy at the following institutions: University of Toronto (1989, 1990), University of Western Ontario (1988), and Queen's University (1988).

A special note of thanks to Shelley Saunders and Susan Pfeiffer for the willing commitment of their own financial resources towards providing and improving some of the materials/technologies used in this study.

Dr. Christopher Ruff (Department of Anatomy and Cell Biology, Johns Hopkins University) served as outside reader, and provided a fair, thoughtful and thorough critique, which is much appreciated.

Finally, my heart and gratitude to my wife Carol Fairhurst for believing, regardless...te quiero mi corazón.

TABLE OF CONTENTS

TABLE OF CONTENTS cont'd

LIST OF TABLES

LIST OF TABLES cont'd...

LIST OF FIGURES

CHAPTER 1. INTRODUCTION

1.1 Research Objectives

This dissertation presents a study of functional adaptation in the human skeleton, focussing on the relationship between macrostructure (cross-sectional geometry) and microstructure (histology). The former reflects changes in size and shape through processes such as expansion of the medullary cavity and continuing periosteal apposition (CPA) of lamellar bone. With advancing age, these processes lead to a reduction in total bone volume and to greater external bone dimensions, respectively. The histological aspect deals with variation in the magnitude and distribution of intracortical porosity (osteoporosis), long recognized as an age-progressive phenomenon resulting in a lower bone volume fraction and apparent density (i.e., the mineral content of the volume fraction). It is also necessarily concerned with bone remodelling as the mechanism of tissue rejuvenation. Older and/or damaged bone tissue is removed and replaced in the form of discrete entities known as Haversian systems (or secondary osteons). To provide a numerical indication of the bone's recent remodelling history (i.e., the rate of rejuvenation), this study has developed an operational model for relative mean bone age (MBA), derived from the apparent density of a region of cortex.

A principal objective of the study is to evaluate a current interpretation of continuing periosteal apposition, in which CPA is seen to serve as a form of mechanical compensation for the age-related expansion of the medullary cavity and increasing porosity. The earliest recognition of CPA dates to the last century (see Israel, 1973a regarding the cranium), but only within the past three decades has systematic investigation and documentation of this process taken place, coincident with the very rapid growth of processual research in skeletal biology (Armelagos et al., 1982). In particular, the last twenty years have witnessed publication of a substantial body of work describing the magnitude and distribution of CPA for a number of different bones and in a variety of living and extinct populations. This dissertation

approaches the question of functional adaptation in the human skeleton through an investigation of how CPA may be distributed according to age, gender, side and lifestyle, as well as to other modelling and remodelling parameters of the skeletal system.

In their revision of the now-classic text *The Human Skeleton in Forensic Medicine,* Krogman and Iscan (1986:126-7) comment upon previous studies dealing with expansion of the craniofacial skeleton: "While much has been written supporting and opposing the hypothesis that cranial bone thickness enlarges, there [was] no histological analysis of the microstructure of the bone, the relationship between the tables and diplöe, and the turnabout rate of bone formation. Research in this area may lead to further elaboration of the aging process in the cranium." This is a telling comment. First, it suggests that no accepted explanatory model that might connect the effect to its cause exists to account for this phenomenon. Second, the search for such a model would seem to hinge on analysis at the histological level. This implies that bone macrostructure, microstructure and ultrastructure are not independent; that is, the properties of bone tissue which originate at one level might promote or constrain properties which originate at some other level. This is a notion that has long been implicitly recognized by skeletal biologists, e.g., Wolff's Law of bone architecture (Roesler, 1987). A recent abundance of models proposed by Harold Frost (1988a-c), e.g., the 'Skeletal Intermediary Organization', the 'Mechanostat' and the 'Three-Way Rule', attempt to identify the operational parameters underlying this structural hierarchy.

This study examines the relationship between two of the above levels, macrostructure and microstructure, in a series of human metacarpals and metatarsals. It incorporates the following comparisons: SOURCE (historic archaeological versus modern cadaveral), AGE (younger versus older), SEX (male versus female) and SIDE (right versus left, for metacarpals). Data for the study are of two general kinds, the first being measures of geometric strength obtained from bone cross-sections using SLCOMM, a recent version of the digitizing program, SLICE. These geometric measures reflect long term functional adaptation, and are used to situate the second category of data, obtained from JAVA, an automated image analysis system applied to

microradiographs prepared from these cross-sections. This category directly measures recent modelling and remodelling activity, providing a view of functional adaptation in the short term.

1.2 Structure of the Dissertation

Chapter 2 reviews the literature for continuing periosteal apposition in the adult human skeleton. This phenomenon is a central focus of this study. Three hypotheses which have been proposed to account for CPA are examined. Consideration is then given to interpretative difficulties that have hindered previous investigations. These originate in the fact that CPA is typified by a small magnitude of change (effect size) at the periosteal surface. Previous nonhistological investigations have been carried out, by and large, at relatively gross levels of measurement and often with small samples. These factors may restrict the likelihood of finding significant differences within cross-sectional or longitudinal studies. This difficulty is illustrated by an analysis of statistical power in three such reports.

Chapter 3 provides a more general literature review of functional adaptation in the skeleton; in addition, it presents the theoretical foundation for this study, beginning with an overview of processes of modelling and remodelling. This overview concludes with a more in-depth consideration of two outcomes of intracortical remodelling, increased porosity and reduced mineral density, which have important effects on the mechanical behaviour of bone tissue. These two characteristics are then incorporated into a mathematical model for determining mean bone age. Justification is offered for viewing MBA as a summary indicator of recent bone turnover, which can subsequently be related to modelling activity at the periosteal surface.

A brief review of existing biomechanical models for functionally adaptive skeletal modelling and remodelling is then provided, with emphasis given to Frost's 'Mechanostat' theory (Burr and Martin, 1989; Frost, 1988a), and Cowin's 'Strain Equilibrium Model' (Cowin, 1987). A more detailed examination of the most frequently cited explanation for CPA-that it acts as mechanical compensation for enocortical and intracortical bone loss-is undertaken beginning with a consideration of the fundamental engineering

principles underlying such an interpretation. At this point, a model for the development of CPA as mechanical compensation is proposed in view of a progressive reduction in activity level, possibly compounded by the loss of neuromuscular coordination which typify aging individuals (Schoutens et al., 1989). These reductions contribute to the necessary quantitative and qualitative changes in the bone tissue's mechanical environment that could determine the occurrence of, or changes in, CPA, porosity and MBA. While the proposed CPA model can not be directly tested without recourse to an experimental design controlling for categories of information that are generally not retrievable from anthropololgical samples (e.g., genetic, behavioural and physiological parameters), it serves to identify probable relationships among variables investigated in the present study.

In chapter 4, the skeletal elements selected for study are described. Much of this chapter is devoted to methodological details, such as the determination of transverse section locations and normalization for body size differences. Also discussed are the stages of sample processing and the technologies used to collect the various kinds of quantitative and qualitative data employed in the study. Chapter 4 concludes with a discussion of the statistical analyses applied to these data.

Results are given in chapter 5, beginning with comparative analyses of the geometric and densitometric data, followed by analyses of variance and correlation aimed at identifying the patterns of relationship that exist for variables among and within cross-sections, and within and between the two categories of data. A summary statement of results concludes the chapter, preparing the way for discussion of these findings, taken up in chapter 6. Particular emphasis on how the results mesh with expectations based on the models of skeletal response to functional change is made. The chapter, and body of the dissertation, ends with a formal statement of conclusions. Appendices incorporating summary descriptive information pertaining to the study (e.g., literature review, sample make-up, statistical data), and bibliography, complete the work.

CHAPTER 2. LITERATURE REVIEW

2.1 Introduction

Continuing periosteal apposition (CPA) of lamellar bone in adulthood produces greater skeletal dimensions in older individuals. Over the last twenty-five years a large body of research has described the magnitude and distribution of CPA for a number of different bones and in a variety of living and extinct populations (e.g., Epker and Frost, 1966; Garn et al., 1972; Israel, 1973; Macho, 1986; Martin and Atkinson, 1977; Ruff and Hayes, 1983b; Ruff and Hayes, 1988; Smith and Walker, 1964). Studies of other aspects of skeletal variability, such as brow ridge surface morphology (Tappen, 1983), cortical bone mineral content (Harper et al., 1984) and histology of archaeological remains (Bassett et al., 1980) also implicate or document CPA in the adult human skeleton.

Among the arguments which have been advanced to account for all or part of the phenomenon are (1) that CPA exists as a cohort effect of a secular trend for stature increase, at least in the femur (Trotter et al., 1968); (2) that it exists as a result of maintaining a viable mechanism for responding to fracture or to increased mechanical loading (Parfitt, 1984); and (3) as concluded by the majority of investigators, that CPA serves at least in part as a form of mechanical compensation for bone loss at the endocortical and/or intracortical surfaces (Garn et al., 1972; Martin and Atkinson, 1977; Ruff and Hayes, 1988). Such bone loss threatens the structural integrity of the skeleton, often leading to traumatic fracture.

Although theoretically well-founded in engineering beam theory, evidence for this latter hypothesis is entirely phenomenological, consisting of repeated observations that bones of older individuals have larger widths, diameters, total areas, etc. To date there are no empirical data which demonstrate periosteal apposition occurring as a discrete modelling event in response to reduction in mechanical strength resulting from intracortical or endocortical bone resorption.

The purpose of this chapter is to review research describing the presence and distribution of CPA in the human infracranial skeleton, most of which has been undertaken since 1960. This chapter also critically evaluates three hypotheses which have been proposed to explain CPA and also considers how skeletal biologists might appropriately interpret it, given that much of the data indicative of CPA reports an effect size often found to be statistically nonsignificant in, e.g., comparisons between different age-cohorts using gross measures of bone size.

Effect size, defined as "the magnitude of the differences among samples" (Hodges and Schell, 1988:176), is a contributing factor underlying the probability of committing a Type II error (accepting a false null hypothesis). For example, a Type II error occurs in accepting the hypothesis that 'total cortical areas in young adults and old adults are equal', when in fact they are not. This probability is the complement of a statistical test's power, and it can be estimated by power analysis (Cohen, 1977; Hodges and Schell, 1988; Lieber, 1990). In addition to effect size, power analysis also considers the level of significance (α) employed in the comparison, and sample reliability (size and number of groups compared). Potential difficulties in the interpretation of the biological versus statistical significance of CPA are illustrated by applying power analysis to data from three studies selected from the literature reviewed: Tallgren (1974), Plato and Norris (1980), and Plato and Purifoy (1982). These studies are among those which have reported nonsignificant age-related geometric change in the cranium (Tallgren) and 2nd metacarpal (Plato).

2.2 CPA in the Human Infracranial Skeleton

CPA has been observed throughout the skeleton. However, given that the skeletal materials used in the present investigation are post-cranial, the following review is restricted to those elements. An overview of cranial studies can be found in Appendix 1. The following summary focusses upon investigations post-1960. Earlier studies do exist that have argued for the existence of continuing periosteal apposition. Boharitchuk (1954:182), for

example, studied macro- and microradiographic changes in hand phalanges from 547 skeletons, noting that " 'Normal' exostosis ... is one of the signs of continuing appositional bone growth after the period of development is completed". Many bones of the infracranial skeleton have provided direct or indirect evidence of adult growth (Table 2.1). These include lumbar vertebrae, ribs, humerus, radius, the second metacarpal, femur and tibia. Garn (1981) identifies the first metatarsal sesamoids as participants in this process, although the source for this observation is not given.

Epker and Frost (1966) have reported histological data for continuing bone growth from the middle third of ribs five through seven. They sampled 92 'metabolically normal' individuals aged two to 70 years who had been given tetracycline at some time within the four years prior to skeletal sampling, which occurred either at autopsy or at thoroctomy. Microscopic examination of transverse thin sections revealed fluorescent labels in some, but not all, individuals in every 10 year age cohort. This would indicate that CPA was an intermittent event. As well, the proportion of individuals with labelled bone progressively decreased in the older cohorts, suggesting that the process responsible occurred less frequently with age. A distinction was also found in the locus of deposition, with the ventral (external or cutaneous) surface being preferentially labelled.

In a series of publications, Garn and co-workers (Garn et al., 1967, 1968, 1972, 1976) amassed and presented a large body of (primarily) cross-sectional radiographic data from both living and skeletal samples on the mediolateral expansion of the second metacarpal at midshaft. Of note is the fact that part of their EuroAmerican sample consisted of participants of the same Fels Growth Study used by Israel in his examination of skull growth (see Appendix 1). Garn's group looked at both males and females, assigning subjects to either younger (25 to 54 years) or older (55 to 84 years) age cohorts. In all cases, the older cohort had larger metacarpals, with many of the differences achieving statistical significance. In most cases, the larger proportional increment was seen in females, prompting the observation that the magnitude of periosteal apposition was tied to the magnitude of endosteal bone loss (both being greater in females). While most of their data

Table 2.1. Summary of Post-Cranial CPA Literature, Through 1990.

Smith and Walker (1964)	2030 adult females, aged 45 to 90 years, measured the mediolateral diameter of the femur in anteroposterior radiographs	the mean periosteal diameter increased 10.9 % at midshaft, less at more proximal locations, contra Sumner (1984a)
Epker and Frost (1966)	tetracycline labelled transverse rib sections from 92 individuals aged 2 to 70 years; cross-sectional data analysed at 10-year cohort intervals	all groups had some individuals with labelled lamellar bone; within cohorts, the proportion of labelled to nonlabelled ribs decreased with advancing age; the ventral surface was preferentially labelled
Garn et al., (1967, 1968, 1972)	2nd metacarpal studied in hand-wrist radiographs from several North and Central American populations; plus a longitudinal component of 87 participants of the Fels Growth Study; the 1972 study involved hand-wrist radiographs of 5660 North American men and women from the Ten State Nutritional Survey	all older cohorts had larger mediolateral diameters; some significantly so; females tended to gain more than males periosteally, and to lose more bone endocortically
Trotter and Peterson (1967)	transverse midshaft diameters of 237 left and 28 right femora; 265 Terry collection females; 25 were radiographed (data corrected for magnification)	actual diameters were slightly larger than the radiographic diameter; the actual diameters increased significantly with age, but less than that reported by Smith and Walker (1964)
Trotter et al., (1968)	male and female black and white femora from 1476 individuals were measured for length and midshaft diameter, and analysed with respect to age at death and birth year	for all except black males, no significant increase in diameter was recorded which could not be accounted for on the basis of a cohort effect associated with a secular trend for greater stature
Adams et al. (1970)	hand-wrist radiographs of 60 males and 54 females, taken 11 years apart, measured for total midshaft diameter and cortical thickness	considerable interindividual variation evident for both variables; reduction in cortical thickness significant for both sexes; females alone show a significant increase in diameter

Perzigian (1973)	122 male and 51 female radii; archaeological; bone mineral content (BMC) and bone width (BW) measured using SPA at two sites: 1/3 (cortical) and 1/10 (trabecular) radial length proximal to the styloid process	at the cortical bone site, BW increased in both sexes between age 20 and 60+, though in females the increase was negligible; at the trabecular bone site, male BW decreased slightly, female BW showed no change
Carlson et al., (1976)	21 female and 19 male femora, archaeological, two cohorts aged 22-40 and 41-55+ years, five transverse sections along the diaphysis, cortical thickness (CT) cortical area (CA), anteroposterior and mediolateral diameter measured	with age, CT and CA lost at all sections, with reduction > in females; mean diameter increased in both sexes, > males, but only significant for the two most distal sites
Martin and Atkinson (1977)	geometric analysis of femoral cross-section images from 4 diaphyseal sites, 16 males and 21 females, aged 2 to 82 years	the anteroposterior and mediolateral bending moments of area increased in males but not in females
Bassett et al., (1980)	subtrochanteric cross-sections from 15 femora from Sudanese X-group individuals (A.D. 350) examined with fluorescence microscopy	older individuals (> 55 years) showed subperiosteal fluorescence in thin bands 5-10 μm thick, consistent with 'tetracycline' labelling
Martin et al., (1980)	geometric and histological analysis of transverse sections from the humerus, 2nd metacarpal and femur in 42 white males aged 37 to 96 years	polar moment of area (J) increased until age 80 in the humerus and femur, and to age 60 in the metacarpal
Pfeiffer (1980)	archaeological left and right humeri, 25 younger (epiphyseal line evident) and 300 older individuals compared	eight osteometric measures showed the older group to have larger humeri; side differences (R > L) noted within cohorts
Ruff and Jones (1980)	an archaeological sample of humeri and tibiae, 79 adult males and females, osteometric and radiographic data collected	side asymmetry found in both sexes, but of different pattern: in tibiae, TA increased in all groups, in humeri females had increases; males decreases with greater age

Plato and Norris (1980)	2nd metacarpal measured in hand-wrist radiographs of 236 male participants of the Baltimore Longitudinal Growth Study on Aging (BLSA), aged 25 to 95 years. Measured for total width (TW), length (LEN), medullary width (MW), combined cortical thickness (CCT), CA, and per cent cortical area (PCA)	with advancing age, the increase in TW and LEN not significant; MW, PCA and CCT was significant; R > L; grip strength was found to be significantly correlated with TW alone, suggests that an association between bone size and stress develops before adulthood is attained
Ruff and Hayes (1983b)	femora and tibiae in an archaeological sample, 59 males, 60 females; geometrical data from several diaphyseal locations	both sexes showed increases with age in cross-sectional properties, eg. I, TA
Plato and Purifoy (1982)	2nd metacarpal measured in hand-wrist radiographs; 176 female, 448 male BLSA subjects; TW, MW, CCT, PCA and LEN measured against age, sex, side and Body Mass Index (BMI)	with advancing age, increased TW n.s., but significant decrease in MW, PCA and CCT was found; in females BMI associated with > PCA and CCT and lower MW. R metacarpals > L, especially in right-handed individuals
Sumner (1984a)	multiple cross-sections assessed in archaeological femora, mediolateral width measured by SPA; cohorts aged 20-39 and 40+ years compared	widths increased between cohorts at all locations; largest increase seen in proximal diaphysis
Burr and Martin (1983)	radii of 86 male and female cadavers, aged 18 to 95 years. SPA, direct measurement of bone width, (BW), torsional loading of excised diaphyseal block and histomorphometry of sectioned loading site. Data: BMC, BW, bone mineral index (bmi), CA, porosity, polar moment of area (J) and torsional rigidity, (R).	with age: male bmi decreased n.s.; CA increased n.s.; porosity increase was significant; J, BW and R all significantly greater; female bmi and CA decreased significantly; J decreased n.s.; porosity and R increased n.s.; authors speculate that mechanical compensation provided to women by means other than CPA, eg., at the tissue level
Ringe et al., (1985)	cross-sectional SPA data (BMC, BW and BMC/BW) for 100 females and 80 males, aged 70 years or over; two radial sites, 1/3 and 1/10 the distance from ulnar styloid to the olecranon process	BMC and BMC/BW declined steadily, BW stable in female radii at both sites, increasing only beyond 90 years of age; in males, BMC loss was accelerated until age 80; rate of loss reduced for BMC/BW due to > BW

Simmons et al. (1986)	four midshaft femoral sites investigated in an unspecified number of males assigned to 20-25, 40-45, 60-65 or 80-85 age cohorts	authors observed "ongoing periosteal new bone formation with endosteal trabecularization and resorption in the older ages" (p. 222)
Fox et al., (1986)	2nd metacarpal of 160 male participants of the BLSA having successive hand-wrist radiographs enabling inclusion in a seven cohort, three-epoch, age-time matrix	some positive gains seen in total midshaft width and in total length occurred but none were significant
Behrents and Harris (1987)	matched hand-wrist radiographs, 28 males and 9 females; mean interval 32.1 years; length of four bones in ray II measured	middle and distal phalanges increased; proximal phalange had no change; metacarpal decreased
Aksharanugraha et al. (1987)	19 hand bones of 60 white males, paired radiographs; cohort mean ages 22 and 54 years	as in Behrents and Harris (1987); changes localized to ends lacking epiphyses
Ruff and Hayes (1988)	ca. 100 each, femur and tibia, male and female cadavers, 3rd to 10th decade, several sites measured for areas and other geometric variables	males alone showed significantly increased dimensions, females showed a positive but nonsignificant trend for greater size
Stini (1989)	longitudinal analysis of radial breadth, mineral content and apparent density of > 1800 subjects using SPA	in subjects > 60 years old, female bone breadth increased and density decreased; males showed no change after age 70
Mosekilde and Mosekilde (1990)	cross-sectional analysis of 90 male and female 2nd lumbar vertebrae, aged 20 to 91 years.	area of male I2 increased with age, female vertebrae did not, cf. Martin and Atkinson, 1977; Ruff and Hayes, 1988; both sexes suffered a decline in load-bearing capacity to age 75.

were cross-sectional in design (e.g., the Ten State Nutrition Survey-see Garn et al., 1976), a smaller subset (34 males and 53 females) of longitudinal data was also analyzed (Garn et al., 1967). Male metacarpal widths

increased an average of 1.5 % over a 24 year interval, while female bones increased 1.4 % over 15 years.[1]

Adams et al. (1970), Fox et al. (1986), Martin et al. (1980), Plato and Norris (1980), and Plato and Purifoy (1982) are among those who have also examined the second metacarpal. The latter three studies involved participants of the Baltimore Longitudinal Study of Aging (BLSA). Fox et al. (1986) partitioned hand-wrist radiographs from 160 male subjects into an age-time matrix comprising seven 8-year age cohorts and three 8-year consecutive epochs. Three cross-sectional analyses; seven longitudinal analyses; and five time-series analyses (five cohorts appeared in each of the three epochs) were performed using the same body of data, allowing the investigators to control for age, secular trend and year of observation independently. Data were collected on medullary width, total width, cortical thickness, per cent cortical area (all at midshaft) and bone length. Only total width and length, however, are relevant in the present context.[2] While some indications for incremental change in total width were observed in the three cross-sectional analyses, as well as in the three youngest longitudinal cohorts, no statistical significance was obtained. Indeed, the four older longitudinal cohorts demonstrated a slight negative trend for total width. Similarly mixed results were obtained in the time-series analysis, and for all analyses concerned with bone length. The authors suggested that, in this sample, neither of these metacarpal dimensions experience directional size change with advancing age.

Plato and Norris (1980) and Plato and Purifoy (1982) examined bilateral hand-wrist radiographs from 236 male, and 176 female plus 448 male participants, respectively, in the BLSA. The subjects were partitioned into 10-year cohorts from age 20 to 99 years. Data for the same variables as

---

[1] This summary is based on information given in the Table 2 of their paper. In the text, the interval range (15 and 24 years) is reversed for the two sexes. This change would render this conclusion inconsistent with that reported above regarding the sex-specific magnitude of growth.

[2] The aim of this discussion is to establish CPA as a real biological phenomenon. Endosteal surface changes (e.g., medullary width) will most certainly become relevant in a consideration of causality.

were later recorded by Fox et al. (1986) were collected. In general, older individuals had larger values for total width up to the seventh decade (females) or eighth decade (males; both studies), though these increments were found to be nonsignificant. Martin et al. (1980) reported increases in cortical area and the polar moment of area (a measure of resistance to torsion) up to age 60, in a series of male subjects aged 37 to 96 years. While it is presumed that increments in these parameters to age 60 reflect periosteal apposition, it is not possible from the data (presented graphically) to determine whether the reduction of these measures, which occurred after age 60, was due solely to endocortical resorption without CPA, or due to endocortical bone loss overwhelming any positive contribution that CPA would provide.

Two studies, Adams et al. (1970) and Behrents and Harris (1987), are important for their use of longitudinal data. Behrents and Harris (1987) investigated length change in matched pairs of hand-wrist radiographs from 37 individuals (28 males and nine females) for the four bones constituting ray II (i.e., 3rd metacarpal plus proximal, middle and distal phalanges). As young adults, this sample had a mean age of 21.7 years, and an average of 32 years (range 19.0 to 37.9) elapsed between observations. Following standardization of growth changes to initial bone size and to duration between observations, a monotonic growth gradient was observed which was more or less uniform for the two sexes: proportionate change was highest in the distal phalanx (1.8 % per decade), slightly less in the middle phalanx, essentially zero for the proximal phalanx and negative for the metacarpal. These investigators have since extended this study, reporting longitudinal data gathered from hand-wrist radiographs on length change for all 19 hand bones from 60 American white males, again with a mean interval of 32 years between cohorts (younger mean = 22 years; older mean = 54 years) (Aksharanugraha et al. 1987). As before, significant length increases of the middle and distal phalanges were found, as were significant decreases in the corresponding metacarpals. This latter result may be contrasted with the BLSA data for the 2nd metacarpal, which indicates a nonsignificant increase in length from age 45 onwards (Plato and Norris, 1980). The proximal phalanges, however, showed no directional change in

length, and represented what Aksharanugraha et al. (1987: 174) have termed a 'point of inflection'. By superimposing each set of radiograph pairs, the authors were able to demonstrate that length increments and decrements occurred "almost exclusively at the articular surfaces *lacking* an epiphysis". In both of these studies the combination of apposition at distal and middle phalangeal surfaces and resorption at proximal metacarpal surfaces resulted in minimal change in net ray length within the hand.

Adams et al. (1970) examined radiographs of the second metacarpal in a British sample of 60 men and 54 women. They were aged 66 to 75 years at follow-up, 11 years after they were first observed. Measures of midshaft diameter and cortical thickness were taken, apparently not standardized for body size differences. Between observations, mean cortical thickness within sexes decreased significantly ($p \leq 0.001$), although the magnitude of loss did not differ between them (0.47 mm in males, 0.62 mm in females). Considerable within-group variation was evident, with some individuals in either sex showing little or no loss of bone. Although males had significantly wider metacarpals at both points in time, and both sexes showed a trend for increasing mean diameter with age, only females showed a significant increase (0.11 mm, $p \leq 0.001$). Again, considerable interindividual variation was present, with some members of each group showing little or no increase, and others showing a decrease in metacarpal diameter.

Long tubular bones of the upper and lower limb have also provided evidence of continuing adult growth. Studies carried out upon bones of the upper limb include the humerus (Martin et al., 1980; Pfeiffer, 1980; Ruff and Jones, 1981) and radius (Burr and Martin, 1983; Harper et al., 1984). For lower limb bones, Carlson et al. (1976), Martin and Atkinson (1977), Martin et al. (1980), Ruff and Hayes (1983b; 1988), Simmons et al. (1985), Smith and Walker (1964), Sumner (1984a), Trotter and Peterson (1967), and Trotter et al. (1968) have investigated age-related changes in femora; while Ruff and Jones (1981), and Ruff and Hayes (1983b; 1988) included data from the tibia. Parameters measured in these studies included cross-sectional geometry (areas, polar and second moments of area), and/or diameters (bone widths). These were measured invasively from bone cross-sections, or noninvasively using photon absorptiometry or radiography.

Aside from documenting the existence of CPA, these studies are valuable in that they identify sources of variability other than age. In particular, the existence of side- and/or sex dimorphism for the second metacarpal) is recorded in a number of these studies (cf. Plato and Purifoy (1982). For example, on the basis of eight osteometric measurements taken on archaeological humeri partitioned into older (n=300) and younger (n=25) cohorts, Pfeiffer (1980) showed that right humeri experienced a greater age-increment than left humeri. Similarly, Ruff and Jones (1981) reported age- and sex-specific bilateral asymmetry for the humerus and tibia in an archaeological sample of 79 adults. In males, right humeri were larger; while in females, left tibiae were larger. The reduction in the magnitude of asymmetry with advancing age was considered "largely attributable to a greater loss of bone with aging from the side with more cortical bone in the younger age groups" (Ruff and Jones, 1981:81).

Carlson et al. (1976) calculated the means for mediolateral and anteroposterior diameters at five loc[illegible]s along the femoral diaphysis in a small archaeological sample (21 females and 19 males). Comparisons were made between a younger (20-40 years) and an older (41-55+ years) cohort, and in all instances the older group means were larger. However, in males only the two most distal locations were found to be significantly different. In samples of modern (cadaveral) human femora (Martin and Atkinson, 1977) and femora and tibia (Ruff and Hayes, 1988), significant periosteal bone growth was also absent in the female component, as measured by cross-sectional areas and moments of area.

Noting the presence of CPA in males and its absence in females, Martin and Atkinson (1977: 229) argued that this disparity between the sexes might "possibly explain the special problems that women have with osteoporosis." They were hesitant to conclude, however, that perio[illegible]al apposition in males was the result of biomechanical factors. On the other hand, Ruff and Hayes (1988) suggested that sex-specific differences in activity profiles might explain the presence of the male-female dichotomy in modern populations, and the fact that in the Pecos Pueblo archaeological sample reported earlier (Ruff and Hayes, 1982; 1983a,b; 1984a,b), both sexes evinced periosteal expansion. They argued that modern women were

more sedentary than both modern men as well as prehistoric men and women. These data should be contrasted with that of others (e.g., Adams et al., 1970, Garn et al., 1967) who observed an opposite effect, with females having greater dimensional change than males, albeit in other bones.[3]

Recently, further attention has been given to documenting CPA in the axial skeleton, notably the lumbar vertebrae. Mosekilde and Mosekilde (1990) hypothesized that sites such as L2 should experience CPA since "the vertebral body is the main-and first-site for age-related osteoporotic fractures" and thus would be expected to undergo a compensatory addition of new bone as a form of compensation. In a sample of 43 females aged 15-91 years and 47 males aged 20-90 years collected at autopsy, they found a significant increase in vertebral body cross-sectional area ($r = 0.33$, $p \leq 0.01$) in male L2, from the age of 20 to 80 years (25-30 %). This increase was not present in females, mirroring results for the femur obtained by Martin and Atkinson (1977) and Ruff and Hayes (1988). Given this dichotomy, it is perhaps surprising that, when tested in compression, both male and female L2s experienced an almost identical decline in load-bearing ability, with males in fact showing a marginally steeper decline, though not significantly so, owing to their having a higher initial capacity. This finding should make one critical of Mosekilde and Mosekilde's (1990) suggestion that compensation is occurring at this site, since this should in theory retard the decline in load-bearing capacity of the male L2.

---

[3] Ruff and Hayes (1988: 892) suggest that these different sex-specific findings may result from (1) the failure of these other studies to control for body size effects, (2) the fact that radiogrammetric and photon absorptiometric techniques possess greater method error, and (3) the metacarpal being "a rather marginal region in terms of general mechanical loadings and remodelling of the skeleton as a whole", and thus a less reliable indicator of sex-specific differences in behaviour (presumably the stimulus for the dimensional dichotomy observed by them in the lower limb). These criticisms, however, fail to explain why several studies demonstrate greater change in female versus male metacarpals.

2.2.1 Discussion

The existence of continuing periosteal apposition of bone throughout adulthood seems well established, despite being found to be of insignificant magnitude in some studies. A number of important points should be noted. First, demonstrating CPA has involved a diversity of populations, living and skeletal. More importantly, a variety of techniques have been used in the documentation of this phenomenon, including direct measurement from individual bones, radiographic analysis, photon absorptiometry and manual stereometry and/or digitized image analysis of transverse bone sections. Furthermore, adult incremental change in the skeleton has been recorded secondarily, in studies formulated to investigate other aspects of skeletal biology (e.g., bone mineral content). Setting aside the tetracycline-based histological demonstration of CPA (Epker and Frost, 1966), these factors alone would seem to rule out the possibility that the occurrence of CPA is a systematically-derived methodological artifact. The fact that studies using comparable methodology have both found (e.g., Adams et al. 1970; Garn et al., 1972; Israel, 1973a) and not found (e.g., Plato and Purifoy, 1982; Fox et al., 1986; Tallgren, 1974), significant incremental growth further substantiates this point.

With the exception of studies by Aksharanugraha et al. (1987), Berhents and Harris (1987), Epker and Frost (1966), and Kokich (1976, in the cranium-see Appendix 1), none of the investigations reviewed is capable of identifying the specific locus of apposition and/or resorption. This is because measurement of lengths, breadths and diameters involves two surfaces. For example, increasing mediolateral midshaft diameter of the second metacarpal might occur at the medial surface, the lateral surface, or both (equally, alternately, and with variable magnitude). Indeed, in the investigations cited above surface-specific changes were noted. These results argue for CPA as a diffuse, but context-dependent phenomenon; thus to assume that CPA occurs on all bone surfaces is overly simplistic. Neither would it be appropriate to consider it a stochastic modelling process. Certainly, the metacarpal-phalangeal pattern of adult growth demonstrated by Behrents and Harris (1987) and Aksharanugraha et al. (1987) suggests otherwise, as does our present understanding of the association between

bone cross-sectional geometry and the distribution of intracortical porosity (Martin and Burr, 1984; Lazenby, 1986b). These latter variables (and, by implication, the processes responsible for them) interact in a manner which conserves the geometric strength of tubular bones.

It is clear that the parameters underlying the occurrence of CPA in such a potentially multivariate context as that of adult growth can only be identified and described by an assessment of skeletal modelling and remodelling dynamics at the histological level. Sumner (1984a: 215) attempted to investigate one particular hypothesis for CPA (that of mechanical compensation) in a series of archaeological femora from the Grasshopper Pueblo site in Arizona using the noninvasive method of computed tomography. This approach was unsuccessful, and Sumner noted that the hypothesis could "not be tested directly because of sampling error in the CT sample". Although it is possible to demonstrate sites of active periosteal bone deposition (and resorption) without invasively sampling the element in question (Bromage, 1982; Saunders, 1985), it is not possible to correlate these surface events with perhaps similarly localized remodelling episodes within the bone (either endosteally or intracortically). At this time, an invasive histological analysis would appear to be the only viable approach capable of providing an integrated view of bone remodelling dynamics among the various bone surfaces.

2.3 Hypotheses

Three explanations have been advanced to account for the continuing growth of the adult skeleton. These are: (1) cohort effect; (2) fracture repair/mechanical response potential; and (3) mechanical compensation. Of these, only the first and last have been suggested by way of an empirical study, and only cohort effect has been explicitly tested.

Any study which uses cross-sectional data must consider the possibility that documented trends exist as artifacts of sample composition and are not reflections of an underlying biological reality. Baer (1956) has identified three possible sources leading to trends in cross-sectional data: true ontogenetic change, secular change and selective survival. Regarding CPA, selective survival refers to a situation in which smaller individuals would be

predisposed to an early death. This would have the consequence that older cohorts would be comprised of individuals with larger mean values for size variables, regardless of the presence or absence of CPA. Selective survival has not been seriously considered in any of the cross-sectional studies reviewed above (indeed, it would be difficult to argue that such a mechanism occurred throughout the diversity of populations studied!). Selective survival would have particular relevance, however, for studies employing archaeological materials spanning a large time period (cf. admonitions by Cadien et al. (1974) regarding the representation of such samples as biological lineages). Ruff (1980:106; see Appendix 1 for discussion) attempted to minimize the significance of this mechanism in his analysis of Indian Knoll crania, noting that the 500 years of site occupation were characterized by "overall physical and cultural homogeneity". The implication is that environmental forces (natural or cultural) that would promote age-specific differential death were not archaeologically evident.

In contrast, CPA has been interpreted as a cohort effect by Trotter et al. (1968). In their analysis of femora from the Terry collection, for which the year of birth spanned approximately nine decades, partial regression of transverse diameter at midshaft on the variables (1) bone length, (2) birth year and (3) death year, indicated the presence of a negative secular trend. Individuals with more recent birth dates tended to have longer, yet narrower, femora. All the same, such a finding does not apply to longitudinal data, nor to Epker and Frost's (1966) cross-sectional data which demonstrated, by histological means, CPA into the 8th decade. This latter point was made by Garn et al. (1968) and recognized by Trotter et al's (1968) study. If anything, the Terry collection results should be taken as a general warning against the incautious use of such skeletal collections in cross-sectional investigations (Ericksen, 1982).

A second hypothesis for CPA suggests that it represents a ubiquitous fracture repair and/or response potential to altered mechanical loading. According to Parfitt (1984: S126) CPA may be "the minimal expression of a mechanism that, although dormant, must remain capable throughout life of responding to the need for fracture healing or to increased biomechanical demand". Much data from the clinical sphere (regarding fracture repair)

and from the experimental sphere (for biomechanical demand) attests to the ability of the skeleton to deal with unexpected or unusual situations. Parfitt's contention, however, conflicts with the results of studies such as Martin and Atkinson (1977) and Ruff and Hayes (1988), in which CPA was found in males only. As formulated by Parfitt (1984), the repair/response potential hypothesis would not permit CPA to be present in one sex and absent in the other, in any population, although the possibility exists that the mechanism might be compromised in one sex.

The hypothesis that CPA is associated with the ability of skeletons to repair fractures or redistribute material resources when faced with novel mechanical situations implies that it will be found wherever such a potential is required. So far as I am aware, all mammalian skeletons are capable of self-repair and self-regulation, the latter attested to by the diverse assortment of large and small mammals involved in experimental work investigating (re)modelling response mechanisms to altered in vivo loading regimens (see Bouvier, 1985; Lanyon 1987 for reviews). As such, CPA should have a wide taxonomic affiliation.

Perhaps more than any other explanation, CPA as an ever present, minimally-expressed potential invokes consideration of the distribution and of the level of control (local or systemic) of this phenomenon. Different bones, and different regions within bones, surely have unequal probabilities for fracture. Buikstra (1975), for example, found 17 healed fractures of long bones and clavicles in 11 of 43 adult *Macaca mulatta* culled from the Cayo Santiago study population, suggesting that such regions are more likely to be broken in the wild (e.g., in falls). Similarly, not all bones are equally likely to experience altered or increased biomechanical loading. Elements involved in locomotion and/or defence, for example, may be reasonably expected to suffer more frequent or more severe demands or insults with possibly life-threatening consequences (Lovell, 1990). In such cases, a repair/response potential will certainly have fitness value, with the attendant implications vis-à-vis selection and adaptation. If control over the bone (re)modelling system is mediated at a systemic level, it might be expected that all bone surfaces would provide evidence of CPA even though selection were acting to ensure an existing potential for but a few such

regions. On the other hand, an adaptationist argument becomes much more complex if control of the cellular mechanisms involved is localized and site-specific. Theoretically, (albeit unreasonably), each site at which CPA occurs could represent an evolutionarily unique adaptational event, and would perhaps be coincident with the evolution of unique behavioural repertoires.

The most frequently cited explanation for CPA argues that it occurs as a form of mechanical compensation. With advancing age, endocortical and intracortical resorption reduces bone volume, thereby weakening the bone, all else being equal. As CPA contributes to an increase in bone volume, it also contributes to an increase in bone strength. The question remains, however, as to the equivalence of the two processes vis-à-vis bone strength.

The hypothesis of mechanical compensation has its basis in engineering beam theory. The ability of a beam to resist an applied bending force perpendicular to its long axis is reflected in a quantity known as the second moment of area (denoted as I). The larger this quantity becomes, the greater the bending strength of the structure (Currey, 1984b; Wainwright et al., 1981). The magnitude of I is calculated as the summed products of each unit of cross-sectional area (theoretically infinitesimal) multiplied by the squared distance of that area to an axis of zero stress, known as the neutral axis of bending. Thus, $I = \text{area}^2 \times \text{distance}^2$, and is expressed in units to the fourth power. It should be clear that a unit of area 'X' mm^2 will contribute more to the summed value of I if it is farther from the neutral axis, i.e., for a given 'X', I increases as an exponential function of distance. Since the periosteal surface defines the maximum distance from the neutral axis in any direction, CPA may be readily perceived, in theory, as mechanical compensation for bone loss occurring in regions nearer the neutral axis. In fact, this relationship would permit a much smaller absolute quantity of periosteal apposition to offset a larger amount of endosteal bone loss.[4]

---

[4] It should be realized that the maintenance of I is specified as an objective for heuristic purposes only, and assumes a constant force (hence a constant resultant stress) which in real life would not apply, as altered lifestyles and concomitant physiological changes in the neuromuscular control system would act to reduce, increase or alter the magnitude and/or the frequency of mechanical loading.

While this argument refers specifically to a bending load, which is the most threatening mode of loading for tubular bones (Bertram and Biewener, 1988), a similar rationale can be described for compression forces and the threat of failure in buckling (see Currey (1984b: 122-6) for discussion).

Two major objections have been raised against the mechanical compensation hypothesis. First, CPA occurs prior to significant endocortical bone loss; and indeed, that it represents a process continuous with adolescent growth (Epker and Frost, 1966; Behrents, 1985). Second, CPA occurs in non-weight bearing bones, e.g., the cranium.

Garn et al. (1972) and more recently Parfitt (1984, taking his cue from Garn, but offering the alternative hypothesis discussed above) have cited the first two objections. From their point of view, neither the cranium nor the second metacarpal can be considered weight-bearing bones in a structural sense, and thus deem it unlikely that CPA in these elements represents an adaptation to withstand mechanical stress (Lanyon, 1987). It must be recognized, however, that weight-bearing (whether static or dynamic) is but one factor in a skeleton's mechanical environment. While the cranium and metacarpal may not qualify as structural members, they are certainly subject to deformation by muscle contraction (e.g., in mastication and manipulation).

It should also be pointed out that Parfitt's (1984) hypothesis and that of mechanical compensation are not mutually exclusive. The presumed motivating factor for any magnitude of CPA as mechanical compensation is bone loss, which will have the effect of increasing the biomechanical demand made upon the remaining bone tissue. Parfitt's hypothesis, however, assumes that CPA occurs in small quantities reflecting a *potential* for responding to increased mechanical loading regardless of prior bone loss. The two hypotheses thus differ significantly at that conceptual level.

The more serious of the objections raised against the hypothesis of mechanical compensation concerns the relative timing of events. As noted, the hypothesis implies that gain follows loss; indeed, that it responds directly to the consequences of loss, viz. increased mechanical strain in the remaining cortex. However, CPA appears to be continuous (albeit intermittent) from the adolescent-adult transition, and as such precedes

bone loss. The latter is not really underway until age 40 or so (Mazess, 1982). This problem does not negate the compensation hypothesis-indeed, Garn et al. (1972) accept CPA as only partial compensation-but it would necessitate accepting the adjunct (improbable?) proposition that the magnitude of future bone loss and/or future levels of physical activity can be predicted by the existing periosteal cell system responsible for CPA (or at least have been, in an evolutionary sense). So far as females are concerned, fracture epidemiology would either argue against this possibility, or for present magnitudes and rates of bone loss as relatively recent phenomena. The alternative to such prediction would be compensation for an unknown reduction of bone volume by excessive deposition of new periosteal bone. This is not only metabolically inefficient, but is inconsistent with the reported magnitude of CPA and contravenes the 'minimum mass' corollary of Wolff's Law.[5]

Martin and Atkinson (1977) and Ruff and Hayes (1988) found adult periosteal expansion in the lower limb bones (femur and tibia) in males but not in females. While this dichotomy may partially explain the greater incidence of osteoporotic fracture in females (Martin and Atkinson, 1977), it does not support mechanical compensation as an adaptive process (though a complex model implicating female menopause and the loss of reproductive capacity, which males retain into advanced years, may be envisioned). Ruff and Hayes (1988) hypothesized that changing age-related activity patterns underlay the dimorphic pattern of CPA. They analyzed two populations, a modern cadaveral sample and an archaeological sample from Pecos Peublo. In both groups, males demonstrated significant periosteal expansion, but only the archaeological females-which they presume to have been active throughout life-showed similar growth. Modern sedentary females showed no significant CPA.

---

[5] This corollary, as stated by Roux in his incorporation of Wolff's Law within the construct of functional adaptation, argues that the self-regulating behaviour of bone tissue seeks to establish maximum strength with a minimum of material expense-see Roesler (1987) for further elaboration and discussion.

2.4 Interpretation

The interpretation of continuing periosteal apposition as an adaptive process in the human skeleton hinges upon three factors: (1) does it occur on all, or only some, skeletal elements; (2) for those elements upon which it occurs, does it do so ubiquitously or do only some surfaces experience it; and (3) what is the absolute and/or relative magnitude of change? The first two have been considered earlier: CPA has been observed in both the axial and appendicular skeleton, and evidence from a number of bones suggests that not all points on a periosteal surface are, at least at any one time, experiencing new bone growth. At the same time, not all bones nor all surfaces been examined; thus, definitive answers for the first two questions can not be given.

The third factor is somewhat more complex given the diversity of methods and variables used to document CPA (Table 2.1). Nonetheless, an appreciation for the magnitude (effect size) of change which might be expected to accrue through the action of CPA is crucial for differentiating between the statistical and biological significance of the phenomenon (Table 2.2), as well as among the various possible hypotheses which might account for it. For example, a small magnitude of change may be in keeping with a basal level of activity for bone-lining cells retaining their ability to actively deposit new bone when called upon to do so (Parfitt's repair/response hypothesis). Alternatively, a small effect size may be all that is required to offset a given magnitude of bone loss, in keeping with the mechanical compensation hypothesis (see section 3.4). In either case, the lack of statistical significance may belie recognition of a biologically meaningful phenomenon, and may lead researchers to accept the statistical null hypothesis that no difference exists between the samples compared (i.e., that $H_0: \mu 1 - \mu 2 = 0$ is true).

Hodges and Schell (1988: 175) have warned that accepting a false null hypothesis may cause researchers to suspend potentially fruitful analyses. Alternatively, it may lead to the proposition of novel hypotheses aimed at accounting for the nonsignificant result, i.e., Ruff and Hayes' (1988) suggestion that the lack of a significant increase in the femoral and tibial dimensions of modern females indicates a more sedentary lifestyle for this

Table 2.2. The Absolute and Relative Magnitude of Age-Related Change in Selected Cranial and Postcranial Elements.

Study[1]	Variable	Mean Interval[2]	Difference[3]	Annual Change
Israel (1968)	mean parietal thickness	18.0	0.62 (+7.86)	0.034
Ruff (1980)	mean parietal thickness	9.8	0.30 (+5.76)	0.03
Garn et al. (1972)	2nd metacarpal width	M: 30.0	0.08 (+0.84)	0.002
		F: 30.0	0.20 (+2.50)	0.006
Trotter and Peterson (1967)	femoral midshaft M-L diameter	40.0[4]	0.80 (+3.19)	0.02

1. See Table 2.1 or Appendix 1 for particulars of these studies.

2. Years.; all other measurements in mm

3. (% difference) calculated as 100 [(older mean-younger mean) ÷ younger mean]

4. 40.0 years between the median age of cohorts, 20-59 years and 60-99 years.

group. In another case, Plato and Norris (1980) have argued that in the absence of a demonstrable age-related increase in 2nd metacarpal total width (TW), the significant association of grip strength to TW found in their male sample indicated that the relationship between bone size and stress (a causal determinant of size) must develop prior to adulthood. This would imply that since total width does not change significantly in adulthood, the bone modelling system responsible for depositing new periosteal bone matrix is not responsive to 'normal' adult stresses; or alternatively, that the adult stresses experienced by the subjects studied are of an insufficient magnitude to activate the system. The merit of either of these hypotheses is premised upon accepting Plato and Norris' (1980) finding as a robust demonstration of adult stasis in second metacarpal total width. This in turn is based upon the statistical power of their analysis.

Cohen (1977: 25) notes that "In new areas of research inquiry, effect sizes are likely to be small...This is because the phenomena under study are typically not under good experimental or measurement control or both". Since a strong theoretical case can be made for a magnitude of CPA which is

small yet biologically meaningful (as outlined above), it is worthwhile examining studies that have reported nonsignificant results vis-à-vis their sample composition and α levels (both of which act with effect size to determine the statistical argument underlying a researchers willingness to accept or reject a result as significant). Three studies from the CPA literature reporting nonsignificant results and providing data in a fashion amenable to an analysis of power are Tallgren (1974) for the cranium; and Plato and Norris (1980) and Plato and Purifoy (1982) for the second metacarpal. The objective of this analysis is to ascertain whether the characteristics of the sample data and experimental design for these studies (sample size, effect size and α) confer power sufficient for acceptance of the specified null hypothesis. When power is lacking, the low probability of rejecting H_0 renders its acceptance vague at best, and meaningless at worst.

For Tallgren (1974), power analysis using the method for the paired t-test (Cohen, 1977: 48-49) was applied to data given in his Tables 2 and 3. Although not specified in Tallgren's paper, I have assumed a 1-tailed design,[6] with $\alpha = 0.05$ and $n = 32$ for all but five of the measurements examined; for these five, $n = 31$ individuals. The effect size index, d_z', is calculated as $d_z' = m_z/\sigma_z$, where m_z is the mean difference for the matched pairs, and σ_z is the associated standard deviation. Power values can then be read directly, or can be linearly interpolated from the appropriate table (e.g., Table 2.3.2 from Cohen (1977) in this case).

The results of this analysis are given in Table 2.3.[7] Power varies from .048 to .7, with 17 of 22 variables having power ≤ 0.5. In other words, given the parameters of Tallgren's research design, the probability that these variables would reject the null hypothesis ranges from 4.8 % to 70.0 %, with

---

[6] Assuming a 2-tailed design would have the effect of lowering power for a given value of d_z'.

[7] In Table 2.3, variables for which the mean difference between cohorts was zero have been omitted, since it would be meaningless to consider the power of a statistical test to reject Ho: $\mu_1 - \mu_2 = 0$ when in fact μ_1 and μ_2 are equal. Also omitted are variables dealing with the outer cranial vault for which the mean difference was less than zero, since these imply dimensional (shape) change with age due to resorption.

Table 2.3. Power Analysis of Tallgren's (1974) Cephalometric Data[1].

Variable	Mean	D	σ	dz′	Power
sella-30° icc	70.90	-0.01	0.31	-0.05	0.048
external diameter	176.63	0.02	0.56	0.05	0.055
nasion-180°	179.08	0.02	0.58	0.05	0.055
sella-150° icc	95.60	-0.02	0.37	-0.08	0.082
thickness at 150°	8.30	0.02	0.33	0.08	0.096
sella-nasion	69.61	0.02	0.32	0.09	0.098
sella-120° icc	98.90	-0.03	0.45	-0.09	0.115
sella-bregma	99.54	0.05	0.47	0.15	0.143
sella-30° ecc	84.14	0.04	0.41	0.14	0.146
nasion-lambda	182.69	0.05	0.47	0.15	0.155
thickness at 30°	7.11	0.05	0.43	0.16	0.165
internal diameter	145.90	-0.06	0.45	-0.19	0.191
thickness at 60°	7.09	0.06	0.44	0.19	0.192
bregma-lambda	132.07	0.07	0.44	0.22	0.227
bregma-basion	137.43	0.13	0.52	0.35	0.408
sella-opisthion	74.49	0.08	0.30	0.37	0.435
nasion-bregma	108.22	0.11	0.40	0.38	0.445
sella-basion	41.71	0.09	0.30	0.42	0.509
sella-60° icc	81.50	-0.14	0.42	-0.47	0.585
glabella-lambda	183.11	0.20	0.58	0.48	0.600
bregma-opisthion	159.14	0.17	0.48	0.50	0.620
sella-glabella	75.75	0.18	0.46	0.55	0.700

1. All dimensions (columns 2-4) are in mm.

Mean = value at first (younger) observation; D = difference between younger and older means; dz′ = the effect size index; ecc = external cranial contour; icc = internal cranial contour.

most having less than a 50.0 % chance of rejection. Indeed, the variable associated with the largest power value (sella-glabella length) did reject H_0, at $p \leq .05$. Clearly, Tallgren's (1974: 293) conclusion that "in the subjects studied no appreciable remodelling of the neurocranial bones had occurred with increasing adult age" appears tenuous.

Data on total width (TW) of the second metacarpal of male participants of the Baltimore Longitudinal Study on Aging (Plato and Norris, 1980; Plato and Purifoy, 1982) were analysed for power using methods for the F-test

(one-way ANOVA, with k means of unequal n) as detailed by Cohen (1977: 359-362). The effect size index, f, is calculated as $f = \sigma_m/\sigma$, where

$$\sigma_m = \sqrt{\frac{\sum_{i=1}^{k} n_i \ (m_i-m)^2}{N}}$$

m_i = the mean of the ith age cohort;
n_i = the size of the ith age cohort;
N = the sum of all n_i's;
m = the weighted mean of the k age cohort means, $\sum n_i m_i \div N$; and
σ = the within population standard deviation.

As with the t-test effect size index, d_z, power values corresponding to f were derived directly or by linear interpolation from tables in Cohen (1977), for $\alpha = 0.05$, u = 7 (u = the degrees of freedom for the F-ratio numerator), and n = 29, which equals the arithmetic mean of the k groups in the sample, i.e., N/k (Cohen, 1977: 362; for Plato and Purifoy (1982), u = 6 and n = 64). Although any of the age cohort σ's could be inserted into the denominator of the equation for f, since they are assumed to be equal, this analysis presents f values for each age cohort standard deviation.

Two things are made clear by this approach. First, as seen in Table 2.4, there was only a ca. 10 % probability of Plato and Norris (1980) rejecting the null hypothesis that the k cohort means were equal, given the parameters of their research design. That is, it was not very likely that a significant age-related trend towards increased total width of the 2nd metacarpal would be found in their sample of 236 males. Second, it seems questionable whether the variances associated with the first (20-29, n=6) and last (90+, n=4) age cohort means satisfy the assumption of equality required by both Plato and Norris' (1980) F-test and this power analysis. Indeed, in the later study, Plato and Purifoy (1982) not only increased the number of individuals in all age cohorts (making N=448), but they collapsed the 90+ cohort into the 80-99 year old group. However, these

Table 2.4. Results of Power Analysis Based on Plato and Norris' (1980) Left (top) and Right (bottom) 2nd Metacarpal Data.

Age Cohort	σ_m	σ	Effect Size Index, f	Power
20-29	0.122	1.10	0.111	0.187
30-39	0.122	2.13	0.057	0.081
40-49	0.122	1.90	0.064	0.092
50-59	0.122	2.44	0.050	0.070
60-69	0.122	2.39	0.051	0.072
70-79	0.122	2.15	0.057	0.081
80-89	0.122	1.95	0.063	0.091
90+	0.122	1.04	0.117	0.220
20-29	0.146	1.04	0.140	0.286
30-39	0.146	2.29	0.064	0.092
40-49	0.146	1.79	0.082	0.121
50-59	0.146	2.57	0.057	0.081
60-69	0.146	2.28	0.064	0.092
70-79	0.146	1.99	0.073	0.107
80-89	0.146	1.95	0.075	0.110
90+	0.146	0.50	0.292	0.908

Table 2.5. Power Analysis for Plato and Purifoy's (1982) Left 2nd Metacarpal Data.

Age Cohort	σ_m	σ	Effect Size Index, f	Power
20-29	0.103	1.51	0.068	0.172
30-39	0.103	2.62	0.039	0.079
40-49	0.103	2.15	0.048	0.098
50-59	0.103	2.66	0.039	0.079
60-69	0.103	2.65	0.039	0.079
70-79	0.103	2.72	0.038	0.076
80-99	0.103	2.08	0.050	0.100

In both Tables 2.4 and 2.5, σ_m = standard deviation of the population means; σ = within cohort standard deviation (calculated from reported cohort standard error and sample size); both σ_m and σ are reported in mm.

changes have had no effect on the power of their analysis for discovering significant increments in total width of the second metacarpal (Table 2.5).

An alternative approach to determining the a posteriori power of an analysis would be to ask, as a matter of research design, what size of sample would be required in order to identify a trend by the F-test, e.g., for an age-related increase in total width of the 2nd metacarpal. This approach requires the investigator to identify how many groups the sample will contain (to determine u), what level of power is desired, the level of significance α, and an estimate of the effect size index (f), expected; based on theory or on previous research. The sample size required for each group, n, can then be read directly from tables (e.g., Cohen, 1977: 381-389), or calculated from the formula

$$n = \frac{n_{.05}}{400\ f^2} + 1$$

where $n_{.05}$ = tabled sample size for the specified α, u and power for an effect size of .05; and f is the effect size index the researcher expects to observe (Cohen, 1977: 390). For example, given u = 6, a desired power of .80, α = 0.05, and an effect size of 0.06 based on Plato and Norris' (1980) data for TW of the 2nd metacarpal, Plato and Purifoy (1982) would have found that the average group n required in each of their 7 age cohorts would be 543 individuals (N would then be 3801). Figure 2.1 presents a series of curves based on Cohen (1977, Table 8.4.5; subtable u = 6) illustrating the relationship between the effect size index and power, for α = 0.05.[8] Clearly, when f is very small, n must be very large in order to have the statistical confidence (i.e., high power) that the nonsignificant result obtained derives from the 'truth' of H_0.

As noted by Hodges and Schell (1988) and others (e.g., Smith et al., 1982), many important biological phenomena typically have small effect sizes. Unfortunately, many anthropological samples employed in skeletal biology research, such as those composed of archaeological and/or

---

[8] See Lieber (1990) for further discussion of the relationship of sample size and statistical power.

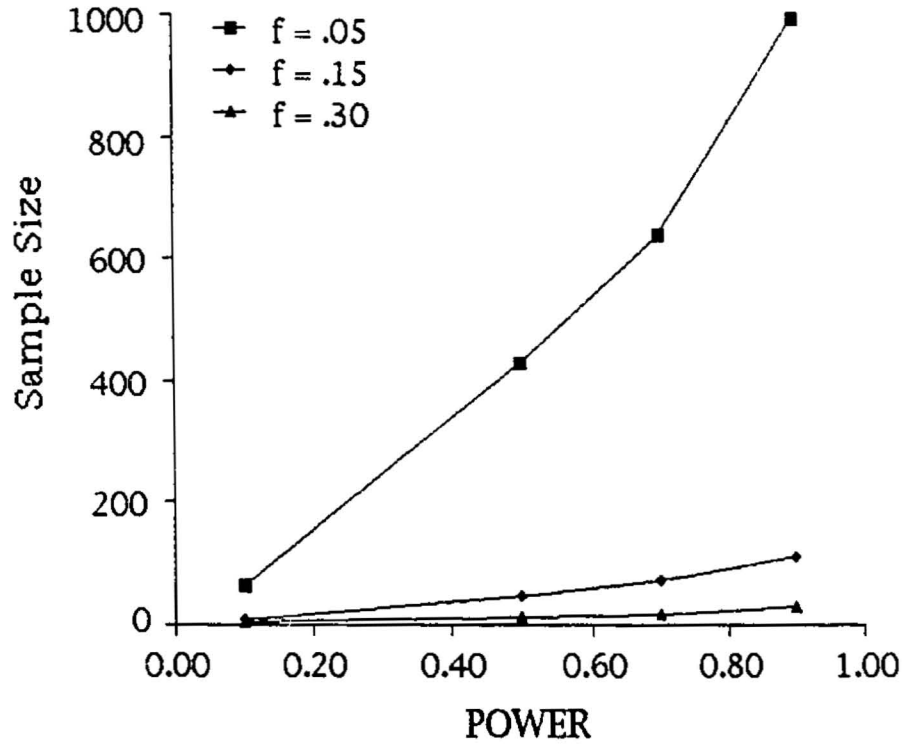

Figure 2.1. The relationship between statistical power and group sample size, n, required to detect an effect size index, f, by the F-test when $\alpha = 0.05$ and $u = 6$.

---

dissecting room populations, are often of an insufficient size to detect small differences between groups. Hodges and Schell (1988: 179) note that statistical power may be enhanced in any one (or more) of three ways: by relaxing α (and accepting, for example, $p \leq 0.1$ as significant, rather than the much more common $p \leq 0.05$); by increasing sample size (n), or by reducing "population variability by defining the population in more restrictive terms". This latter alternative has the effect of decreasing the sample error, thereby increasing the effect size index and, in turn, increasing the associated level of power. The viability of any of these alternatives will, of course, be dictated by the particular research problem under investigation. Often, there is no option for increasing n, and

restricting the population variability may not be desirable since it necessarily restricts the generality (and thus the applicability) of the investigations results (Hodges and Schell, 1988). It would appear, then, that in such instances researchers should give serious consideration to the level of probability of Type I errors (α) they are willing to accept.

2.5 Summary

The review and critique undertaken in this chapter supports the following conclusions. First, continuing periosteal apposition (CPA) in the adult skeleton is a bone fide component of skeletal aging, in spite of a number of studies having reported nonsignificant dimensional change. Second, CPA appears to be widely distributed in the skeleton. However, the precise nature of the surficial distribution for individual bones is unclear, although evidence does exist (e.g., Epker and Frost, 1966) suggesting that CPA is differentially distributed over an element's periosteal surface. Third, the majority of studies which document CPA have measured the result of the process, such as larger bone dimensions in e.g., older individuals. The relationship this external phenomenon may have with specific bone remodelling events at the intracortical and/or endocortical surfaces remains to be adequately described. This fact makes it impossible to distinguish from among the various hypotheses proposed to account for the observed dimensional change, nor even to draw definitive conclusions as to the adaptive character of the process. Finally, interpretation has been hampered by the small effect size which typifies CPA, and the small sample sizes which so typify skeletal biology research. Future studies that explore this process at gross levels of measurement should consider the potential statistical power of their analyses in research design formulation, although admittedly, large *and* representative skeletal samples are a rarity. A more promising approach that has received relatively little attention is that undertaken by the current study, namely histological analysis, which alone offers the possibility of identifying intersurface (periosteal, intracortical, endocortical) relationships.

CHAPTER 3. THEORETICAL ARGUMENTS

3.1. Introduction

This chapter presents the theoretical and interpretive framework relating to the objectives of this research, ostensibly five in number. The first of these is to histologically verify the existence of CPA: can recent circumferential lamellar bone modelling at the periosteal surface be demonstrated unequivocally? The reviewed literature supports this possibility, in which case the second objective is to describe the spatial distribution of CPA: is it diffuse over the periosteal surface or localized? A third goal involves discovering how CPA may or may not relate to other aspects of structural variability, such as cross-sectional geometry, intracortical porosity and bone turnover. A fourth objective is to determine the degree of contextual (source, age, sex and side) variability expressed for CPA within the present sample of individuals and elements. The final goal, of course, is to evaluate the above with respect to mechanical compensation, the favoured hypothesis purporting to explain CPA.

It becomes necessary to delve into a number of aspects of bone biology to achieve these goals. These aspects include the processes of skeletal modelling and remodelling responsible for CPA and the observable microstructural variation. An informal, descriptive approach is first employed, situating these processes and their effects within the hierarchical structure of cortical bone (e.g., Burr and Martin, 1989; Frost, 1980, 1988; Jaworski, 1984a, b, 1987; Martin and Burr, 1982; Parfitt, 1984a, b). Afterwards, a more formal, mathematical perspective is explored (e.g., Frost, 1987a, b; Hattner and Frost, 1963; Polig and Jee, 1987), anticipating development of an operational model for the determination of relative mean bone age (MBA) within a cross-section. MBA provides a single numerical indicator of the recent Haversian remodelling history of the bone at the level of the section, and offers-for certain applications-a more useful approach to characterizing remodelling history than other methods, notably that of 'paleophysiology' (Wu et al. 1970; Frost, 1987b), as applied by

Martin et al. (1985), Lazenby et al. (1989) and Stout (1986; Stout and Teitelbaum, 1976) in tasks ranging from dietary reconstruction to forensic identification.

Since CPA is most often viewed as mechanical compensation, an evaluation of biomechanical models which have been advanced for interpreting cortical bone variation vis-à-vis external stimuli is provided (e.g., Burr and Martin, 1989; Cowin, 1984, 1987; Cowin et al., 1985; Frost, 1982, 1983, 1988a-c; Hart et al., 1984; Hart and Davy, 1989; Jaworski, 1987; Lanyon, 1987; Rubin and Lanyon, 1987). With this background established, more focussed theoretical modelling of mechanical compensation is presented, relating CPA to the maintenance of mechanical strain equilibrium in a context of reduction in bone mass and modified physical activities.

3.2 Functional Adaptation in Skeletal Tissue

Functional adaptation denotes "the ability of living tissue to respond to changes in its environment" (Hart, 1990: 241). Skeletally, this response occurs through change in size, shape and/or quality of bone tissue, for which the processes of growth, modelling and remodelling are accountable (Frost, 1988a-c; Martin and Burr, 1989). Frost (1988a) defines growth as size increase through the addition of cells and intercellular matrix independent of modification in shape or organization; growth per se is not the principal concern of this study.[1] More pertinent are the processes of modelling and remodelling, which alter not only bone size, but its shape and/or quality as well.

Modelling alters bone shape and mass through localized resorption (R) or formation (F), following cellular activation (A). The sequence is thus A-R or A-F (Martin and Burr, 1989). Tissue formed through physiologic modelling is primary, circumferential lamellar bone. In certain circumstances, such as excessive mechanical loading, a pathologic modelling

---

[1] Factors affecting skeletal growth, such as childhood activity and nutrition, can have a very significant effect upon the phenomena studied in this research, in terms of contributions to the magnitude of peak bone mass attained in young adulthood.

response leads to woven bone formation (Burr et al., 1989b). Alternatively, remodelling involves the resorption and subsequent formation of secondary bone at a given site (sequence = A-R-F), and is thus concerned with tissue renewal. Both processes require the activation and coordination of multinucleate osteoclasts and/or mononucleate osteoblasts, operating as basic multicellular units or BMU (Coupron, 1981; Jaworski, 1984a, b; Parfitt, 1984b). While both modelling and remodelling may take place at the periosteal or endocortical surfaces, remodelling alone occurs intracortically. The classic view of remodelling is that which produces Haversian systems intracortically, (i.e., concentric lamellae around a central vascular canal containing blood vessels and nerve fibres).

There are important temporal and spatial associations for modelling and remodelling. Both processes are predominant features of the immature skeleton responsible for adjusting the gross architecture and mass of bones in coordination with growth of adjacent soft tissues. During adulthood, however, Frost (1980, 1987a) reports that modelling as a general phenomenon occurs at a rate that is less than five per cent of that seen during growth. Consequently, most bone cellular activity during adulthood is due to remodelling. Martin and Burr (1989: 181) seem to preclude the occurrence of modelling in adults, although they later (p. 183) indicate a willingness to accept periosteal expansion as "a special case of modelling which persists on this bone envelope into adulthood", in order to reconcile particular experimental data within the parameters of Frost's Mechanostat theory (see section 3.5). In support of this position, Martin and Burr (1989: 181) note that fluorochrome studies indicate that periosteal expansion (cf. CPA) "occurs around a large proportion of the circumference of the bone, rather than in discrete foci", that "(r)esorption cavities are infrequently found on the periosteal surface", and that "formation is seldom associated with a well-defined cement line" characteristic of a remodelling event.

Two concepts of the cellular dynamics of bone remodelling, coupling and balance, are especially relevant in the context of aging (Burr and Martin, 1989; Jaworski, 1984a). The former is a qualitative characteristic with potentially quantitative ramifications, referring to the sequential activity of osteoclasts and osteoblasts. When a remodelling (A-R-F) event is

uncoupled, no formation at all occurs resulting in a net loss of bone mass equal to that resorbed. It should be noted that such an occurrence is pathological, and does not constitute a resorptive modelling (A-R) event. Balance, on the other hand, is a quantitative aspect of remodelling which indicates an equivalency in the mass of bone resorbed and subsequently formed. Burr and Martin (1989) give a detailed review of the relationship of coupling and balance to the development of numerous metabolic bone diseases, including the osteoporoses.

The process of remodelling is ostensibly adaptive, given that it consumes energy and materials; does not occur randomly (Martin, 1984; Polig and Jee, 1987); and produces a relatively weaker structure compared to primary bone (Currey, 1975, 1984c; Vincentelli and Grigorov, 1985). While its specific purpose has been the focus of some contention, an emerging consensus points toward adaptive remodelling as an outcome of two independent aspects of normal mechanical loading history (Burr and Martin, 1989). These are fatigue microdamage repair following prolonged dynamic loading, and mass adjustment following unloading, such as occurs with extended periods of immobilization.

Martin and Burr (1982) proposed that Haversian remodelling represents a response to fatigue damage occurring in the form of microcracks, an accumulation of which would threaten failure of the element. From literature extending back to Currey's (1962) work on voids in bone as sites of stress concentration, they suggested that the approximately circular shape of secondary osteons would prevent microcrack propagation through the cortex. Experimental studies (e.g., Carter and Hayes, 1977) showed that in cortex under tension, a developing crack is captured within the cement sheath at the osteon periphery, resulting in the dissipation of the energy behind its formation. This resulted in the osteon becoming debonded from adjacent lamellae. In compressed regions, microcracks tended to travel across concentric lamellae, again disrupting the association between adjacent layers of bone. It was postulated that debonding and/or disruption stimulated the formation of a new osteon by modifying existing stress fields or piezoelectric potentials at the Haversian canal wall, known from other

work (e.g., Tappen, 1977) to be the site at which new secondary osteons originate.

In a following paper, Burr et al. (1985) reported significant associations between cyclical physiological loading of canine ulnae and radii in vivo, and the amount of microdamage observed in thin section when compared with contralateral controls. They also found a 44-fold increase in the proximity of resorption spaces to microcracks than expected by chance alone. More recently, Forwood and Parker (1989) studied torsional loading of whole rat tibiae in vitro. They observed an inverse relationship between the frequency of microcracking and osteon debonding with parameters such as stiffness and energy absorption. Schaffler et al. (1989) considered the effects of physiological strain rate on the development of fatigue microdamage in bovine cortical bone. Tests in a range of 0-1200 microstrain were performed using 10^6 cycles of tensile strain at rates of 0.01 s^{-1} and 0.03 s^{-1}. The presence of fatigue damage associated with both strain rates was demonstrated through a reduction in stiffness, and confirmed histologically through an increase in microcrack density (cracks/mm^2). Observations were consistent with expectations based on models of fatigue in composite laminates: the higher (0.03 s^{-1}) strain rate specimens lost more stiffness and had more microdamage than lower strain rate specimens, relative to a group of unloaded controls. However, only the former series gave results which were significantly different from the control group. It was also found that osteonal bone specimens showed a greater loss of stiffness than unremodelled (plexiform) bone specimens, confirming earlier work showing secondary bone to be relatively weaker than primary bone. These results suggest that a process whereby microdamage is removed could have significant adaptive value by extending the fatigue life of the structural element.

Prior to this experimental support, Currey (1984b: 264) had criticized the Martin and Burr model on grounds that cracks in bone orient such that "there will be no great tendency for the crack front to travel around the cement sheath"; reducing the likelihood of osteonal debonding. Based on work with paired cat tibiae, Currey argued further that the high degree of left-right symmetry in observed patterns of remodelling weakens the

microdamage hypothesis, since it would require a similar, and in his view an unlikely, symmetry in the formation of microcracks. Currey (1984b, c) outlines other possible objectives for Haversian remodelling, such as the removal of necrotic bone tissue following in vivo cell death; and mineral homeostasis. In his view, neither of these explanations are entirely satisfactory. The former suffers from the same criticisms as the fatigue microdamage hypothesis, i.e., why should bone tissue 'die' with such a high degree of side-symmetry? A major criticism of the latter is the lack of an apparent correspondence between the degree of interspecific variation in remodelling and the likelihood of calcium imbalance. Currey wonders why, for example, adult Americans should show high degrees of Haversian remodelling, while tending not to suffer from a dietary calcium balance sufficiently negative to account for it. At the same time, smaller mammals and birds exhibit little or no remodelling yet are more likely candidates for experiencing mineral imbalance.

The symmetry observed by Currey in the paired cat tibiae might be accounted for by the second objective of Haversian remodelling, namely to reduce bone mass in regions which have undergone a reduction in the level of mechanical loading. If this reduction follows from a nonpathological decline in physical activity, the qualitative symmetry noted by Currey (1984b, c) would be expected, rather than surprising. This is because such a decline might impart a solely quantitative modification to the bone's mechanical environment, keeping constant the qualitative aspects of loading (e.g., direction of bending). However, if aging results in a decline in physical activity (unlikely in Currey's experimental cats), one might expect both quantitative and qualitative changes in mechanical loading; the latter associated with age-progressive impairment of balance and muscular coordination. More will be said of the relationship between modelling, remodelling and mechanical history in section 3.5.

3.3 Hierarchical Structure in Cortical Bone

Bone tissue is heterogeneous in its construction (Currey, 1984b). The structural strength of a skeletal element is derived from a combination of physical properties, principally orientation, porosity, mineralization and

reconstruction (Currey, 1984c). Geometric properties such as cross-sectional area and second moments of area are also major contributors.[2] These properties are not independent (Lazenby, 1986b; Martin and Burr, 1984; Ascenzi et al., 1987); but act and interact within the structural hierarchy of cortical bone (Table 3.1). Variation within hierarchical constituents can have significant positive or negative effects upon a bone's mechanical properties, such as the elastic modulus, yield strength, and work of fracture. Mineral content and porosity are two factors which exert such effects, and illustrate the contribution that lower level structural variation can make to the mechanical properties of whole bones (Burr and Martin, 1983; Currey, 1969a, b; 1975, 1984a, c; 1988; Keller et al., 1990; Laval-Jeantet et al., 1983; Lazenby, 1986a, b; Martin, 1972, 1984; Martin and Burr, 1984; Schaffler and Burr, 1988).

Bone mineral consists of "a mixture of hydroxyapatite crystals and amorphous calcium phosphate" (Vaughan, 1975: 104) which osteoblasts infuse into a scaffolding of maturing, cross-linked collagen during bone formation (Burr and Martin, 1989). With progressive mineralization, collagen and hydroxyapatite become inextricably bound together (Currey, 1984a), with the latter occupying a space of some 18.6 Å between adjacent mineral crystals (McCutchen, 1975). This intimate association contributes to the anisotropy and viscoelasticity of bone material as factors which render theoretical modelling of the mechanical behaviour of bone as a porous, multiphase composite tissue such a difficult task (e.g., Carter and Spengler, 1978; Cowin, 1989b; Currey, 1984a, b).

---

[2] Orientation refers to the fact that bone is anisotropic, meaning that its mechanical properties differ according to the direction of applied load. A long bone , for example, is strongest when loaded parallel to its long axis, weaker when loaded normal to this axis. Reilly and Burstein (1974) provide an excellent account of these issues. Reconstruction is a term used by Currey (1984c and elsewhere) in reference to Haversian remodelling. In addition, characteristics of the loading environment such as strain rate, magnitude and distribution (Rubin and Lanyon, 1987) also contribute to structural strength. For example, the viscoelastic nature of bone tissue sees stiffness as a positive function of strain rate (e.g., Currey, 1975).

Table 3.1. A Constitutive Hierarchy for Cortical Bone.

Analytical Level	Major Components	Major Constituent	Characteristics Affecting Mechanical Properties
Ultra-structure	Organic	Collagen	varies in orientation between, and possibly within, lamellae; preferred orientation likely nonrandomly distributed throughout cortex
	Inorganic	Mineral	varies in content re: bone and age; affects material properties e.g., stiffness
	Primary Bone	Lamellar Bone	slowly deposited as tightly organized circumferential sheets ca. 5 mm thick; separated by a thin (.1 mm) interlamellar layer cf. the cement sheath of Haversian osteons
		Laminar Bone	deposited on fast growing surfaces; struts of parallel fibred bone infilled with lamellar bone
		Woven Bone	rapidly deposited (e.g., in fracture callus) short, fine fibres randomly organized; mineral content greater than lamellar or laminar bone
Micro-structure	Secondary Bone	Haversian Systems	organized as concentric lamellae around a central vascular canal; varies in mineralization
		Cement Sheath	highly mineralized matrix surrounding Haversian systems; negligible organic content
	Porosity	Resorption Cavities; Osteocyte Lacunae	nonrandomly distributed throughout cortex; tending to be proportionately greater near the endosteal surface
Macro-structure	Matrix	Cortical and Trabecular Bone	differentiable along a continuum of bone volume fraction, ash content and in size and shape (geometry)

Much work has examined the relationship of bone mineral to the mechanical behaviour of both trabecular (e.g., Carter et al., 1987, 1989; Whalen et al., 1988) and cortical (e.g., Carter et al, 1981; Currey, 1988) bone tissue. Currey especially has given considerable attention to the adaptive significance of interspecific differences in the mineralization of cortical bone (e.g., Currey, 1979, 1988, 1990). In the following discussion,

concentrating on the physical properties of cortical bone, reference is made to 'true' mineral density, apparent density and bone volume fraction. True mineral density (p_m) refers to the amount of mineral present in fully mineralized bone material, ignoring tissue porosity (Laval-Jeantet et al., 1983), and is most often reported in the literature as the per cent ash content of dry bone (e.g., Currey 1969, 1988). Bone volume fraction is equal to 1-P, where P is the volume of porosity. Apparent density (p_a) is a measure of the mineral content of the volume fraction, such that $p_a = p_m$ (1-P) (Schaffler and Burr, 1988: 15). Bone volume fraction and apparent density both decline with advancing age as a consequence of increasing porosity, while true mineral density remains more or less constant (Laval-Jeantet et al., 1983). In normal mammalian cortical bone (e.g., the bovine femur), the latter approximates an ash content of 65-70 % by weight or 50 % by volume (Wainwright et al., 1981: 183). More specialized mineralized tissues such as the whale temporal bullae and deer antler deviate above and below this value, respectively. Currey (1969a, 1984a-c) has argued that such deviation reflects the specific adaptive character of such elements. The deer antler is often subjected to high energy impact, especially during the rutting season, and thus benefits from a lower mineral content since this would lower the modulus of elasticity and concomitantly increase the work of fracture (see Currey, 1984b: 90). On the other hand, the whale bulla is protected from externally applied dynamic loads due to its anatomical position and the fact that whales are sea living creatures. As noted by Currey (1984a: 517), the very large stiffness of the whale bulla "increases the impedence mismatch between the otic bones and the rest of the skull, so preventing sound reaching the inner ear except via the tympanic ligament, the whale's equivalent of the tympanic membrane".

Variation in true and apparent density also occurs ontogenically, since newly deposited bone is always less mineralized than mature bone (see section 3.4). Bone tissue from subadults, or from regions of varying remodelling rates within adult skeletons, might be expected to differ with respect to true mineral density, and will thus differ in terms of tissue properties and mechanical performance. One effect of a lower elastic modulus is that, for equal magnitudes of stress, such tissue will experience

more strain than that with a higher modulus (Keller et al., 1985). In other words, a similar amount of mechanical loading will produce a greater amount of elastic deformation in immature or more actively remodelled bone (less mineralized, low modulus) versus mature or less actively remodelled bone (more mineralized, high modulus). The significance of this lies in the general acceptance of strain rather than stress as the stimulus for bone modelling or remodelling activity (e.g., Carter et al., 1981; Martin and Burr, 1989), and suggests that the osteogenic potential of younger bone tissue will be more sensitive to variations in strain history. This could in part account for the accumulation of bone tissue in the growing skeleton (Carter, 1983, 1984), in which a lower modulus tissue is subjected to relatively higher levels of physical activity, and thus to more or less constant osteogenic stimuli. The role such an interactive mechanism might play in the modelling and remodelling of adult bone having regional variation in mineral density, and subjected to age-related declines in physical activity, remains to be explored.

Hart (1989, 1990) has recently examined the effects of tissue maturation on the bone remodelling response in a series of finite element models, observing that while little difference in response existed between the various 'maturation rules' used,[3] all exhibited a fundamental distinction from the (nonphysiological) no-maturation case: the response was biphasic, with an initial accelerating rate followed by deceleration, presumably coincident with the increasing material stiffness associated with maturation. This scenario would fit logically into constructs of mechanically adaptive bone (re)modelling, (considered in section 3.5 below) which purport their objective as a return to an equilibrium strain environment.

Bruce Martin (1984:179) has defined porosity as "void volume per unit volume of whole bone", and its appearance in cross-sections of both cortical and trabecular bone is self-evident. Typically, the former has a porosity of less than 15 %; the latter a porosity of greater than 70 % (Schaffler and

---

[3] The term 'maturation rule', as defined by Hart (1990: 242) denotes a "mathematical description of the gradual stiffening, consolidation and calcification of osseous tissue over time".

Burr, 1988).[4] Voids in any material have a strength and stiffness equal to zero (Wainwright et al., 1981). It is thus not surprising that porosity in cortical bone exerts a significant influence on its physical properties: the greater the porosity per unit tissue volume (i.e., the higher a tissue's apparent density), the lower its strength and stiffness.[5] As a general rule, an increase in porosity of 10 % is thought to reduce the absolute value of the elastic modulus by as much as 20 % (Wainwright et al., 1981:157).

Schaffler and Burr (1988) examined the stiffness of bovine cortical bone under uniaxial tension at two strain rates (0.01/s and 0.03/s), with regard to porosity, ash content and apparent density. The expected increase in stiffness with greater strain rate (see footnote 2) was not found, purportedly due to the greater influence on viscoelasticity exerted by porosity and mineralization. After pooling the two samples, Schaffler and Burr (1988) were able to demonstrate a reduction in stiffness, measured in GPa,[6] as a power function of increasing porosity (exponent = -0.55). Interestingly, least squares analysis for log elastic modulus against the log values for porosity, bone volume fraction, apparent density and ash content gave r^2 values of 0.71, 0.71, 0.70 and 0.41, respectively. In a stepwise multiple regression, only bone volume fraction (the complement of porosity) was significantly associated with the elastic modulus. True mineral density (ash content) thus appears to exert less effect on elastic properties than the amount of bone present. A perhaps more significant finding was that the elastic modulus of their cortical bone specimens increased as a power function of apparent density (exponent = 7.4). This is much different that that reported for

---

[4] These definitions lead one to wonder what bone tissue with a porosity between 15 % and 70 % might be called!

[5] Voids in bone may also act to reduce strength by acting as 'stress concentrators'; i.e., artifacts such as osteocyte lacunae, canaliculi and vascular spaces (Haversian systems and primary osteons) may increase regional stress in bone tissue by 300 to 700 % (Currey, 1962, 1984).

[6] GPa is GigaPascals, commonly the unit of measurement for bone stiffness as a reflection of its modulus of elasticity, E. Expressed in Pascals (Newtons per square metre), the stiffness of various types of bone material varies from 4-32 x 10^9Pa; alternatively, from 4-32 GPa (Currey, 1984a, b).

trabecular bone (exponent = 3.0, Carter and Hayes, 1977), indicating that the elastic modulus of cortical bone is more severely affected by changes in porosity than that of trabecular bone. As noted by Schaffler and Burr (1988:16), it also suggests that "compact and trabecular bone should be regarded functionally as distinct structural materials", rather than as one material differentiated solely in terms of the amount of porosity present (contra Martin, 1984).

A similar analysis is reported by Currey (1988), who examined the relationship between elastic modulus, true density and volume fraction in cortical bone samples from 18 species of mammals, birds and reptiles. In this series, the elastic modulus (in GPa) varied from 2.23 to 34.06; calcium content (mg/g) from 174.3 to 315.3; and volume fraction from 66.3% to 98.1%. Not unexpectedly, the lowest values were derived from Roe deer antler and the highest values from Fin whale bullae. Currey found over 80 % of the variance in the elastic modulus was explained by variation in volume fraction and calcium content. Most recently, Keller et al. (1990: 602) examined the relationship among the elastic modulus, bending strength and various physical properties in samples of human femur midshaft. They also report that "one of the most important determinants of the mechanical properties of bone is its apparent density or porosity."

As noted earlier, bone volume fraction and apparent density decrease with age as a function of increasing porosity (Burr and Martin, 1983; Laval-Jeantet et al., 1983). A greater proportion of porosity, as well as most of the age-related increase, occurs primarily adjacent to the endosteal surface (Martin and Burr, 1984). The circumferential distribution of porosity is also not random, but occurs in regions which enjoy large contributions to structural strength from cross-sectional geometry (Martin and Burr, 1984; Lazenby, 1986a, b). These aspects of microstructural variation and their role in functional adaptation of skeletal tissue will be considered more fully in section 3.5.

3.4 Mean Bone Age

At present, a quantified view of the past remodelling history of a region of cortical bone useful in comparative analyses can be obtained, without

recourse to tissue time markers such as tetracycline (Frost, 1969), using a method developed by Wu et al. (1970; see also Frost, 1987b). The method, termed 'paleophysiology' by Martin et al. (1985; also Stout, 1986), is based on the histological analysis of cortical bone cross-sections and requires data for a minimum of five different histomorphometric variables in order to achieve a meaningful reflection of bone remodelling dynamics. This dynamic is represented in the form of subsequently derived variables such as 'annual osteon creations' and 'Haversian bone formation rate'. At present, paleophysiology is applicable only to the middle-series ribs (i.e., ribs 5 to 7) for which good normative data are available. It also does not provide the investigator with a view of the most recent remodelling history, since the variables named above are averaged over the effective age of adult compacta. In the human rib, effective age is considered equal to chronological age minus 12.5 years (Wu et al., 1970). The method is further hindered by the fact that the derived variable 'total osteon creations', which is used in determining more meaningful variables indicative of remodelling dynamics, reaches an asymptotic value in older adults. This is because in heavily remodelled bone cortex, newly formed secondary osteons obliterate all evidence of one or more previously existing structures.

A more advantageous estimate of remodelling dynamics is found in the concept of mean bone age. Mean bone age consists of a single value, obtained directly from the frequency and quantity of bone turnover events. The concept can also be applied to any region of bone tissue, cortical or trabecular, and at all ages. Finally, the resultant can be more meaningfully interpreted vis-à-vis the bone's biomechanical behaviour and structural strength. The following discussion describes the concept of mean bone age, and the derivation of an operational model for its determination.

The addition of new bone, removal of older bone or replacement of existing bone within a region of tissue necessarily alters the age of that tissue. In the absence of modelling or remodelling, the age of any region in the skeleton would approximate the chronological age of the individual, a condition which exists only at birth (Frost, 1987a). A number of factors, not the least of which is mechanical history, create skeletal regions with varying modelling and remodelling rates. The skeleton as a whole will thus possess a

range of MBAs, all of which will be less than the individual's chronological age. Since it is unlikely that any natal bone remains in an adult skeleton, the youngest region of bone will be that with the highest remodelling rate. The concept of mean bone age thus originates in the notion that any given region of bone tissue is continually rejuvenated through the combined processes of modelling (resorption or deposition) and remodelling (sequentially coupled resorption and deposition).

3.4.1 Theoretical Models

Several formal models for mean bone age have been proposed. An early model by Hattner and Frost (1963) rested upon the effects of linear versus probabilistic remodelling distributions. In linear remodelling, sites of bone turnover are evenly spaced and newer areas avoided; thus, older bone is preferentially removed. Under a probabilistic distribution, considered most common by Hattner and Frost, "newer bone is as likely to be remodelled as its proportional amount is to the whole amount of bone present" (p. 203). Given this condition, the mean age of probabilistically-remodelled bone (Tm) is found as [their equation (16)]:

$$Tm = [(\frac{V_0}{V})\ t] + [(\frac{V_n}{V})\ Tm_n]$$

where V_0 = volume of original bone; V_n = volume of new bone; V = volume of the whole region; t = time (in years); and Tm_n = mean age of newly formed bone. Verbally, mean bone age is equal to the volume fraction of original bone times its residence period (≈ ontogenic age), plus the volume fraction of newly formed bone times its residence period (= time between formation and observation). This model assumes that the total amount of bone, V, and the bone formation rate over the period of observation remain constant.

Hattner and Frost (1963) formulated their model in order to study skeletal tracer physiology, and viewed mean bone age as a determining factor for the uptake or removal of 'bone seeking tracers' (e.g., Ca^{45}). They reasoned that because the final ca. 30 per cent of mineralization occurs in

the weeks or months following initial deposition, new bone is always less dense than older, more fully mineralized bone. Since the transfer of a tracer from blood to bone is an inverse function of mineral content, the age of bone tissue will affect the rate of tracer uptake, and the mode of remodelling will determine its period of residence in the skeleton.

More recently, Polig and Jee (1987) provided a more formal treatment of bone age as a function of remodelling. Mean bone age was determined as the probability distribution of lifetimes for individual bone elements (not to be confused with a bone structural unit or BSU, such as a secondary osteon). In turn, this probability was determined by a 'stochastic law of remodelling', such that [their equations (1) and (13)]:

$$p(t, t + \delta t) = g(t)\delta t \quad [\text{nb. } g(t) \geq 0]$$

and

$$g(t) = \lambda t^{\beta}$$

where t specifies the resident age of each individual element; λ is the period of quiescence between remodelling events and β represents "the degree of age-dependence of remodelling. For $\beta = 0$, there is no age dependence, and random remodelling occurs. For $\beta \rightarrow \infty$, the limit of "deterministic" remodelling, i.e., the case where all bone elements remodel after a fixed time interval" (Polig and Jee, 1987: 132-3) is approached. The above cases of 'random' and 'deterministic' remodelling correspond to Hattner and Frost's (1963) 'probabalistic' and 'linear' modes of remodelling distribution, respectively.

Polig and Jee (1987) specify four postulates (assumptions or simplifications) for the development of their model: (1) a bone consists of a collection of single elements which are sufficiently small as to be entirely remodelled during a single event; (2) a skeleton can be regionally sub-divided with respect to a common remodelling rate; (3) these regions are composed of elements constituting a statistical population whose lifetime is regulated by a stochastic remodelling process; and (4) skeletal maturity is characterized by a bone turnover rate which varies insignificantly (i.e., less than 10 per cent) between remodelling events.

Frost (1987a) has outlined a model for the mean tissue age (MTA) of bone, differentiated into two fractions: basal mean tissue age (the age of previously existing cortex exclusive of secondary osteons, i.e., primary bone), and global mean tissue age (the age of all compact bone). Frost's paper deals primarily with the former, and focusses upon the effects of modelling 'drifts' during growth, which move the bone through 'tissue space' in order to maintain its functional relationships vis-à-vis muscles and articulations. Determining the mean tissue age (MTA) for an area of bone comprised of numerous tissue domains formed independently during various drift events requires that the investigator find "both the MTA and cross section area of each domain, weight each domain's MTA by its area as a fraction of the total area of all the domains being averaged, and sum them to find the overall MTA" (Frost, 1987a: 229). Thus [his equation (7)]:

$$MTA = \frac{a_1b_1 + a_2b_2 + \ldots a_mb_m}{\sum b_m}$$

where a = the age of a given domain and b = the cross-sectional area of that domain. While Frost's equation was derived specifically for determining the basal mean tissue age of bone, Frost (1987a: 330) observes that it could be adapted to the find the global MTA provided that osteon area "be subtracted from the area of the whole section to find the area of the remaining original circumferential and endosteal lamellae and/or natal bone".

While the above models are useful for identifying general factors and/or assumptions involved in attempting to derive mean bone age, they do not provide a method for its actual estimation, required in order to derive inferences regarding recent remodelling history and, by implication, past biomechanical history (as will be detailed in section 3.5). While single (Polig and Jee, 1987) and/or double (Frost, 1987a) labelling with in vivo tissue markers, such as tetracycline (Frost, 1969), will identify those surfaces actively forming at a given point in time, they will not discriminate among the various ages of tissue domains which are relatively new (i.e., not yet fully mineralized) but are no longer actively 'forming'. Furthermore, such

approaches are restricted to samples obtained from individuals who have been administered one or more labels, and thus cannot be applied to nonlabelled materials (e.g., most archaeological or cadaveral samples). The following section describes an operational model for determining a relative MBA, which is applicable to all remodelled bone samples, based on the variable mineral content seen, for example, in microradiographs.

3.4.2 An Operational MBA

In the following analysis, the assumption is made that all elemental volume fractions of bone which constitute the units of remodelling are equal, making it possible to treat collections of such units of similar age in terms of frequencies, rather than volumes. As noted by Frost (1987a), conversion of these frequencies to volume fractions entails correction by the ratio of their unit volume to the volume of the region (or whole bone) under consideration. An example of how this is accomplished is given at the end of this section.

A region of bone tissue is composed of discrete elements of various ages. All newly deposited elements, whether or not preceded by a resorption event, can be assigned an age of t_1. For the present, it is assumed that there is an equivalent interval, ∂, between each differently aged element. Previously synthesized elements thus can be assigned an age based upon their order of appearance, e.g., ∂t_1, ∂t_2, ∂t_3 etc., where 3 is older than 2, 3 and 2 are older than 1, and all subscripted ∂t's are older than t_1. The aggregate bone age (BA_a) of a given tissue volume therefore is equal to the sum of the ages of each individual element of newly synthesized bone, plus the sum of the various elements of previously synthesized bone:

$$BA_a = \sum t_1 + \sum \partial t \qquad (1)$$

By treating bone elements of equal ages as frequencies rather than volumes, the mean bone age, MBA is found as:

$$\text{'MBA'} = \frac{(n_0 t_1 + n_1\ \partial t_1 + n_2\ \partial t_2 \ \ldots + n_m\ \partial t_m)}{(n_0 + n_1 + n_2 \ \ldots\ n_m)} \qquad (2)$$

where n through m = the number of elements occurring for each ∂t. To simplify the argument still further, assume that all ∂t's appear with a constant frequency; thus $n_0, n_1, n_2 \ldots n_m$ will equal n, and equation (2) becomes:

$$\text{'MBA'} = n\left(t + \sum_{j=1}^{m} t_j\right) + \sum_{j=1}^{m} n_j \qquad (3)$$

This equation further assumes that the oldest matrix is preferentially removed at each remodelling event, which has the effect of keeping 'n' constant for all values of ∂t. This scenario corresponds to the linear and deterministic remodelling distributions proposed by Hattner and Frost (1963) and Polig and Jee (1987), respectively. Under a probabilistic or random remodelling distribution, 'n' will vary among the existing ∂t moities. As noted by Polig and Jee (1987), however, 'linear' and 'probabilistic' remodelling should be viewed not so much as separate entities, but as points along a continuum defined in terms of either mineral content (Hattner and Frost, 1963) or age-dependence (Polig and Jee, 1987),[7] where the latter refers to the period of residence of individual bone elements prior to their being remodelled. At one extreme, the oldest matrix is preferentially removed, while at the other, the youngest matrix is the focus of new remodelling activity. This latter scenario is considered pathological by both Hattner and Frost (1963: 214) and Polig and Jee (1987: 132).

An additional factor affecting the MBA among a group of tissue regions will be the relative rates at which bone is removed and/or added (i.e., the frequency of appearance and disappearance). Equation (3) can be visualized by considering two equal 'volumes' of bone, comprised of 20 distinct elements (Figure 3.1). If volume 'A' is assigned a remodelling rate twice that of volume 'B', then twice as many elements will be turned over

---

[7] In fact, the two are related, since the degree of mineralization of remodelled bone is in part a function of its residence time in the bone.

Volume 'A'				
0	4	3	2	1
0	4	3	2	1
0	4	3	2	1
0	4	3	2	1

Volume 'B'				
0	9	8	7	6
0	9	8	7	6
5	4	3	2	1
5	4	3	2	1

Figure 3.1. Two equal volumes of bone, A and B, undergo remodelling at rates of 2r and r, respectively. There will thus be twice as many resorption spaces present in A than in B. Resorption spaces are marked '0', since as voids they do not contribute to the 'MBA' of the sample. As a result of the slower rate of turnover, B contains a greater diversity of element ages as well as elements of a much older age than any found in A. In all cases of linear remodelling distribution, the ratio of 'MBA' for two equal volumes of bone will equal the inverse of the ratio of their respective remodelling rates; in the above example, 'MBA'$_{A/B}$ = 2.5/5 = 2; r/2r = 1/2.

---

per unit time. As per equation (3),

$$\text{'MBA'}_A = \frac{4\ (1\ +\ 2\ +\ 3\ +\ 4)}{(4\ +\ 4\ +\ 4\ +\ 4)} = \frac{40}{16} = 2.5\ \text{'age units'}$$

and

$$\text{'MBA'}_B = \frac{2\ (1\ +\ 2\ +\ 3...\ +\ 9)}{(2\ +\ 2\ +\ 2...\ +\ 2)} = \frac{90}{18} = 5.0\ \text{'age units'}$$

Marotti (1976) has published formation rates for various bones in the dog skeleton, which can be used to further illustrate the model. Relative to the tibia, assigned a rate (r) of 1.0, the femur turns over at 0.8r, the left seventh rib at 1.4r and the seventh thoracic vertebra at 2.4r. Given the above hypothetical region of bone consisting of 20 elements of equal volume which are initially of uniform age (e.g., t_1, indicating all new bone); and given four turnover events occurring per unit remodelling time, r, then at any given moment there will be four resorption cavities, four units equal to t_1, and four units for each ∂t value.

After four remodelling cycles, when r = 1.0, 'MBA' will equal 2.5 (i.e., the situation as depicted in Figure 3.1, for volume 'A'). When the remodelling rate equals 0.8, as in Marotti's dog femora, the initiation of four remodelling events requires a length of time 1.25 that required for the tibia, i.e., 1.0 ÷ 0.8 = 1.25. This simply reflects the fact that, at a slower turnover rate, there is a longer residence time for a given element of bone tissue. Under the assumption of equal volume per element turned over, one can calculate corresponding ∂t values for the femur as

$$\partial t_{femur} = \frac{\partial t_{tibia}}{0.8}$$

which gives

$$\text{'MBA'}_{femur} = \frac{\text{'MBA'}_{tibia}}{0.8} = 3.13 \text{ 'age units'}$$

Using the same general relationship, MBA for the seventh thoracic vertebra will be 1.04 'age units', and for the left seventh rib, 1.79 units. For the conditions specified in this example, and following a linear remodelling distribution, bone sampled from the femoral diaphysis will be three times as old as that from the seventh thoracic vertebra.

The result of bone remodelling is the removal of existing bone with replacement by new bone. Remodelling has the effect of making a given region of bone younger, and the greater the number of simultaneous remodelling events, the greater the reduction in MBA. On the other hand, MBA at any point in the bone cortex can increase only in the absence of bone remodelling, i.e., between successive turnover events at that point. The rate at which a regional MBA increases will be a function of (1) the number of simultaneous remodelling events initiated; (2) the interval between successive events at any point in the region; and (3) the MBA of the tissue which is removed. In the above examples, it has been assumed that the volume of bone resorbed was of a uniform age, each event thereby reducing MBA by an equal amount. Under a probabilistic distribution, it is more likely that the tissue removed will be comprised of elements of varying MBAs, which may or may not approximate MBA for the region as a whole. It

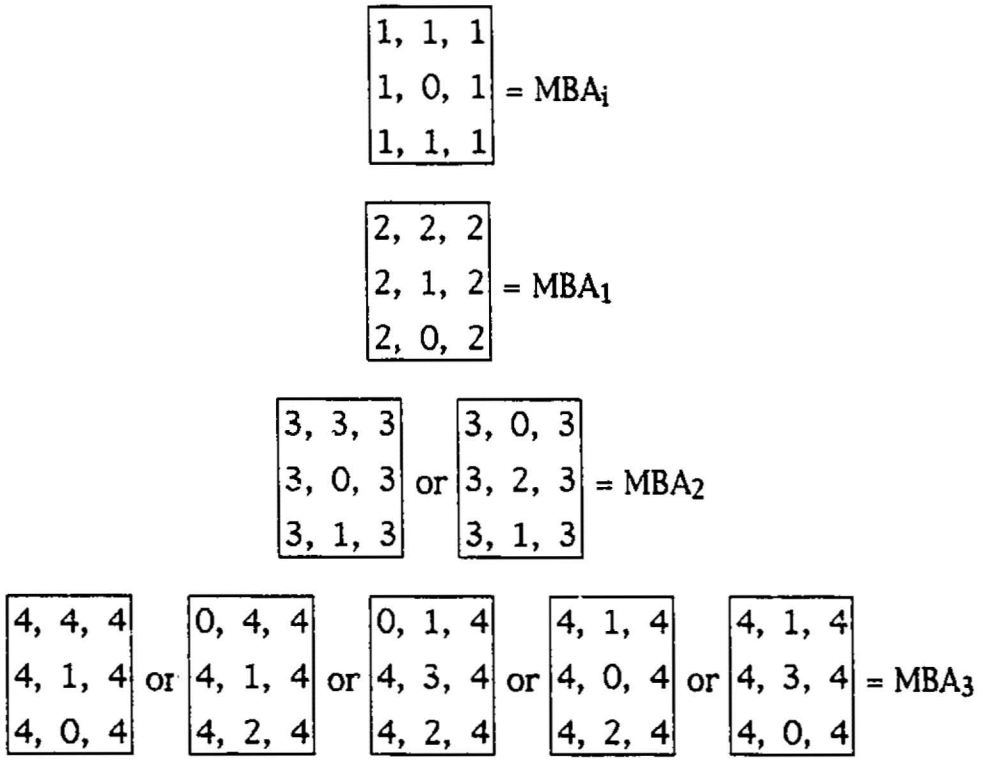

Figure 3.2. A region of bone having 8 discrete remodelling elements, initially of uniform age, t_1, giving and MBA_i of 1.0. One remodelling cycle produces a unique solution, MBA_1 = 1.88. The next remodelling cycle produces two possible solutions, and after this, five possible solutions. Note that, for MBA_3, solutions 2 and 4 are identical with respect to MBA. Again, a '0' indicates a resorption space, i.e., an element which has been most recently resorbed and which will appear in the following series as new bone with an age equal to t_1.

---

follows that for any given interval between remodelling events, mean bone age over a large tissue area will increase at a rate which depends upon whether the bone subsequently resorbed is relatively younger or older than the regional MBA. If there is no preference for the age of existing bone to be turned over; that is, if probabilistic remodelling holds, the theoretical probability that the age of the bone removed is less than the regional MBA

will equal the probability that it is older than the regional MBA. In fact, this theoretical probability will equal 0.5. The actual probability will be a function of the relative volume fractions of bone elements having ∂t values greater or less than the MBA for the region. Over time, if no preference exists for the age of bone being removed,[8] the actual probability should approximate the theoretical probability of 0.5, and the ∂t values for the elements in the region will be normally distributed.

Under a probabilistic remodelling distribution, the increase in MBA can be modeled as a function of the number of remodelling cycles. Given a volume of newly formed bone in which all the elements are of equal age, t_1, after one remodelling cycle, MBA will be 1.88 (Figure 3.2) This represents the only solution. After the second remodelling cycle, there will be two solutions, since there were elements of two different ages available for removal, even though of unequal probability given their vastly different volume fractions. These two solutions give MBA values of 2.63 and 2.75, depending upon whether the oldest or youngest tissue was resorbed, respectively. Following the third remodelling cycle, five possible solutions exist, but only four possible MBA values, since two solutions are for all intents identical. MBA varies from 3.25 to 3.63. The next remodelling cycle would provide a total of 15 solutions and a range of seven possible MBA values, from 3.75 to 4.5. The most frequent solution gives a MBA of 4.13.

It becomes evident that the rate at which MBA increases will have a range of values bounded by an upper and lower limit:

Lower MBA_m =

$$(m+1)\,MBA_i - MBA_i\,[\{m\,(V_{r_m}) + (m-1)(V_{r_{m-1}}) + (m-n)(V_{r_{m-n}})\}\,V_t^{-1}] \qquad (4)$$

---

[8] This presumes that there is no causal relationship between the MBA of an element of bone and the probability of microcrack formation. This may not be true, given the relationship between mineral density and the element's stiffness or toughness, as discussed in section 3.5.1.

Upper MBA_m =

$$(m+1)\ MBA_i - (m\ V_{r_m} V_t^{-1}) \qquad (5)$$

where MBA_m is the mean bone age after 'm' remodelling cycles; MBA_i is the initial age of the whole region, V_t; and V_r is the volume of bone remodelled during the specified cycle, m through m-n (with n = m-1). The value in square brackets will always be negative, since bone turnover reduces MBA at the site of remodelling.

These limits represent the linear remodelling distribution on the one hand [eq. (4)], in which the oldest bone is removed with each new cycle, and the pathological or redundant remodelling distribution on the other [eq. (5)], in which the newest bone is preferentially removed. These limits will bracket MBA resulting from a probabilistic remodelling distribution, as noted by Polig and Jee (1987). If no remodelling occurs, $V_r = 0$, and MBA will increase as a linear function of the number of remodelling cycles, m. Relative mean bone age (hereafter, MBA) can then be calculated as the average of these upper and lower limits.

Obtaining the upper and lower bounds for MBA of any given region of bone tissue requires that one know, or is able to assign, values for MBA_i, m, V_t and V_r. While it is not possible to determine these values absolutely, it is possible to derive a relative MBA for any given bone region through the discrimination of remodelling elements sharing common ∂t values from among a population of such elements. This possibility can be realized by quantifying regional variation in mineral density resulting from the fact that full mineralization of newly deposited bone is achieved over a period of several months (Hattner and Frost, 1963; Martin and Burr, 1989). This variation in the degree of mineralization can be visualized and subsequently quantified in microradiographs of bone sections (Boiven and Baud, 1984; Lloyd and Hodges, 1971; Phillips et al., 1978; Pugliese and Anderson, 1986). Pugliese and Anderson (1986), for example, assessed mineral variation in an iliac crest biopsy using a semiautomated video digitizing system (Leitz 'Bioquant II'). Grey levels from one to 255, calibrated against an aluminum

foil step wedge, were subdivided into five 50-level categories and one 5-level category (e.g., 1-50 as the least dense, to 251-255 as the most dense). Using the video image of the microradiograph, the per cent 'area' of pixels[9] falling into each mineral content category was determined, relative to the total number (40832) of pixels. Pugliese and Anderson (1986: 93) report a reproducibility of ≈ 1.5 %.

This approach would lend itself favorably toward the determination of MBA: for a video screen filled with an image of bone material, V_t would equal the total number of pixels corresponding to mineralized bone tissue. Thus, one would subtract from the total number of pixels those which correspond to regions of 'nonbone', i.e., intracortical porosity, medullary cavity and so on. V_r would equal the number of pixels falling into each category, and 'm' would equal the number of categories, which can be user-defined. Each category of mineral content would correspond to a previous remodelling cycle. Finally, for the purposes of determining relative MBA, MBA_i in eqs. (4) and (5) can be assigned a value of 1.0. Thus, regions of bone having high rates of bone turnover or new bone formation would have a greater proportion of pixels falling into the lower content categories, and would therefore have a younger MBA than regions with lower rates of turnover. An assumption of this approach is that individuals being compared in an analysis of bone remodelling do not differ with regard to the pattern of mineralization of newly formed bone. That is, all newly formed bone should progress through a similar sequence of rapid initial mineralization followed by a much longer period (several months) of protracted mineralization. A limitation of this approach lies in the number of user-defined categories, m, since the MBA will always be less than or equal to m+1.

Densitometric data from Pugliese and Anderson (1986) can be used to exemplify the method (Table 3.2). These data were obtained from microradiographs of trans-iliac crest biopsies taken two years apart from a woman with postmenopausal osteoporosis who had been treated through

---

9 Pixels are the picture-points on the video display screen. Per cent area = (# pixels at level n ÷ total # of pixels) x 100.

Table 3.2. An Example of the Microradiographic Determination of MBA (Data from Pugliese and Anderson,1986, Table 1).

No. of Cycles	Mineral Level	Pre-Treatment[1]	Post-Treatment[1]
m	6	14.8	8.3
m-1	5	21.4	16.1
m-2	4	22.7	15.1
m-3	3	22.7	23.7
m-4	2	14.7	24.7
m-5	1	3.2	11.9
	Σ	100	100
Lower	MBA	3.1*	3.8
Upper	MBA	6.1**	6.5
	MBA	4.6	5.2

1. Expressed as % total bone present.

* 3.127 = 7-[{6(14.8) + 5(21.4) + 4(22.7) + 3(22.7) + 2(14.7) + (3.2)} 0.01]

** 6.112 = 7-[6(14.8) 0.01]

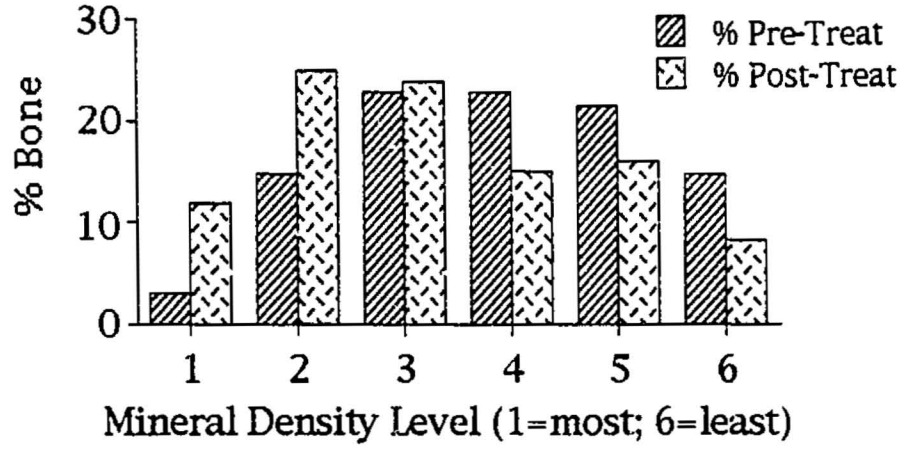

Figure 3.3. Histogram constructed from data in Table 3.2.

Coherence Therapy (Frost, 1981). The post-treatment data indicate an increase in the amount of bone tissue imaged (17.6 % versus 6.87 %); however, mean bone age has increased over the two year span, from 4.6 to 5.2 'age units'. Interestingly, Pugliese and Anderson (1986: 93) remark that

the post-treatment image (their Figure 3) shows a "thicker but less dense" trabecula. This conclusion is not borne out by their tabulated data (Figure 3.3), which indicates a greater percentage of pre-treatment bone falling into the lower content categories. The aim of coherence therapy is to stimulate bone resorption and then to suppress it; but the initial stimulation causes the A-R-F sequence to proceed. The effect is to minimize resorption and still end up with the normal amount of formation: hence a positive bone balance is achieved and an increase in bone mass results. It would seem that what Pugliese and Anderson have wrought in the administration of coherence therapy is to impose a 'pathological' linear remodelling distribution. Resorption of the newest tissue was instigated, then stopped, and redeposition of new tissue proceeded. The existing unremodelled tissue ages, while the newest tissue is continually turned over, with more added at each coherence treatment than is removed. This alone explains the appearance of low density and high MBA; note that in the histogram of Figure 3.3, the pre-treatment distribution is approximately normal (as expected), the post-treatment values approximate a bimodal distribution, with 1-3 (ca. 55 % of bone volume = most dense), and 4-6 (ca. 45 % of bone volume = least dense) forming somewhat distinct distributions.

It would also be possible to visually assign values to the variables m, V_r and V_t using more traditional approaches, such as histomorphometric stereology (Recker, 1983). Such approaches would be considerably more time-consuming and are known to suffer significant inter-observer error in spite of standardizing analytic methods such as section preparation and microscopy (Compston et al., 1986). Section 4.5.2, along with Appendix 5, provide additional details concerning the microradiographic determination of MBA undertaken in the present study.

3.5 Strain Equilibrium and Cortical Bone Modelling and Remodelling

Biomechanical models which attempt to describe the integrated functional adaptation of whole skeletons, skeletal elements and skeletal tissue invoke the application of engineering methods and theory. It becomes necessary to conjoin processes of bone modelling and remodelling, which alter a bone's external and internal architecture, with those

mechanical stimuli which initiate and/or terminate these activities. Hart and Davy (1989) have recently reviewed a variety of engineering-oriented models for mechanical strain-induced remodelling. They note that the interpretation of functional adaptation in skeletal tissue must reference the concept of an equilibrium strain state, defined by Hart and Davy (1989: 255) as "the normal loading situation where...there is no net change in the macroscopic bone properties or geometry". This concept is central to constructing a model of CPA as mechanical compensation in light of the bone loss and modified physical activity which accompany human aging, the latter impinging on various aspects of the skeletal strain environment, including peak strain magnitude, distribution, rate, etc. Two existing theoretical frameworks, among others, offer useful insights for such model-building. These are Frost's 'Mechanostat' (Burr and Martin, 1989; Frost, 1983, 1987c, 1988a-c; Martin and Burr, 1989) and Cowin's 'Adaptive Elasticity' (Cowin, 1987; Hart et al., 1984; Hart and Davy, 1989).

Frost's Mechanostat originates in the observation that from birth to maturity, normal mechanical usage (MU) generates typical peak strains ca. 1,500 (tension) and ca. 3,000 (compression) microstrain[10] (μE), in spite of the fact that peak loads increase 20 to 25+ times over this period (Frost, 1988a, b).[11] Frost (1988a: 146) suggests that the constancy of these peak strains "mean that mechanically controlled architectural adaptations probably fit the needs of the largest daily repeated dynamic loads and

---

[10] A microstrain is defined as a millionth of a unit strain. For example, a compressive strain of 2000 μE shortens a structure 0.02 %, or from 100 % to 99.98 % of its length.

[11] Most work on the determination of in vivo strain magnitude etc. has been carried out on long tubular bones, many of which are subject to eccentric loading which generates a combination of axial (compressive) and bending (tensile and compressive) strains. The larger peak compressive strains reflects the superimposition of the axial and bending strains. As there are no axial tensile strains which might be summed to the bending tensile strains, peak tensile strains will always be the lesser of the two (Martin and Burr, 1989). The tensile-compressive strain differential also reflects the shift in the neutral axis of bending towards the tensile surface which occurs under eccentric loading.

strains, rather than the needs of frequent and small, or single or rare large ones." Thus, the long bones of dedicated weight lifters will be more massive than those of marathon runners (Frost, 1988c), since the former alone will tend to generate atypical peak strains, evoking architectural adaptation aimed at reducing these strains to more typical levels. This conclusion is supported by experimental work illustrating the greater osteogenic potential of high strain rate (cf. impact) loading compared to more moderate dynamic loading (see Martin and Burr, 1989: 160 for discussion). At the upper limit of the typical peak strain range lies the Minimum Effective Strain or MES.[12] Strains in excess of the MES turn on physiologic modelling, leading to net bone gain or loss in the course of 'architecturally adapting' skeletal structure. At some point beyond the MES, a level of strain termed E_{sat} (Frost, 1988b) is reached at which the modelling response switches from a physiologic to a pathologic state, with consequent woven bone formation or 'anarchic bone resorption'. The lower limit of the typical peak strain range is suggested to be in the range of 100-300 μE, below which remodelling BMUs are activated. In this range, a negative imbalance is promoted, leading to a net bone loss and a downward adjustment of bone mass. The limits, or setpoints, of the 'typical peak strain range' and E_{sat} are

---

[12] It is not clear how proximate the typical peak strains are to either tensile MES or compressive MES. Martin and Burr (1989) suggest that the peak compressive strain may lie closer to its MES than does the peak tensile strain, since experimental data indicate that smaller increments in compressive strain elicit a modelling response, while large increments in tensile strain do not. Lanyon (1987:1087-88) has criticized Frost's restriction of the MES to the peak strain range, noting that sufficient experimental data exists pointing to other factors such as strain distribution and strain rate as significant contributors to the modelling and remodelling response. He suggests modifying MES to MESS, the Minimum Effective Strain-related Stimulus. Frost (1988a: 145), however, recognizes though chooses to ignore these other factors for the time being, explicitly those related to the viscoelastic nature of skeletal tissue, noting that "they have minimal bearing on the major thrust of the proposed concepts of how biology fits architecture to mechanical demands". Frost acknowledges that if the MES concept proves correct, these others factors can then be accommodated within a more precise formulation of the model.

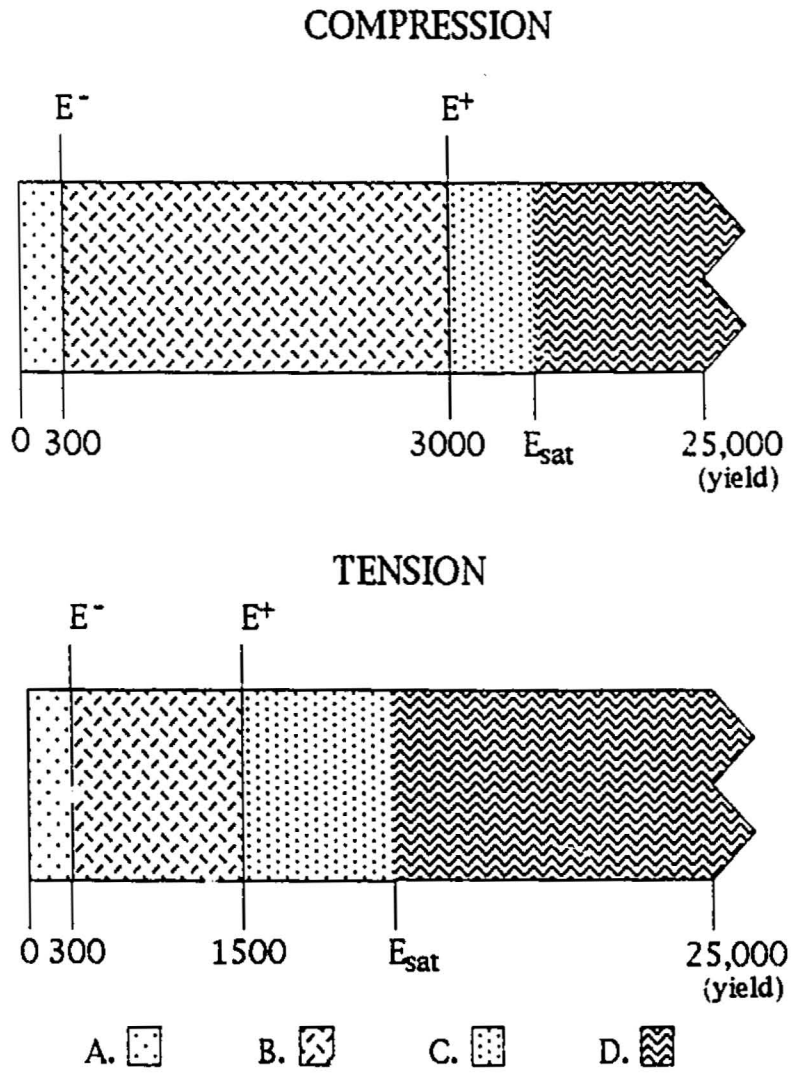

Figure 3.4. Four genetic setpoints 'determine' bone size, shape and structural integrity through the promotion or suppression of (re)modelling activity on the one hand, and failure of the element under dynamic loading on the other. A = increased remodelling activity; B = (re)modelling equilibrium; C = lamellar bone modelling promoted; D = physiologic lamellar bone deposition replaced by pathologic woven bone. At ca. 25,000 με, fracture results. E^- and E^+ refer to parameters of Cowin's Adaptive Elasticity model (see text for discussion).

presumably established genetically, and as noted above differ with regard to strain polarity (tension versus compression). To further complicate matters, recognition of these setpoints by the bone cell systems responsible for architectural adjustment (osteoclasts and osteoblasts) may depend upon prevailing nonskeletal (e.g., hormonal, metabolic) conditions (Burr and Martin, 1989). The process of functional adaptation in bone tissue thus occurs when peak strains above the MES are actually experienced, or when such a change is perceived by the bone cells following a metabolically-mediated 'reduction' of the MES setpoint; while a state of functional adaptation exists when peak strain falls below the MES.

A fundamental tenet of Frost's Mechanostat theory states that the processes of modelling and remodelling have independent setpoints, and are in fact antagonistic responses to altered mechanical loading (Burr and Martin, 1989). Simply put, modelling and remodelling cannot occur on the same surface at the same time. Martin and Burr (1989: 182) point out that, while the suppression of remodelling by normal peak strains seems at variance with general perceptions (i.e., increased strain promoting remodelling), it makes perfect sense that a process which can only lead to greater porosity, and thus lower bone strength, should be promoted only when the skeleton can afford such a reduction; that is, if and when strains fall to or below a particular non-threatening level.

As indicated above, Frost suggests the MES for modelling should be ca. 1,500 μE (longitudinal tension) and ca. 3,000 μE (compression). Strains lower than these values are not likely to 'turn on' modelling. On the other hand, remodelling tends to be suppressed by strains >100 to 300 μE (Burr and Martin, 1989; Frost, 1988a, b), but is enhanced at strain magnitudes below this narrow range. Thus, a downward adjustment of bone mass will occur at the endocortical surface as a result of a remodelling imbalance; however, above 300 μE, remodelling is inhibited[13] and bone mass is conserved. Functional adaptation towards an equilibrium strain state

---

[13] As noted by Burr and Martin (1989: 191) "the accumulation of microdamage within the tissue may eventually also activate a remodelling response", although remodelling per se is inhibited at high strain ranges. However, if the strain environment within an osteon is altered, due to

follows from the adjustment of skeletal architecture and mass as a result of resorption and formation 'drifts', at higher strains. These processes would have the effect of increasing and decreasing, respectively, the level of strain associated with a given deformation, all else (e.g., stiffness) being equal. It is reasonable to suspect as well that 'zero' strain resulting from complete disuse (e.g., paralysis) would see a progressive loss of bone tissue until a genetic baseline for bone mass is reached (Frost, 1988c; Rubin and Lanyon, 1987). It is thus possible to identify four critical genetically-based strain setpoints (Figure 3.4): remodelling disequilibrium (< 300 μE); (re)modelling equilibrium (300 μE to MES); physiologic modelling disequilibrium (MES to E_{sat}), and pathologic modelling disequilibrium ($> E_{sat}$). Together, these setpoint established processes act to determine and/or adjust bone mass, architecture and, ultimately, its structural integrity.

Frost developed his Mechanostat theory over a long career focussed on the clinical investigation of the (patho)physiology of human skeletal tissue during development, growth and senescence. His work in skeletal biology (and that of others e.g., Garn, Jaworski, Jee, Kimmel, Mazess, Nordin, Parfitt, Riggs; see Frost, 1988b, c; 1989a-d) has been primarily directed towards understanding deviations from a normative state, as seen in metabolic bone diseases such as the osteoporoses, osteopetrosis, osteomalacia, and osteogenesis imperfecta. Awareness of what constitutes functional adaptation in skeletal tissue has developed as well within orthopaedic bioengineering. Significant contributions in this arena have been made by individuals such as Ascenzi, Carter, Cowin, Currey, Evans, Lanyon, Pauwels, Rubin and others (Ascenzi, 1980; Currey, 1984; Cowin, 1989a). A strong emphasis of this group has been the experimental and mathematical modelling of bone as a distinctively configured and self-adjusting material under dynamic loading. Skeletal pathophysiology as such receives relatively little attention. Theoretical developments have progressed in conjunction with much in vivo and in vitro experimental research (e.g., Lanyon, 1987). One of the more significant models of functional adaptation in bone to

---

lamellar debonding, then such remodelling is not inconsistent with Mechanostat expectations.

come out of this school is that of Adaptive Elasticity proposed by Cowin and his associates. The development of this theory over the last 15 years has been recently recounted (Hart and Davy, 1989; Martin and Burr, 1989). While comparatively little cross-over has occurred between what might be termed the 'clinical' and 'engineering' schools,[14] a number of workers have undertaken research which bridges this gap (e.g., Burr, Martin, Ruff and Schaffler; see Martin and Burr (1989) for a recent synthesis).

Adaptive Elasticity is also a theory of surface remodelling[15] as a function of strain history (Cowin, 1987; Hart and Davy, 1989; Hart, 1990). In agreement with Frost, Cowin proposes that cellular activity in bone depends upon the current strain state relative to a range of normal, equilibrium strain. The version of Adaptive Elasticity followed here does not define the upper and lower bounds of this equilibrium range in terms of microstrain, but simply denotes them as E^+ and E^- (Cowin, 1987). Strain which exceeds E^+ prompts a net deposition of bone tissue, while that which falls below E^- results in net resorption. This nonspecificity reflects Cowin's decision to model these over- or under- non-equilibrium strains as "the time averaged values [of strain]...over a period of a day or longer" (Cowin, 1987:1112). Although other alternatives, e.g., peak strains, strain amplitude or strain rate may be equally valid stimuli, they are considered more complex entities from a mathematical modelling perspective. An important outcome of dealing with time-averaged strains is the posited existence of a

---

[14] Frost (1988c) provides an interesting commentary on the failure of these two groups to effectively communicate, to the detriment of both.

[15] Cowin and associates use of the term 'adaptive remodelling' parallels that of others engineering-oriented researchers (e.g., Lanyon and Rubin) , and as pointed out by Martin and Burr (1989: 143), should be considered synonymous with 'adaptation' in the sense of something rendered more fit to some use. In vivo experiments recently published by Burr et al. (1989b, c) produced qualitatively comparable results to those reported by the early 1980s work of Lanyon and Rubin; however, Burr et al. make a point of differentiating between A-R-F remodelling and A-F or A-R modelling as cell-based biological phenomena (noting in particular that the tissue reaction observed in their animals (Beagles) was a product of modelling activity, with very little surface remodelling observed).

'fading strain memory' for bone tissue (Hart and Davy, 1989). This would ensure that bone responds to its most recent loading history, while ignoring (i.e., forgetting) those strains which occurred some time ago and which are perhaps no longer relevant vis-à-vis functional adaptation. Lanyon (Lanyon, 1987; Skerry et al., 1988, 1990) has opined that the reorientation of proteoglycan molecules[16] under dynamic loading may, provide such a time-averaged strain memory of ca. 24 hour duration.

Cowin's Adaptive Elasticity differs from Frost's Mechanostat in several important ways. Based on the demonstrated constancy of peak strain magnitude under diverse loading conditions, Frost nominates this parameter as the objective of functionally adaptive modelling or remodelling. His position would argue for a genetic-based communality for the activating signal within all bone tissue, keeping in mind that variation in mechanical properties would see this parameter achievable under a variety of stress states. In other words, depending upon factors such as bone volume fraction, apparent density and stiffness, loads of differing magnitude and stress could exceed the MES (i.e., 1,500 to 3,000 μE). Thus, in some bone tissue a given load would produce an equilibrium strain, while in others the same load could initiate a modelling response. On the other hand, the theory of Adaptive Elasticity accepts the existence of site or bone specific strain equilibrium functions. This accomodation follows from the fact that different bones perform different functions in life (Hart and Davy, 1989), and should not be expected to possess some genetically determined uniform equilibrium strain under all loading scenarios. Thus, the time-

---

[16] Proteoglycans are large, highly charged molecules which are closely associated with bone cells (Lanyon, 1987: 1092). These molecules are reorientated under dynamic loading, possibly through relative movement of bone matrix constituents or from "strain-induced flow of (charged) fluid through the tissue" (Skerry et al., 1988: 549). This reorientation not only provides a memory of the most recent strain history, but because it is subject to continual upgrading through repeated loading, provides a mechanism for time-averaging of strain history and thus of degrading the significance of rare and exceptional over- and under-strains. This reorientation has been observed both in vivo and in vitro, and in rapid response to as few as 50 load reversals (Skerry et al., 1990).

averaged equilibrium strain at one site may be 1,000 μE; at another 3,500 μE and at a third, 700 μE. This accomodation would allow elements which experience comparatively low mechanical loadings, such as the human calvarium, the possibility of strain-related biomechanical adaptation. Frost's Mechanostat is presently unable to deal with such cases and must therefore appeal to certain "baseline properties" (e.g., genetic, metabolic and hormonal potentialities) (Frost, 1988c: 82) . A further important distinction is that, because Adaptive Elasticity uses the term remodelling to encompass all bone cellular activity, it is unable to offer insight into the antagonism which Frost's Mechanostat proposes for modelling processes which alter size and shape and remodelling processes which affect bulk and apparent density.[17]

Adaptive Elasticity is certainly the more phenomenological of the two; for example, Martin and Burr (1989: 177) observe that as presently formulated it "is incapable of describing adaptation to mechanical usage in any sort of generalized way". However, as discussed above, there are constructs within the model which may be usefully incorporated within, or appended to, the Mechanostat. The following sections develop an informal theoretical model for CPA as mechanical compensation which integrates the antagonistic character of the Mechanostat with that aspect of Adaptive Elasticity emphasizing site specific equlibrium strain states as a (re)modelling objective. The model is situated within a context of variation in mechanical loading associated with reduced levels of activity and/or with the loss of precise neurological control over muscular function and coordination (the latter especially a consequence of aging).

---

[17] Although Cowin retains the dichotomy between external (periosteal) and internal (intracortical) changes, the 'Cell Biology-Based' expansion of Adaptive Elasticity offered by Hart and Davy (1989) removes even this distinction, identifying both simply as surface remodelling activities (after Martin, 1972, 1984). Hart and Davy (1989; also Hart et al., 1984) purport to accommodate a greater diversity of strain-related parameters within the Adaptive Elasticity model (cf. Lanyon, 1987), potentially including the effects of nonmechanical mediators on the cellular response to strain, such as cell number, cell recruitment rate, activity level and duration, along with hormonal and metabolic constraints.

3.6 Modelling Mechanical Compensation

The mechanical compensation hypothesis postulates that CPA offsets lower bone strength following from age-related endocortical bone loss. The hypothesis is rooted in engineering beam theory, and its proponents reasonably assume that bones, and in particular long tubular bones, are deformed primarily by bending (Bertram and Biewener, 1988). The effect of such deformation is to place the largest stresses at a point furthest from the transverse neutral axis in the plane of bending (Wainwright et al., 1981). The neutral axis is that axis within a beam at which stress and strain are zero, and represents the point of transition between tensile and compressive deformation.

For any given cross-section, geometric rigidity under bending is quantified as the second moment of area (I), the magnitude of which is determined as product of two quanta relative to a given axis. These are the distance squared of a unit area of bone perpendicular to the axis. These multiples are then summed over the entire cross-sectional area on either side of the axis, with I reported in units to the 4th power (Martin et al., 1980). An important outcome of this area-distance relationship which is fundamental to the mechanical compensation hypothesis is that, for any two equal units of bone tissue, the unit which is situated further from the neutral axis will contribute more to geometric strength than the unit which is closer.

Other ways in which bones (or beams) might be deformed include torsion and axial compression. The geometric resistance to torsion about a longitudinal neutral axis is quantified as the polar moment of area (J); for approximately circular geometries J is equal to the sum of the second moments of area (I) about any two orthogonal axes. The cross-sectional cortical area (CA) of a section is considered proportional to that section's geometric resistance to axially compressive (and tensile) loads (Ruff, 1987b: 10). Bertram and Biewener (1988: 75) have noted that axially compressive loads are seldom found in vivo, as they tend to be transformed into bending moments due to the curvature present in most tubular bones. Similarly, Cowin (1987: 1119) has suggested that significant torsional loads are not

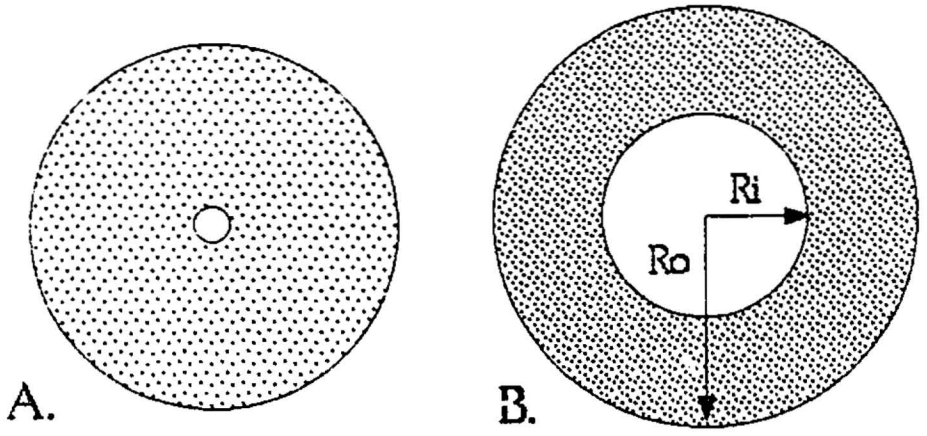

	Section A	Section B	% Difference
R_i ≈	0.491	2.82	474
R_o ≈	4.91	5.64	15
CA ≈	75	75	0
I ≈	457	746	63

Figure 3.5. Schematic depiction to two right circular sections of equal cortical area, showing the relationship between the magnitude of the second moment of area (I) and the two radii, R_i and R_o. In spite of a ca. 475 per cent increase in the endosteal radius, R_i, the figure on the right has a much larger resistance to bending (I = 746.04 units^4 vs. 456.64 units^4) as a result of a more modest ca. 15 per cent increase in the periosteal radius, R_o.

normally experienced by long bone diaphyses, but are borne instead by the epiphyseal regions.

Whatever the force or combination of forces operating, it would serve an animal well if it could resist these forces with a minimum of skeletal material, since both acquiring, distributing and maintaining skeletal mass exerts an energetic and metabolic cost on the animal. This line of argument has led Currey (1984b; Currey and Alexander, 1985), among others, to suggest that the cross-sectional shape of tubular bones reflects the direction

and magnitude of predominant time-averaged bending loads applied to them. A form-function continuum is suggested which sees bones experiencing loads equally in all axes over time being best designed as cylinders; while those which experience loads predominantly in a single preferred axis are optimally designed as I-beams. This logic underlies the use of cross-sectional long bone geometry as a basis for drawing behavioral inferences in both human (Ruff et al., 1984; Bridges, 1989a; see following section) and nonhuman (Schaffler et al., 1985; Burr et al., 1989) primates. Bone tissue can thus be economized by placing it where it will serve the greatest purpose, given a particular loading history. Since the more distant units of bone tissue contribute more to geometric strength, an animal can also economize on the cost of materials by building more hollow bones; i.e., by placing a given allotment of bone further from the axis of bending and leaving empty areas closer to that axis. Were these areas to be filled with bone, their contribution to overall geometric strength would not warrant the additional cost of producing and maintaining the tissue required (Figure 3.5). An important constraint on this option is the propensity for hollow thin-walled cylinders to fail in Euler buckling, when the ratio of wall thickness to cylinder diameter exceeds a critical value (Currey, 1984b).

The relation for stress (σ) in a beam can be expressed as $\sigma = My/I$ (Wainwright et al., 1981: 247), where I is the second moment of area, M is the applied bending moment and y is the distance from the neutral axis of bending at which s is measured. Larger magnitudes of stress (and hence of strain in any given bone tissue) will result from increasing M or decreasing I. When M and I are constant, larger stresses and strains will occur in proportion to the distance from the neutral axis, y.

The reduction in mass which occurs in the bones of aging individuals is well established (eg. Garn, 1970; Mazess, 1982; Kelsey, 1987). In cortical bone this takes place primarily through expansion of the medullary cavity, along with increasing porosity, as a result of a negative endocortical remodelling imbalance. Skeletons also experiences bone growth as a result of continuing periosteal apposition (CPA). Often, both bone gain and loss are observed within the same skeletal element. This juxtaposition has led to a general acceptance of the hypothesis that CPA serves as mechanical

compensation for the reduction in mass resulting from prior endocortical bone loss. In tubular bones, data on CPA generally consists of larger values in older cohorts for midshaft diameters in radiographs of long or short tubular bones (eg., Smith and Walker, 1964; Garn et al., 1972), or for various geometric measures such as cortical areas and moments of area (eg., Martin and Atkinson, 1977; Ruff and Hayes, 1983b). These measures, however, do not in themselves constitute direct evidence for CPA as mechanical compensation. This is because they are nonspecific vis-à-vis the magnitude, location and timing of modelling events at the periosteal surface to (re)modelling events occurring endosteally or intracortically. As well, they often do not consider potential effects of changes in biomechanical environments, such as would occur when individuals become more sedentary with advancing age. All the same, such measures are suggestive of mechanical compensation, and have in fact been often cited as more or less conclusive evidence that such a mechanism exists (Garn et al., 1990).

In accordance with the general tenets of Wolff's Law (Roesler, 1987), the objective of mechanical compensation would be maintenance of the skeleton's structural integrity in a manner consistent with the functional demands placed upon it. At the same time, the metabolic and material cost of that maintenance is expected to be minimized. In spite of such hypothesizing, however, fractures (especially in the elderly) continue to occur at sites having a large proportion of cortical bone, such as the proximal humerus, the distal radius, and the subtrochanteric femur. Such occurrences suggest an apparent contradiction: why do some individuals fail to benefit from the compensation provided by periosteal bone growth in adulthood, if the intent of such compensation is the preservation of bone strength? Are they breaking their bones and in so doing breaking Wolff's Law? This contradiction is made even more apparent by studies (e.g., Martin and Atkinson, 1977; Ruff and Hayes, 1988) which suggest that mechanical compensation occurs preferentially in males, thereby leaving women deprived of its benefits, and thus consequently more susceptible to (age-related) fracture (Kelsey, 1987).

3.6.1 Maintaining Strain Equilibrium by CPA

The basic theoretical relationship of periosteal compensation for endosteal bone loss can be explored using a series of circular geometric models (sensu Cowin, 1984) as analogues for tubular bone diaphyses.[18] The objective of each solution is the maintenance of the second moment of area, and reasonably assumes that the diaphyses of tubular bones can be modeled as beams (Ruff, 1987b, 1989). The intent of the following analysis is to show how the apparent contradiction noted above, and hence the mechanical compensation hypothesis, is in fact consistent with factors now recognized to be of importance in preventing fractures symptomatic of osteoporosis. These factors include (1) the magnitude of peak bone mass (Garn, 1975; Lindsay, 1987);[19] and (2) the relationship of physical activity to bone mineral status (Meade, 1989; Smith and Raab, 1986; Smith and Gilligan, 1989).

Minimum mass analysis approaches a design problem from the perspective of minimizing the materials required to perform some function (Currey, 1984b). A logical extension of this approach applied to the problem of bone loss and gain would consider what parameter(s) would minimize the cost of maintaining bone strength via CPA in the face of endocortical bone loss. Two questions become evident: (1) what factors determine how much compensation is necessary; and (2) what factors determine how much CPA is possible? When 'possible' is less than 'necessary', broken bones are likely to result.

---

[18] For simplification, the following discussion considers bone loss in terms of medullary expansion alone, in spite of the fact that intracortical porosity may be one of the more significant factors underlying reductions in the mechanical properties of bone (Schaffler and Burr, 1988).

[19] The environmental (i.e., lifestyle) factors underlying the magnitude of peak bone mass achieved during growth are both many and varied. In a sample of 101 healthy women, aged 20 to 35 years, a recent retrospective study (McCulloch et al., 1990) examined correlations between calcaneal bone density and current versus recalled levels of childhood activity and calcium intake, along with current lifestyle variables (cigarette smoking, caffeine consumption). In their study, only childhood activity level showed a strong positive correlation with current bone density.

Modelling the relative magnitude of periosteal apposition required to maintain I in response to a specified relative magnitude of endocortical bone loss can provide an initial response to the first question. To this end, hollow circular sections can be considered analogous to transverse sections of tubular bone diaphyses (Cowin, 1984). For such sections, the magnitude of I relative to a bisecting neutral axis is determined by the formula:

$$I = \frac{\pi}{4}(R_o^4 - R_i^4) \qquad (6)$$

where R_o denotes the radius to the periosteal surface, and R_i the radius to the endosteal surface. As endosteal resorption proceeds, R_i increases by an amount, ∂R_i. Maintaining a given value of I requires that R_o also increase, by ∂R_o, which satisfies the equation

$$\partial R_o = \sqrt[4]{\frac{I + \frac{\pi}{4}(R_i^4 + \partial R_i^4)}{\frac{\pi}{4}}} - R_o \qquad (7)$$

The initial radii (R_i and R_o) represent the situation which exists prior to the onset of progressive endosteal bone loss, that is, when the element at the level of the section is at its peak bone mass, CT_0. At any given moment, the ratio R_i/R_o is a relative measure of cortical thickness.

Three series of circular models, each with three variants, are developed in order to identify the factor(s) relevant to maintaining the geometric bending strength of tubular bones (Table 3.3; Figure 3.6). Series 'A' specifies that prior to the onset of endosteal bone loss, R_o is equal, making total area (TA) equal for all sections. However, R_i is allowed to vary, the consequence of which is that cortical area (CA) differs for each section. Series 'B' permits both radii to vary, such that both TA and CA differ among the sections. Series 'C' allows TA to vary, while CA is held constant. For comparative purposes, the values of R_i and R_o are set arbitrarily in order to keep R_i/R_o ratios constant among the three series of models, at 0.1, 0.25 and 0.5. Using

Table 3.3. Values assigned to the three series of models, A to C, for the periosteal radius (R_o) and the endosteal radius (R_i) such that the R_i/R_o ratios are: 0.1, 0.25 and 0.5. R_i and R_o are used to calculate the magnitude of the second moment of area (I).[1]

Series: (R_i/R_o)	R_o	R_i	I	TA	CA
A: (0.10)	3.9894	0.3989	198.9238	50.0	49.5
A: (0.25)	3.9894	0.9974	198.1676	50.0	46.875
A: (0.50)	3.9894	1.9947	186.5097	50.0	37.5
B: (0.10)	4.9106	0.4911	456.6662	75.7576	75.0
B: (0.25)	5.0463	1.2616	507.3064	79.9999	75.0
B: (0.50)	5.6419	2.8209	746.0388	99.9999	75.0
C: (0.10)	10.0	1.0	7853.1962	314.1593	311.018
C: (0.25)	5.6	1.4	69.3823	98.5203	92.3628
C: (0.50)	3.0	1.5	59.6412	28.2743	21.2058

1. $I = \pi/4 (R_o^4 - R_i^4)$; all values are in arbitrary units.

equation (7), the absolute change in the response ∂R_o was determined for a series of successive increments of ∂R_i (e.g., $\partial R_{i1} = (0.5\ R_i) + R_i$; $\partial R_{i2} = (1.0\ R_i) + R_i$; $\partial R_{i3} = (1.5\ R_i) + R_i$....$\partial R_{i8} = (4.0\ R_i) + R_i$). The tubular bone cross-sections modeled in this analysis are assumed equivalent with regard to their nongeometric properties (e.g., stiffness); and that the incremental geometric change is isometric (shape-preserving).

Tables 3.4 to 3.6 give the values of $R_i + \partial R_i$, $R_o + \partial R_o$ and ∂R_o expressed as a percentage of R_o for 50 % increments in R_i, from 0 to 400 % (0 to 300 % for the R_i/R_o ratio 0.5, since beyond 300 %, the radius $R_i \approx R_o$). The analysis indicates that maintaining the second moment of area (I) in these tubular bone analogues is independent of the initial values for TA and CA; rather, this maintenance is dependent upon the initial ratio of the endosteal and periosteal radii; that is, CT_0 (Figure 3.7). The greater the proportion R_i is of R_o at CT_a, the larger ∂R_a must be to maintain bending rigidity for any given ∂R_i. These results are not unexpected, of course, since I is not an intrinsic property of the cross-section, but is simply a mathematical description of the amount and distribution of material relative to some axis of bending.

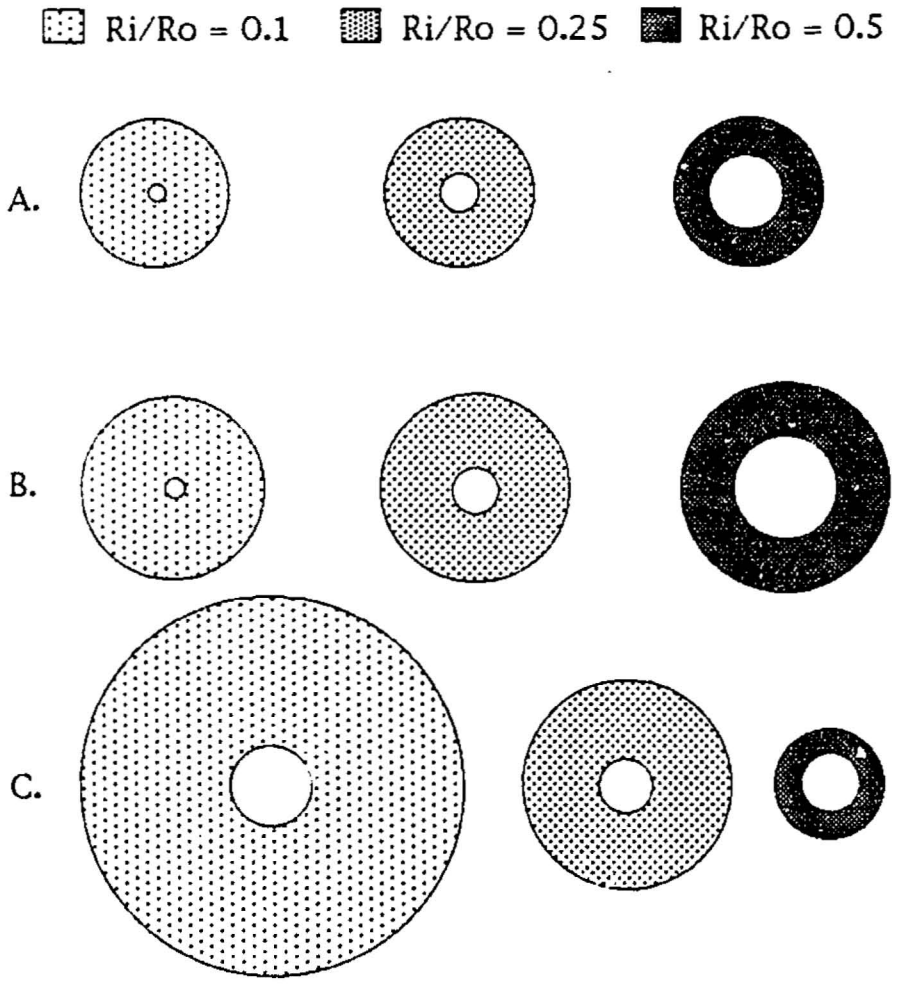

Figure 3.6. Schematic depiction of the nine right circular section tubular bone analogues modeled in this analysis. R_i/R_o is the ratio of the two surface radii, i.e., endosteal radius/periosteal radius. The three series, A-C, correspond to the constancy of Total Area (Series A), Cortical Area (Series B) or neither (Series C). (Illustrated at ca. 0.5x values given in Table 3.3.)

Table 3.4. Absolute and relative change in the endosteal and periosteal radii for three series of models accumulating 50 % increments in R_i; R_i/R_o = 0.1.

∂R_i	A			B			C		
(%)	$R_i+\partial R_i$	$R_o+\partial R_o$	∂R_o(%)	$R_i+\partial R_i$	$R_o+\partial R_o$	∂R_o(%)	$R_i+\partial R_i$	$R_o+\partial R_o$	∂R_o(%)
0[a]	0.399	3.989	0.0	0.491	4.911	0.0	1.0	10.0	0.0
50	0.598	3.99	0.01	0.737	4.911	0.01	1.5	10.001	0.01
100	0.798	3.991	0.038	0.982	4.913	0.038	2.0	10.004	0.038
150	0.997	3.993	0.1	1.228	4.915	0.095	2.5	10.01	0.095
200	1.197	3.997	0.199	1.473	4.92	0.199	3.0	10.02	0.199
250	1.396	4.004	0.371	1.719	4.929	0.371	3.5	10.037	0.371
300	1.596	4.015	0.632	1.964	4.942	0.632	4.0	10.063	0.636
350	1.795	4.03	1.007	2.21	4.96	1.007	4.5	10.101	1.007
400	1.995	4.05	1.525	2.455	4.986	1.525	5.0	10.153	1.525

[a]When ∂R_i(%) = 0, $R_i+\partial R_i = R_i+0 = R_i$, and $R_o+\partial R_o = R_o+0 = R_o$, and ∂R_o(%) = 0.

Table 3.5. Absolute and relative change in the endosteal and periosteal radii for three series of models accumulating 50 % increments in R_i; R_i/R_o = 0.25.

∂R_i	A			B			C		
(%)	$R_i+\partial R_i$	$R_o+\partial R_o$	∂R_o(%)	$R_i+\partial R_i$	$R_o+\partial R_o$	∂R_o(%)	$R_i+\partial R_i$	$R_o+\partial R_o$	∂R_o(%)
0[a]	0.997	3.989	0.0	1.262	5.046	0.0	1.4	5.6	0.0
50	1.496	4.005	0.395	1.892	5.066	0.394	2.1	5.622	0.394
100	1.995	4.047	1.434	2.523	5.119	1.434	2.8	5.680	1.434
150	2.493	4.13	3.526	3.154	5.224	3.526	3.5	5.798	3.526
200	2.992	4.27	7.035	3.785	5.401	7.035	4.2	5.994	7.035
250	3.491	4.475	12.156	4.416	5.66	12.156	4.9	6.281	12.156
300	3.989	4.742	18.863	5.046	5.998	18.863	5.6	6.656	18.863
350	4.488	5.065	26.957	5.677	6.407	26.957	6.3	7.11	26.957
400	4.987	5.432	36.164	6.308	6.871	36.164	7.0	7.625	36.164

[a]When ∂R_i(%) = 0, $R_i+\partial R_i = R_i+0 = R_i$, and $R_o+\partial R_o = R_o+0 = R_o$, and ∂R_o(%) = 0.

Table 3.6. Absolute and relative change in the endosteal and periosteal radii for three series of models accumulating 50 % increments in R_i; R_i/R_o = 0.5.

∂R_i	A			B			C		
(%)	$R_i+\partial R_i$	$R_o+\partial R_o$	∂R_o(%)	$R_i+\partial R_i$	$R_o+\partial R_o$	∂R_o(%)	$R_i+\partial R_i$	$R_o+\partial R_o$	∂R_o(%)
0[a]	1.995	3.989	0.0	2.8209	5.642	0.0	1.5	3.0	0.0
50	2.992	4.222	5.82	4.231	5.97	5.82	2.25	3.175	5.82
100	3.989	4.707	17.981	5.764	6.656	17.981	3.0	3.54	17.981
150	4.987	5.409	35.58	7.052	7.649	35.58	3.75	4.067	35.58
200	5.984	6.244	56.509	8.4628	8.83	56.509	4.5	4.695	56.509
250	6.982	7.15	79.218	9.873	10.111	79.218	5.25	5.377	79.218
300	7.979	8.093	102.87	11.284	11.446	102.87	6.0	6.086	102.87

[a]When ∂R_i(%) = 0, $R_i+\partial R_i = R_i+0 = R_i$, and $R_o+\partial R_o = R_o+0 = R_o$, and ∂R_o(%) = 0.

What is important is the relationship between the relative magnitude of CT_o and the amount of periosteal apposition required to compensate for a given relative increase in R_i, since CPA is a cellularly-based phenomenon having intrinsic physical and/or biological limitations which determine how much bone can be deposited within a specific time period. These limitations speak to the second question: how much CPA is possible?

Considering the results from bone biopsy studies using double fluorochrome labelling, Frost (1988b:15) remarks that "The largest physiologic formation drifts (e.g., drifts of lamellar bone, not woven bone) that have been reported in such studies so far are ≈ 3 microns/day". At this rate, ≈ 1 mm^3 per mm^2 of newly acquired bone tissue could be added each year. This would be more than enough to offset endocortical bone loss over a similar period. However, a variety of factors extrinsic to the bone cell system, such as raw material availability for bone matrix production, or reduced efficacy of the signal transducers activating the bone formation sequence, may effectively limit CPA as mechanical compensation for bone loss. An important consequence of the presumed existence of such factors limiting a CPA response is that a skeleton of lower peak bone mass is more likely to be threatened with structural failure than is a skeleton having a

high peak bone mass, if maintenance of a specified level of geometric strength is required, since they require a greater ∂R_o for any given ∂R_i.

Figure 3.8 depicts ∂R_o in bending versus axial compression, for an initial R_O = 4 units, and an R_i/R_o ratio of 0.25. These two curves indicate that the magnitude of ∂R_o required to maintain compressive strength (CA) is much larger than that required to maintain bending strength. It may also be inferred from this relationship that massive increases in I would result as a consequence of maintaining CA, if axial compressive strength was the selective factor determining the magnitude of ∂R_o. Were this the case, tubular bones would become increasingly resistant to bending loads in

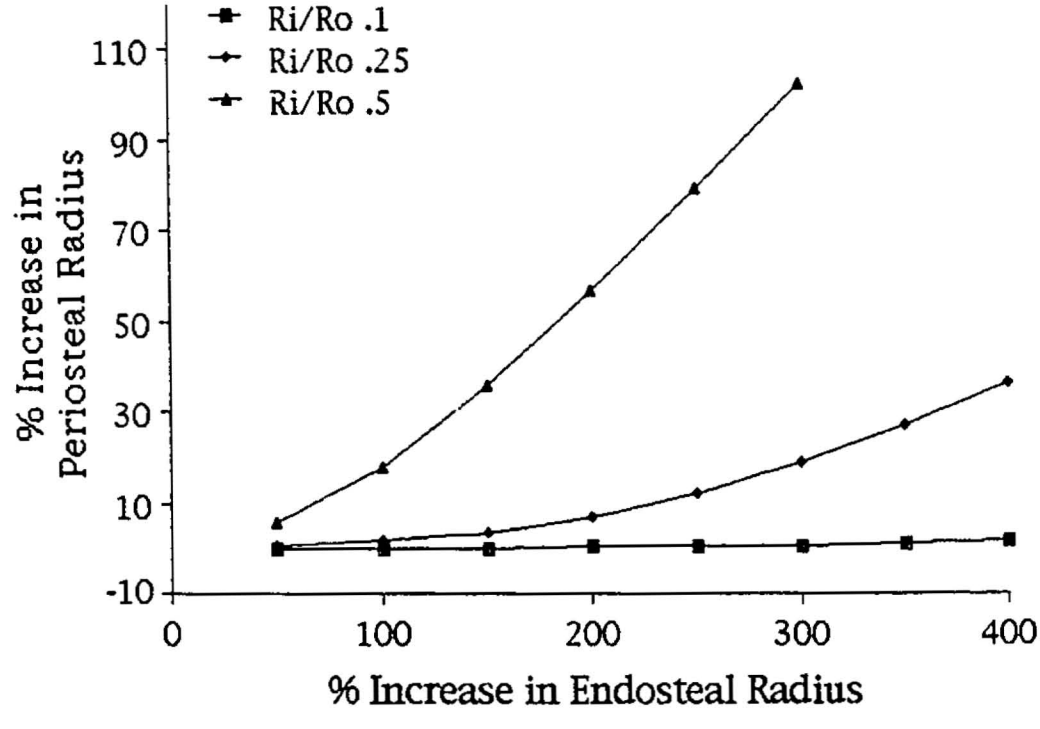

Figure 3.7. The relationship between % change at the periosteal surface, ∂R_o, in response to % change at the endosteal surface, ∂R_i, for three initial peak bone masses (0.1, 0.25 and 0.5).

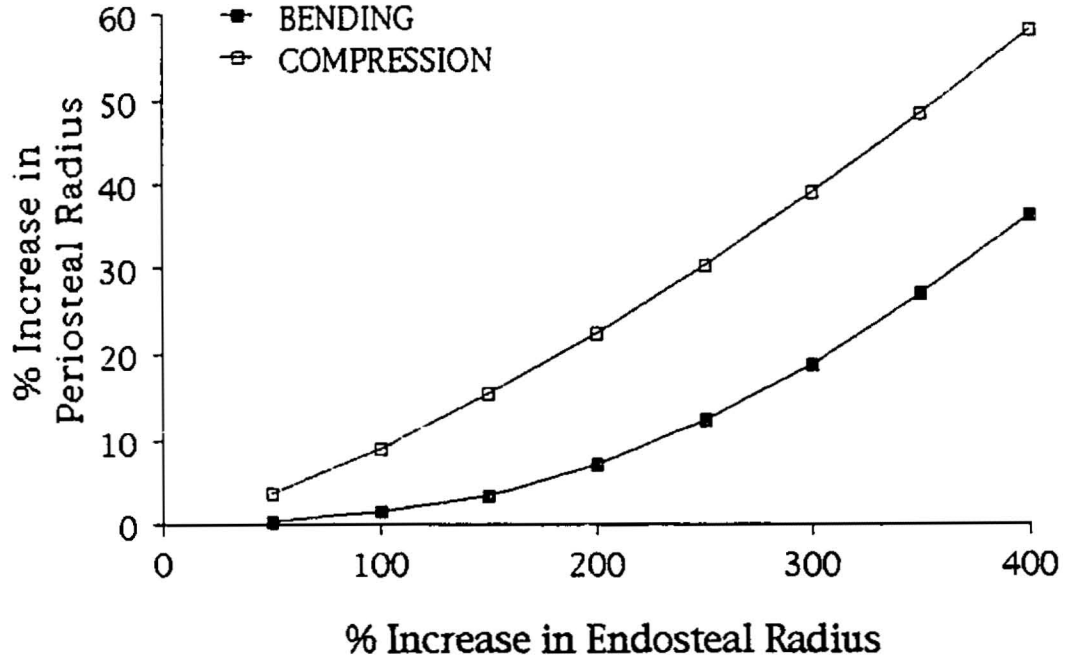

Figure 3.8. Curves illustrating the relative magnitude of periosteal change required in response to a specified change at the endosteal surface, for a tubular section having an initial R_i/R_o ratio of 0.25. The top curve indicates the response necessary to preserve the section's initial compressive strength; the bottom curve indicates the response required to preserve bending strength.

consequence of preserving a given cortical area. Since a large body of literature documents a reduction in cortical area in older groups (e.g., Ruff and Hayes, 1988), maintaining geometric resistance to compression likely does not determine ∂R_o. This is not unexpected given Bertram and Biewener's (1988) suggestion that axial compressive loads seldom occur in vivo, and since bone tissue is materially stronger under axial compression than in either bending or torsion (Currey, 1984b).

In the above analysis, the bending moment M (from the relation $\sigma = My/I$ for stress in a beam) was assumed to be constant for the purpose of determining the magnitude of compensatory apposition at the periosteal

surface to a given magnitude of endosteal resorption. A further assumption is that the objective of CPA is to maintain a given cross-sectional (and by extension, diaphyseal) geometric bending strength. As stipulated by contemporary interpretations of Wolff's Law (Roesler, 1987) and suggested by numerous studies involving experimentally-modified loading regimens (reviewed by Bouvier, 1985; Lanyon, 1987; Martin and Burr, 1989), tubular bones are seen as minimum mass solutions adapted to particular levels of functional strain vis-à-vis their time-averaged loading histories (Frost, 1985; Rubin and Lanyon, 1987). As such, the objective cited above, re-stated in terms of strain rather than bending strength, would be that CPA acts to limit increases in functional strain given the constancy of M and a reduction in the value I engendered by endosteal bone loss. In other words, CPA serves to maintain/restore strain equilibrium, viz. the objective proposed by the Mechanostat and Adaptive Elasticity models of Frost and Cowin.

However, casual observation clearly does not support the premise that bending moments remain constant. The frequency and the magnitude of dynamic loading which people impart to their skeletons varies with a variety of factors, including lifestyle, sex and age (e.g., Lips et al., 1990). With increasing age in particular, it could also be argued that neuromuscular control over functional loading becomes less precise, and is one factor predisposing older individuals to falls (Tideiksaar and Kay, 1987). As far as our bones are concerned, the rest of the body becomes less predictable. Thus, in addition to experiencing applied loads which are both less frequent and less strenuous, there may also be altered distributions of strain within the bone tissue. Such a scenario may raise or lower the level of strain at a given point in the bone tissue that was previously recognized as normal. Such factors will affect how much and where CPA occurs.

3.6.2 Activity Differentials and CPA

In bending, the magnitude of stress and strain increases along a gradient proportional to the distance from the centroidal neutral axis. For a cross-section at equilibrium (e.g., that moment when CT_0 is achieved) the endosteal surface can be visualized as E^-, and the periosteal surface as E^+. This terminology is adapted from Cowin, who uses E^- and E^+ to denote the

range of strain permissible at a single point on a bone surface which would not induce a 'remodelling' response. Here, they refer to a gradient of strain from the endosteal to the periosteal surface. The absence of bone matrix between the section centroid and the endosteal surface reflects the existence of strain levels below E^-, leading to net resorption which ensures the presence of a medullary cavity, as per Frost's Mechanostat. At the same time, the absence of periosteal apposition reflects the fact that equilibrium peak (or time-averaged) strains < MES.

This range of normal strain, E^- to E^+, can be visualized as the outcome of a range of activity differentials, A^- to A^+, that is, as a range of dynamic loading events which, averaged over a given time-period, give a mean value, $\tilde{A}$. The length of time over which bone tissue averages these cyclic loading events is presently unknown, however, it is clear that it must be of a sufficiently short duration (e.g., 24 hours) as to permit differentiation among excessive use ($\tilde{A}$ + tissue physical properties = strain > E^+ (MES), leading to net deposition), use ($\tilde{A}$ + tissue physical properties = 300 μE < strain < E^+ (MES) = (re)modelling equilibrium) and disuse ($\tilde{A}$ + tissue physical properties = strain < 300 μE (E^-), leading to net resorption).

Experimental work on the in vivo response to altered loading environments (Rubin and Lanyon, 1984) indicates that a remodelling 'equilibrium', in which the geometric and histological morphology of the experimental limb ≈ that of the control limb, can be maintained in the functionally-isolated turkey ulna by applying as few as four physiological load reversals (cycles) per day. Thirty-six such cycles produced a significant positive remodelling response at both the periosteal and endosteal surfaces, while zero cycles led to an eventual negative remodelling response at the endosteal and intracortical surfaces in moving towards a 'genetic' baseline level of bone mineral content which was ca. 88 % below control levels. From these results and related studies, Rubin and Lanyon (1987) suggest that the significant parameters recognized by the bone remodelling system appear to be both the magnitude and the distribution of dynamic loading events imparted to the skeleton. Increasing the former and/or altering the latter from that which has been perceived as 'normal' elicits an adaptive remodelling response with the presumed aim of equilibriating bone mass

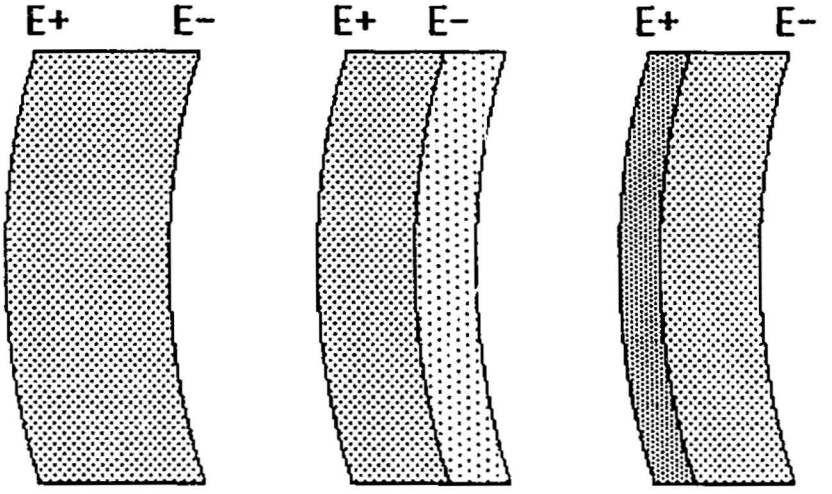

Figure 3.9. Schematic representation of how change in activity differentials results in endocortical bone loss and subsequent periosteal apposition. E^+: periosteal surface; E^-: endocortical surface.

LEFT: Peak Bone Mass (CT_0): The mean activity differential, $\tilde{A}$, of children and young adults establishes the strain equilibrium range, E^+ to E^-. Greater values for $\tilde{A}$ lead to a greater peak bone mass and CT_0.

CENTER: Endocortical Bone Loss: Reductions in activity sees the value of $\tilde{A}$ decreasing; this effectively shifts the lower limit of the strain equilibrium window, E^-, towards the periosteal surface. This leads to (1) a net resorption of endosteal bone tissue; (2) an adjacent increase in cortical porosity; (3) a net reduction in the value of I; and (4) an increase in tissue compliance (i.e., lower stiffness = greater strain per unit stress).

RIGHT: CPA as mechanical compensation: (3) and (4) above produce an increase in strain levels within the remaining bone tissue, and any subsequent occurrence of loads beyond $\tilde{A}$ leads to strain at the periosteal surface which exceeds E^+. This excess strain promotes a net apposition of bone, and the repetition of this and the above sequence leads to the phenomenon recognized as CPA.

and geometry to accommodate the 'new' criteria. For example, Rubin and Lanyon (1984) consider their results to have derived from alterations in strain distribution, since the loads which were applied to the isolated element were within the physiological range for the turkey ulna as registered during normal wing-flapping. Presumably, this altered strain distribution effectively established a state of disequilibrium at those surface locations which subsequently underwent net deposition or net resorption. This would account for the deposition of new bone at both the periosteal and endocortical surfaces.

While the quantitative results obtained from experimental studies carried out on the turkey ulna can not be translated to the human skeleton directly, the qualitative aspects are intriguing in the present context of activity-related bone loss and gain. Consideration should be given to the possibility that reductions in activity differentials predispose an individual to a lower mean activity state, $\tilde{A}$, and in consequence thereof to a lower strain level (frequency and magnitude). As well, altered strain distributions may result from age-related loss of neuromuscular control over body movement. A change in strain distribution would create regionally novel strain environments. Moreover, if these regions varied in terms of their recognizable peak strains or MES magnitudes (as postulated by the Adaptive Elasticity model), a change in strain distribution could have significance for (re)modelling equilibrium irrespective of any change in strain magnitude. The argument made here is that such occurrences may at least in part be responsible for both endocortical bone loss and CPA.

Figure 3.9 schematically depicts how CPA might occur. Since bending strain increases from the neutral axis outward, the reduction in time-averaged strain following an increase in sedentary behaviour will first be perceived at the endocortical surface. Conversely, an increase in strain would first be perceived at the periosteal surface. A widening or narrowing of the width of the strain equilibrium range, E^+ to E^-, is registered at only one surface because the strain parameters at the opposite surface remain within the recognized range, and thus no net (re)modelling occurs at the nonaffected surface. Thus, any change to a lower mean activity state ($\tilde{A}$) effectively shifts the value of E^- our bones recognize as the lower

equilibrium limit towards the periosteal surface. The bone tissue which exists between the centroidal neutral axis and this new location of E^- now exists in remodelling disequilibrium, and net endocortical bone loss, as well as increasing porosity near the endocortical surface, follows. This decreases the second moment of area and lowers the elastic modulus. Given these changes in strength and compliance, subsequent bending moments will produce larger strains within the remaining tissue. The result is that the strain magnitude at the periosteal surface may exceed E^+, and net periosteal apposition ensues, increasing geometric strength and tissue stiffness.

The scenario envisioned here is of a progressive and continual reduction in Ã, not necessarily linear, which promotes a negative endocortical bone balance. In turn, bending strength, I, is reduced establishing a potential for strain at the periosteal surface which exceeds E^+ following from any short term activity on the A+ side of Ã. These intermittent excursions beyond E^+ at the periosteal surface elicit successive net depositional responses, the accumulation of which are measured as CPA.

The reduction in the geometric strength of the bone associated with a lower Ã predisposes, but does not predict, the occurrence of higher levels of stress and strain within the remaining tissue. It follows that these elevated strain levels will be proportional to the reduction in I in the context of the value of Ã, and not simply to the reduction in I. This would see the magnitude and frequency of CPA set by the magnitude and frequency of excursions beyond E^+ at the periosteal surface, and not directly by the magnitude of endocortical bone loss.

Changes in strain distribution create a more complex scenario. Theoretically, such situations may promote formation or resorption, endosteally or periosteally, depending on the new strain state relative to that which was previously recognized as 'normal'. It is understood that cross-sectional geometry reflects strain history, and that irregular geometries possess orthogonal axes of maximum and minimum bending strength which are indicative of strain distribution. It can be argued then, that the distribution of surface modelling relative to these axes may be indicative of novel strain distributions.

So far as the models developed previously are concerned, the ratio R_i/R_o, (initially a reflection of peak bone mass, CT_0), can be viewed as a measure of our time-averaged activity levels established in young adulthood; and hence of the initial strain equilibrium window width, E^- to E^+. When the ratio R_i/R_o is small (i.e., cortical thickness is large) the endocortical resorption which follows from lowering activity differentials will at first register only slight decrements in the magnitude of I. However, when the initial R_i/R_o ratio is large, say 0.5, a situation exists in which the strain equilibrium window is narrow at the outset. Any further reduction in the width of E^- to E^+ will necessitate a much larger CPA response if and when E^+ is, on occasion, sufficiently exceeded to elicit a response. The problem, however, is that individuals with high initial R_i/R_o ratios are likely to have been habitually less active as young adults. In all probability, their mean activity differential was low at the outset. Should these individuals become even more sedentary with increasing age, they face the potential result of maximally narrowing the strain equilibrium window without exceeding E^+ and thus fail to elicit a biologically significant amount of CPA as compensation. While these individuals will be most susceptible to breaking their bones, it cannot be argued that they have broken Wolff's Law!

Throughout this section, arguments have been presented which consider the interactions among differential stress (i.e., changes in Ã) and cross-sectional geometry (i.e., changes at the endosteal and periosteal surfaces) in producing strain disequilibrium as a stimulus for bone modelling and remodelling. What has not been taken fully into account, for the sake of simplicity, are the confounding interactions among apparent density and porosity, and their effects on the stiffness and compliance of the tissue (i.e., the relationship of stress and strain). While it is true that, given no change in stress, a negative endocortical bone balance alone will increase strain throughout the remaining tissue, it is also true that this increase will be influenced by the amount of mineral and porosity present. Table 3.7 presents the effects of various permutations of high versus low mineral and porosity on the level of strain along an axis of constant geometry subjected to constant stress; as well as an indication of whether

Table 3.7. The relationship of high (H) versus low (L) mineral content and porosity on tissue stiffness and resultant strain under a constant stress, and the likelihood of more (M) or less (L) CPA.

Mineral	Stiffness	Porosity	Stiffness	Strain	CPA
H	↑	L	↑	↓	L
L	↓	H	↓	↑	M

CPA is more or less likely to occur. Because mineral density and porosity are inversely related, as detailed earlier, combinations such as High-High or Low-Low should not be encountered.

3.7 Summary

A. Strain-related bone modelling and remodelling leading to a net change in bone architecture and/or mass occurs in response to two stimuli: (1) overstrain, exceeding the upper modelling setpoint, (E^+) MES, promoting apposition of periosteal lamellar bone; and (2) understrain, which promotes a negative remodelling imbalance at the intracortical and endocortical surfaces.

B. Modelling and remodelling can exert significant effects on the physical properties of bone tissue, primarily by changing mineral density and porosity. For a given volume of tissue, lower density or higher porosity = reduced stiffness/increased compliance. Consequently, there will be greater strain (deformation) per unit stress (load).

C. The addition of new bone (modelling) or replacement of existing bone (remodelling) will always lower the mean bone age (MBA) of a given region of tissue, irrespective of the age of the bone tissue resorbed, because newly deposited bone is always the least mineralized bone tissue in any given area/volume of bone. Variation in regional bone tissue density, as can be seen in microradiographs, is quantifiable using grey-level analysis, and can be used to derive an objective MBA. This numerical value is interpretable with regard to the remodelling history of different regions of bone: a lower value indicates a greater rate of local bone turnover.

D. Bone modelling and remodelling are strain sensitive processes; any departure from an equilibrium strain state towards either end-point leads to a net accretion or net reduction in bone mass. These departures may occur through actual or perceived changes in recent strain history; the former mediated by behaviour and the latter by physiology. As noted, factors such as true and apparent density, while not affecting the genetically established or physiologically modified setpoints for functional adaptation, will mediate the resultant strain under any given applied load.

E. All else being equal (e.g., material stiffness and geometry) the peak bone mass achieved in young adulthood is likely the primary factor determining how much CPA constitutes sufficient mechanical compensation for endocortical bone loss. Constraints on achieving sufficient CPA are most likely extrinsic to the bone cell system (e.g., metabolic/nutritional status).

F. Changes in the magnitude (quality) and distribution (quality) of strain within bone tissue will determine the amount and circumferential location of CPA, intracortical porosity and MBA. Variation within these parameters will be effected by a combination of behavioural (e.g., activity level and muscular coordination) and physiological (hormonal and metabolic) factors extrinsic to the skeletal system.

CHAPTER 4. MATERIALS AND METHODS

4.1 Introduction

There are three requirements for achieving the objectives identified in Chapter 3: (1) a sample of cortical bone cross-sections from individuals differing in terms of strain history; (2) an assessment of the geometric properties of these sections; and (3) an assessment of their recent modelling and remodelling history, i.e., CPA, mean bone age, porosity. In this chapter, specific details are given pertaining to sample composition and description, to cross-section preparation, and to data acquisition and analysis.

The bones used for this study are the left second metatarsal and the left and right second metacarpal. Both metacarpals were collected in order to test for side differences. The rationale for selecting these particular elements was to sample skeletal sites which are structurally similar (i.e., both are short, tubular bones) but functionally different (i.e., manipulation versus locomotion). Appendix 2 provides details regarding the structural and functional similarities and differences for the 2nd metacarpal and 2nd metatarsal, with respect to osteology, arthrology and myology, as well as the principal deformations of these elements.

4.2 Samples: Sources and Description

The following section provides a demographic summary of the sample by element, since not every individual sampled was able to contribute all of the bones selected for study. Appendix 3 catalogues the provenience of the entire sample, by individual and source, and Appendix 4 gives the summary descriptive statistics for the osteometric data.

Human bones were acquired from two primary sources: (1) teaching cadavers from the Anatomy Departments of Queen's University, the University of Toronto and the University of Western Ontario, and (2) a small historic archaeological sample obtained from a 19th century EuroCanadian cemetery located in southwestern Ontario (Saunders and Lazenby, 1991).

In the cadaver group, there were instances in which the chosen elements were either unavailable or were no longer sufficiently intact to warrant sampling. The latter difficulty follows from several conditions: collection followed student dissection; specimens were often sequestered for preparing new prosections; and other researchers were also competing for tissue samples. Age, sex and cause(s) of death were documented by each Anatomy department. Collection was undertaken by gross dissection; in total 90 bones were obtained from 39 individuals, aged 49 to 88 years (32 males and seven females; Appendix 3). An additional 20 bones were contributed by the seven archaeological individuals, aged ca. 30 to 98 years (five males and two females). There were 33 metacarpal pairs in the combined sample, the composition of which is summarized in Table 4.1.

The archaeological skeletons are from an historic pioneer cemetery; personal identities are documented for some, and can be inferred for others (Saunders and Lazenby, 1991; Appendix 3). There is thus good support for the assigned age and sex of the individuals included in this study.

4.3 Sex Dimorphism

All comparative analyses must be confident in the fact that the data employed are, so far as possible, unadulterated measures of the properties under investigation. Since bone size is not independent of body size (Ruff, 1987c), a primary concern for studies of skeletal size and shape variability, whether ontogenetic or phylogenetic, is to control for effects due to body size. Normalizing or standardizing variables for body size effects can permit interpretation of between-group skeletal differences with regard to group-specific characteristics, e.g., behaviour or inheritance (Ruff, 1984; Burr et al., 1989a). A primary source of body size differences, of course, is gender: males, on average, are larger than females for many functionally significant skeletal dimensions (Ruff, 1987c).

Body weight provides the most useful and valid criterion for body size (Fleagle, 1985; Jungers, 1984; Ruff, 1987b). Other measures such as bone lengths and widths may not be appropriate factors for size standardization,

Table 4.1. Sample Composition by Sex, Source and Element.

Males					
Source	LMC	RMC	MT	Total	MC Pairs
Cadaver (Y/O)	26 (15/11)	27 (16/11)	22 (13/9)	75	22
Historic (Y/O)	5 (2/3)	5 (2/3)	4 (1/3)	14	5
Total	31	32	26	89	27
Females					
Source	LMC	RMC	MT	Total	MC Pairs
Cadaver (Y/O)	5 (2/3)	6 (2/4)	4 (1/3)	15	4
Historic (Y/O)	2 (1/1)	2 (1/1)	2 (1/1)	6	2
Total	7	8	6	21	6

Y=younger cohort (≤ 67 years); O=older cohort (≥ 68 years); an age of 67 years corresponds to the mean and median age for the largest component of the sample, cadaver males.

since they may not scale geometrically with body weight (Jungers, 1984);[1] however, body weight data are often not available to investigators working with skeletonized (e.g., archaeological) samples. While some researchers have been able to estimate body weight for skeletal data using regression formulae (Burr et al., 1989a), more often than not the tendency has been to resort to a presumed reflection of body size which is readily accessible. In most instances, this has been some measure of bone length. Ericksen

[1] If a variable scales geometrically with body weight, it maintains the same proportional relationship over all body weights, and thus could serve for weight as a scaling factor. If the relationship is not geometric, e.g., if a linear measure does not conform to the proportional relationship 'length $\propto$ mass$^{1/3}$' or an areal measure to the relationship 'area $\propto$ mass$^{2/3}$', then "erroneous functional interpretations of skeletal allometry and proportionality" can result (Jungers, 1984:79). In the present context, attempting to correct for body size differences by a factor which does not scale geometrically with the most valid indicator of body size (i.e., weight) may result in controlling for input from a source other than body size, e.g., a behavioral factor, thereby defeating the intent of the exercise.

(1976), for example, corrected cortical diameter data obtained from a series of archaeological femora and tibiae by dividing by 'maximum bone length'. Ruff (1984) points out, however, that maximum lengths are often not representative of 'true' functional length, and may be biased if substructures show independent variability (e.g., the contribution to maximum length from the femoral head and neck may be an independent function of the collodiaphyseal angle). In an analysis of chimpanzee femora, Sumner et al. (1989) normalized bone mineral content and cortical area data by 'diaphyseal length'. This length was taken to be the distance from the junction of the femoral shaft and the patellar surface of the condyles to the point of intersection between the femoral neck and the shaft in the vicinity of the base of the greater trochanter (see Fig. 1 in Sumner, 1984b; also Ruff and Hayes, 1983:363).

Ruff (1984) analyzed the allometric relationship between bone length and different cross-sectional variables, areas (mm^2) and moments of area (mm^4) in three human skeletal samples (two prehistoric groups and one modern autopsy group). Approximate isometry was found, with cortical area scaling $\approx$ length^2, and moments of area scaling $\approx$ length^4, leading Ruff (1984:356) to suggest that "in general, comparisons of long bone geometric properties between populations of different size or bone length should divide cross-sectional areas by length^2 and second moments of area by length^4". This was done in the analysis of structural change in the femur consequent with the shift from hunting and gathering to agriculture on the Georgia coast (Ruff et al., 1984). This study provides a useful illustration of the effect and necessity of controlling for inputs from large variations in body size within and between samples. Prior to normalization for bone length differences, a significant difference in magnitude was found for 11 of 12 subtrochanteric geometric variables (six each, male and female). After size standardization, only five of these 12 variables remained significantly different, and these much less so (from $p \leq 0.001$ for 73 % of the 11 significant differences before correction, to $p \leq 0.05$ for 60 % of the five significant differences afterwards). A similar result is reported by Bridges (1989b) in her analysis of cortical bone area from hunter-gather versus agriculturalist femora and humeri. In male femora, all but one of the

significant differences for cortical area between these two groups disappeared following size correction; in female humeri, significant differences appeared in the size-corrected data, where none previously existed, although only for the most proximal of site along the diaphysis.[2]

As noted by Ruff (1984), size correction is required in cases where the groups compared evidently differ in body size. 'Groups' can be identified according to various referents, the most outwardly apparent being gender. Since the present study intends to examine sex differences in geometry and histology as a function of behavioral rather than genetic input, results of analyses for sex dimorphism of are given in Table 4.2. Significant sex differences were found for both samples. Consequently, all geometric analyses were performed using data standardized by the appropriate power of bone length: areas by [(physiological length)^2 ÷ 10^2], and moments of area by [(physiological length)^4 ÷ 10^5].

4.4 Sample Processing and Section Preparation

When collected, each individual was assigned a code indicating source, year collected and sample number, e.g., in Appendix 3, T8906 indicates the sixth cadaver sampled in 1989 from the University of Toronto. Defleshing of the cadaver material at first involved delicate manual removal of as much of the adhering soft tissue as possible, followed by soaking in tap water with the enzyme-active laundry presoaking agent Bio-Ad. This approach is recommended for its lack of volatility and toxicity (Mooney et al., 1982). Similar agents have been shown to have no effect upon the dimensional characteristics of bone, even after three weeks immersion (Kokich, 1976). Elements from a single individual were placed in a glass jar, sprinkled with Bio-Ad and covered with tap water. Several jars at a time were immersed together in a water-filled enamel canner, and set on a hot plate to bring the

---

[2] In an expanded analysis of the relationship between lower limb bone geometry and 'subsistence' behaviour, Ruff (1987c:393) chose to use ratios of bending moments of area (Ix/Iy and Imax/Imin). One reason for this decision was to avoid "complexities associated with the standardizing of raw data for body size differences between the sexes or population samples".

Table 4.2. Human Sex Dimorphism Results for Metacarpals and Metatarsals, Based on Data Summarized in Appendix 4 (Unpaired, 1-Tailed t-Test).[1]

Variable	Sample	L 2nd MC	R 2nd MC	L 2nd MT
Maximum Length	Cadaver	- 3.729*** (28)	- 2.923*** (28)	- 3.349*** (23)
	Historic	- 2.287** (5)	- 1.812* (5)	- 2.563** (4)
Physiological Length	Cadaver	- 3.452*** (29)	- 2.597*** (28)	- 2.945*** (23)
	Historic	- 2.222 (5)	- 1.779* (5)	- 1.699* (4)
Proximal Width	Cadaver	- 6.017*** (28)	- 3.298*** (27)	- 0.226 (23)
	Historic	- 1.372 (5)	- 0.815 (5)	- 0.026 (4)
Dorsopalmer (-plantar) Diameter	Cadaver	- 4.306*** (29)	- 4.968*** (24)	0.768 (25)
	Historic	- 1.813* (5)	- 1.909* (5)	- 4.657*** (4)
Mediolateral Diameter	Cadaver	- 2.779** (29)	- 3.301*** (24)	0.349 (25)
	Historic	- 1.412 (5)	- 0.967 (5)	- 2.246** (4)

1. A '-' sign denotes males > females; d.f. given in parentheses.
* $p \leq 0.1$; ** $p \leq 0.05$; *** $p \leq 0.01$.

temperature to just below boiling. Both water and detergent were renewed after three to five days. This method produced bone samples which were totally defleshed and partially degreased after seven to 10 days, depending on the amount of adhering soft tissue. After a few samples had been processed in this manner, it was found unnecessary to manually remove any soft tissue. The soap and water bath performed this task admirably, though they required a few extra days, and as such minimized the possibility of damaging the periosteal surface, and eliminated the often unpleasant and onerous task of handling materials steeped in formalin. This method leaves the bone samples still somewhat greasy (Mooney et al., 1982); however,

further efforts to chemically degrease or bleach the samples were not undertaken, for fear that this might damage the periosteal surface (e.g., Rangel et al., 1985), which would negatively affect the CPA data subsequently collected. Once defleshed, the elements were allowed to air dry, after which they were individually labelled with an indelible marker.

Osteometric data were recorded, as tabulated in Appendix 4. In addition to assessing the magnitude of sex dimorphism, these data were used to determine the three thin section locations for histological analysis. Sections were located at 50 %, 60 % and 70 % of the physiological length of the bone (Figure 4.1), measured from the proximal end using 0.05 mm Helios dial calipers, and marked on the bone surface with an indelible pen. In all, 339 section locations were initially identified from both samples: however, attrition during processing resulted in a sample size for geometric analysis of 326 sections: 268 cadaveral and 58 archaeological.

Sections 250-350 mm thick were cut using a Buehler Isomet Slow Speed Saw, with a diamond wafering blade. Once removed, they were placed in a solution of tap water and Bio-Ad and ultrasonicated for 10 to 15 minutes to remove marrow and grit, then rinsed in the ultrasonicator for an additional 10 minutes in tap water. Images for geometric analysis were prepared prior to grinding the sections to an appropriate thickness for microradiography (see below). The cross sections were then hand ground between two sheets of 400 or 600 grit carborundum paper attached to large glass plates, in order to minimize variation in final thickness. The ground sections were then ultrasonicated in de-ionized water and Liquinox, followed by straight de-ionized water. Between the various stages of preparation (sectioning, geometric analysis, grinding, microradiography), the cross-sections were stored in 70 % ethyl alcohol (Anderson, 1982).

Thickness was monitored during grinding at several locations around the circumference of each section using a 0.001 mm Mitutoyo digital-outside micrometer, and final thickness was recorded at four locations corresponding to the intersection of the periosteal boundary with the major and minor moment axes, as determined by the geometric analysis. For 61 right metacarpal sections the average thickness among sections was 72.5 ±

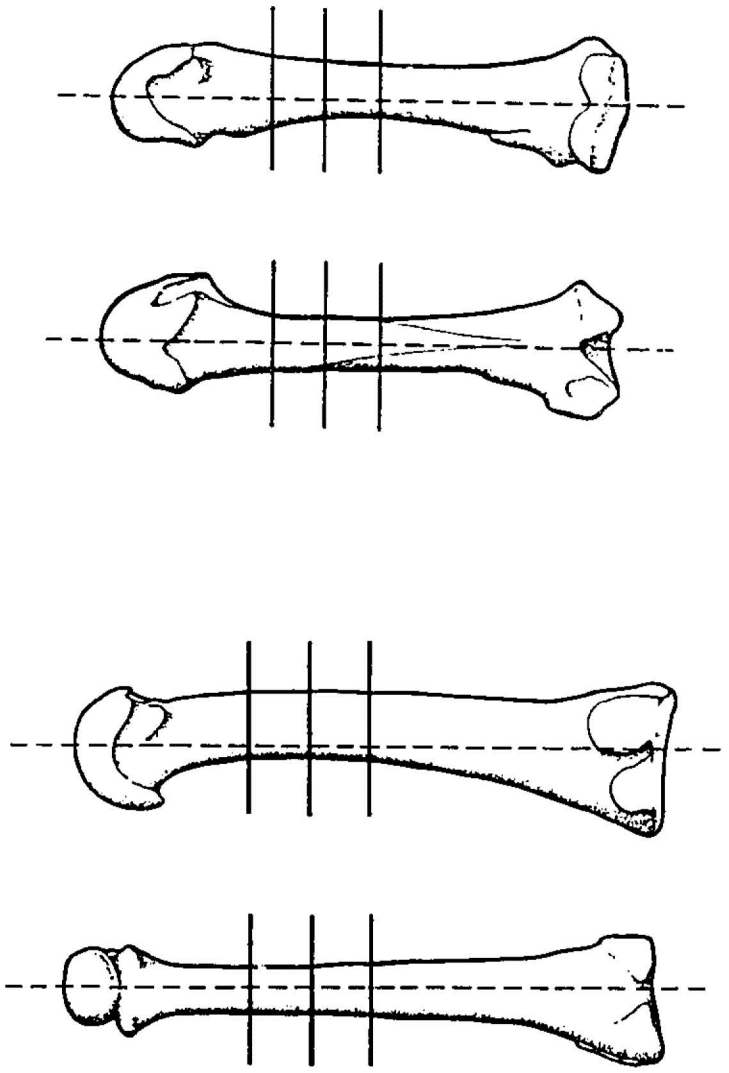

Figure 4.1. Superior (below) and lateral (above) views of the 2nd left metacarpal (top pair) and 2nd left metatarsal (bottom pair), showing the three section locations (50 %, 60 % and 70 % of physiological length).

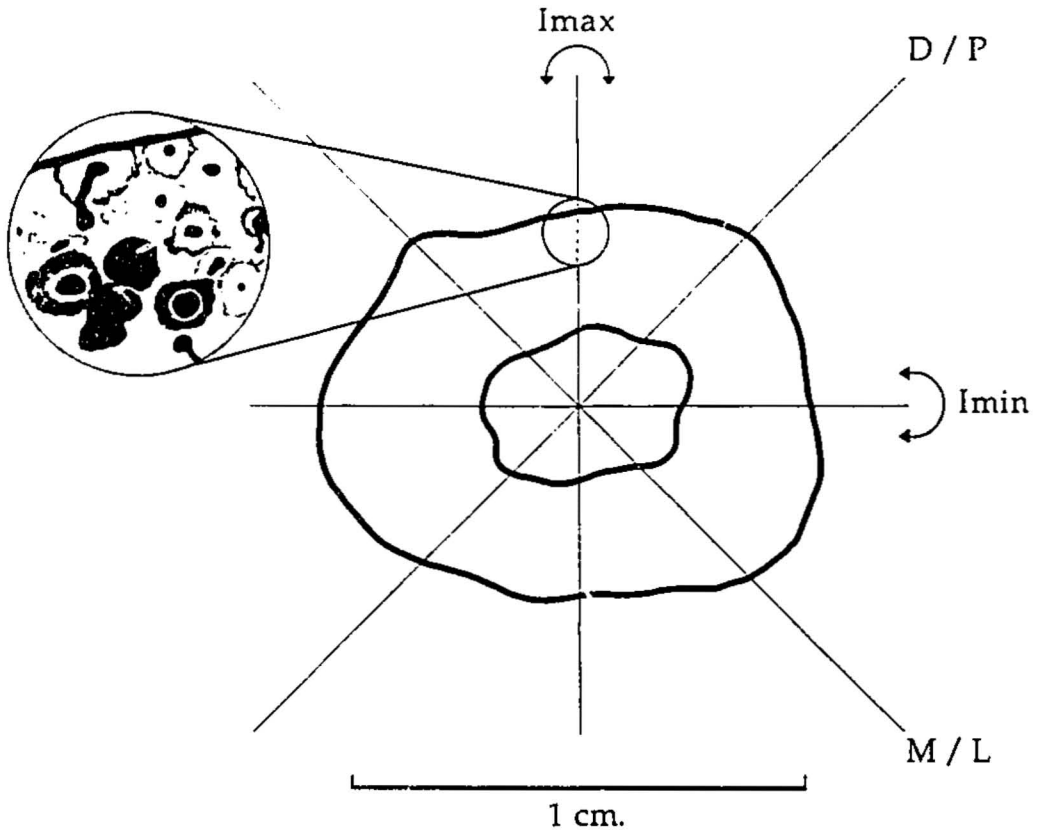

Figure 4.2. A representative metacarpal cross-section (50 % location) showing the reference dorsopalmer (D/P) and mediolateral (M/L) axes, and relative to these, the major (Imin) and minor (Imax) axes of bending. Also illustrated is a view of microradiographic mineral density variation. In this study, the entire periosteal-endocortical cortex was evaluated.

14 μm,[3] the mean deviation in thickness around the circumference was 4.01 μm. Although it is desirable to have uniformly thin sections for microradiography, it should be remembered that the resulting density data are used to evaluate relative remodelling history; and not absolute bone mineral status. Variation in section thickness was partially compensated for by varying the exposure time during radiography, giving microradiographs of similar visual appearance (see below).

4.5 Data Collection

Data for this study are of two general kinds: geometric (size and shape) data representative of structural strength independent of physical property variation; and densitometric ('mass') data, indicative of the modelling and remodelling history of the sections. The former data were collected with regard to each section in its entirety; the latter were obtained with regard to discrete quadrants within each cross-section.

4.5.1 Geometry

Geometric properties of all metacarpal and metatarsal sections were measured using SLCOMM (Eschman, 1990), a modified version of the SLICE program (Nagurka and Hayes, 1980; Ruff, 1989). SLCOMM calculates the geometric properties of each irregular section based upon digitized perimeter (periosteal and endosteal) coordinates collected from enlarged section images (Figure 4.2). The following geometric data are output by SLCOMM: total area (TA), cortical area (CA), the maximum (Imax) and minimum (Imin) moments of area, centroidal x and y coordinates, moments

---

[3] The rather large deviation in thickness among sections reflects a change from 100 μm to 70 μm as the objective for final thickness during grinding. This change was prompted during initial evaluations of the microradiographic procedure, which showed that the thinner sections gave somewhat better visual discrimination of mineral density variation. The recommended 100 μm 'gold standard' for microradiography can be traced to Jowsey (1960), although others (e.g., Bohatirchuk, 1954; Mjör, 1963) indicate that thinner sections (30-80 μm) give as good or better resolution than thicker sections. Over 80 % of the sections were prepared with a 70 μm final thickness in mind.

of area about the x and y axes,[4] and theta, a measure of rotation from the x-axis to the major (Imin) axis, in both degrees and radians. This study uses TA and CA as measures of size and resistance to axial strain; and Imax and Imin as measures of bending rigidity about the minor and major axes, respectively; three additional variables were derived from them: medullary area (MA), a proxy measure for endocortical bone loss; the polar moment of area (J), indicative of resistance to torsional strain; and the Imin/Imax ratio, a measure of cross-sectional shape-values departing from unity (1.0) indicate increasing noncircularity (Table 4.3).

The perimeter coordinate data were obtained first by preparing image outlines of the periosteal and endocortical margins of the cross-sections. Black and white photographic negatives for each series of sections were obtained, adjacent to a 10 mm x,y scale, and grouped by element and individual. The processed negatives were then projected onto metric graph paper under darkroom conditions, and the margins traced. The scale was also marked in order to record the magnification in x, y coordinate space for each series of section tracings. Each tracing and scale was then enlarged

---

[4] The precise determination of these reference axes is especially important when interpretations are to be drawn relative to them (Ruff and Hayes, 1983a). In this study, these axes are used only as a basis for locating the principal second moment of area axes, Imin and Imax, which SLCOMM determines with respect to any two orthogonal arbitrary axes. Therefore, the stringent requirement for precise location of the x-y axes is considerably relaxed. All the same, it was considered prudent to identify these axes for future reference (Figure 4.2). For metatarsals, the dorsoplantar (DP) axis was located by a line connecting a point at the maximum convexity of the margin of the head, viewed dorsally, to a point of maximum concavity of the dorsal margin of the proximal articular facet. The mediolateral (ML) axis corresponded to a line connecting the point of maximum concavity of the lateral margin of the head to a point adjacent to the inferior margin of the dorsal articular facet for the third metatarsal. For the metacarpals, the dorsopalmer (DP) axis was a line joining the proximal notch of the trapezoidal articular facet to a point at the maximum concavity of the margin of the head, viewed dorsally. The ML axis corresponded to a line connecting the point of maximum concavity of the head margin to the point of maximum concavity of the trapezoidal articular facet.

Table 4.3. Variables Collected From Entire Sections.

Variable	Definition	Method
Total Area, TA	area circumscribed by the periosteal margin, in mm^2	SLCOMM
Cortical Area, CA	TA-CA, in mm^2	"
Medullary Area, MA	medullary area circumscribed by the endocortical margin, in mm^2	derived
Maximum Moment of Area, Imax	maximum resistance to bending, in mm^4	SLCOMM
Minimum Moment of Area, Imin	minimum resistance to bending, in mm^4	"
Polar Moment of Area, J	a measure of resistance to torsion for approximately circular sections, in mm^4	derived
Imin/Imax	the ratio of moments of area; a measure of shape: a value of 1.0 indicates circularity	derived

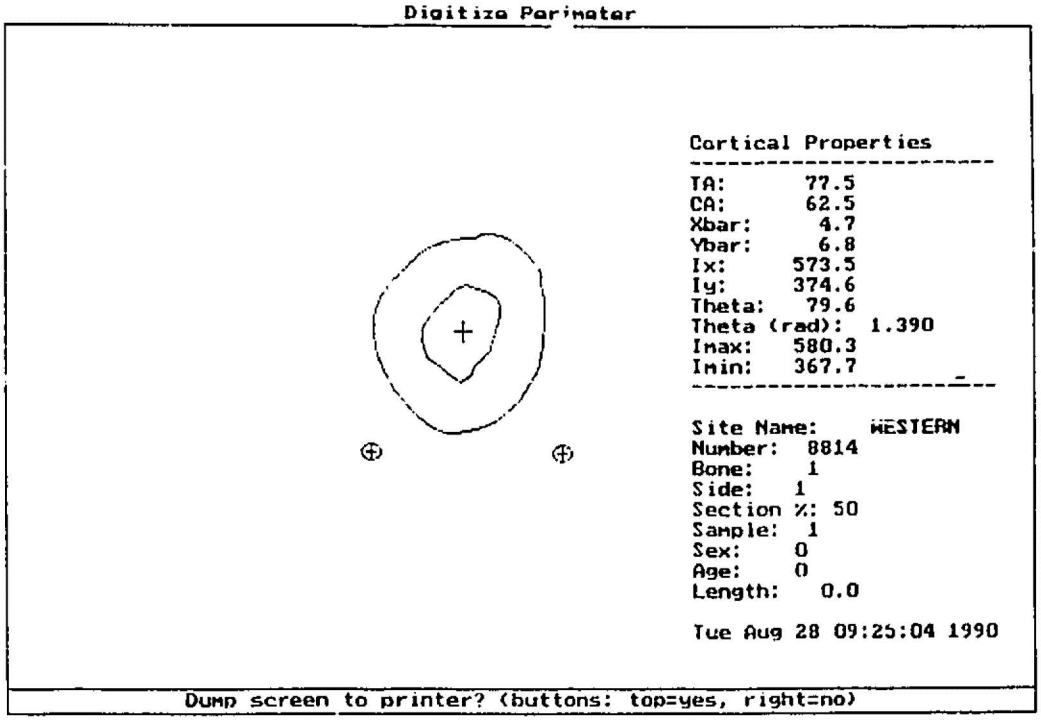

Figure 4.3. An example of SLCOMM output.

Table 4.4. SLCOMM Error.

Regular & Irregular Geometries [1]	A	B	σ	% σ^2
Shapes				
Areas (n = 4)	55.8	55.2	0.40	0.72
Moments (n = 6)	344.1	337.0	5.40	1.57
Variables				
TA (n = 21)	64.2	64.4	0.38	0.59
CA (n = 21)	43.7	44.1	0.35	0.80
Imax (n = 21)	370.3	371.5	4.90	1.32
Imin (n = 21)	261.7	263.3	3.37	1.29

1. Areas reported as mm^2, moments of area as mm^4; 'A' = mean values for shapes (determined algebraically), or from the first set of digitized images; 'B' = mean SLCOMM estimated values for shape parameters, or second set of irregular image observations. The four shapes tested were a solid right triangle, a solid rectangle, a hollow circle and a hollow oval; the different n's for rows 1 and 2 are due to the fact that moments of area are calculated relative to specific axes, data for six of which are given.
2. Calculated as [σ/A] x 100.

150 %, and digitized on a Summagraphics SummaSketch II Professional graphics tablet interfaced to an IBM-compatible microcomputer. Total magnification for the section images ranged from 6.9 to 9 times; SLCOMM corrects for this magnification according to a scaling factor entered at the tablet prior to tracing. The system is rapidly learned and extremely fast: a section can be digitized and the data screen dumped in under three minutes (five minutes if a hard copy is required; Figure 4.3).

There are two possible sources of method error in image digitization using SLCOMM. The first may occur prior to digitization, when entering the scaling factor by locating two points on the tablet which were previously assigned keyboard x, y coordinates. The program uses this factor when translating the geometric properties of the enlarged image to those of the actual section. The second source of error, of course, may accrue when actually tracing the image. Tests for method accuracy and precision are

reported in Table 4.4.[5] The former was evaluated by comparing SLCOMM estimates for a series of regular shapes (circles, rectangles, triangles) for which the true geometric properties could be determined algebraically (Muvdi and McNab, 1984). Intraobserver reliability for the method applied to irregular shapes was evaluated using a duplicated series of 21 human metacarpal and metatarsal section images. Together, these tests suggest a method accuracy and replicability < 2.0%, consistent with that others report for comparable technology (e.g., Ruff and Hayes, 1983a).

4.5.2 Microradiography

Microradiography was carried out on a subsample (n = 52; Table 4.5) of the sections[6] using facilities of the Dept. of Pathology, Ontario Veterinary College, University of Guelph. Sections were placed on Kodak SO 343 high resolution plates and exposed to low kilovoltage x-radiation in a Hewlett-Packard Faxitron, model 8050, having a focal spot size = 0.5 mm, tungsten target, and a 0.064 mm (0.025") beryllium window. The sections were kept in close contact with the film emulsion using removable cellulose tape, a method found to be preferable to the use of a vacuum cassette (McQueen et al., 1972; Dunn et al., 1974; Bowes and Dunn, 1975), since a greater number of sections (10 -12 per plate) could be exposed at once.

Table 4.6 gives examples of microradiographic exposure data from the literature. Several factors are involved when producing a microradiographic image, including specimen thickness, distance from the x-ray source, energy

---

[5] Error was calculated using the formula (Horsman and Kirby, 1972):

$$\sigma = \sqrt{\frac{\sum_{i=1}^{n} (x_i - x'_i)^2}{2n}}$$

[6] This sample size reflects the number of microradiographic images obtained of sufficiently high quality to permit analysis using the JAVA system. The reason for the inconsistency in image quality is unclear.

(kVp), current (mA)[7] and exposure time. Preliminary test exposures were undertaken to determine the optimal values for specimen thickness, energy, target-to-film distance, and time. Settings of 20 kVp, 2.75 mA at 20 cm for 160-205 minutes gave good visual discrimination among degrees of mineralization. Time was varied according to average section thickness: longer for thicker and shorter for thinner sections.

An important outcome of the geometric analysis was locating the axes associated with the maximum (Imax) and minimum (Imin) moments of area, translated to the section centroid (cf. the center of mass).[8] MBA, IP and CPA were evaluated within individual quadrants, for all bone tissue lying between the periosteal and endocortical margins, bisected by the Imax and Imin axes (Table 4.9). These quadrants are designated DJ, DN, PJ or PN, according to whether they occur in the dorsal or palmer (plantar) half of the section, and whether they are bisected by the major (J) or minor (N) axis. For each quadrant, the distance along the major or minor axes between the endocortical and periosteal margins, constituting cortical thickness (CT), was measured from the traced sections using 0.05 mm Helios dial calipers, and corrected for enlargement. Similarly, the respective section moduli, Z, were determined. In simple beam theory, Z reflects the maximum stress expected at the outermost fibre of a cross-section: the larger the value of Z, the lower the resultant stress, for any given material.

---

[7] In the Faxitron, current (mA) is a function of energy (kVp), and cannot be independently adjusted.

[8] In this case, the section centroid is determined based on static geometry alone; however, in living animals the centroid of a section is determined with regard to geometry and the nature of dynamic loadbearing to which it is subjected. For example, in a long bone such as a femur loaded eccentrically at the acetabulum, a significant compressive strain will be superimposed on the principal bending strain (combining both compressive and tensile strains). The summation of axial and bending strains serves to make peak compressive strains (e.g., in the anteromedial femoral midshaft) much more significant than peak tensile strains, and to laterally shift the centroid and the neutral axis of bending (Martin and Burr, 1989:151).

Table 4.5. Microradiographic sample composition by level.

Element	LMC	RMC		MT
Sex =	M	M	F	M
70 %	2	1	1	4
60 %	7	6	2	7
50 %	6	7	3	6
Total	15	14	6	17

Table 4.6. Exposure details for microradiography of cortical bone sections.

Study	ST[1]	kVp	mA	Distance[2]	Time[3]	Film
Dunn et al. (1974)	75-125	20	3	20	75	Kodak high resolution plates*
Ortner (1975)	ca. 80	10.5	2.5	20	60-80	"
Richman et al. (1979)[4]	ca. 80	11	na	20	65-70	na
Pugliese and Anderson (1986)	100	20	3	30	90	Kodak SO-343*
Martin et al. (1990)	100	25	3	na	60	"
this study	ca. 70	20	2.75	20	160-205	"

kVp = kilovoltage; mA = milliamperage.

1. Section thickness, in mm; 2. Focal spot-to-film distance, in cm; 3. Length of exposure, in minutes; 4. Picker 'Minishot', Model 1; all other studies used the Hewlett-Packard Faxitron.

* Kodak 'high resolution plates' and 'SO 343' refer to the same, slow speed photographic film, which offers a resolving power > 2000 lines/mm (Boivin and Baud, 1984).

Table 4.7. Variables Collected From Each Quadrant.

Variable	Definition	Method
Mean Bone Age, MBA	A measure of recent remodelling history; see Appendix 5 for methodological particulars; chapter 3 for derivation	JAVA
Porosity, IP	The proportion of the number of pixels in the range 0-40 relative to the total number of pixels for the quadrant	"
Continuing Periosteal Apposition, CPA	The proportion of pixels visually identified as having a lower mineralization that the subjacent bone matrix, relative to the total number of pixels in the quadrant comprising bone cortex	"
Section Modulus, Z	An indicator the maximum stress at the periosteal surface in the plane of bending, calculated as the ratio: [bending moment ÷ perpendicular distance, c, from the centroid to the periosteal surface]; e.g., DJ Z = Imax ÷ DJ c, etc.	SLCOMM; Helios dial calipers
Cortical Thickness, CT	The distance along the major and minor axes between the endosteal and periosteal margins, in mm.	Helios dial calipers

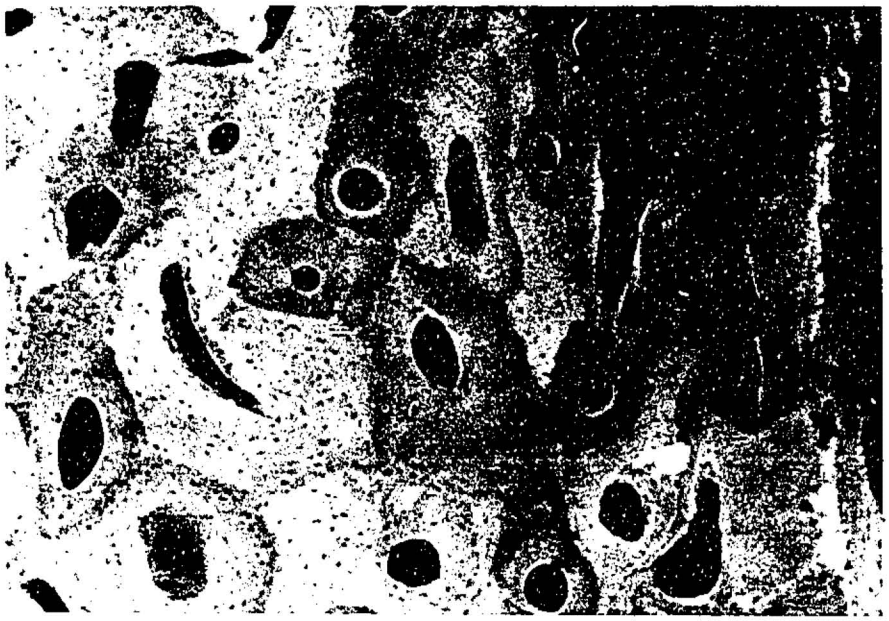

Figure 4.4. A microradiograph from a 56 year old male metacarpal, depicting intracortical porosity and variation in mineralization associated with Haversian remodelling. Several bands of circumferential lamellar bone, representative of CPA, can be seen at the periosteal surface (right side).

The microradiographic data were obtained using the Jandel JAVA multipurpose video analysis program interfaced with an IBM-compatible microcomputer. The microradiographs were mounted between standard 50 x 75 mm glass slides and viewed through a JVC High Band Saticon video-camera (Model Gx-S 700) attached to a Nikon Labophot microscope providing Koehler illumination, at a lamp voltage setting of 5.0-6.0. This system combined a 4x objective with a 1x/16 video ocular. No attempt was made to standardize the area evaluated as a fixed proportion of section size, since the dimensions of histological structures indicative of remodelling are independent of body (and thus of bone) size and age in humans (i.e., larger Haversian systems, or larger resorption spaces, and not found in larger or older individuals; Jowsey, 1968; Takahashi et al., 1965). Thus one can expect, all else being equal, to be able to measure an equivalent number of remodelled units in a given area of bone cortex from individuals of diverse sizes and ages; presumably, any variation in histology within a standard unit of cortex should reflect variation in strain history. Appendix 5 summarizes procedures followed for a typical JAVA session.

4.6. Hypotheses

As noted in Chapter 1, a rigorous test of the Mechanostat and Mechanical Compensation models developed in this thesis would require an experimental (animal) model which could control for categories of information (e.g., genetic/behavioural/physiological) that in general are poorly delimited in anthropological samples. However, as documented in Chapter 3, a principal factor underlying macroscopic (size and shape) and densitometric (porosity, CPA, MBA) variation is a real or perceived difference in functional strain history. Such differences might accrue between bones within an individual, as a function of bilateral asymmetry, or among individuals differentiated along lines of age, sex or lifestyle. It is thus possible to undertake an investigation of functionally adaptive modelling and remodelling within the context of an anthropological sample, if certain fundamental strain inequalities can be presumed to exist among the different sample components.

In the present study, these inequalities are as follows. Higher magnitudes and/or frequencies of strain-related stimuli are expected: (1) in the right rather than the left metacarpal, as a function of handedness; (2) in males rather than females; (3) in younger rather than older individuals; and (4) in historic rather than contemporary lifestyles. The latter three expectations follow as functions of cultural and/or sociological biases, as argued in e.g., Ruff (1987c) and Ruff and Hayes (1988). Assuming that these inequalities are valid, then some expectations regarding the nature and interaction of geometric and densitometric variation can be put forward, based on the Mechanostat model.

(1) Functional overstrain should typify the antecedent in the above pairs. Thus, modelling effects should dominate over remodelling effects, leading to larger cortical geometries, thicker cortices, smaller medullary areas, lower porosity, higher MBA and more CPA.

(2) Functional understrain should typify the latter group in each pair, leading to more remodelling effects and inhibited modelling. Larger medullary areas and thinner cortices are expected as a result of endocortical bone loss, as well as greater porosity and lower MBA via intracortical remodelling, and an absence of CPA.

(3) It is possible to envision a scenario in which the latter categories, experiencing a relative reduction in bone volume through remodelling, may show CPA as a result of diminished structural strength and intermittent loading beyond the E^+ setpoint. This defines mechanical compensation in the strict sense, as outlined in section 3.8. The association of remodelling effects with CPA is thus also anticipated.

In all instances, the null hypothesis is that no difference exists between groups, i.e., $H_0=\mu_1-\mu_2=0$.

4.7 Statistical Analyses

Rankit analysis for individual observations (Sokal and Rohlf, 1969) was first carried out on the individual SLCOMM and JAVA datasets to assess goodness of fit to the normal distribution assumed by parametric statistics. In this method, appropriate for small sample sizes, a linear plot of 'y' observations versus 'x' rankits (ranked normal deviates, corrected for ties)

indicates normality. This visual examination of the data revealed a number of cases for which the data departed from normality. No single method of transformation (e.g., log, square root or power) was able to satisfactorily resolve these departures.

Univariate locational analyses for the geometric and densitometric data were investigated using nonparametric methods. For the SLCOMM data, Source, Sex and Cohort differences were evaluated using Mann-Whitney U; and Side differences (in metacarpals) using the Wilcoxon Signed Rank test. In each case, a 1-tailed test was used, given the directional nature of the hypotheses specified for each comparison. For each element, a parametric Model 1 Anova was carried out on rank-transformed variables (Conover and Iman, 1981) to investigate whether differences occurred among the three levels, and Fisher's Protected Least Significant Difference test was used to identify specific differences. For the JAVA data, Mann-Whitney U was used to investigate Source, Cohort, Sex, and Side differences; this test was applied in the latter analysis since few matched pairs were involved. Anova was used to investigate the effects of Level, Quadrant and the 1st order interaction, Level x Quadrant, within each element. Finally, the association between geometric and densitometric variables was evaluated using Kendall's rank correlation coefficient, tau.

In this study α was set = 0.1 to accomodate the small sample sizes employed, as argued in chapter 2. Niemcryk et al. (1990:100) have noted that "A more liberal alpha of .10 may also be chosen. Larger alphas are particularly acceptable in exploratory or pilot studies [in which] the investigator is often still working out the "bugs" in the design." This qualification applies in the present case, given that novel methods-and models-are being employed to evaluate a heretofore poorly quantified phenomenon; i.e., CPA. The above analyses were performed using the statistical package Statview 512+ for the Macintosh.

CHAPTER 5. RESULTS

5.1 Geometric Variation

5.1.1 Source Differences

Results of an analysis to detect if the historic and cadaver samples differed in terms of cross-sectional geometric properties are reported in Table 5.1 for sexes combined (A), and for males (M) alone. So far as Source is concerned, broadly similar patterns in cross-sectional geometry are evident in all bones. In the metacarpals, there is a general absence of significant differences for total area (TA) at any of the three locations, suggesting similarity for overall size between the historic and cadaver samples, although the latter tends to have larger values overall (Figure 5.1). However, there are a considerable number of significant differences for cortical and medullary areas (CA and MA), and for measures of bending and torsional strength (Imin, Imax and J). This was especially so for the right metacarpal.

As indicated by the direction of difference in Table 5.1, as well as in Figure 5.1, historic metacarpals have larger MAs and smaller CAs than the cadaver group. Considered in conjunction with the relative similarity for TA, these results do not confirm the expected directionality: the historic bones are significantly less robust than the presumably more sedentary cadaver individuals. It may be that the equation 'modern dissecting room samples=more gracile individuals' does not hold for all bony elements. This may be especially true for an older cadaver sample that, for the above comparison, would be more contemporaneous with a recent historic sample, and thus may have differed little in terms of activity level.

A rather different picture appears for the metatarsal (MT) data: the historic group possesses larger dimensions for all variables, and only CA at all three locations along the distal diaphysis fails to achieve significance. The 'activity-geometry' model would appear to have currency in this case, and it is perhaps noteworthy that Ruff's (1987c; Ruff and Hayes, 1988) conclusions regarding habitus and bone geometry are based on analyses of

the lower limb (femur and tibia). The shape index, Imin/Imax, shows cadaver males to possess modestly more circular bones than their historic counterparts, although the differences were not significant. Since numerous experimental studies have demonstrated that changes in strain distribution promote changes in cross-sectional shape (e.g., reviewed by Rubin and Lanyon, 1987), the absence of such change here suggests that at least the qualitative aspects of the respective mechanical environments of these two groups did not differ appreciably.

5.1.2 Cohort Differences

There is little significant age dimorphism in either metacarpal, excepting CA (younger > older) and MA (older > younger) in comparisons involving the combined historic/cadaver sample, or male/female sample (Tables 5.2a, b). Figure 5.2 depicts the situation for male cadaver data; the absence of a significant aging effect is quite apparent. The opposite directional change noted for variables such as CA and MA is not surprising since both result from the same phenomenon: an age-related endocortical bone loss indicative of type II ('senile') osteoporosis (Resnick and Greenspan, 1989; Stini, 1990). In the majority of instances, particularly for 60 % and 50 % levels, TA in the older cohort is larger than in the younger, and although not differing significantly, this direction of change would be expected had continuing periosteal apposition occurred. No significant age differences in bending and torsional strength were discovered.

The metatarsal results (Table 5.2c) reveal a greater number of significant differences, especially at the 60 % and 50 % levels and again involving comparisons combining sexes or sources (for males). TA is often significantly larger at all levels, as is MA. CA does not differ significantly for any comparison. While CA is generally reduced in older individuals, there are exceptions, particularly at midshaft: e.g., the 'cadaver' (sexes combined), 'male all' (sources combined), and 'male cadaver' comparisons. All three variables, TA, CA and MA, are larger in the older cohort, indicating that any new bone added at the periosteal surface must have exceeded that lost through medullary cavity expansion. Such a result implies an impetus for CPA beyond that engendered solely by endocortical bone loss. In other

words, compensation beyond that required has occurred, and has, on average, been translated into greater structural strength for older versus younger individuals at this location. The significant differences found for Imin, Imax and J are undoubtedly a function of changes in TA, since these properties are most affected by that bone mass which is more distantly removed from the neutral axis of bending or torsion.

No significant change in cross-sectional shape was found for any comparison, at any level, again suggesting that the pattern of loading (and hence the resulting strain distribution) has not changed appreciably over the time span represented by this sample.

So far as the female metacarpals are concerned, the results obtained in this study are rather more inconclusive. At some levels older females exhibit larger values for variables such as TA, thereby agreeing with studies such as those of Garn et al., (1968; 1972), while at other sites the younger women have bigger bones.

5.1.3 Sex Differences

For the metacarpals, male dimensions were in general significantly greater than those of females (Table 5.3a, b; Figure 5.3), with the exception of medullary area for which no significant differences were found, and no consistent directional bias was apparent.

Though often not significant, the Imin/Imax ratio showed females to have more circular cross-sectional shapes, especially at the 60 % and 50 % levels. Thus, the size dimorphism discovered in chapter 4 appears to extend as well to shape, implying that both quantitative and qualitative differences between the sexes for manipulative behaviors.

A far different picture emerges regarding metatarsal geometry (Table 5.3c): female dimensions were consistently, and often significantly, larger than those of males. A notable exception occurs for comparisons restricted to older cohort individuals: males had larger CAs than females at all three locations along the shaft, albeit not significantly so. This result is consistent with older females having lost more bone endocortically, resulting in larger MAs and smaller CAs. At the same time, females may have acquired more

Table 5.1. Comparison of Historic Versus Cadaver Samples; Direction and Significance of Difference for Geometric Variables[1].

	M LMC	M RMC	M MT	A LMC	A RMC	A MT
70 % n =	31, 7	33, 7	26, 6	26, 5	27, 5	22, 4
TA	<	<	>	<	<	>
CA	< *	< *	<	< *	< *	>
MA	>	> *	> *	>	> *	> *
Imin	< *	< *	> *	< *	< *	> *
Imax	<	< *	> *	<	< *	> *
J	< *	< *	> *	< *	< *	> *
Imin/Imax	<	<	<	<	<	>
60 % n =	31, 7	33, 7	26, 6	26, 5	27, 5	22, 4
TA	<	<	> *	<	< *	> *
CA	< *	< *	>	< *	< *	>
MA	>	>	> *	> *	> *	> *
Imin	< *	< *	> *	< *	< *	> *
Imax	< *	< *	> *	< *	< *	> *
J	< *	< *	> *	< *	< *	> *
Imin/Imax	<	<	<	>	<	>
50 % n =	30, 6	33, 7	26, 6	25, 4	27, 5	21, 3
TA	<	<	> *	<	< *	> *
CA	< *	< *	>	< *	< *	>
MA	>	> *	> *	> *	> *	> *
Imin	<	< *	> *	<	< *	> *
Imax	<	< *	> *	<	< *	> *
J	<	< *	> *	<	< *	> *
Imin/Imax	<	<	<	>	<	>

1. > = historic > cadaver; < = historic < cadaver; * = significant at $p \leq 0.1$.

n = sample size for: cadaver, historic.

A = All (males & females); M = males only.

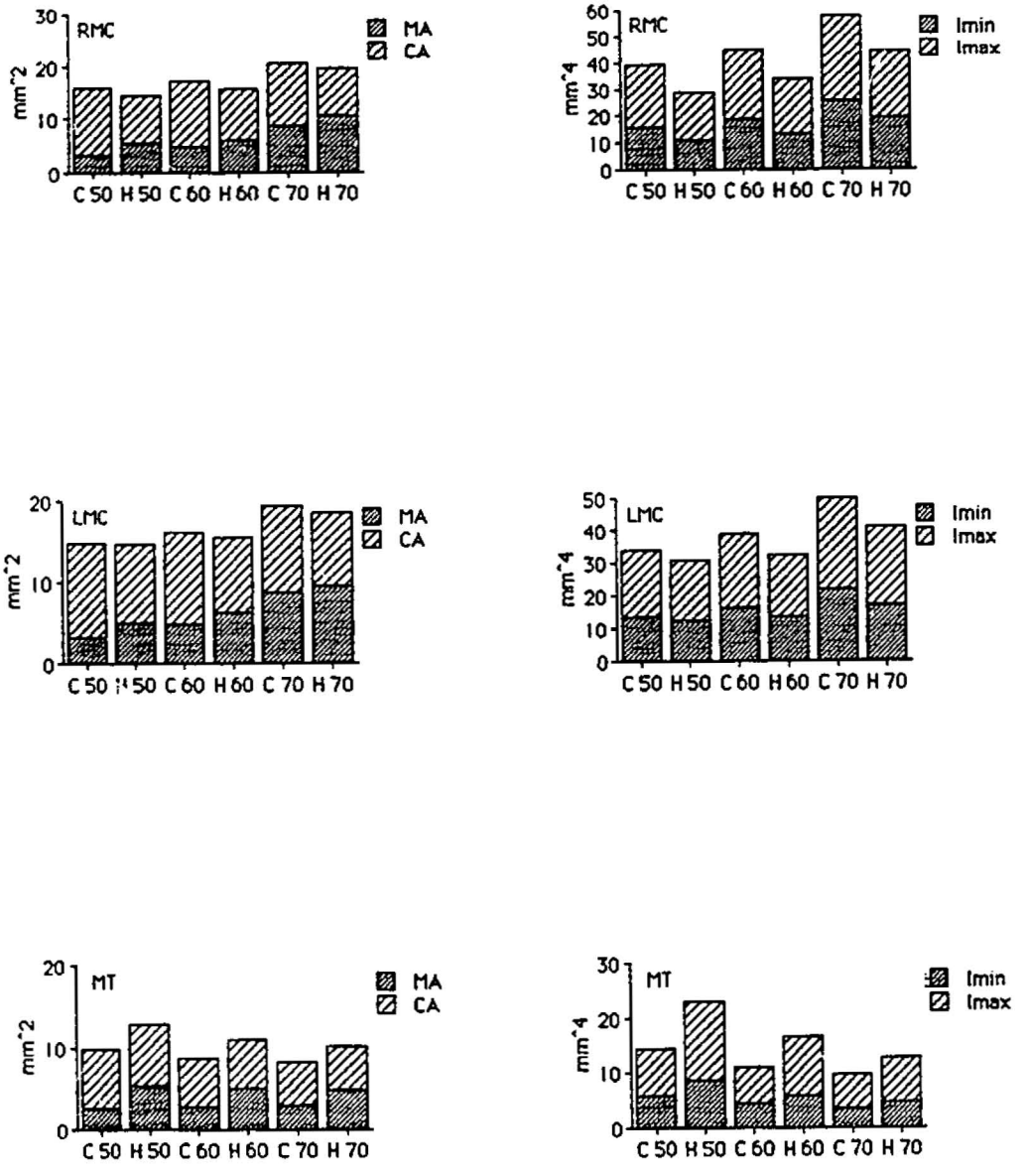

Figure 5.1. Source differences (C = cadaver, H = historic) revealed in stacked histograms for CA, MA (left) and Imin, Imax (right) means, male data. The total height of each column approximates TA and J, respectively.

Table 5.2a. LMC Age Comparison, Direction and Significance of Difference[1].

	ALL			CADAVER		
	M	F	M & F	M	F[2]	M & F
70 %, n =	17, 14	3, 5	20, 19	15, 11	2, 4	17, 15
TA	<	<	<	<	<	<
CA	>	>	> *	>	>	>
MA	<	<	<	<	<	<
Imin	>	>	>	<	<	>
Imax	>	>	>	<	>	>
J	>	>	>	<	>	>
Imin/Imax	>	<	>	>	<	<
60 %, n =	17, 14	3, 5	20, 19	15, 11	2, 4	17, 15
TA	<	<	<	<	<	<
CA	>	>	> *	>	>	>
MA	<	< *	< *	<	<	< *
Imin	<	<	>	<	<	<
Imax	<	<	>	<	<	<
J	<	<	>	<	<	<
Imin/Imax	>	>	>	>	>	>
50 %, n =	17, 12	3, 5	20, 17	15, 10	2, 4	17, 14
TA	<	<	<	<	<	<
CA	>	>	> *	>	>	>
MA	< *	<	< *	< *	<	< *
Imin	>	<	>	>	<	>
Imax	<	<	<	<	<	<
J	<	<	>	<	<	>
Imin/Imax	>	>	>	> *	>	>

1. > = younger larger than older; < = younger smaller than older.

2. Not tested for significance.

* = significant at $p \leq 0.1$; n = sample size for: young, old.

Table 5.2b. RMC Age Comparison, Direction and Significance of Difference[1].

	ALL			CADAVER		
	M	F	M > F	M	F[2]	M > F
70 %, n =	18, 14	3, 5	21, 19	16, 11	2, 4	18, 15
TA	<	>	>	<	>	>
CA	> *	> *	> *	> *	>	> *
MA	< *	<	< *	<	<	< *
Imin	>	>	>	>	>	>
Imax	>	>	>	>	>	>
J	>	>	>	>	>	>
Imin/Imax	0	<	<	<	<	<
60 %, n =	18, 14	3, 5	21, 19	16, 11	2, 4	18, 15
TA	<	<	<	<	>	<
CA	>	> *	> *	>	>	> *
MA	< *	<	< *	< *	<	< *
Imin	<	>	>	<	>	>
Imax	>	<	>	<	>	>
J	<	>	>	<	>	>
Imin/Imax	<	>	<	<	>	<
50 %, n =	18, 14	3, 5	21, 19	16, 11	2, 4	18, 15
TA	<	<	<	<	<	<
CA	> *	>	>	>	>	> *
MA	< *	<	< *	< *	<	< *
Imin	<	<	<	<	>	>
Imax	>	<	>	<	<	>
J	<	<	>	<	<	>
Imin/Imax	<	>	<	<	>	<

1. > = younger larger than older; < = younger smaller than older.

2. Not tested for significance.

* = significant at $p \leq 0.1$; n = sample size for: young, old.

Table 5.2c. MT Age Comparison, Direction and Significance of Difference[1].

	ALL			CADAVER		
	M	F[2]	M > F	M	F[2]	M > F
70 %, n =	14, 12	2, 4	16, 16	13, 9	1, 3	14, 12
TA	< *	>	< *	<	>	<
CA	<	>	>	>	>	>
MA	< *	<	< *	<	<	< *
Imin	<	>	<	<	>	<
Imax	<	>	<	<	>	<
J	< *	>	<	<	>	<
Imin/Imax	>	<	>	>	<	>
60 %, n =	14, 12	2, 4	16, 16	13, 9	1, 3	14, 12
TA	< *	>	< *	<	>	< *
CA	<	>	>	>	>	>
MA	< *	<	< *	<	<	< *
Imin	< *	>	< *	<	>	< *
Imax	< *	>	< *	<	>	<
J	< *	>	< *	<	>	< *
Imin/Imax	>	>	>	<	<	<
50 %, n =	13, 11	2, 4	15, 15	12, 9	1, 3	13, 12
TA	< *	>	< *	< *	>	< *
CA	<	>	>	<	>	<
MA	< *	<	< *	< *	<	< *
Imin	< *	>	< *	< *	>	< *
Imax	< *	>	< *	<	>	<
J	< *	>	< *	<	>	< *
Imin/Imax	>	>	>	<	>	<

1. > = younger larger than older; < = younger smaller than older.

2. Not tested for significance.

* = significant at $p \leq 0.1$; n = sample size for: young, old.

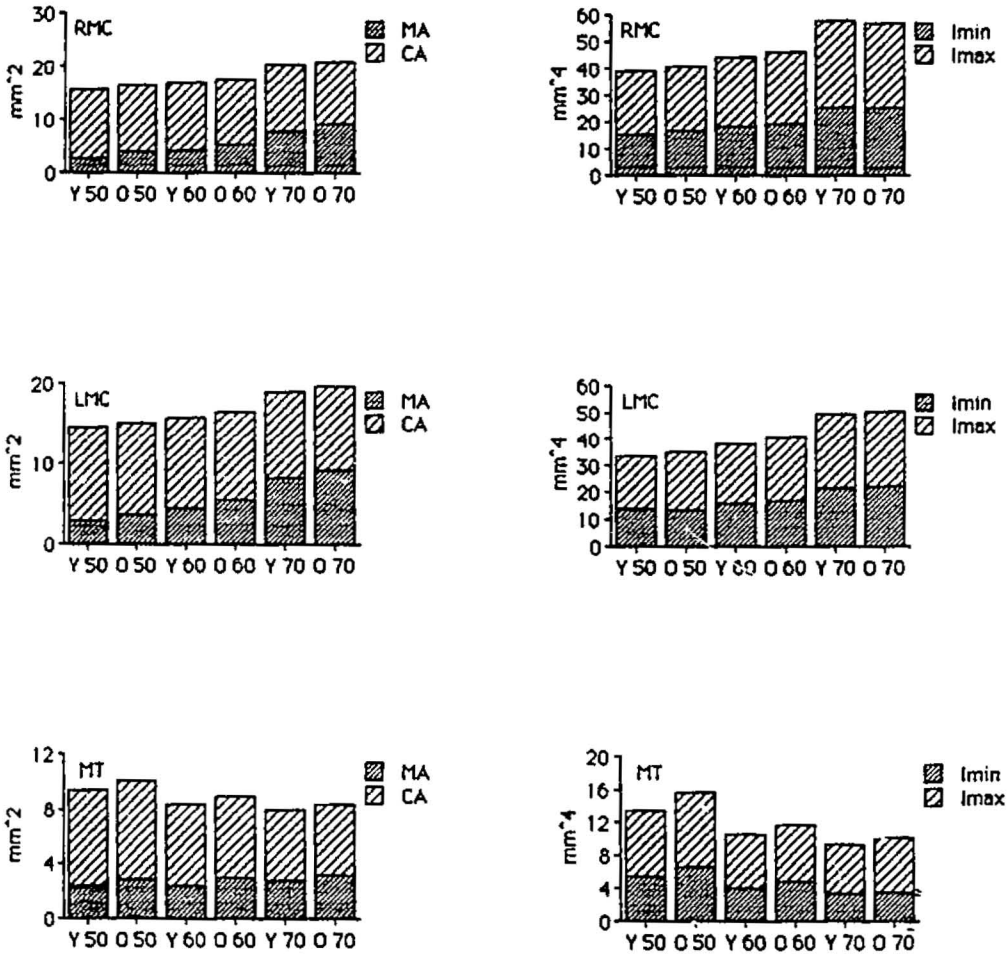

Figure 5.2. Cohort differences (O = old, Y = young) revealed in stacked histograms for CA, MA (left) and Imin, Imax (right) means, male data. The total height of each column approximates TA and J, respectively.

Table 5.3a. LMC Sex Dimorphism, Direction and Significance of Difference[1].

	ALL			CADAVER		
	young	old	both	young	old	both
70 %, n =	17, 3	14, 5	31, 8	15, 2	11, 4	26, 6
TA	> *	>	> *	>	>	> *
CA	>	> *	> *	>	> *	> *
MA	>	<	>	>	<	<
Imin	> *	> *	> *	> *	> *	> *
Imax	> *	> *	> *	>	> *	> *
J	> *	> *	> *	> *	> *	> *
Imin/Imax	<	<	<	>	<	0
60 %, n =	17, 3	14, 5	31, 8	15, 2	11, 4	26, 6
TA	> *	>	> *	> *	>	> *
CA	>	> *	> *	>	> *	> *
MA	>	<	<	>	<	<
Imin	> *	> *	> *	> *	> *	> *
Imax	> *	> *	> *	> *	> *	> *
J	> *	> *	> *	> *	> *	> *
Imin/Imax	<	<	< *	<	<	<
50 %, n =	17, 3	12, 5	29, 8	15, 2	10, 4	25, 6
TA	> *	>	> *	> *	>	> *
CA	> *	> *	> *	> *	> *	> *
MA	>	<	<	<	<	<
Imin	> *	> *	> *	> *	> *	> *
Imax	> *	> *	> *	> *	> *	> *
J	> *	> *	> *	> *	> *	> *
Imin/Imax	<	< *	< *	<	< *	< *

1. > = males larger than females; < = males smaller than females.

* = significant at $p \leq 0.1$; n = sample size for: males, females.

Table 5.3b. RMC Sex Dimorphism, Direction and Significance of Difference[1].

	ALL			CADAVER		
	young	old	both	young	old	both
70 %, n =	18, 3	14, 5	32, 8	16, 2	11, 4	27, 6
TA	>	> *	> *	>	> *	> *
CA	>	> *	> *	> *	> *	> *
MA	>	>	>	>	>	<
Imin	> *	> *	> *	>	> *	> *
Imax	>	> *	> *	>	> *	> *
J	>	> *	> *	>	> *	> *
Imin/max	>	<	<	>	>	>
60 %, n =	18, 3	14, 5	32, 8	16, 2	11, 4	27, 6
TA	> *	> *	> *	> *	> *	> *
CA	> *	> *	> *	> *	> *	> *
MA	>	<	<	<	<	<
Imin	> *	> *	> *	> *	> *	> *
Imax	> *	> *	> *	> *	> *	> *
J	> *	> *	> *	> *	> *	> *
Imin/Imax	< *	<	< *	< *	<	< *
50 %, n =	18, 3	14, 5	32, 8	16, 2	11, 4	27, 6
TA	> *	> *	> *	> *	> *	> *
CA	> *	>	> *	> *	> *	> *
MA	>	>	<	<	<	<
Imin	> *	> *	> *	> *	> *	> *
Imax	> *	> *	> *	> *	> *	> *
J	> *	> *	> *	> *	> *	> *
Imin/Imax	< *	<	< *	< *	>	<

1. > = males larger than females; < = males smaller than females.

* = significant at $p \leq 0.1$; n = sample size for: males, females.

Table 5.3c. MT Sex Dimorphism, Direction and Significance of Difference[1].

	ALL			CADAVER		
	young	old	both	young[2]	old	both
70 %, n =	14, 2	12, 4	26, 6	13, 1	9, 3	22, 4
TA	< *	<	< *	<	<	< *
CA	<	>	<	<	>	>
MA	<	<	<	<	<	< *
Imin	< *	<	< *	<	<	< *
Imax	< *	>	<	<	<	<
J	< *	>	< *	<	<	< *
Imin/Imax	<	<	< *	<	<	<
60 %, n =	14, 2	12, 4	26, 6	13, 1	9, 3	22, 4
TA	< *	<	< *	<	< *	< *
CA	< *	>	<	<	>	<
MA	<	<	<	<	< *	< *
Imin	< *	<	< *	<	<	< *
Imax	< *	>	< *	<	<	< *
J	< *	>	< *	<	<	< *
Imin/Imax	<	<	<	>	>	>
50 %, n =	13, 2	11, 4	24, 6	12, 1	9, 3	21, 4
TA	< *	<	< *	<	< *	< *
CA	< *	>	<	<	>	<
MA	<	<	<	<	< *	< *
Imin	< *	<	< *	<	<	< *
Imax	< *	<	< *	<	<	< *
J	< *	<	< *	<	< *	< *
Imin/Imax	<	<	<	>	>	>

1. > = males larger than females; < = males smaller than females.

2. Not tested for significance.

* = significant at $p \leq 0.1$; n = sample size for: males, females.

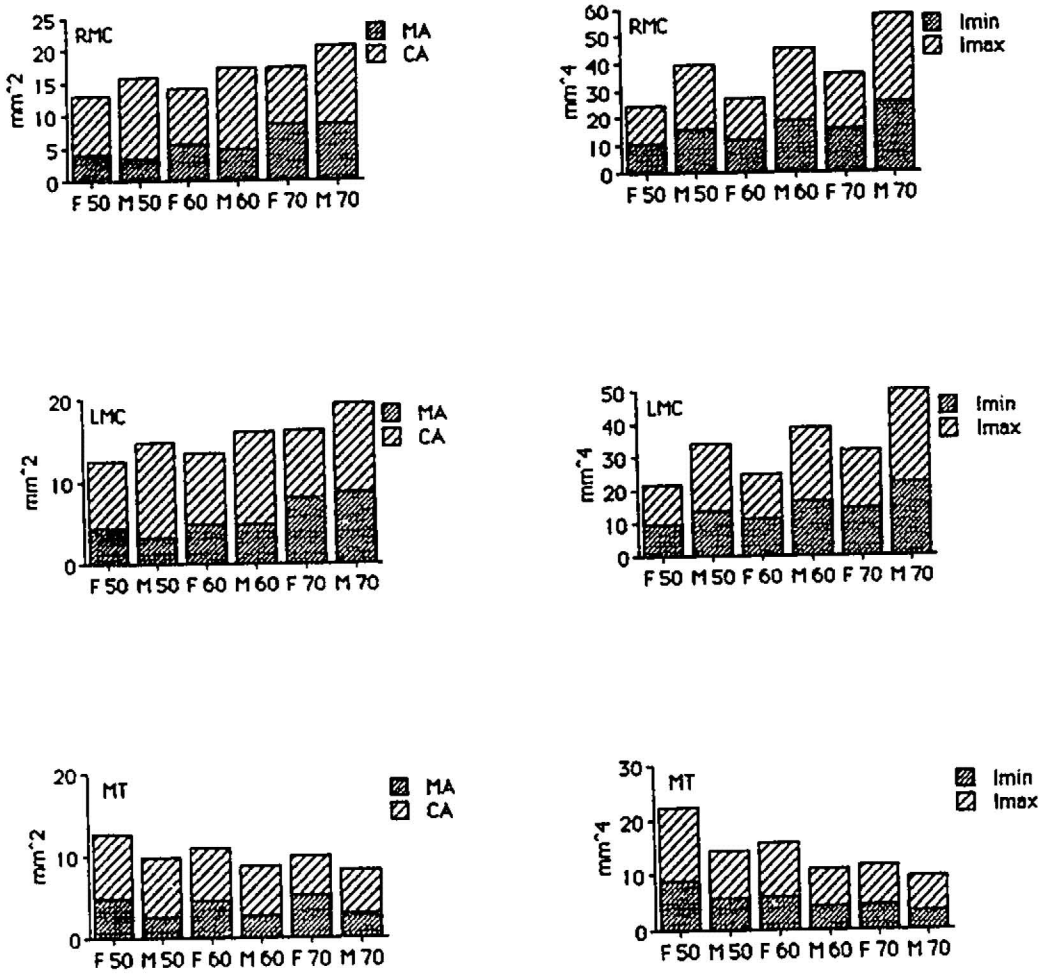

Figure 5.3. Sex differences (F = female, M = male) revealed in stacked histograms for CA, MA (left) and Imin, Imax (right) means, cadaver data. The total height of each column approximates TA and J, respectively.

Table 5.4. Side Dimorphism, Direction and Significance of Difference[1].

	All		Young	Old	Male		Female
	C	H	C	C	C	H	C & H
70 %, n =	26	7	15	11	22	5	6
TA	> *	> *	> *	>	> *	>	>
CA	> *	>	> *	>	> *	>	>
MA	>	> *	>	>	>	>	>
Imin	> *	> *	> *	>	> *	>	> *
Imax	> *	> *	> *	>	> *	>	> *
J	> *	> *	> *	>	> *	>	>
Imin/Imax	<	>	<	>	<	>	<
60 %, n =	26	7	15	11	22	5	6
TA	> *	>	> *	>	> *	>	> *
CA	> *	>	> *	>	> *	>	>
MA	>	>	<	>	>	<	>
Imin	> *	>	> *	> *	> *	<	> *
Imax	> *	> *	> *	>	> *	>	>
J	> *	>	> *	>	> *	>	>
Imin/Imax	>	<	>	>	>	<	>
50 %, n =	25	6	15	10	21	< 5	6
TA	> *	>	> *	>	> *	na	>
CA	> *	>	> *	>	> *	na	>
MA	<	> *	<	<	>	na	<
Imin	> *	>	> *	>	> *	na	> *
Imax	> *	>	> *	>	> *	na	> *
J	> *	>	> *	>	> *	na	> *
Imin/Imax	>	<	<	>	>	na	<

1. > = right larger than left; < = right smaller than left.

* = significant at $p \leq 0.1$, 2-tailed (or $p \leq 0.05$, 1-tailed).

C = cadaver; H = historic.

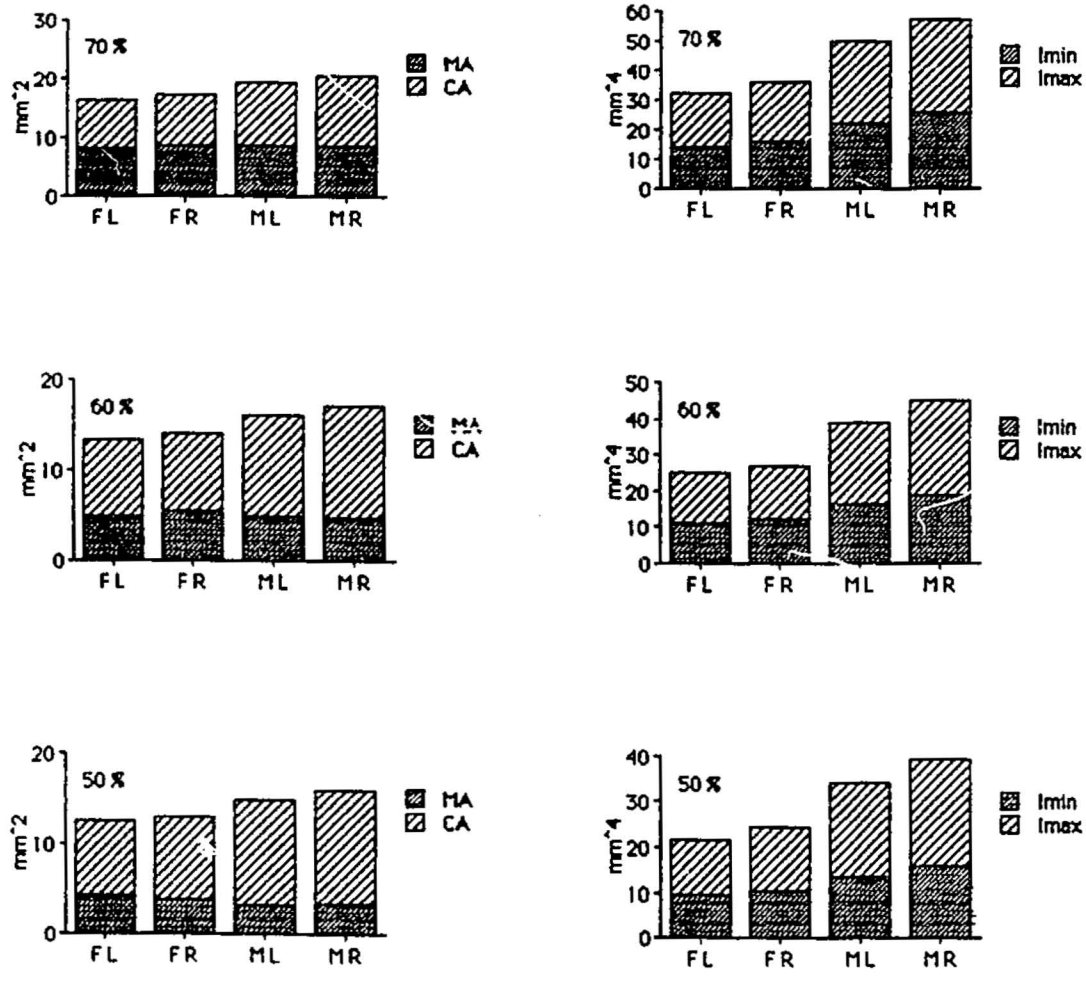

Figure 5.4. Side differences revealed in stacked histograms for CA, MA (left) and Imin, Imax (right) means, cadaver data. The total height of each column approximates TA and J, respectively.

bone at the periosteal surface, giving them larger total areas and greater bending and torsional strength.

5.1.4 Side Differences

Results from the present study confirm the side asymmetry reported elsewhere (e.g., Plato and Purifoy, 1982; Kimura, 1990a, cited in Kimura, 1990b). Analysis of side dimorphism was carried out (1) for all metacarpal pairs, age and sex combined; (2) by age (sexes combined); and (3) by sex (ages combined). Results of Wilcoxon's Signed-Rank test are reported in Table 5.4 (see also Figure 5.4) for each source independently, given a sample size sufficient to assess significance. In general, RMCs possess significantly larger dimensions than LMCs, the only consistent exceptions being for the two variables MA (especially at midshaft) and the Imin/Imax ratio. Relatively few of the historic comparisons achieve significance, probably due to the small sample size; neither do most of the old cadaver, nor the combined female, comparisons achieve significance.

5.1.5 Intra-element Differences

The F-ratios from a one-way Anova of rank-transformed variables across the three levels are given in Table 5.5. Analyses were undertaken for the historic sample, ages and sexes combined; and for the cadaver sample by age (sexes combined) and by sex (ages combined). In the majority of cases at least two of the levels differ significantly. Where the Anova for TA is significant, the analysis for bending and torsional strength indicators is also significant, a not unexpected result since these latter variables are most affected by changes at the periosteal surface that would lead to greater Total Areas (e.g., Jee et al., 1991). There are only four exceptions to this generalization: LMC historic Imax and J; RMC old cadaver Imax; and MT historic Imax. Of particular interest are two variables, metacarpal CA and metatarsal MA, for which no significant differences among levels were observed, suggesting that these two geometric measures are typified by considerable intra-level variability (i.e., they exhibit relatively large within group Mean Square values).

Table 5.5. Inter-Level Differences, 1-Way Anova F-ratios[1].

	Historic	Cadaver			
	All	Young	Old	Males	Females
LMC, df =	2, 17	2, 48	2, 38	2, 74	2, 12
TA	4.258*	14.294*	11.401*	26.798*	11.004*
CA	0.246	0.726	0.403	1.551	0.167
MA	6.221*	39.397*	15.971*	48.735*	4.269*
Imin	4.807*	10.301*	9.393*	24.349*	10.406*
Imax	1.783	5.262*	2.475*	8.351*	7.419*
J	2.582	7.218*	6.088*	15.608*	9.054*
Imin/Imax	0.471	1.722	4.271*	6.805*	0.222
RMC, df =	2, 18	2, 51	2, 42	2, 78	2, 15
TA	11.573*	20.109*	8.313*	30.043*	10.040*
CA	0.112	0.440	0.658	1.396	0.278
MA	10.159*	41.748*	21.766*	56.870*	5.287*
Imin	11.314*	18.437*	5.207*	26.714*	8.856*
Imax	2.786*	8.726*	2.147	12.653*	8.018*
J	4.892*	13.329*	3.502*	20.377*	9.080*
Imin/Imax	1.610	3.321*	5.670*	9.206*	0.554
MT, df =	2, 14	2, 38	2, 33	2, 62	2, 9
TA	1.650	9.274*	6.523*	10.565*	6.789*
CA	5.203*	14.931*	10.567*	18.310*	4.759*
MA	0.116	0.990	0.054	0.969	0.113
Imin	4.596*	15.064*	11.778*	19.742*	12.660*
Imax	2.677	7.561*	10.183*	9.270*	9.800*
J	3.097*	12.813*	12.751*	13.912*	9.800*
Imin/Imax	1.625	2.845*	3.288*	6.325*	0.016

1. * = significant at $p \leq 0.1$; df = between, within.

Table 5.6. Inter-Level Differences, Fisher's PLSD Results (* $p \leq 0.1$).

Historic (age & sex combined)

	LMC			RMC			MT		
	50-60	50-70	60-70	50-60	50-70	60-70	50-60	50-70	60-70
TA		*			*	*			
CA							*	*	
MA		*	*		*	*			
Imin		*	*		*	*		*	
Imax					*				
J					*	*		*	
Imin/ Imax									

Young Cadavers (sexes combined)

	LMC			RMC			MT		
	50-60	50-70	60-70	50-60	50-70	60-70	50-60	50-70	60-70
TA	*	*	*	*	*	*	*	*	
CA							*	*	*
MA	*	*	*	*	*	*			
Imin		*	*	*	*	*	*	*	*
Imax		*	*		*	*	*	*	
J		*	*	*	*	*	*	*	*
Imin/ Imax					*			*	

Old Cadavers (sexes combined)

	LMC			RMC			MT		
	50-60	50-70	60-70	50-60	50-70	60-70	50-60	50-70	60-70
TA	*	*	*		*	*	*	*	
CA							*	*	*
MA	*	*	*	*	*	*			
Imin	*	*	*		*	*	*	*	*
Imax		*			*		*	*	
J		*	*		*		*	*	*
Imin/ Imax		*		*	*			*	

Table 5.6 cont'd. Inter-Level Differences, Fisher's PLSD Results (* $p \leq 0.1$).

Male Cadavers (ages combined)

	LMC			RMC			MT		
	50-60	50-70	60-70	50-60	50-70	60-70	50-60	50-70	60-70
TA	*	*	*	*	*	*	*	*	
CA							*	*	*
MA	*	*	*	*	*	*			
Imin	*	*	*	*	*	*	*	*	*
Imax		*	*	*	*	*	*	*	
J	*	*	*	*	*	*	*	*	*
Imin/ Imax		*	*	*	*	*		*	*

Female Cadavers (ages combined)

	LMC			RMC			MT		
	50-60	50-70	60-70	50-60	50-70	60-70	50-60	50-70	60-70
TA		*	*		*	*	*	*	
CA								*	*
MA		*	*		*				
Imin	*	*	*	*	*	*	*	*	*
Imax		*	*		*	*	*	*	*
J	*	*	*		*	*	*	*	*
Imin/ Imax									

Table 5.6 reports results of Fisher's Protected Least Significant Difference test for paired comparisons among the three levels. Relatively few of the historic comparisons were found to be significant (28.6 %); this most likely reflects the inclusion of both sexes and all ages within the analysis, and a consequent increase in within-group variability. For the cadaver sample, an approximately equal number of significant comparisons was found when the sample was separated by sex (ages combined), rather than age (sexes combined) (66.7 % versus 62.7 %, respectively). Most of the significant differences in the metacarpals involve the 70 % section location, which generally falls within the diaphyseal region over which the shaft is expanding in medial, lateral and palmer directions towards the

head, involving considerable size and shape change from more proximal locations. In the metatarsals, the 50 % location is most often implicated; in this element, the reverse pattern holds, with the diaphysis tapering from midshaft towards the head. As might be expected, in both metacarpals and the metatarsal, the majority (43.6 %) of significant differences found over all five analyses were for comparisons involving the 50-70 % locations.

5.2 Densitometric Variation[1]

The data sets employed for analysis of densitometric variation suffer numerous deficiencies as a result of attrition during sample preparation and microradiography. For example, some of the microradiographs, while revealing seemingly good quality contrast when viewed microscopically, were found to be deficient when interpreted using JAVA, and consequently had to be eliminated.[2] As a result of these difficulties, there are relatively few historic and/or female cases available for analysis; as well, the 'old' cohort and the 70 % section location are poorly represented. This being the case, the analysis of the densitometric data for Source, Cohort, Sex and Side dimorphism was undertaken for discrete subsets of the overall sample, with the effect that small sample sizes typify all comparisons. Given the above restrictions, the results obtained should be interpreted and accepted with appropriate caution. All the same, as will be seen below and in the correlation analysis (section 5.3), some consistent and theoretically consonant patterns do emerge.

---

1 Reference is made throughout this and the following sections to the four quadrants evaluated, DJ, DN, PJ and PN. These quadrants generally possess the following relationships to the bone's four 'surfaces':

	DJ	DN	PJ	PN
LMC	laterodorsal	mediodorsal	mediopalmer	lateropalmer
RMC	laterodorsal	mediodorsal	mediopalmer	lateropalmer
MT	dorsal	lateral*	plantar	medial*

*A frequent exception occurs for the 50 % location, with DN situated medially, and PN laterally.

2 In a number of instances, these sections were microradiographed a second, and even a third time. This process managed to retrieve some, but not all, of the original sample.

5.2.1 Source Differences

Two analyses were undertaken: (1) LMC 60 % old males; and (2) RMC 50 % males, cohorts combined (Table 5.7). There were only two historic sections retained in the metatarsal data set, one for 50 % old males and one for 60 % old males.

For each of these analyses 7/20 significant differences were found, five more than expected by chance alone (with a set at 0.1, 2/20 comparisons might be significantly different even though the null hypothesis is true). Cadavers tended to exhibit greater values overall; for example, in Cortical Thickness, MBA and Z. Historic metacarpals had significantly greater porosity for the dorsal major axis quadrant. CPA did not differ significantly in either section, for any quadrant, though a slim majority of comparisons (5/8 quadrants over both sections) showed cadavers exhibiting more CPA than the historic individuals.

5.2.2 Cohort Differences

The analyses undertaken here, and reported in Table 5.8, included: (1) LMC 60 %; (2) RMC 50 %; and (3) MT 60 %; all restricted to male cadavers. For both the RMC and the MT, there were no more significant differences than expected by chance alone. As for direction of difference, older metacarpals show greater porosity, cortical thickness and section moduli. The LMC and RMC appear to differ with respect to CPA, with the former showing greater values in the younger of the two cohorts, and the latter tending towards larger values in the older. The metatarsal data exhibit a somewhat different pattern: older individuals tend towards greater MBA, lower porosity, less CPA and larger section moduli.

5.2.3 Sex Differences

Three statistical analyses were performed (Table 5.9): RMC 50 % and 60 %, and MT 60 %, all using cadaver data for combined cohorts. In the right metacarpals, the majority of significant results showed males with greater section moduli (all quadrants) and thicker cortices (lateral quadrants, DJ and PN). Females tend to have larger values for CPA and IP, and lower MBA.

Table 5.7. Source Differences for Densitometric Variables (* $p \leq 0.1$)[1].

	QUADRANT			
LMC 60 % n = 4, 2	DJ	PJ	DN	PN
IP	< *	<	>	<
CPA	<	<	>	<
MBA	> *	> *	>	> *
Z	> *	>	>	> *
CT	>	> *	>	>
RMC 50 % n = 7, 2	DJ	PJ	DN	PN
IP	< *	<	>	>
CPA	>	>	>	>
MBA	> *	>	>	>
Z	>	>	> *	>
CT	> *	> *	> *	> *

1. > = cadaver greater than historic; < = cadaver less than historic.
n = sample size for: cadaver, historic.

Table 5.8. Cohort Differences for Densitometric Variables (* $p \leq 0.1$)[1].

	QUADRANT			
LMC 60 % n = 4, 3	DJ	PJ	DN	PN
IP	>	>	>	>
CPA	<	<	<	<
MBA	>	<	<	> *
Z	> *	>	>	> *
CT	<	> *	>	>
RMC 50 % n = 3, 4	DJ	PJ	DN	PN
IP	>	>	>	>
CPA	> *	<	>	>
MBA	>	>	>	<
Z	>	<	>	>
CT	>	>	> *	<
MT 60 % n = 2, 5	DJ	PJ	DN	PN
IP	>	<	<	<
CPA	<	<	<	<
MBA	> *	>	>	>
Z	> *	<	>	>
CT	<	>	<	>

1. > = older greater than younger; < = older less than younger.
n = sample size for: old, young.

Table 5.9. Sex Differences for Densitometric Variables (* $p \leq 0.1$)[1].

	QUADRANT			
RMC 50 % n = 7, 3	DJ	PJ	DN	PN
IP	>	>	<	>
CPA	<	>	<	<
MBA	>	>	>	<
Z	> *	> *	> *	> *
CT	> *	>	<	> *
RMC 60 % n = 6, 2	DJ	PJ	DN	PN
IP	< *	<	<	<
CPA	>	< *	<	<
MBA	>	>	>	>
Z	> *	> *	> *	> *
CT	> *	<	>	> *
MT 60 % n = 7, 2	DJ	PJ	DN	PN
IP	< *	< *	< *	< *
CPA	>	<	>	>
MBA	>	>	>	>
Z	<	>	<	>
CT	>	>	> *	> *

1. > = males greater than females; < = males less than females.
n = sample size for: males, females.

Table 5.10. Side Differences for Densitometric Variables (* $p \leq 0.1$)[1].

	QUADRANT			
50 % n = 7, 6	DJ	PJ	DN	PN
IP	<	<	<	>
CPA	>	>	>	>
MBA	> *	> *	> *	>
Z	>	> *	>	>
CT	> *	> *	>	> *
60 % n = 6, 7	DJ	PJ	DN	PN
IP	>	>	< *	>
CPA	>	<	<	>
MBA	<	<	> *	>
Z	> *	> *	>	>
CT	>	>	<	>

1. male cadavers, cohorts combined; > = right greater than left; < = right less than left;
n = sample size for: right, left.

In the metatarsal, 7/20 significant differences were found. Females tended towards more intracortical porosity (significant for all quadrants), lower MBA, more CPA and thinner cortices.

5.2.4 Side Differences

This analysis was done for 2 subsamples, 50 % and 60 % male cadavers, combined cohorts: Table 5.10 provides results. For both comparisons, a greater than expected number of significant differences (11/40) was found and, for all except one of these, the RMC exhibited larger values for CPA, Z, CT and MBA.

5.2.5 Intra-element Differences

Variation due the fixed effects of level and quadrant was evaluated by two-way factorial Anova of the rank-transformed variables, and results are given in Table 5.11. Three separate analyses were performed for the following subsets: LMC, RMC and MT male cadavers. The analyses represent unbalanced designs, that is, there are unequal n for each cell (location x quadrant). This means that it is not possible to partition the total sum of squares (SS) into discrete components attributable uniquely to each main effect (Kirkwood, 1988). Thus, the SS for Level will include variation due to the main effect, Quadrant. As the second factor entered into the analysis, the SS for Quadrant represents variation remaining after adjustment for differences due to Level. Reversing the order in which the main effects were allowed for in the analysis of variance, a procedure recommended for unbalanced designs in which the order is not contingent upon theoretical premises (Kirkwood, 1988), had no effect on the distribution of the sum of squares or F-ratios. To assist in the interpretation of the Anova, the mean rank values from the resulting incidence tables are plotted in Figures 5.5 to 5.9, with each point representing the cell value corresponding to a particular quadrant-level combination, e.g., DJ 50 %, PN 70 % and so on.

Intracortical Porosity, IP:

In the metatarsal, both main effects were found to be significant (Figure 5.5). The greatest porosity occurs with the 50 % level, and while the DJ

quadrant retains a high degree of porosity at both 60 % and 70 %, the other quadrants show a significant reduction in porosity from 50 % to 60 %. In the metacarpals, Quadrant was not a significant factor in either case, and Level only for the RMC. As with the foot bone, the distal section location suffers less porosity than midshaft, but unlike the metatarsal, most of the reduction takes place between the 60 % and 70 % locations. In all three elements, the DJ quadrant tends to exhibit most porosity, and PN the least.

Continuing Periosteal Apposition, CPA:

In the metatarsal, only Level was found to be significant, and barely so ($p = .0959$), while for the metacarpals, neither main effect could account for the data variance. This lack of significance is apparent in the graphs of the cell values (Figure 5.6), in which no real pattern can be discerned among quadrants at any given level or across the different levels.

Mean Bone Age, MBA:

For all three bones, Level was a significant factor while Quadrant was not (Figure 5.7). In the foot, the 50 % location differs from the more distal levels, while in the hand it is the 70 % section which appears most distinctive. Overall, MBA tends to exhibit the lowest values at midshaft, increasing towards the head in all bones; this is the reverse of the pattern seen for IP in Figure 5.5.

Section Modulus, Z:

In the MT and RMC both Level and Quadrant were significant factors contributing to variation in Z; in the LMC neither was (Figure 5.8). The differences in shape along the shaft noted earlier (section 5.1.5) for the MT and MC appear here as well: the MT section modulus decreases from midshaft, indicating a smaller size for the more distal locations. In the metacarpals, the magnitude of Z tends to increase distally (thus, 70 % sections tend to be larger than 50 % sections).

Cortical Thickness, CT:

For all three elements, both main effects were significant factors (Figure 5.9). In the metatarsal there is a gradual and more or less uniform reduction in cortical thickness from midshaft towards the head (the decline somewhat greater between 60 % and 70 %); within levels, thickness tends to decrease around the circumference, with the DN quadrant substantially thinner than all others. In the metacarpals, the major axis quadrants (DJ, PJ) tend to have thicker cortices than the minor axis quadrants (DN, PN), with exceptions noted for the 70 % location: in the RMC, dorsal quadrants are thicker than palmer, while in the LMC the converse is approximated.

Table 5.11. 'Densitometric' Intra-Element Differences, Anova F-ratios.

Source	df	IP	CPA	MBA	Z	CT
LMC						
Level	2	1.140	0.080	12.522*	1.634	3.946*
Quadrant	3	1.360	1.278	0.527	2.043	3.153*
Interaction	6	0.716	0.862	1.296	0.156	0.804
error	48					
RMC						
Level	2	2.52*	0.744	3.971*	12.961*	8.116*
Quadrant	3	0.789	2.11	0.087	3.237*	3.708*
Interaction	6	0.41	1.262	0.426	0.494	1.07
error	44					
MT						
Level	2	9.208*	2.445*	3.091*	7.121*	6.263*
Quadrant	3	6.331*	1.035	0.651	6.604*	4.696*
Interaction	6	1.02	1.371	0.253	0.184	0.074
error	56					

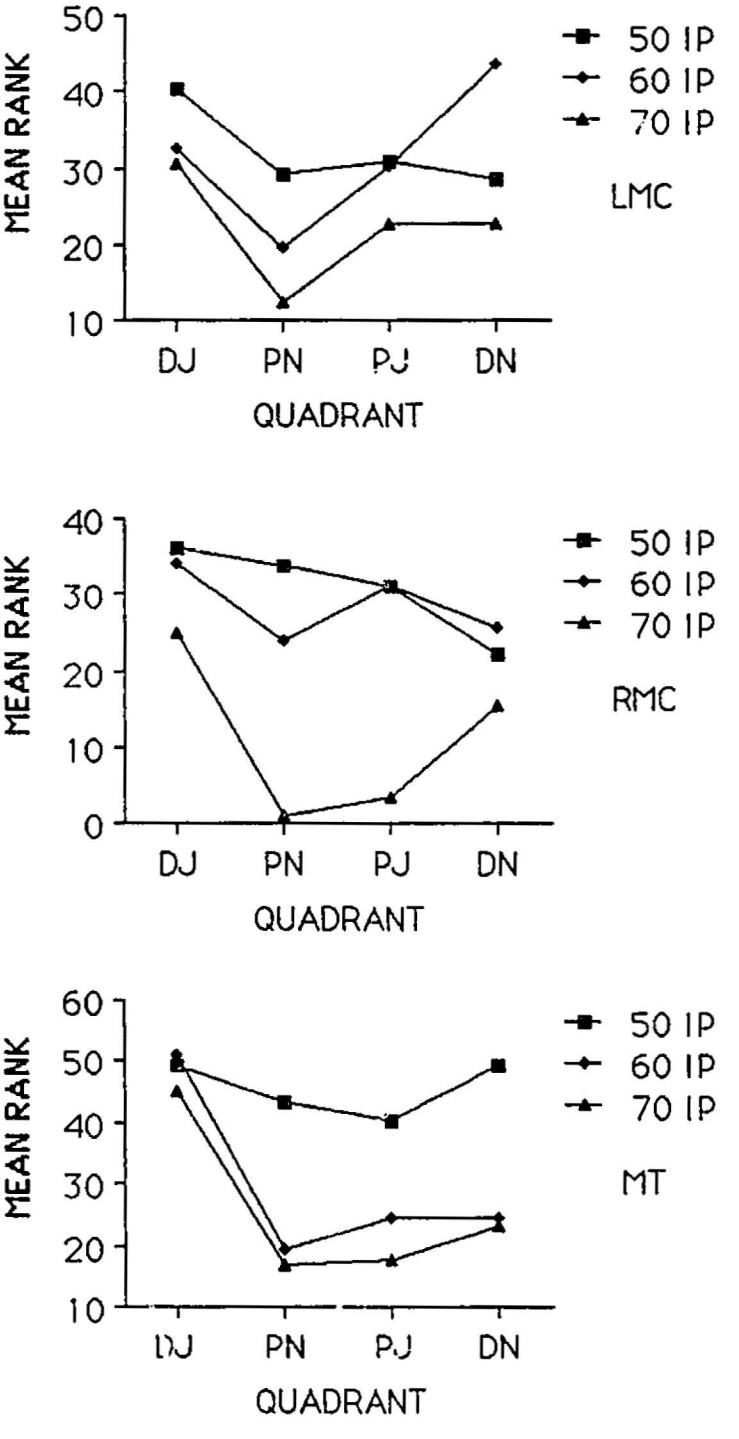

Figure 5.5. Plot of incidence table values for IP.

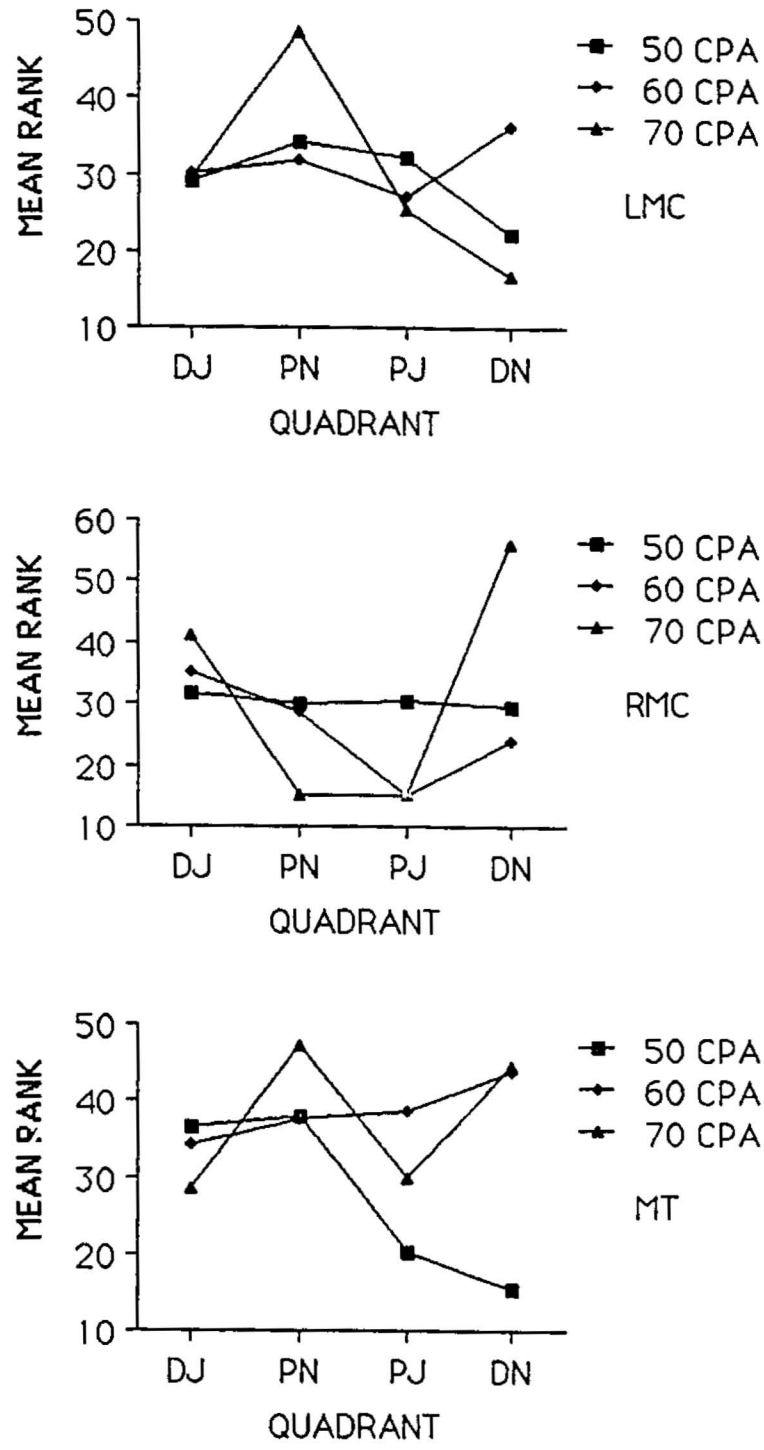

Figure 5.6. Plot of incidence table values for CPA.

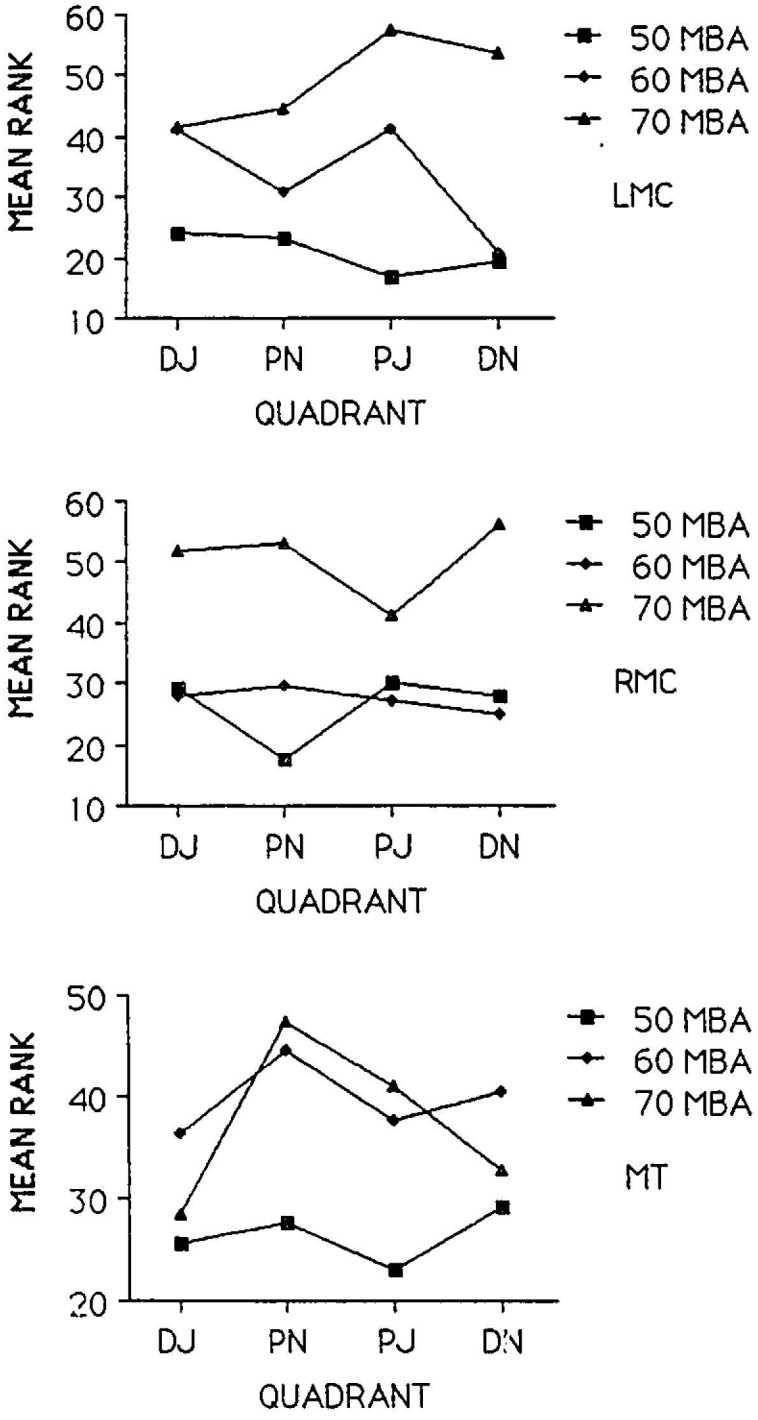

Figure 5.7. Plot of incidence table values for MBA.

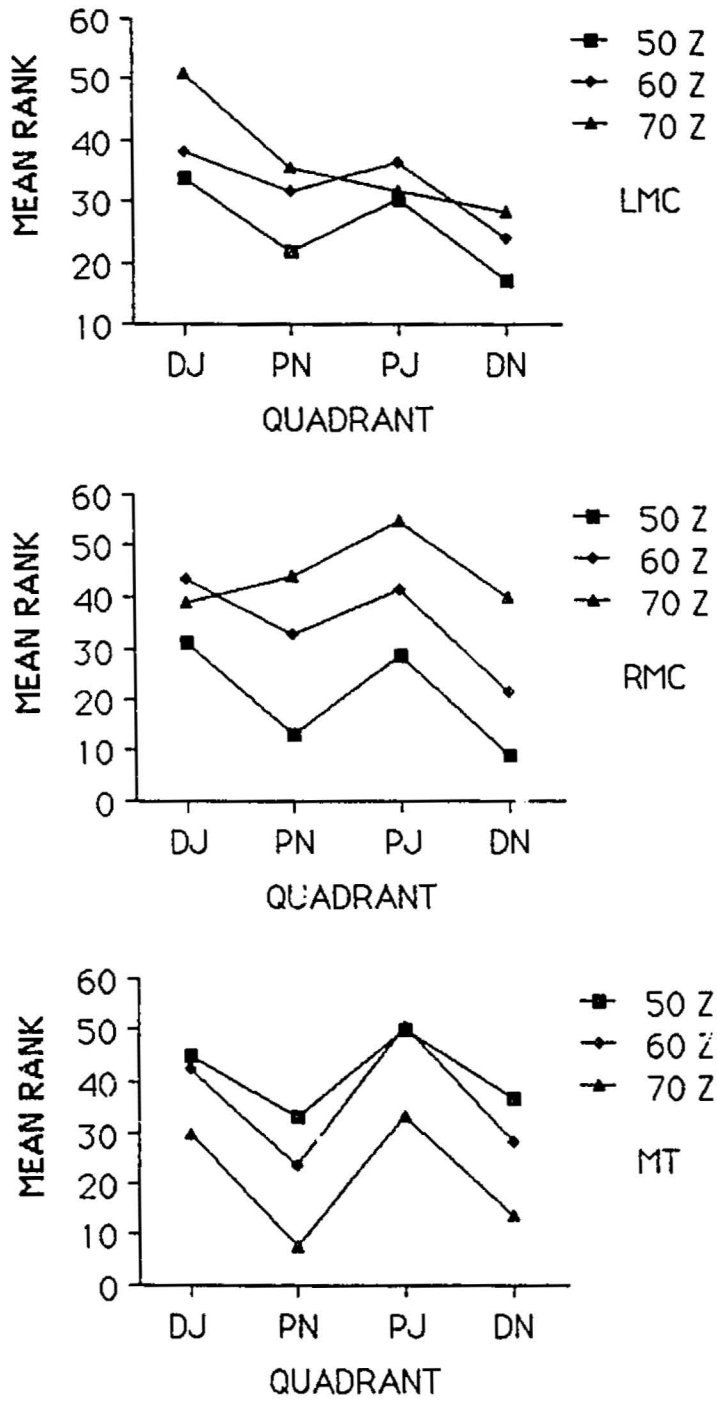

Figure 5.8. Plot of incidence table values for Z.

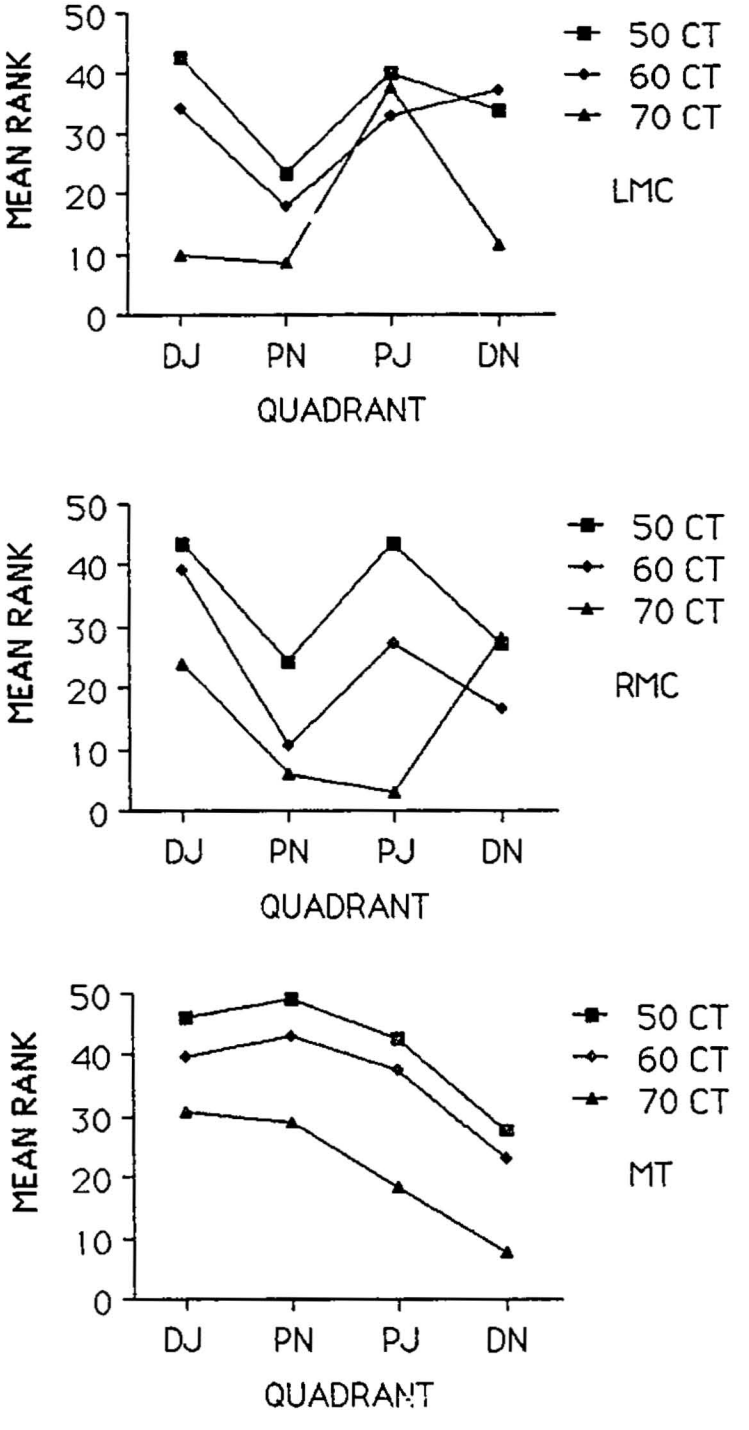

Figure 5.9. Plot of incidence table values for CT.

5.3 Geometric-Densitometric Relationships

The strength of association between the geometric and densitometric variables, and between the densitometric variables from different quadrants, was evaluated using Kendall's rank-order correlation coefficient, tau. While this measure gives conservative estimates of association (i.e., lower values than Spearman's rho, for example) it is the more appropriate nonparametric measure when tied values are common (Norman and Streiner, 1986). Ties were particularly prevalent for the variable CPA, in which a number of quadrants exhibited no recent new periosteal bone formation. This analysis was carried out using male cadaver data, cohorts combined. Based on similarities discovered in the preceding analyses, the metacarpal 50 % and 60 % location data were combined, as were the metatarsal 60 % and 70 % location data. This was done to ensure an $n > 10$ for all correlations, permitting significance to be determined against the normal approximation (Sokal and Rohlf, 1969), using values for a two-tailed test. As elsewhere, $\alpha = \leq 0.1$, in this case against H_0: tau = 0.

5.3.1 The Correlation Matrices

Given their interdependency, it is not unexpected that the majority of geometric variables reveal large positive correlations among themselves (Tables 5.12 to 5.14). Exceptions to this generalization are, for metacarpals: (1) MA versus CA (both sides), and Imax (RMC only); and (2) Imin/Imax versus all others. For metatarsals, the exceptions are: (1) MA versus all others, and (2) Imin/Imax versus CA and Imax, in addition to MA. Of interest is the suggestion that in the hand bones, size and shape, the latter represented by the ratio of the two principal moments of area and the former by TA through J, seem to be independent, while in the foot this is not the case: more circular sections possess significantly larger total areas, in addition to a greater resistance to torsion and to bending perpendicular to the major axis, Imin.

The majority of significant geometric-densitometric associations within quadrants occur for the variables section modulus and cortical thickness. This again is not surprising as both of these quantities are de facto measures of bone size (i.e., are not actual densitometric quantities, but are

included under this heading since they were evaluated on a per quadrant basis). For the most part, the remaining ('true') densitometric variables (IP, CPA and MBA) reveal few significant correlations with gross bone geometry, with a few noteworthy exceptions. In the LMC, Intracortical Porosity within the medial quadrants DN and PJ possess relatively large positive correlations with all geometric measures save for CA and the Imin/Imax ratio, many being significant at $p \leq 0.1$. In the RMC, CPA within the PJ (mediopalmer) quadrant is inversely related to geometry, significantly so for MA, Imin, J and Imin/Imax; while MBA within the PN (lateropalmer) quadrant reveals a number of significant positive correlations. These variable-quadrant 'patterns' are asymmetrical, i.e., they do not appear in the opposite metacarpal. As with geometry, the densitometric variables are independent of shape, with only 4/40 metacarpal correlations, and 3/20 metatarsal correlations significant.

There are relatively few significant correlations within quadrants among the densitometric variables, IP versus MBA excepted. However, between quadrants (e.g., DJ versus PJ, DN or PN; PJ versus DN or PN; DN versus PN), a greater number of significant correlations are evident. For example, in the RMC, the variables IP, MBA, Z and CT all possess significant, positive tau values for the two lateral quadrants DJ and PN; similarly, all variables are significant for the two medial quadrants, DN and PJ (IP, MBA, Z and CT being positive, and CPA negative). A similar pattern occurs for both the MT and LMC, albeit more weakly expressed in the latter. Interestingly, in all bones the densitometric variables generally possess weak correlations when quadrants along an axis (i.e., major = DJ versus PJ, minor = DN versus PN) are compared, the section modulus singularly excepted.

Figures 5.10 to 5.15 depict relationships of particular interest to the mechanism for continuing periosteal apposition relative to porosity and mineral density, in terms of the Mechanostat model.

In all bones and in all quadrants save one (MT DJ), an inverse relationship exists for Intracortical Porosity and MBA (Fig. 5.10). This means that more porous quadrants tend to be younger (that is, composed of more recently formed bone substance) than less porous quadrants. Such a relationship is consistent with variation in the rate of bone turnover. When

remodelling is high, a larger number of resorption spaces and forming osteons of lower mineralization should result. When remodelling is inhibited, fewer forming osteons should occur and the compact bone which is present should be more fully mineralized.

Figure 5.11 shows the relationship of CPA to the section modulus, Z, and suggests the following tendency for periosteal new bone formation. In the left metacarpal, CPA is inversely related to Z on laterally oriented surfaces, positively on medial surfaces. In the foot bone, CPA on the dorsal and medial surfaces are positively correlated, and the plantar and lateral surfaces negatively so, with the section modulus. A yet different pattern appears for the RMC, with CPA increasing in conjunction with Z dorsally, but decreases with larger values of Z in the palmer half of the axis. Indeed, it is evident in all bones that the association between these variables is reversed along both axes; i.e., if positive/negative at DJ or DN, it will be negative/positive at PJ or PN, respectively. Since Z, for any given load and assuming equality of properties such as bone density and porosity, reflects the level of stress, and thus of strain, at the bone's surface (Wainwright et al., 1981), the above findings argue that strain magnitude is not accurately reflected by measures such as the section modulus, Z. This would be the case if variables such as porosity and mineral density varied among quadrants, which they do; such variation is not accounted for in the determination of Z, but could significantly affect strain levels.

Figures 5.12 and 5.13 explore the relationship between the modelling (CPA) and remodelling (IP, MBA) densitometric variables. Under a strict interpretation of the tenets of Frost's Mechanostat, an inverse relationship is expected: tissue strain sufficient to elicit periosteal modelling (CPA) should inhibit intracortical and endocortical resorption and formation, and CPA should be absent when strain falls to a level which promotes intracortical bone turnover and endocortical expansion (Jee et al., 1991; Li and Jee, 1991). Thus, CPA would be associated with lower IP and greater MBA, i.e., tau should be negative for CPA versus IP and positive for CPA versus MBA. However, as discussed in chapter 3, if might also be expected that, since CPA represents new bone formation, it will of its own accord reduce MBA since it is less mineralized than the subjacent tissue. Thus, a negative relationship

for CPA and MBA might also be anticipated. Such a result could be expected for quadrants having thin cortices, since a given volume of CPA constitutes a greater proportion of the matrix from which MBA is calculated.

While generally insignificant, Figure 5.12 reveals a number of instances in which CPA varies directly with porosity, thus contravening the strict Mechanostat model. However, it is possible for CPA and IP to be positively associated, given that increases in IP produce lower bone mass, and a resulting increase in tissue strain for any given load (Schaffler et al., 1990; Viceconti and Seireg, 1990). If CPA occurs in response to such an overstrain, then CPA should vary directly with IP: this in fact constitutes the Mechanical Compensation model described in chapter 3. The pattern for CPA versus MBA (Fig. 5.13) adheres to Mechanostat expectations for the metacarpals (the RMC in particular), although all of the MT results run contrary to them. However, the MT cross-sections are quite thin, and the negative CPA-MBA association logically follows from the argument given previously.

Particular relationships between MA, and both CPA and IP are also postulated. CPA versus MA should possess negative tau values, if strain that induces periosteal expansion concurrently inhibits endocortical expansion. However, a similar argument can be made for CPA and MA as for CPA and IP: expansion of the medullary cavity reduces bone mass, and presumably will engender larger strains in the remaining tissue. These strains may elicit a CPA modelling response; therefore, a positive correlation between these variables would not be totally unexpected. At the same time, porosity and medullary area should be positively correlated, since both are actively increased in response to reduced strain levels.

Figures 5.14 and 5.15 depict the tau values for these variables obtained in this study. For the most part, expectations based on the Mechanostat are confirmed: for CPA versus MA, negative tau values predominate (i.e., the expansion of MA has not, for the most part, lead to a modelling response). However, the relationship between IP and MA is less clear: the LMC results are entirely consistent with expectations; but both the MT and the RMC results show directional patterning. In the MT, the adjacent dorsal-medial quadrants (DJ and PN) alone comply with the model, while in the RMC the only the two medial quadrants, DN and PJ, are in agreement.

Table 5.12. Left Metacarpal Ta((Matrix (* p ≤ 0.1).

Variable	TA	CA	MA	Imin	Imax	J	Imin/ Imax	DJ IP	DJ CPA	DJ MBA	DJ Z	DJ CT
TA	1.0											
CA	.641*	1.0										
MA	.538*	.179	1.0									
Imin	.923*	.615*	.564*	1.0								
Imax	.872*	.615*	.513*	.795*	1.0							
J	.974*	.667*	.513*	.897*	.897*	1.0						
Imin/Imax	.077	-.077	.128	.154	-.051	.051	1.0					
DJ IP	.256	.205	.154	.231	.333	.282	-.410*	1.0				
DJ CPA	-.242	-.333	-.272	-.272	-.272	-.242	.212	-.212	1.0			
DJ MBA	.051	-.051	.154	.128	.077	.026	-.103	-.128	-.061	1.0		
DJ Z	.462*	.615*	.359*	.538*	.436*	.487*	.051	.077	-.182	.077	1.0	
DJ CT	0.0	.205	-.308	-.026	.077	.026	-.256	.128	.363*	.077	-.128	1.0
PJ IP	.323	.065	.555*	.348*	.297	.297	.090	.194	-.350*	.090	.297	-.477*
PJ CPA	.113	-.049	.081	.049	.178	.113	.016	.210	.134	-.210	-.210	.178
PJ MBA	-.026	-.026	.128	.051	.051	0.0	.179	-.154	.091	.308	.051	.154
PJ Z	.718*	.564*	.410*	.795*	.590*	.692*	.103	.179	-.061	.231	.487*	.128
PJ CT	.231	.538*	-.128	.205	.308	.256	-.282	0.0	-.030	-.051	.462*	.154
DN IP	.462*	.256	.564*	.538*	.436*	.436*	.154	.282	-.242	.128	.436*	-.179
DN CPA	.307	.307	.016	.340	.275	.340	.178	-.146	.286	.243	.113	.437*
DN MBA	-.154	.103	-.359*	-.179	-.128	-.128	-.154	-.282	.061	.179	-.128	.385*
DN Z	.641*	.538*	.385*	.718*	.513*	.615*	.282	.103	-.030	0.0	.615*	-.051
DN CT	.179	.385*	-.128	.205	.154	.205	.231	-.205	-.091	-.051	.154	.308
PN IP	-.103	-.065	.013	-.039	-.090	-.039	-.400*	.374*	-.228	-.090	-.142	-.142
PN CPA	-.357*	-.271	-.157	-.300	-.271	-.328	.043	.157	.118	-.385*	-.243	-.014
PN MBA	-.026	-.128	.077	.051	-.051	.051	.385*	-.154	.030	.205	.205	-.103
PN Z	.538*	.590*	.333	.615*	.462*	.564*	.333	0.0	-.030	.051	.718*	0.0
PN CT	.077	.282	-.179	.103	.051	.103	.077	-.103	.151	-.103	.103	.308

Table 5.12. cont'd. Left Metacarpal Tau Matrix (* $p \leq 0.1$).

Variable	PJ IP	PJ CPA	PJ MBA	PJ Z	PJ CT	DN IP	DN CPA	DN MBA	DN Z	DN CT
PJ IP	1.0									
PJ CPA	.081	1.0								
PJ MBA	-.258	-.194	1.0							
PJ Z	.284	.097	.103	1.0						
PJ CT	-.052	-.065	-.026	.256	1.0					
DN IP	.335	-.162	.255	.436*	-.051	1.0				
DN CPA	-.277	.102	.307	.469*	-.016	.081	1.0			
DN MBA	-.387*	-.226	.256	-.128	.256	-.436*	.324	1.0		
DN Z	.310	.065	.026	.718*	.282	.513*	.226	-.256	1.0	
DN CT	-.206	.129	.077	.256	.231	0.0	.291	.308	.231	1.0
PN IP	.195	.016	-.219	.013	-.116	.090	-.277	-.245	-.090	-.271
PN CPA	-.187	.450*	.128	-.300	-.128	-.128	-.198	-.128	-.243	-.128
PN MBA	.206	-.259	.077	.154	.026	.051	-.162	0.0	.231	.077
PN Z	.206	-.129	.179	.615*	.282	.564*	.162	-.103	.795*	.333
PN CT	-.103	.194	-.231	.154	.231	-.205	.421*	.154	.179	.282

Variable	PN IP	PN CPA	PN MBA	PN Z	PN CT
PN IP	1.0				
PN CPA	-.043	1.0			
PN MBA	-.258	.171	1.0		
PN Z	-.258	-.228	.282	1.0	
PN CT	-.516*	-.114	-.026	.128	1.0

Table 5.13. Right Metacarpal Tau Matrix (* $p \leq 0.1$).

Variable	TA	CA	MA	Imin	Imax	J	Imin/ Imax	DJ IP	DJ CPA	DJ MBA	DJ Z	DJ CT
TA	1.0											
CA	.462*	1.0										
MA	.436*	-.103	1.0									
Imin	.872*	.436*	.462*	1.0								
Imax	.769*	.641*	.256	.641*	1.0							
J	.949*	.513*	.385*	.821*	.821*	1.0						
Imin/Imax	.026	-.205	.333	.154	-.205	-.026	1.0					
DJ IP	-.168	.013	-.090	-.039	-.090	-.168	.219	1.0				
DJ CPA	.107	.107	.160	.187	.080	.107	.027	.081	1.0			
DJ MBA	.179	.154	.077	.205	.154	.128	-.077	-.103	.187	1.0		
DJ Z	.487*	.308	.385*	.359*	.462*	.487*	-.026	-.310	.347*	.282	1.0	
DJ CT	.205	.436*	-.051	.231	.282	.205	.051	.026	0.0	.103	.256	1.0
PJ IP	-.051	-.128	.154	.026	-.077	-.051	.103	.129	-.107	-.051	-.256	-.282
PJ CPA	-.314	-.105	-.384*	-.454*	-.175	-.349*	-.559*	.070	-.327	-.070	-.349*	-.210
PJ MBA	.103	.231	-.051	.128	.179	.051	-.051	.026	-.160	.410*	.051	.179
PJ Z	.538*	.410*	.282	.462*	.564*	.538*	-.026	-.310	.027	.231	.487*	.513*
PJ CT	-.256	.231	-.513*	-.231	-.077	-.256	-.308	.026	.214	.256	-.103	-.128
DN IP	.039	-.065	.245	.116	.013	.039	.168	.247	-.121	-.116	-.271	-.065
DN CPA	0.0	.032	-.096	.032	.032	-.032	.032	.097	.433*	.480*	.128	0.0
DN MBA	.103	.282	-.205	.128	.128	.051	0.0	.026	.107	.308	.051	.077
DN Z	.436*	.205	.436*	.410*	.359*	.436*	.231	-.206	.187	.231	.692*	.205
DN CT	-.026	.410*	-.385*	.051	.051	-.026	.077	.258	.027	.128	-.077	.308
PN IP	-.205	.026	-.308	-.128	-.128	-.205	0.0	.490*	-.214	-.205	-.667*	-.026
PN CPA	.271	.471*	-.128	.271	.328	.271	-.100	.503*	-.134	-.100	-.214	.157
PN MBA	.487*	.359*	.231	.410*	.462*	.487*	-.077	0.0	.027	.385*	.487*	.051
PN Z	.615*	.333	.462*	.590*	.590*	.615*	.154	-.232	.214	.308	.615*	.333
PN CT	-.231	.154	-.436*	-.256	-.051	-.231	-.231	-.206	-.294	-.128	-.179	.359*

Table 5.13. cont'd. Right Metacarpal Tau Matrix (* $p \leq 0.1$).

Variable	PJ IP	PJ CPA	PJ MBA	PJ Z	PJ CT	DN IP	DN CPA	DN MBA	DN Z	DN CT
PJ IP	1.0									
PJ CPA	.140	1.0								
PJ MBA	-.026	.140	1.0							
PJ Z	-.205	-.524*	.154	1.0						
PJ CT	-.026	.140	.128	-.205	1.0					
DN IP	.658*	.299	.065	-.116	-.168	1.0				
DN CPA	-.128	-.436*	0.0	.096	.288	-.193	1.0			
DN MBA	-.333	-.419*	.385*	.103	.282	-.413*	.352*	1.0		
DN Z	-.103	-.245	.103	.436*	-.308	-.077	0.0	-.051	1.0	
DN CT	-.051	-.175	.051	.026	.359*	.026	.448*	.205	.026	1.0
PN IP	.333	.140	.026	-.308	.231	.413*	-.032	-.128	-.564*	.205
PN CPA	.185	.175	.300	-.071	.157	.330	-.232	.043	-.157	.300
PN MBA	-.154	.035	.410*	.333	-.103	-.181	-.128	.256	.487*	-.026
PN Z	-.128	-.559*	.128	.718*	-.231	-.103	.032	.077	.718*	.051
PN CT	-.103	.105	.256	.128	.154	-.232	-.064	.205	-.179	.179

Variable	PN IP	PN CPA	PN MBA	PN Z	PN CT
PN IP	1.0				
PN CPA	.471*	1.0			
PN MBA	-.410*	.143	1.0		
PN Z	-.436*	-.057	.462*	1.0	
PN CT	.103	.143	-.026	-.103	1.0

Table 5.14. Left Metatarsal Tau Matrix (* $p \leq 0.1$).

Variable	TA	CA	MA	Imin	Imax	J	Imin/ Imax	DJ IP	DJ CPA	DJ MBA	DJ Z	DJ CT
TA	1.0											
CA	.636*	1.0										
MA	.018	-.345	1.0									
Imin	.818*	.527*	-.018	1.0								
Imax	.745*	.745*	-.164	.564*	1.0							
J	.927*	.709*	-.055	.745*	.818*	1.0						
Imin/Imax	.527*	.236	.055	.709*	.273	.455*	1.0					
DJ IP	.220	.220	.294	.183	.183	.220	.110	1.0				
DJ CPA	.039	.078	-.156	0.0	-.078	.039	.156	-.157	1.0			
DJ MBA	.273	.200	.091	.382	.164	.273	.164	.128	-.097	1.0		
DJ Z	.636*	.345	.164	.527*	.600*	.564*	.382	-.092	-.175	.127	1.0	
DJ CT	.236	.309	-.236	.200	.200	.236	.200	-.055	.019	-.273	.236	1.0
PJ IP	.309	.236	-.236	.200	.273	.382	.055	-.128	.331	-.127	.309	.491*
PJ CPA	.112	.187	-.187	.224	.075	.112	.449*	.038	-.040	-.337	.112	.262
PJ MBA	-.309	-.091	-.127	-.200	-.200	-.236	-.127	.055	-.175	.273	-.455*	-.273
PJ Z	.491*	.200	.164	.382	.382	.418*	.236	-.165	-.097	-.018	.709*	.382
PJ CT	.382	.600*	-.455*	.200	.564*	.382	.055	-.202	.097	.018	.382	.273
DN IP	.127	.200	-.200	.018	.164	.127	-.127	.055	-.097	-.600*	.127	.600*
DN CPA	.019	-.170	.208	.057	-.208	-.019	.170	.210	-.020	-.283	-.057	.208
DN MBA	.164	.309	-.236	.273	.200	.164	.200	-.055	.019	.527*	.018	-.164
DN Z	.600*	.236	.200	.636*	.418*	.527*	.491*	-.128	-.058	.164	.818*	.273
DN CT	.564*	.564*	-.273	.527*	.455*	.491*	.382	.055	.214	.127	.418*	.164
PN IP	.183	.037	.037	.073	0.0	.110	-.073	.148	.354	-.294	.110	.367
PN CPA	-.183	-.220	0.0	-.220	-.110	-.183	-.147	-.593*	.039	.073	.037	-.367
PN MBA	.055	.127	-.127	.164	.091	.055	.164	-.018	-.057	.636*	.055	-.055
PN Z	.600*	.236	.273	.636*	.418*	.527*	.564*	.018	.019	.091	.745*	.345
PN CT	.382	.236	-.091	.418*	.273	.309	.345	-.275	-.058	-.055	.673*	.491*

Table 5.14. cont'd. Left Metatarsal Tau Matrix (* $p \leq 0.1$).

Variable	PJ IP	PJ CPA	PJ MBA	PJ Z	PJ CT	DN IP	DN CPA	DN MBA	DN Z	DN CT
PJ IP	1.0									
PJ CPA	.112	1.0								
PJ MBA	-.564*	-.243	1.0							
PJ Z	.382	.056	-.600*	1.0						
PJ CT	.200	.168	-.127	.236	1.0					
DN IP	.382	.206	-.382	.273	.091	1.0				
DN CPA	.170	.136	-.170	.132	-.397*	.170	1.0			
DN MBA	-.309	-.131	.527*	-.273	.273	-.418*	-.321	1.0		
DN Z	.345	.243	-.491*	.745*	.200	.091	.057	-.018	1.0	
DN CT	.164	.056	-.164	.273	.455*	.127	-.057	.236	.309	1.0
PN IP	.514*	.113	-.587*	.183	.073	.477*	.038	-.330	.147	.037
PN CPA	0.0	-.226	.073	.110	.037	-.330	-.229	.037	0.0	-.110
PN MBA	-.273	-.168	.418*	-.236	.236	-.382	-.359	.600*	.018	.127
PN Z	.345	.243	-.491*	.673*	.200	.164	.208	-.091	.855*	.382
PN CT	.418*	.393*	-.491*	.600*	.418*	.236	-.094	-.018	.709*	.309

Variable	PN IP	PN CPA	PN MBA	PN Z	PN CT
PN IP	1.0				
PN CPA	-.407*	1.0			
PN MBA	-.385*	-.018	1.0		
PN Z	.165	-.128	.018	1.0	
PN CT	.385*	-.055	-.055	.564*	1.0

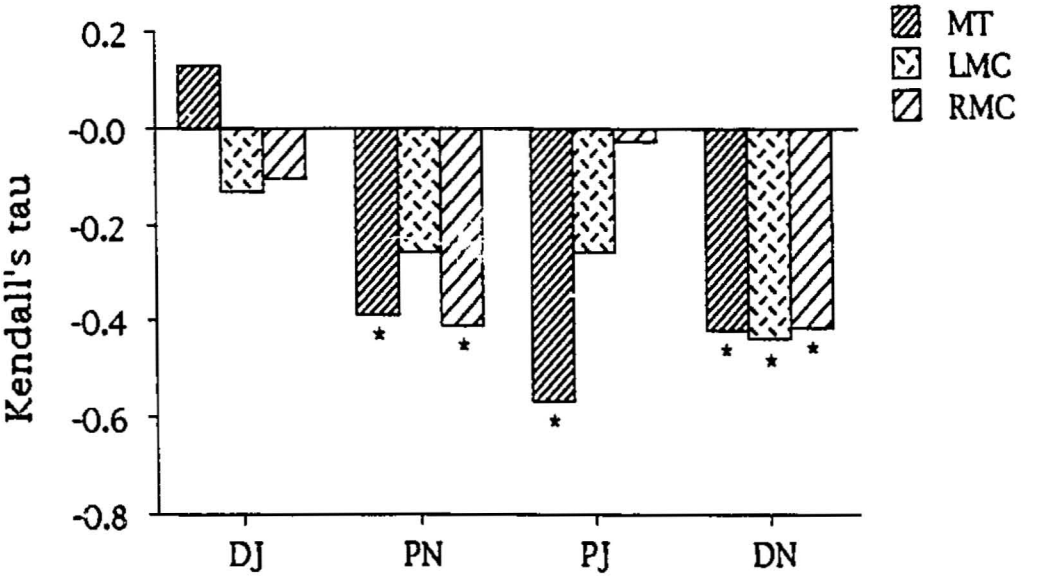

Figure 5.10. Kendall's tau, IP versus MBA (= significant, $p \leq 0.1$).*

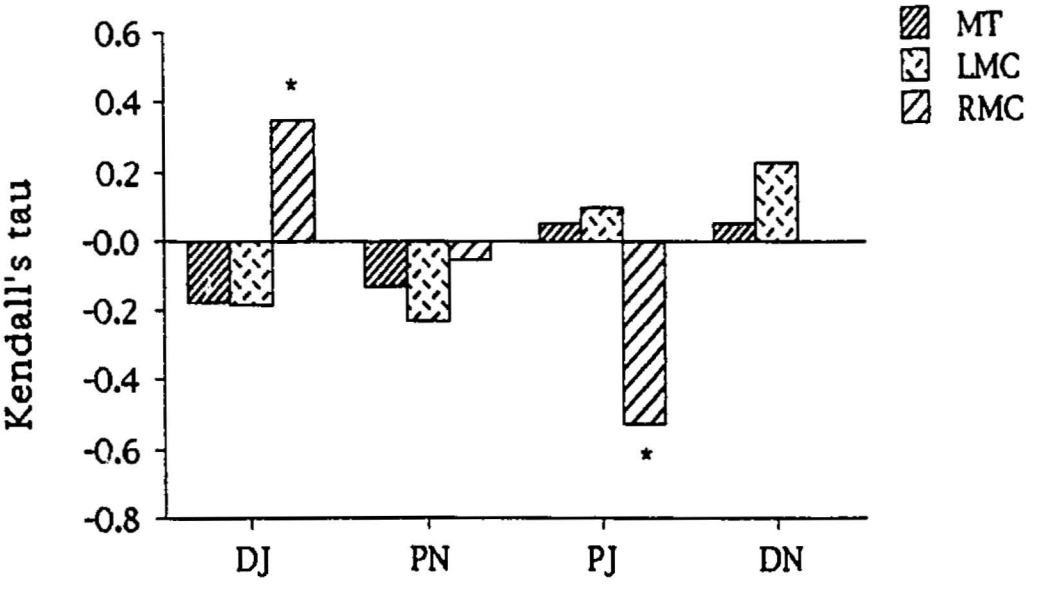

Figure 5.11. Kendall's tau, CPA versus Z (= significant, $p \leq 0.1$).*

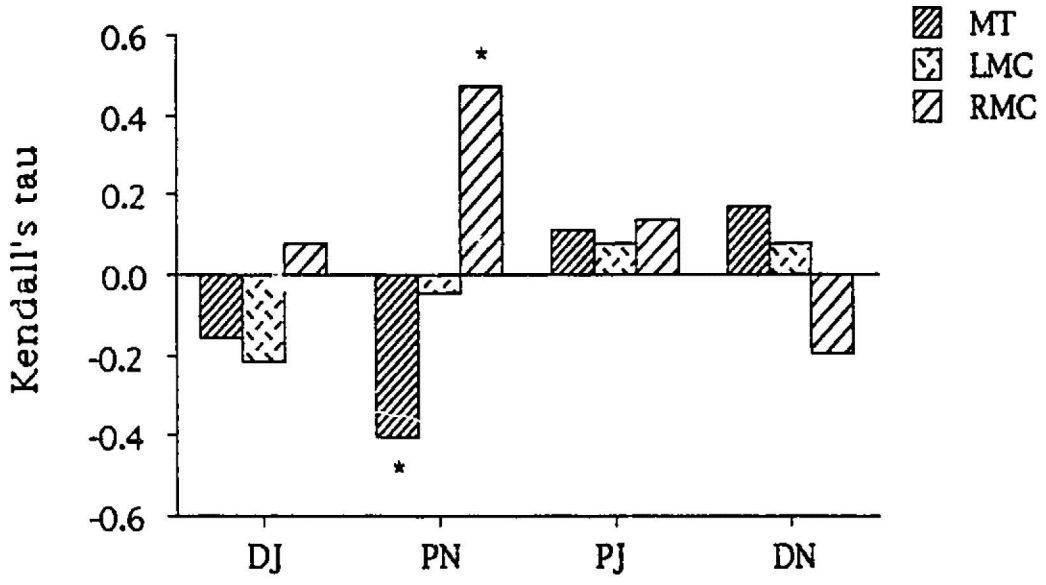

Figure 5.12. Kendall's tau, CPA versus IP (= significant, $p \leq 0.1$).*

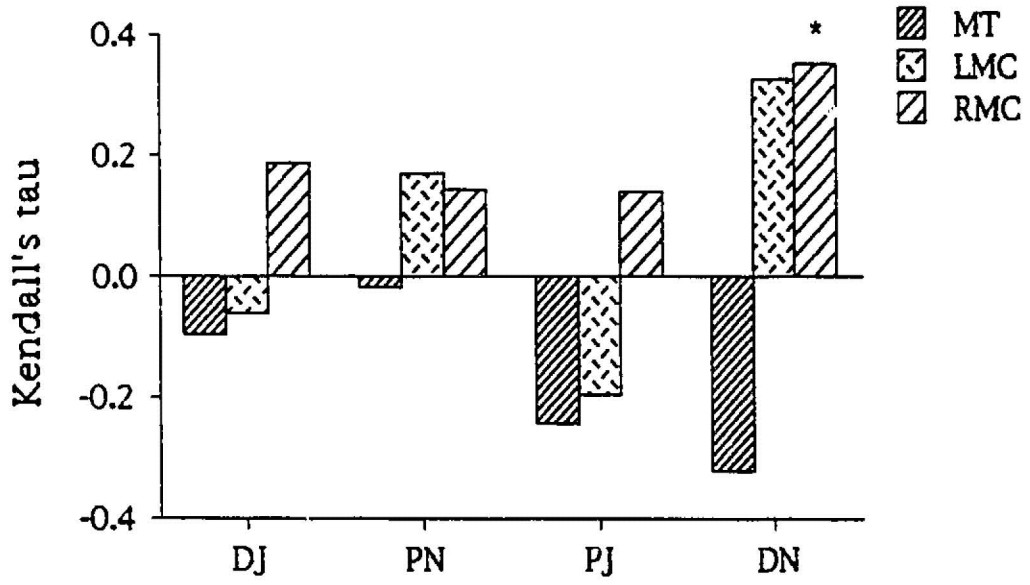

Figure 5.13. Kendall's tau, CPA versus MBA (= significant, $p \leq 0.1$).*

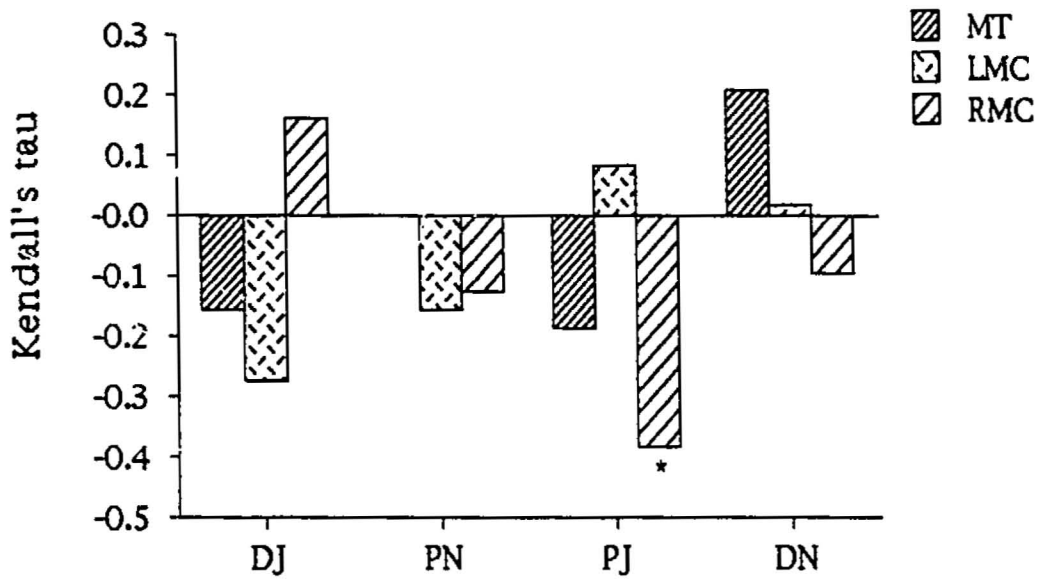

Figure 5.14. Kendall's tau, CPA versus MA (= significant, $p \leq 0.1$).*

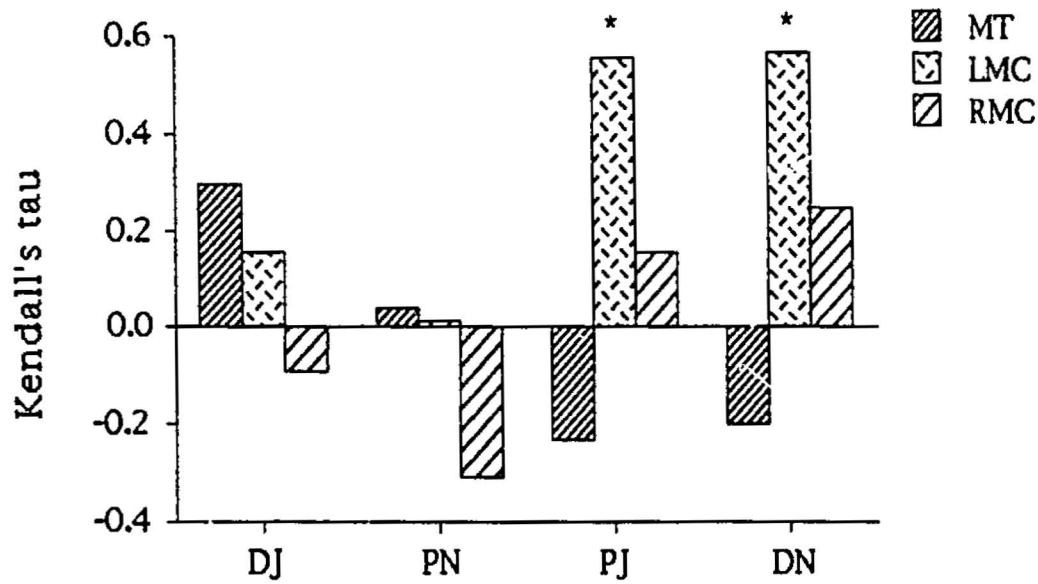

Figure 5.15. Kendall's tau, IP versus MA (= significant, $p \leq 0.1$).*

5.4 Summary of Results

A. Geometry:

1. The dissecting room sample possessed larger metacarpal dimensions, medullary area excepted, and smaller metatarsal dimensions. There were no significant differences in shape (Imin/Imax).

2. For metacarpals, there were no significant directional differences with regard to cohort membership, except that older individuals had larger medullary areas, and smaller cortical areas. In the metatarsal, older individuals consistently had larger values, often significantly so. This did not occur when the female data were considered separately: older members of this subsample were smaller. Younger cohort MTs and LMCs were rounder than those of the older group; alternatively, a tendency for greater circularity was evident in older, rather than younger, RMCs.

3. Males had larger metacarpals than females for all variables except medullary area; females generally had significantly larger metatarsals. Females tended to have rounder bones than males. Many MC comparisons were significant; however, most MT comparisons were not so.

4. The right metacarpal was typically larger than the left. The shape index showed no significant side dimorphism, nor was a predominant directional difference evident for this variable.

5. Most variables revealed significant intra-element variation; in the metacarpals, the most distal location (70 %) was involved, while in the metatarsal it was the midshaft (50 %) location. Within the shaft, significant shape differences were expected and noted.

B. Densitometry:

1. For the metacarpal comparisons, cadavers exhibited larger values for almost all variables, with the exception of intracortical porosity. Less than half the comparisons were significant.

2. There was a general absence of significant age-related differences for all comparisons. Older individuals tended to have larger values than younger, especially in the metacarpals.

3. In an analysis restricted to the MT and the RMC, males were shown to have thicker cortices and larger section moduli; females more porosity, CPA and lower MBA.

4. The RMC exhibited larger values than the LMC for all but one of the significant differences. Only the PN quadrant revealed a consistent directional difference (right > left), for all variables and both section locations.

5. The two-way Anova (level x quadrant) showed that differences within variables occurred between levels, and to a lesser extent among quadrants. Few significant F-ratios were found for metacarpal porosity or CPA, and no significant interaction effects for any of the variables.

C. Correlation Analysis:

1. With few exceptions, the geometric variables are significantly and positively intercorrelated (negatively for those comparisons involving medullary area). The size and shape of metacarpals were found to be independent; in metatarsals this was not so, as more circular sections tended to have greater compressive, bending and torsional rigidity.

2. Within quadrants, the majority of significant geometric-densitometric correlations involved the size variables Z and CT; few significant correlations occur between geometry and porosity, CPA or MBA.

3. The densitometric variables were, for the most part, independent of shape.

4. A greater number of significant correlations among densitometric variables occurred between, rather than within, quadrants, so long as the two quadrants do not share one of the principal geometric axes.

5. A definite inverse relationship was found between intracortical porosity and mean bone age within quadrants, consistent with bone turnover rate.

6. The expected positive relationship between CPA and the section modulus, Z, was not found in a majority of quadrants, and likely reflects the fact that Z is not an accurate reflection of periosteal strain, failing to take full or partial account of factors such as medullary expansion, nor the lower

mineralization and increase in porosity which may have accrued from prior remodelling activities.

7. While mostly nonsignificant so far as strength of association was concerned, the direction of correlation for CPA-MBA, CPA-MA and MA-IP offered qualified support for Frost's Mechanostat model, although not all quadrants complied with expectations. However, the direction of association for CPA-IP departed from expectations, with the majority of quadrants showing positive values. It is possible that this result reflects the adverse effect porosity has on tissue strength and stiffness, leading to higher levels of strain and an increased probabilty of CPA.

CHAPTER 6. SUMMARY AND CONCLUSIONS

6.1 The Functionally Adapted Skeleton

Varying interpretations of the functionally adapted skeleton can be found in the literature, e.g., "Bone morphology represents a dynamic compromise between structural and metabolic criteria: through adjustments of form and mass the skeleton must achieve sufficient strength to accommodate the demands of activity, yet retain the advantages of tissue economy..." (Rubin et al., 1990b:43); or "Bone structure represents an optimum balance between the cost of excessive bone mass and the cost of excessive bone fragility." (Turner, 1991:203); or "(Bone) mass is costly in terms of the energy required for its construction and transport, and for the time taken to produce it. Therefore, there must generally be a balance between the mass of the structure and its mechanical virtues." (Currey, 1984d:S7). Certain underlying themes implicitly or explicitly invest all such interpretations: (1) there exists, at least theoretically, some optimal configuration of skeletal structure and the location and progression of bone cellular activity through which a balance is achieved among the skeleton's various demands and obligations; (2) maintaining this balance requires that bone size and/or shape be modifiable in light of altered circumstances, i.e., that skeletal morphology is a dynamic rather than a static proposal; (3) the altered circumstances leading to modification in bone mass and distribution may originate at the local (e.g., biomechanical) and/or systemic (e.g., biochemical) levels. As described in chapter 3, the processes through which this balance is obtained and maintained are modelling and remodelling (Martin and Burr, 1989), and there are numerous theoretical constructs which attempt to reconcile the operation of these processes with known or presumed mechanical and metabolic regulation. As yet, no single body of theory accommodates all known adaptive bone modelling/remodelling behaviour.

In attempting to derive an interpretive framework from which to investigate Continuing Periosteal Apposition (CPA) in particular, this

this dissertation has focussed on aspects of two middle-range theories, the principal one being Frost's Mechanostat, to which one particular feature of Cowin's Adaptive Elasticity model has been appended.

The Mechanostat proposes that a physiological range of typical peak strain exists within which the skeleton can be deemed functionally adapted, i.e., little or no (re)modelling occurs and all demands are satisfied. There is considerable support for the basic tenets of Frost's Mechanostat model, particularly the view that modelling and remodelling are antagonistic in both effect (gain versus loss) and stimulus (over- versus understrain, respectively; Martin and Burr, 1989). Cowin's Adaptive Elasticity model proposes-among other things-that the critical strain range leading to cellular activation is not uniform throughout the skeleton, but is 'site specific'. Consequently, rather than stipulating specific strain setpoints for the activation of (re)modelling, no numerical values are assigned to these lower and upper equilibrium limits, the labels E^- to E^+ serving in their place. This lack of standardization in the critical strain range ventures the possibility that, for a given strain experience, one bone surface might undergo modelling or remodelling, while another would remain quiescent. Given this possibility it can be argued that skeletal elements usually considered 'non-weight-bearing' (e.g., the second metacarpal: Ruff and Hayes, 1988) might adhere to Mechanostat expectations in the same manner as, e.g., the femur, but in response to a quantitatively different mechanical loading history.[1]

---

[1] There is experimental support for this view. In reviewing their previous work involving experimentally modified functional loading of the avian ulna, Rubin et al. (1990b) note that strains within the physiologically normal range often resulted in substantial new bone formation (modelling). Since the osteogenic stimulus was not an 'overstrain' in the strict sense, the response must have occurred as a result of the registered strain being recognizably different from the habitual strain. It was also noted that sites of new bone formation did not correspond to areas experiencing the peak strain magnitude (i.e., the largest strains). Presumably, given the absence of bone formation, these areas would have been within their strain equilibrium window, while the sites at which bone formation occurred would have been

Excluding biochemical modulation of strain perception (i.e., alteration of setpoint values), departures from typical or habitual equilibrium strain ranges might occur through a variety of behavioral shifts, including changes in the quantity, quality or aptitude of activity performance (the latter as a product of degraded neuromuscular coordination). Such shifts may be the outcome of normal aging and/or different lifestyles, with the differences originating in gender or residence/occupation (viz. urban industrial versus rural farming). Acting alone or in combination, these changes would result in a modified cross-section geometry (size/shape) and/or histology (i.e., intracortical porosity, MBA, CPA). Indeed, under the E^- to E^+ Mechanostat model, variation in geometry and histology within a sample of bones connotes the existence of functional variation, although not necessarily suggesting the precise nature of the change(s): quantity and/or quality and/or aptitude (the last perhaps most difficult to infer). However, interpretation of differences in geometry or histology between different skeletal elements (e.g., left versus right metacarpals) presents a more formidable challenge: are they due to differences in functional loading or to the two elements having dissimilar equlibrium strain ranges? This question remains unresolvable pending additional experimental studies. While not assuming equivalent equilibrium strain ranges for different skeletal sites, this study does assume that variation in geometry and/or histology at any given skeletal site derives from variation in functional strain history.

6.2 Summary

A number of significant differences have been noted in comparisons involving samples classified according to source, age, sex and side, although many others lacked significance as a result of inadequate sample size and/or small effect size for the measured variables. Larger functional strains were expected: (1) in the right rather than the left metacarpal;[2] (2)

---

beyond their local equilibrium window, although at strain levels below the peak strain.

[2] Perhaps especially since the samples employed consisted of older rather than younger individuals: Plato et al. (1984) noted a cohort effect

in males rather than females; (3) in younger rather than older individuals; and (4) in historic rather than contemporary lifestyles. Accepting that departures from the habitual strain range (E^- to E^+) will elicit a response, as documented in considerable experimental work, e.g., Raab et al., (1991), expectations based on the Mechanostat would be that the less vigorous individuals within a comparison will tend to exhibit more remodelling effects (larger medullary areas, smaller cortical areas and moments of area, lower MBA, less CPA and greater intracortical porosity), and that the converse individual would manifest effects associated with modelling (larger total areas and moments of area; more CPA, less porosity, greater MBA).

These expectations were generally realized in the present study. For instance, pertaining to remodelling: (1) female, older and left metacarpals had larger medullary areas, smaller cortical areas, and greater porosity than male, younger and right metacarpals; (2) cadaver and older metatarsals met expectations with regard to medullary area and cortical area; however, the older metatarsals tended to be less porous than those from younger individuals, although not significantly so; (3) the female metatarsal had a larger medullary area and greater porosity than that of males, a result which was expected; however, they also had larger total areas and as a result, larger cortical areas.

One comparison that consistently countered expectations involved the historic metacarpal. A larger medullary area, smaller cortical area, and greater porosity compared to the cadaver bones is evident. Although the combination of character states remains intact so far as Mechanostat expectations are concerned, the predicted direction is reversed. A possibile explanation is that the larger medullary area and greater porosity of historic hand bones might reflect post-depositional changes, such as fungal destruction of the cortex at the intracortical or endosteal surfaces (Hanson and Buikstra, 1987). However, the histology of these bones does not support such an interpretation, either for these particular elements or for

---

for hand dominance in a BLSA sample, with older individuals exhibiting significantly lower frequencies of left-handedness.

other tissue samples (e.g., of long bones) obtained from the same skeletons prepared for histological age estimation (Lazenby et al., 1991).

Expectations pertaining to modelling are more difficult to define. Modelling effects (larger total areas, greater bending and torsional rigidity) should characterize groups living more vigorous lifestyles (presumptively, the historic, male, younger and right metacarpal subsamples). However, because remodelling lowers both bone mass and stiffness, it contributes to an increase in strain within the remaining tissue (Schaffler et al., 1990; Viceconti and Seireg, 1990), possibly beyond the local E^{+}. In other words, bones of a seemingly more 'sedentary' disposition might also be expected to show modelling effects, in particular CPA, as a result of such mechanical compensation (see Table 3.7). In the present study, we might expect such an occurrence for the cadaver, female, older and left metacarpal samples. However, recent experimental work by Rubin et al. (1990a) suggests that the modelling response may be impaired by aging. Their older animals-in this case male turkeys-failed to show a periosteal response to altered dynamic loading, while the younger animals did. This lack of response likely reflects a failure to recognize the load-induced strain as 'appropriate'. In terms of the Mechanostat, age-related changes might have modified the setpoint values in the older birds. In the present study, with samples comprised of primarily older individuals, modelling activity as measured by CPA tended to be greater in the cadaver metacarpals (the right side especially), in older right metacarpals, in female metacarpals, in male metatarsals; and in the right rather than the left hand. Thus, there is evidence that either age has not imparied this potential in humans, or that strain was of a sufficient magnitude to overcome any change in setpoint values. It was also found that larger total areas and greater structural rigidity characterized older bones, especially the metatarsal. More specifically: cadaver metacarpals, historic metatarsals, male metacarpals, female metatarsals, and the right side in both sexes all had larger cortical geometric properties. Such effects might reflect recent modelling activity or, also likely, the existence of large peak bone masses associated with young adulthood.

Table 6.1. Summary of conformance to 'Mechanostat' expectations, for those groups presumed to have experienced the less vigorous lifestyle.

Group	Modelling Suite[1]	CPA[2]	RemodellingSuite[3]
cadaver MC	no	yes	no
cadaver MT	yes	na	yes
old MC	no	no[4]	yes
old MT	no	no[4]	yes (except IP)
female MC	yes	yes	yes
female MT	no	no[4]	yes (except CA)
left MC	yes	no	yes

1. Smaller TA, Imin, Imax and J.

2. Greater CPA, due to overstrain associated with decreased bone mass.

3. Smaller CA, larger MA, greater IP, lower MBA.

4. See text for explanation of these results.

na = condition not evaluated.

Table 6.1 summarizes the results obtained in terms of whether or not Mechanostat expectations were met. The cadaver versus historic results can be explained if we assume that a fundamental distinction between the historic sample and the (principally male) cadaver sample occurs with regard to mobility, but not manipulation. The results obtained would be consistent with an assumption that the more recent group was less mobile, in terms of walking or running. The (re)modelling changes expected on the basis of reduced activity levels are not seen in the metacarpals, however. The higher CPA response found in the cadaver group, while itself generally not statistically significant, contributed to significantly larger geometric properties such as Imax, TA, etc. This suggests that the recent group benefitted from a somewhat greater modelling response to functional overstrain, consistent with Mechanostat expectations.

The fact that older cohort bones agreed with Mechanostat expectations so far as remodelling effects were concerned, but not for modelling effects, could account for the negative CPA results. In spite of the expected greater loss of bone mass via endocortical resorption and increasing intracortical

porosity, the remaining tissue may have been of sufficient robusticity (possessing larger total area and greater structural rigidity-perhaps from prior periosteal apposition no longer identifiable in microradiographs) that a recent CPA response was not necessary. A similar argument applies to the female metatarsal, where large values for TA and Imin etc. also occurred.

The female metacarpal results suggest that hand activities were insufficient to maintain strain within the equilibrium range, resulting in a remodelling-based bone mass deficit at the endocortical and intracortical surfaces. Their lower size-standardized measures of structural strength (e.g., TA, Imax, Imin) relative to males might reflect a typical low peak bone mass for this sex. The expected outcome would be a greater propensity for CPA as a compensatory mechanism to intermittent excursions beyond E^+, which indeed seems to be the case. This latter result, consistent with Mechanostat theory, runs contrary to results obtained from studies of long bone geometry (Martin and Atkinson. 1977; Ruff and Hayes, 1988) which identified a female deficit for structural compensation to lower bone mass.

Although the left metacarpal conforms to Mechanostat expectations for both modelling and remodelling expectations, on the presumption of a lower level of functional strain, CPA appears to favor the right metacarpal. Indeed, the relative structural strength deficit for the LMC (e.g., lower values for variables such as total area, Imin, Imax and J) may reflect the fact that CPA as a response to functional overstrain in the right metacarpal would effectively increase all of these properties. The fact that cortical area was also significantly larger in the RMC, that porosity was lower and that MBA was greater (for most comparisons) suggests that the CPA observed resulted from experience of an activity-induced overstrain, rather than through a reduction in bone mass and tissue stiffness associated with the accumulation of remodelling effects. While some studies have reported little side dimorphism in the metacarpal (e.g., Adams et al., 1970), most demonstrate a bias towards larger right versus left bones (e.g., Plato and Purifoy, 1982; Kimura, 1990a, cited in Kimura, 1990b). This suggests that side asymmetry is related to hand dominance, given the propensity of right-handedness in human populations. The inference that metacarpal bone size is to a large degree functionally determined is supported by studies such as

Plato and Purifoy (1982), who found that in left-hand dominant individuals, the 'right > left' difference was rendered nonsignificant. Recently, Roy et al. (1991), in a further study of male and female BLSA participants, reported on the relationship of functional hand dominance to second metacarpal bone size. In males they observed that, irrespective of side, significantly larger values for Total Width, Medullary Width, Cortical Area and an estimate of bending strength about the mediolateral axis were all associated with hand dominance.

6.3 Conclusion: CPA, Adaptation and Mechanical Compensation

As stated in the opening chapter of this study, a principal objective of the research was to consider whether or not CPA could serve as mechanical compensation for the reduction in structural strength associated with expansion of the medullary cavity and increased intracortical porosity. Such a reduction in bone mass and strength has been most often uniquely associated with aging, and indeed a massive clinical literature exists documenting a decline in bone tissue associated e.g., with age-related changes in endocrine function (Type I osteoporosis). However, given the current state of theoretical development in skeletal biology and biomechanics (e.g., Cowin, 1989a; Frost, 1989a-d; Martin and Burr, 1989) an equally legitimate interpretation would equate reduced bone mass with reduced mechanical loading, either independent of age, or consequent to age-related declines in physical activity (Type II osteoporosis). Recognition of this fact allows for comparison of samples contrasted along lines other than age which might differ with regard to their respective mechanical loading histories, such as the sex, side, or source comparisons explored in this study. It is thus possible to test what is essentially the same hypothesis in a series of different models.

In chapter 3 of this study, it was demonstrated theoretically that Continuing Periosteal Apposition is capable of maintaining or restoring a state of functional adaptation in the 'structurally-challenged' skeleton. In at least one case, female metacarpals, it appears that newly deposited lamellar bone at the periosteal surface-CPA-occurred consequent to endocortical and intracortical bone loss. This finding is consistent with an hypothesis of

mechanical compensation. The regulation of mechanical compensation is described as a special case of Frost's Mechanostat theory, which also received support in comparisons of cadaver versus historic, and right versus left, metacarpals.

The results obtained are not consistent with existing alternative hypotheses. For example, the cohort effect hypothesis (Trotter et al., 1968), as the sole explanation for larger dimensions in older individuals, is negated by the histological demonstration of newly deposited lamellar bone in elderly adults. Parfitt's (1984) 'fracture repair' hypothesis fails to account for the fact that CPA appears to occur preferentially in one sex (e.g., the female metacarpal) or on one side of the body (e.g., the right metacarpal). This latter result is especially significant since both left and right elements would be subject to the same systemic effects (e.g., hormonal changes) that could affect interindividiual comparisons. Neither is the implicit null hypothesis tenable: that CPA is nothing more than a non-adaptive corollary of aging, cf. a mild albeit randomly diffuse hyperostosis. The fact that CPA occurs variously throughout the skeleton, but not necessarily consistently in a given location, is evident from the literature review. However, this does not mean that CPA is nonadaptive, i.e., that it 'just is'. As discussed in chapter 3, the distribution of CPA throughout the skeleton, under the interpretation offered above, would simply reflect unique juxtapositions of strain equilibrium ranges (E^- to E^+) and activity profiles. The adaptive nature of CPA would be assured by demonstrating its absence in elements subject to minimal or no functional strain. Such bones have not yet been identified in humans to my knowledge, though e.g., the ethmoids and/or ear ossicles may be candidates.

Clearly, the research offered in this dissertation does not purport to be the last word on the subject. Future studies dealing with issue of Continuing Periosteal Apposition should rigorously consider e.g., the distribution of the process throughout *individual* skeletons; its relationship with parameters such as peak bone mass; its manifestation in other (primate) species; and its relationship with variation in the equilibrium strain range.

Appendix 1: CPA in the Craniofacial Skeleton

Longitudinal studies of living populations, primarily using lateral cephalometric data, and cross-sectional studies of archaeological samples using craniometric data, have documented age-related size change in a number of skull dimensions (Table A1). Both sexes have been included in these analyses, although often not within individual studies. Israel (1973a) gives a concise review of investigations prior to 1960.

Two early studies of white males, aged 22 to 34 years, reported significant increases for four of five vertical, and five anteroposterior, measurements (Thompson and Kendrick, 1964; Kendrick and Risinger, 1967). These studies were carried out on a series of 71 paired lateral cephalographs, taken one year apart. Israel (1967, 1968, 1970, 1973a,b, 1977, 1979) has provided the most comprehensive documentation for continuing age-related alteration of skull dimensions. His data primarily derive from selected lateral cephalographs of participants of the Fels Longitudinal Study. His 1968 paper reported cranial data from 43 males and 53 females, with a mean interval between recording episodes of ca. 18 years. All subjects were 24 years of age or older when first examined. In this study, 11 midsagittal cranial measurements were taken: five thicknesses, two diameters and four intersutural distances, involving both the inner and the outer vault tables. Seventy-five to 97 % of male and female subjects showed significant ($p \leq 0.01$) increases of about 6 % in thickness and 3 % in diameter. The magnitude of gain was found to be poorly correlated with either the age of the subject at initial exposure or the interval between exposures (with the exception of female ectocranial diameter versus age, $r=0.29$, $p \leq 0.05$). Israel hypothesized that reducing measurement error may be required in order to resolve the issue of age and/or interval length to the magnitude of change. The most anterior and most posterior locations for cranial thickness measurement showed the least increment in both sexes, and females had the largest absolute mean increments at four of the five

locations. Israel concluded that size increase was likely a combination of periosteal apposition and intersutural growth.

Comparable cranial data were provided by Israel (1973a, 1977) using additional subjects drawn from the Fels study group. While a generalized expansion of 4 % to 5 % was manifested in a variety of skull dimensions, those specific to vault thickness, sinus size and sella turcica area showed an increase of approximately 10 %, leading Israel (1977) to conclude that adult skull growth follows a dichotomous pattern.

Israel's results were criticised by Tallgren (1974), primarily on methodological grounds. Specifically, Fels cephalographs prior to 1964 had been taken without the benefit of a headholder, a device designed to minimize inadvertent systematic positioning errors. In theory, increasing the distance between the film and the mid-sagittal plane of the head could result in the symmetrical enlargement reported by Israel in his 1968 and 1973 papers. Tallgren provided cephalometric data on 32 Finnish women, spanning an interval of 15 years. For 33 variables descriptive of skull size, results indicated "no significant changes in neurocranial size or skull thickness", although "in half of the subjects a slight appositional thickening in the glabella region of the frontal was noted" (p. 289). Israel's 1977 paper was, in fact, a response to Tallgren's criticism, and from his perspective the existence of a dichotomous pattern of craniofacial expansion removed "the likelihood that improper radiographic methods spuriously manufactured a biological phenomenon" (p. 52). This would seem to be a reasonable conclusion. It should also be noted that Tallgren's sample had a much older mean age, which may have mitigated the potential for a significant result.

An important study documenting cranial CPA is that of Kokich (1976), who undertook a radiographic, histological and gross examination of the bony region around and including the frontozygomatic suture in a series of 61 cadavers aged 20 to 95 years. Apart from documenting the patency of this suture through the 10th decade of life, Kokich also observed several layers of new, unremodelled, lamellar bone covering the facial periosteal surface at all ages, interspersed with 'resting' lines indicative of intermittent activity. The orbital periosteal surface, however, was seen to be resorptive over the adult period. With advancing age the thickness of the facial

lamellar zone decreased and the subperiosteal regions became progressively remodelled with Haversian systems. This would suggest that the process responsible becomes less active with age, a finding consistent with that of Epker and Frost (1966) in the rib.

Macho (1986) analyzed data for 13 craniometric variables, consisting of 10 linear and three angular dimensions. These were obtained from lateral cephalographs of a cross-sectional sample of 154 males and 199 females aged 21 to 83 years; and trends in metrical change among five 10-year age cohorts were compared by analysis of variance. In both sexes, four of 13 variables (two angles, two chords) had significant F-ratios, three of which decreased in magnitude with advancing age. Within each sample, two additional variables indicated significant reductions in cranial size between the third and ninth decades of life. Macho (1986: 58) suggests that a secular trend may be the 'causal' factor underlying her results, particularly with regard to reductions in neurocranial height. She cites two studies (Morita and Ohsuki, 1973; Facchini and Gualdo-Russo, 1982) which had previously reported secular decremental change in head dimensions in samples of Japanese and Italian adults.

A recent longitudinal study, however, substantiates the existence of adult craniofacial size increase. Behrents (1985) analyzed 524 paired lateral cephalographs from 163 participants (age range 17 to 83 years) of the Bolton-Brush Growth Study. Throughout all ages, continuing growth of the craniofacial complex was observed. However, while Israel (1973a) argued that the 'symmetrical enlargement' he measured represented a uniquely adult relationship between the neurocranium and viscerocranium, Behrents suggested that his observations indicate a pattern of adult growth "similar to typical adolescent alterations but of lesser magnitude and rate" (p. 315). Consequently, both size and shape changes were noted. Interestingly, in the young adult period the direction of continuing growth was individually dependent upon the direction of growth present through the period of late adolescence. That is, "'horizontal growers' grew horizontally and 'vertical growers' grew vertically" (p. 315). In late adulthood, however, all subjects experienced vertically-directed growth. A further distinction between the two studies is reflected in the magnitude of female growth. In Behrents'

sample, women showed less adult growth than men, while in Israel's group the females had absolutely larger increases (e.g., in cranial vault thickness). It is unclear why such fundamental differences should exist between the two data sets. A partial explanation may lie in the fact that Behrents' study included individuals of middle to late adolescent age, whereas Israel purposely excluded all participants who were less than age 24 at first examination. In spite of specific differences in patterns or magnitude of change, the majority of available longitudinal data supports the existence of continuing growth of the adult craniofacial complex.

Forsberg (1979) studied dimensional change in lateral cephalographs of 25 male and 24 female dental students over a ten year interval, from a mean age ca. 24 years to ca. 34 years. Twenty-seven linear and angular measurements of the skeletalprofile were taken using a digital-electronic apparatus to reduce method error. Significant increments were noted in vertical height measurements, primarily associated with the lower face; and significant (in females, nearly so in males) decrements were noted in lower anteroposterior dimensions associated with the mandibular profile. Sutural growth as a mechanism for vertical height change was discounted, with Forsberg arguing that such growth would have ceased prior to the mean age at onset for his study. This suggestion disagrees with Kokich's (1976) histological finding for the frontozygomatic suture. While Forsberg (1979: 22) acknowledges the occurrence of CPA (citing both Epker and Frost, 1966 and Garn et al., 1967), he suggests that "this apposition is normally very slight and is not likely to give any measurable change on a cephalogram during a 10-year period". Rather than posit CPA, Forsberg argues that the changes noted in his study are more likely a result of a posterior rotation of the mandible, due to tooth eruption and occlusal positioning (particularly of the 3rd molars). This would have the effect of both lengthening the lower face vertically, and shortening it in the A-P plane. Behrents (1985) noted that in his male sample forward rotation of the mandible occurred; yet vertical height increments, rather than decrements, were still observed. Still, the possibility that positional changes among structures, rather than actual growth changes within structures, contributes to dimensional change deserves consideration. For example, Behrents' (1985) female subjects

showed posterior mandibular rotation and greater vertical height change than males, in accordance with Forsberg's (1979) hypothesis.

Two cross-sectional craniometric studies have been undertaken using archaeological samples with the specific intent of testing the hypothesis of adult skull growth. Ruff (1980) analyzed a data set of 16 variables, collected by Snow (1948) on a series of 136 adult male skulls from Indian Knoll, Kentucky. Based upon morphologically estimated ages, a young (mean age of 28.6 years) and an old (38.4 years) cohort were compared. Fourteen of the 16 dimensions were larger in the older group, six of which were significant ($p \leq 0.05$). The fact that cranial vault thickness showed a larger percentage increase than other dimensions (e.g., those pertaining to height and length) led Ruff to conclude that, as in Israel's samples, the Indian Knoll males showed a dichotomous pattern of expansion. Furthermore, as all of the significant differences were positive (larger in the older group), Ruff argued that the adult growth observed reflected size rather than shape change. This conclusion, of course, presumes that the differences are of a similar relative magnitude, in addition to having the same sign (i.e., positive incremental change).

Heathcote (1986) reported data for 80 variables from 187 adult male crania collected from sites in Alaska, the Yukon Territory and southern Ontario. These were arranged into three age cohorts (young, middle and old adults) on the basis of published age estimates or estimates made by Heathcote. All ages were based on tenuous 'cranioscopic' criteria (e.g., suture closure). Fourteen of the 80 variables showed significant age-regression, with the majority of these pertaining to the facial skeleton. Contrary to Ruff's study, however, not all of the changes were incremental. While 11 of the measurements did increase significantly, one decreased (basion to nasal border point length) and two first increased and then decreased with advancing age (basion to prosthion length and the prosthion radius). This pattern suggested to Heathcote that the conventional wisdom of ectocranial deposition and endocranial resorption was over-simplified, and that age-related craniofacial growth indicated the presence of more complex remodelling processes. Heathcote (1986: 87) suggests that adult growth changes in the skull "may be processually continuous with the

complex remodelling changes of childhood" (cf., Behrents, 1985). While substantiating dimensional change in the lateral plane, the cross-sectional craniometric studies are important for also demonstrating growth in other planes, which is not possible to achieve from lateral cephalographs. In Ruff's 1980 study, for example, two of five skull breadths (bizygomatic breadth; bigonial breadth) increased significantly in the older Indian Knoll cohort.

In the lower jaw, Israel (1973a) reported data on six mandibular dimensions which increased with age. All concerned aspects of the horizontal and ascending ramus. One of these, gonial angle, was also measured by Ruff, and constituted one of the 'two major discrepancies' among the set of nine comparable measurements for the two studies (the remainder concerned the two cranial chords: sagittal and frontal). The smaller increment in gonial angle obtained by Israel[1] was ascribed to measurement error engendered by growth in bigonial breadth, documented by Ruff (1980) but not measurable in Israel's lateral cephalographs. Ruff argued that enlargement of the breadth dimension would foreshorten the radiographic image of the lateral mandibular body, thereby minimizing or eliminating any increase in gonial angle. While possible, it might also be the case that a sex-effect may be confounding the comparison, since the Fels study measured females and the Indian Knoll study measured males. In a later study, Israel (1979) published mandibular data from the Terry and Todd collection. In these 90 white male specimens, three body widths taken at, above and below the mandibular foramen, and one ascending ramus width were found to increase significantly over the four decade period. An approximate increase of 2 % per decade was noted.

Israel (1967) provided data of a different sort pertinent to mandibular body growth in adults. A cross-sectional sample of 119 males and 94 females, aged 6 to 64 years, was measured for four mandibular heights in the region of the second premolar. These were (1) jaw height from the

---

[1] There is a reporting error in Israel's (1973a) Table 6. The published figure of a 4 % increase in gonial angle should be 0.31 %, based on the 'raw' data given in the same table. Ruff (1980, Table 2) cites this value as 0.4 %, as calculated by him from the differences between the younger and older group means published by Israel.

alveolar crest to the mandibular base; (2) tooth-bearing bone height, from the alveolar crest to the root apex; (3) basal bone height, from the root apex to the inferior border of the horizontal ramus; and (4) cortical bone thickness, at the mandibular base below P_2. Those dimensions inclusive of the alveolar crest were found to decrease through the adult age range, while those which were exclusive of the alveolus at the 2nd premolar increased. Israel (1967:1727) concluded that "Even though loss in jaw height is demonstrated here, it cannot be construed to mean that the loss is shown to be the result of either periodontal disease or age change alone, it is probably the sum of both".

Whittaker (1985) has argued that much of what is generally interpreted to be alveolar bone loss due to chronic inflammatory periodontal disease (CIPD) is actually an artifact of continuous tooth eruption in response to attrition. Whittaker examined the premolar and molar dentitions of 500 skulls from the Romano-British Poundbury site (ca. AD 300). Dental attrition (as an estimator of age, cf. Brothwell, 1963), position of the alveolar crest, position of the root apex, position of the cemento-enamel junction (CEJ), and position of the inferior mandibular border were ascertained. The various positional attributes were measured with regard to the inferior alveolar canal, considered to be a stationary point of reference. It was found that, with increasing age the distance from the inferior alveolar canal to the lower mandibular border increased, as did the distance to the CEJ and to the root apices. However, the distance from the alveolar crest to the occlusal surface remained more or less constant, in spite of increasing amounts of attrition. It was hypothesized that as enamel is ablated, tooth eruption continues in order to maintain effective occlusal contact. This being the case, if alveolar crestal bone was being resorbed due to CIPD, the distance from the crest to the occlusal surface would increase. This was not the case in this sample, so if bone was being lost it must also have been replaced periodically. The increase in the distance between the inferior border and the inferior alveolar canal further attests to depositional events in the adult mandible.

Two additional studies deserve mention, though neither was undertaken with the expressed purpose of investigating continuing bone growth in

adults. Dahlberg et al. (1978) discuss the results of a 1968 cephalometric study of Wainwright Eskimos, undertaken as part of the International Biological Program Human Adaptability studies of circumpolar peoples. A total of 188 adult individuals (92 females, 96 males) were radiographed in *norma lateralis*, some of whom contributed multiple exposures with intervals of approximately one year. In all, 361 cephalographs were analyzed. Among the more notable age-related changes found was "an increase in all linear dimensions for both males and females" (Dahlberg et al., 1978:104).

A study with a completely different focus is that of Tappen (1983), who investigated the vermiculate pattern of the superciliary arch in Indian Knoll crania of unassigned sex. Tappen noted that the superciliary arch continued to develop with increasing age in adults, cf. Ruff's (1980) finding that the older males from this same archaeological site had a greater glabella-opisthicranion length. Tappen (1983: 535) suggests that both results "could be part of the same growth process, since the arches are adjacent to glabella and are not clearly demarcated from this measuring point".

Two of the above cranial studies provide contradictory results regarding dimensional changes in the cervical spine. Israel (1973a) measured the anteroposterior diameter of the spinal canal for C2 and C3 from his series of lateral cephalographs, noting a significant increase of approximately 4 % ($p \leq 0.05$). On the other hand, Behrents (1985:311), whose data disagree with Israel's on other points as discussed above, reported that in C3 "all dimensions (anteroposterior and vertical) [were] increasing in size, except the case of the spinal aperture which was decreasing in anteroposterior dimensions". Behrents attributed such changes to biomechanical adaptation in response to weight change and to continued adult growth. It should be noted that only Behrents' data are consistent with a process of continued apposition, i.e., the reduction of the 'negative space' of the spinal canal by bone growth on the surfaces which surround and define it. Israel's data, indicating an increase in aperture size, implies resorption on these surfaces. Vertebral body growth in C3 was noted by Israel (1973b) in a cross-sectional series of lateral cephalographs from females aged 26 to 89.4 years. A smaller (n=18) longitudinal sample was also included. While outer body

height did not change significantly, a perpendicular measure of width showed highly significant dimensional change ($p \leq 0.01$). In the longitudinal series, both height and width had increases of ca. five per cent over the interval (14 to 20 years) of observation.

Discussion

It seems clear that, at least in the craniofacial skeleton, adult skeletal growth may not be a simple matter of periosteal (ectocranial) apposition and endocranial resorption as was suggested by Garn (1981: 238) in his consideration of Israel's cephalometric data: "As bone is added to the outer side of the skull by subperiosteal apposition, the skull becomes both longer and wider...At the same time, there is resorption at the inner surfaces of the skull...Notably, there is an excess of appositional gain over resorptive loss, leading to a considerably thicker skull - especially in the older female". (The reference to increasing width is, of course, presumptive, as such change could not have been ascertained from Israel's lateral cephalographs.) The perspective offered by Garn possibly derives from Israel's (1968, 1973a) finding that endocranial and intersutural distances both increased in the older cohorts studied. Endocranial resorption would seem a reasonable supposition given the observation that internal (endocortical) resorption occurs within postcranial tubular bones with aging. However, the endocranial surface is, in fact, a periosteal surface; the diplöic space is analogous to the medullary cavity of tubular bones. Israel (1968:134) recognized this distinction, describing the cranium as a "flattened round bone", but he did not go on to consider why the two cranial tables should demonstrate opposite remodelling processes. Garn (1981: 238) suggests that endocranial resorption may serve to "leave more room for the brain within", a proposition with which Lanyon (1987:1084) would agree so far as the growth period is concerned, noting that: "It is after all the gentle pressure from the expanding brain on the cells which line the cranium and inhabit the sutures, which allows the [genetically-determined size of the] brain to control cranial capacity".

The endocranial surface may indeed be resorptive as a result of pressure necrosis. Orthopaedists have witnessed progressive osteolysis at

periosteal sites of fracture healing (ostensibly sites of active deposition) in response to extreme fixation (Treharne, 1981). However, since adult brain size is effectively reached in childhood (Young, 1971), the source of pressure-induced resorption in aging adults would have to be sought elsewhere. Data on nonpathological age-related increases in the intracranial pressure of the cerebrospinal fluid in the subarachnoid space (between the arachnoid and the pia mater) would substantiate-but not prove-this hypothesis. Depressions resulting from pressure exerted by arachnoid granulations (Pacchionian bodies), more characteristic of the aged endocranial surface, may represent foci of such a process, though these tend to be restricted to the midsagittal plane (Steele and Bramblett, 1988).

A more likely explanation for increasing endocranial dimensions would be continuous intersutural growth. This was suggested by Israel (1968-see also Kokich, 1976 regarding the frontozygomatic suture). However, Israel (1973a:124) noted that sutural obliteration characterized his study group, leaving unresolved how such a mechanism could lead to larger endocranial distances. All the same, pre-obliteration 'sutural drift', if of the right kind (i.e., away from the cranial vertex), would displace defined cephalometric landmarks and could produce the directional size change reported by Israel. Intersutural growth is characteristic of the child and adolescent cranium (Enlow, 1982), and if Behrents (1985) and Heathcote (1986) are correct in supposing adult growth to be a continuation of more youthful processes, this hypothesis would warrant investigation.

Table A1. CPA in the Adult Human Cranium.

Study	Design	Major Finding(s)
Thompson and Kendrick (1964); Kendrick and Risinger (1967)	1 year interval paired lateral cephalographs, 71 white males, aged 22 to 34, 5 vertical & antero-posterior dimensions measured	4 of the 5 vertical dimensions; and 5 of 5 anteroposterior dimensions, increased significantly
Israel (1967)	lateral-oblique mandibular radiographs, 119 males and 94 females, aged 6 to 64 years, from the Fels Growth Study (FGS)	4 measurements taken at P2 indicate growth at the inferior border of the ramus, with reduction of alveolar crest height

Israel (1968)	paired lateral cephalographs, 43 white males, 53 white females from the FGS, initially aged 24 years or older, interval range 13 to 25 years (mean ca. 18 years)	75% to 97% of male and female subject showed significant growth in 11 midsagittal dimensions
Israel (1973a)	paired lateral cephalographs from 26 white females, cf. Israel (1968), interval range 13 to 28 years (mean 19.48 years); cranial and cervical dimensions measured	41 cranial dimensions show a generalized uniform growth with few exceptions (eg., palatal length); in vertebrae, the antero-posterior diameter of the spinal canal increased with age
Israel (1973b)	vertical height and anteroposterior width measured in the 3rd cervical vertebrae in lateral cephalographs of 189 females, 26 to 89.4 years old; longitudinally in 18 females aged 24.9 to 47.8 years at 1st exposure; 41.9 to 64.8 years at 2nd exposure; minimum interval, 14 years	cross-sectional: height change was not significant; width change was highly significant; longitudinal: technical factors with respect to enlargement made interpretation problematic, though change in both height and width was observed
Tallgren (1974)	paired lateral cephalographs from 32 Finnish females, aged 20 to 73 years, interval = 15 years	no significant change noted for 32 of 33 neurocranial dimensions
Kokich (1976)	61 cadavers, aged 20 to 95 years, gross, histologic, radiographic examination of the frontozygomatic suture and adjacent bone	orbital surface resorptive, facial surface intermittently appositional at all ages, new bone layers thinner in older individuals
Israel (1977)	paired lateral cephalographs, 26 each males and females, age range 24.9 to 78.8 years, mean interval ca. 19.5 years	a dichotomous pattern of expansion observed in the 4 variables studied, for different dimensions
Dahlberg et al. (1978)	lateral cephalographs of 92 male, 96 female adult Eskimos	all linear dimensions in both sexes showed some increase with age
Israel (1979)	90 Terry and Todd collection mandibles, white males, 20 to 69 years; measured body width at 3 sites and ramus width	over 4 decades, width at all sites increased significantly, ca. 2% per decade

Forsberg (1979)	lateral cephalographs of 25 males, 24 females, initial mean age ca. 24 years, final mean age ca. 34 years; 27 linear & angular measurements of the hard tissue profile taken	vertical height changed significantly, esp. lower face; negative anteroposterior change in length of lower face, significant in females; posterior rotation of the mandible suggested causal mechanism, rather than CPA
Ruff (1980)	cross-sectional craniometry, 136 adult Indian Knoll males, grouped into young & old cohorts	6 of 16 sagittal and coronal dimensions significantly larger in the older cohort
Behrents (1985)	paired lateral cephalographs from 163 male and female participants of the Bolton-Brush Growth Study (BBGS), aged 17 to 83 years over the period of evaluation; cranial and 3rd cervical dimensions measured	growth continued through all ages, significant sex dimorphism noted with regard to vertical height and mandibular rotation patterns; in vertebrae, all anteroposterior and mediolateral dimensions increased, except spinal canal diameter
Heathcote (1986)	cross-sectional craniometry of 187 adult males from a variety of Eskimo and Indian archaeological sites	14 of 80 variables showed significant age regression, with both increases & decreases ,suggesting a complex pattern of remodelling
Macho (1986)	cross-sectional craniometric study using lateral cephalographs from 154 males, 199 females, aged 21 to 83 years	6 of 13 variables had significant age-related change, 5 of which decreased in magnitude

Appendix 2: Functional Anatomy of the Second Metacarpal and Metatarsal

The following anatomical descriptions are based primarily on Gardner and Osburn (1978), Lampe (1989), Lewis (1989), Thomas (1985) and Warwick and Williams (1973).

I. The Second Metacarpal: Osteology

Morphology: The metacarpals, numbered 1 through 5 from the lateral (radial) to medial (ulnar) side, may be classified as short, tubular bones consisting of a proximal base, an intervening shaft and a distal head. With the phalanges fully flexed, the metacarpal heads are revealed as 'knuckles'.

The 2nd metacarpal is the longest of the five, the base of which is grooved in the dorsopalmer plane to accomodate the trapezoid. The

bifacetted medial ridge articulates with the capitate and the base of the 3rd metacarpal, while the lateral edge rises dorsally to meet the trapezium. The longitudinal axis of the shaft is curved, convex dorsally and concave in its palmer aspect. A triangular expansion occupies the distal third of the dorsal surface, with the apex directed towards the midshaft, and the base adjacent to the neck, the latter is a narrow constriction just proximal to the head. The head is convex and rectangular, being longer in its dorsopalmer axis.

Ossification: The 2nd metacarpal ossifies from two centers, one primary and one secondary. The primary center for the shaft begins to ossify at about the 9th week of intrauterine life, while the secondary center for the head begins to form between 1.5 and 2.5 years (males) and ca. 2.0 years (females). Fusion of these two centers occurs around 18 years of age in males, and 15 years of age in females.

Arthrology

Joints: All joints in the hand are synovial, with the carpometacarpal and intercarpal joints of the arthrodial type, permitting only gliding motion. The metacarpophalangeal joints are condyloid, and allow more or less all angular motions except rotation. The bases of the medial four metacarpals articulate with the distal row of carpals and with one another, and the heads with the first (proximal) phalanges.

Ligaments: Proximally, the 2nd to 5th metacarpal bones are connected by dorsal, palmer and interosseous ligaments; the names indicating general location. The dorsal ligaments, crossing the carpometacarpal joint, are considered to be the strongest. The 2nd metacarpal receives two dorsal and two palmer ligaments, with the two articulating carpal bones (trapezium and trapezoid) supplying one apiece of each class. Fibres of the dorsal and palmer ligaments also pass transversely between the bases of the four medial metacarpals, assisting the interosseous ligaments in binding the proximal transverse palmer arch.

Distally, the metacarpal heads are joined by the strong bands of the deep transverse metacarpal ligaments, as well as palmer and collateral ligaments. The former ligaments maintain the distal metacarpal arch of the

palm; the collateral ligament firmly connects the head of each metacarpal to the base of its adjacent proximal phalange.

Myology

Muscles of the hand are classified as either intrinsic (I) or extrinsic (E), depending on whether they take their origin proximal or distal to the wrist. A further distinction can be made according to aspect: palmer (P) or dorsal (D). The following muscles act directly on the 2nd metacarpal: flexor carpii radialis (EP); extensor carpii radialis brevis (ED); extensor carpii radialis longus (ED); adductor pollicis, oblique head (IP); 2nd palmer interosseus (IP); 1st dorsal interosseous (ID); and 2nd dorsal interosseous (ID). Table A2 describes the origin, insertion and action of these muscles.

Principal Movements and Deformations

There are four principal movements of the hand relative to the wrist: adduction, abduction, extension and flexion. These movements also apply to the phalanges relative to the metacarpus. As noted above, there is little movement possible at the carpometacarpal and intercarpal joints, since these are constrained by a combination of irregular bony morphology and tight ligamentous connection. Although these ligaments permit some mediolateral gliding movement of the 4th and 5th metacarpals (15° and 30° respectively), little or no independent motion is afforded the 2nd and 3rd metacarpals. This stability is further supported by the flexor carpii radialis muscle proximally, and the extensor carpii radialis brevis and longus muscles, distally (see Table A2). At the metacarpophalangeal (MCP) joints, movement is much freer, with flexion, extension, abduction and adduction all possible, along with a limited degree of rotation; the 1st metacarpal excepted. It hardly bears mention that the greatest amount of movement of the latter involves flexion, contributing to the wide variety of possible 'grips' (e.g., power, precision and hook) the human hand may perform.

Given the above, the principal deformation of the 2nd metacarpal will be bending, placing the dorsal surface in tension and the palmer surface in compression. Considered as a cantilever, fixed at the proximal end and loaded across the MCP joint (e.g., by the long extensors and flexors), any bending moment should increase from the MCP joint toward the base. While

deflection will be greatest distally, deformation (strain) should increase towards the base.

II. The Second Metatarsal: Osteology

Morphology: As for metacarpals, the metatarsals are classifiable as short, tubular bones consisting of a proximal base, an intervening shaft and a distal head. Unlike metacarpals, metatarsals are numbered 1 through 5 from the medial (tibial) to lateral (fibular) side. Metatarsals 2 through 4 are most alike, being narrow with a shaft which tapers from proximal to distal ends. The dorsal surface is slightly convex; the plantar surface more strongly concave, especially towards the base. Unlike the 2nd metacarpals, the 2nd metatarsal expansion of the shaft proximal to the neck is not particularly strong. The shape of the base is like an inverted wedge, having a shallow concavity; while that of the head is rectangular, and strongly convex in the dorsoplantar direction. In humans, the second is the longest of the five metatarsals.

The 2nd metatarsal normally has four proximal articular facets, although a good deal of variation is common (Singh, 1960). The largest single facet is for the intermediate cuneiform; medially, there occurs a single superior facet for the medial cuneiform, and laterally there is one superior and one inferior facet separated by a nonarticular depression. Each of these facets exhibits two aspects, for proximal articulation with the lateral cuneiform and distal articulation with the 3rd metatarsal bones.

Ossification: There are two centers: a primary one for the shaft and a secondary center for the head. The former begins to ossify about the 9th week of interuterine life, the latter between 2 and 4 years of age, with girls somewhat advanced over boys (Garn et al., 1967, cited in Steele and Bramblett, 1988). Fusion occurs between the ages of 17 and 20.

Arthrology

Joints: All joints in the foot are synovial, with the tarsometatarsal and intertarsal joints of the plane arthrodial type, permitting only gliding

motion. The metatarsophalangeal joint is condyloid, allowing somewhat more angular motion.

Ligaments: Proximally, the articulations of the 2nd metatarsal bone are reinforced by a dorsal tarsometatarsal ligament (to the intermediate cuneiform) and by interosseous ligaments (to the medial cuneiform and 3rd metatarsal). Distally, the head is fixed to the proximal phalange by medial and lateral collateral ligaments, and to the adjacent metatarsophalangeal capsules by deep transverse metatarsal ligaments. Additionally, the plantar metatarsal ligament joins the bases of the 2nd and 5th metatarsals.

Myology

Three muscles, tibialis posterior, adductor hallucis and dorsal interosseous, have direct attachment to the 2nd metatarsal. The origin, insertion and action of each is given in Table A3.

Principal Movements and Deformations

While the 3rd metacarpal is perhaps least mobile in the hand, the 2nd metatarsal holds this distinction in the foot. Proximally, tarsometatarsal and intermetatarsal movements are essentially restricted to slight gliding, most pronounced during inversion (medial tilting) and eversion (lateral tilting) while loadbearing. Dorsiflexion and plantarflexion are also important movements so far as the 2nd metatarsal in concerned. The latter especially so, since during locomotion it involves raising the heel off of the ground (e.g., during push-off) and transference of body weight and thrust through the metatarsal heads and the great toe.

An important aspect of the force deformations of the second metatarsal concerns its position with respect to the two major arches of the human foot: the longitudinal (medial component) and transverse. These arches, not found in other primates, reflect our unique adaptation to bipedal stance and locomotion. The apex of both arches occurs towards the medial border of the foot, resulting in an inclination of the base of the 2nd metatarsal, and the distribution of static force through the talus to the calcaneal tuberosity behind, and in front through the heads of metatarsals I - V, primarily I - III (Salathé et al., 1986); the majority of stress is transmitted through the second metatarsal head.

Table A2. Muscles Acting Directly on the Second Metacarpal.

MUSCLE	ORIGIN	INSERTION	ACTION
		PALMER	
flexor carpii radialis	medial epicondyle of humerus	base of 2nd meta-carpal	flexes and abducts wrist
adductor pollicis longus, oblique head	capitate, base of 2nd and 3rd metacarpals	base of 1st phalanx of thumb, medially	adducts thumb
2nd palmer interosseous	ulnar side, palmer surface of shaft	digital expansion of the index finger	adducts finger towards the midline of hand
		DORSAL	
extensor carpii radialis brevis	common tendon, lateral epicondyle of humerus	base of 2nd and 3rd metacarpals	extends and abducts wrist
extensor carpii radialis longus	lower lateral supra-condylar ridge of humerus	base of 2nd metacarpal	extends and abducts wrist
1st dorsal interosseous	medial side of 1st, lateral side of 2nd metacarpal	extensor expansion of 2nd metacarpal	abducts index finger from hand's midline
2nd dorsal interosseous	medial side of 2nd + lateral side of 3rd metacarpal	extensor expansion of 3rd metacarpal	abducts index finger from the hand's midline axis

Table A3. Muscles Acting Directly on the Second Metatarsal.

MUSCLE	ORIGIN	INSERTION	ACTION
tibialis posterior	interosseous membrane of tibia and fibula	bases of MT II - IV, navicular, cuneiforms	principal inverter of foot
adductor hallucis	plantar surface of MT II base (oblique head); transverse meta-tarsophalangeal ligaments (transverse head)	lateral sesamoid and base of MT I proximal phalange	flexion of great toe; binds metatarsal heads and supports transverse arch
dorsal interosseous	medial and lateral shaft surfaces	base of the proximal phalange	toe flexion at MTP joint

Appendix 3. Sample Provenience and Description

Table A4. The Cadaver Sample

ID*	AGE	SEX	CAUSE OF DEATH / REMARKS	2nd MC	2nd MT
Q8801	75	M	pneumonia, prostrate carcinoma, carotid artery disease	L, R	L
Q8802	73	M	broncopneumonia	L, R	L
W8801	56	M	aspiration pneumonia; thrombic brainstem infarct; diabetes mellitus; hypertension	L	L[2]
W8802	81	M	natural causes; ht: 168 cm; wt: 59.1 kg	L	
W8803	63	M	natural causes; Huntington's chorea	R	L
W8804	80	F	cardiac arrest; arteriosclerosis	L	L
W8805	69	M	respiratory failure; progressive pulmonary fibrosis; ht: 159 cm; wt: 50 kg		L
W8806	88	F	chronic obstructive lung disease; arteriosclerosis	L, R	L
W8807	83	M	ischemic heart disease; chronic obstructive lung disease; ht: 175 cm; wt: 77 kg	L, R	L
W8808	56	M	cardiac arrest; thoracic aneurysm; generalized arteriosclerotic heart disease; ht: 185 cm; wt: 102 kg	L, R	L
W8809	62	M	coronary thrombosis; ischemic heart disease; Charcot-Marie-Tooth disease; ht:180 cm; wt:86.4 kg; *C-M-T disease affects foot muscles	L, R	L[2]
W8810	73	M	bronchopneumonia; arteriosclerosis; ht: 175 cm; wt: 75 kg	R	L
W8811	64	F	pneumonia; pancytopenia; nonHodgkin lymphoma; ht: 157 cm; wt: 52 kg	L, R	L
W8812	67	M	congestive heart failure; cardiac arrhythmia; coronary artery disease; ht: 180 cm; wt: 95 kg	L, R	L
W8813	67	M	respiratory failure; bilateral cerebral infarcts; ht: 175 cm; wt: 50 kg	L, R	L
W8814	76	M	chronic obstructive pulmonary disease; left upper lobe aspergilloma	L, R	L
T8901	65	M	acute pulmonary edema; coronary artery atherosclerosis		L
T8902	83	M	acute myocardial infarction	R	L
T8905	70	M	probable pulmonary embolism	L, R	L
T8906	66	M	pneumonia; emphysema; chronic obstructive lung disease	L, R	

T8907	85	M	pulmonary embolism; metastatic carcinoma to brain and lungs	L, R[1]	
T8908	64	M	cardiac arrest; metastatic esophygeal carcinoma	L, R	
T8909	62	M	metastatic pancreatic carcinoma	R	
T8910	65	M	arteriosclerotic heart disease	R	
T8911	49	M	probable acute myocardial infarction	L	L
T8912	71	F	cardiac arrest; possible well-healed fracture of metatarsal ≈ 27 mm from proximal end	R	L
T8913	50	M	anterior myocardial infarction;	L, R	
T8914	68	M	acute myocardial infarction	L, R	L
T8915	62	M	intracerebral hemorrhage	L, R	L
T8916	58	M	myocardial infarction	L, R	L
T8917	67	M	acute myocardial infarction	L, R	L
T8918	54	M	atherosclerosis coronary heart disease	L, R	L
T8919	60	M	cardiac arrest; ischemic heart disease	L, R	L
T9002	76	M	aspiration pneumonia	L, R	
T9005	88	F	myocardial infarction	R	
T9006	62	F	metastatic cancer	L, R	
T9012	63	M	metastatic cancer	L, R	
T9015	75	M	metastatic lung cancer	L, R	
T9016	76	F	cardiac arrest; myocardial infarction	L, R	

M = male; F = female; L = left; R = right

* Initial indicates Department of Anatomy source: Queen's University (Q), University of Western Ontario (W) or University of Toronto (T).

1. Section locations estimated with respect to the left side.
2. Bone incomplete; axes and locations estimated visually re: elements of similar size.

Table A4 cont'd. The Historic Sample

ID*	AGE	SEX	2nd MC	2nd MT
3	31	M	L, R	
4	71	M	L, R	L
6	71	M	L, R	L
7	98	F	L, R	L
8	71	M	L, R	L
11	31	F	L, R	L
14	65	M	L, R	L

Appendix 4: Osteometric Data

Table A5 summarizes the descriptive osteometric data collected (mean, sd and CV) beginning with a definition of each variable. In addition, the age and sample size for each of component of the total sample is provided.

1. Age (years): Documented for the cadaver sample by the originating institution, and recorded or estimated for the historic sample.
2. Maximum Length (mm) : This is the length measured from the most proximal to most distal points longitudinally.
3. Physiological Length (mm): Measured from the midpoint of the proximal articulation (for metacarpals, this will be in the notch separating medial and lateral 'halves') to the apex of the head, distally.
4. Proximal Width (mm): The maximum mediolateral distance on the epiphysis perpendicular to length; for metacarpals, the entire epiphysis is included, while for metatarsals the articular surface alone is measured.
5. Dorsopalmer (-plantar) Diameter (mm): Perpendicular to length, this is the shaft width measured at 50% of physiological length.
6. Mediolateral Diameter (mm): The midshaft width taken perpendicular to Maximum Length and Dorsopalmer (-plantar) Diameter.

Table A5. LMC Osteometrics (males above; females below)

	CADAVER				HISTORIC			
#	n =	MEAN	sd	CV	n =	MEAN	sd	CV
1	25	66.52	9.87	14.83	5	61.80	17.40	28.18
2	24	71.87	3.53	4.91	5	71.06	2.79	3.92
3	25	67.84	3.15	4.64	5	67.91	2.69	3.96
4	24	19.74	1.00	5.05	5	19.42	1.52	7.82
5	25	9.69	0.83	8.51	5	9.43	0.72	7.65
6	25	9.00	0.86	9.52	5	8.76	1.07	12.18
1	6	75.50	10.46	13.86	2	64.50	47.38	73.45
2	6	66.12	2.61	3.95	2	66.25	0.71	1.07
3	6	63.11	2.28	3.62	2	63.38	0.88	1.40
4	6	16.93	1.15	6.80	2	17.78	1.03	5.77
5	6	8.17	0.50	6.07	2	8.45	0.07	0.84
6	6	7.95	0.72	9.02	2	7.63	0.25	3.25

Table A5 cont'd. RMC Osteometrics (males above; females below)

	CADAVER				HISTORIC			
#	n =	MEAN	sd	CV	n =	MEAN	sd	CV
1	25	67.04	8.39	12.51	5	61.80	17.40	28.18
2	25	71.64	3.39	4.73	5	70.79	3.15	4.45
3	25	67.94	3.15	4.64	5	67.42	2.82	4.19
4	25	19.90	1.27	6.37	5	18.95	2.03	10.73
5	25	9.95	0.74	7.45	5	9.29	0.82	8.84
6	25	9.15	0.80	8.74	5	8.65	1.05	12.17
1	5	75.60	12.52	16.56	2	64.50	47.38	73.45
2	5	66.92	2.70	4.04	2	66.50	0.64	0.96
3	5	64.02	2.64	4.13	2	63.65	0.50	0.79
4	4	17.56	1.65	9.42	2	17.53	2.30	13.11
5	5	8.19	0.60	7.32	2	8.10	0.28	3.49
6	5	7.87	0.74	9.39	2	7.88	0.39	4.94

Table A5 cont'd. MT Osteometrics (males above; females below)

	CADAVER				HISTORIC			
#	n =	MEAN	sd	CV	n =	MEAN	sd	CV
1	23	66.70	9.04	13.55	4	69.50	3.00	4.32
2	21	79.21	4.10	5.17	4	78.26	2.62	3.35
3	21	75.10	3.89	5.18	4	74.14	3.55	4.79
4	21	13.17	2.50	19.01	4	12.63	2.53	20.03
5	23	8.94	0.87	9.77	4	9.56	0.32	3.29
6	23	7.75	0.82	10.54	4	9.35	0.97	10.40
1	4	75.75	10.47	13.82	2	64.50	47.38	73.45
2	4	72.01	2.67	3.71	2	72.60	2.33	3.21
3	4	69.04	2.85	4.13	2	69.33	2.23	3.21
4	4	12.88	1.85	14.37	2	12.58	0.81	6.47
5	4	9.30	0.87	9.32	2	8.13	0.46	5.66
6	4	7.90	0.45	5.71	2	7.45	0.99	13.29

Appendix 5: Video Densitometry of Bone Microradiographs

1. Preparing the image.

Ensure microscope is set-up for Koehler Illumination, daylight filter off. Establish correction for shading distortion. Shading distortion is a form of system noise which occurs due to the interaction of the optical systems of the microscope and videocamera (Martin et al., 1990). The visual effect is an uneven gradient of brightness which is not a reflection of the "original scene" (Inoué, 1986: 45-6). Since image analysis operates on the gray level (Vg) value of an x, y pixel array, shading distortion can be a serious problem since, when present, the digitized gray value for a given pixel will be a function of its location in the field of view and not necessarily of its 'true density'. Correction or compensation for shading distortion can be achieved in digital image processing through various techniques, including subtraction or division of the image of interest by an Image Transformation Function, ITF. Martin et al. (1990: 85) discuss a version of the latter; JAVA contains a subtraction subroutine on its Image Processing menu, so this method, though less preferable than a specific ITF (which could not be applied due to software limitations), was chosen in the present case. Various kinds of image noise, including hotspots (condensed areas of brightness) and mottling in addition to uneven illumination, can be compensated for using the method of image subtraction (Inoué, 1986). Set illumination to an appropriate level which will give good visual discrimination of gray level variation (e.g., 5.0-6.0). Locate the field of interest, reduce illumination 1 full step (e.g., from 6.0 to 5.0). This step was found necessary in this analysis in order to prevent total subtraction of image contrast; it may not be appropriate to all applications. Raise or lower the stage to place the image slightly out of focus (Inoué, 1986); capture this image and store it on disk, identified as SUB. If a previous SUB file exists, chose 'rewrite' when prompted by the program. Unfreeze the image, re-focus and return to desired illumination. Freeze, and select SUB from the Image Processing menu.

2. Data Collection

Visually identify lamellar bone at the periosteal surface (CPA) which appears less mineralized than the adjacent matrix. Define this region as an Area of Interest (AOI) independent of the rest of the bone in the field of view. Using the Histogram function, record the number of pixels within it. Remove the AOI. Determine '% CPA' as: (CPA pixels / total of bone pixels) x 100. Create and save a look-up table (LUT) which simplifies the image into fewer gray levels, e.g., 8 - 10. In the present case, the following ranges were 'compressed': 0-40 = 0; 41-60 = 41; 61-80 = 61; 81-100 = 81; 101-120 = 101; 121-140 = 121; 141-160 = 141; 161-180 = 161; 181-255 = 181. Apply the LUT, followed by the Histogram function. Go to the datafile (column 11) and obtain the simplified Vg values for the above table; these are presented as the total number of pixels falling within the defined range. In column 11, the most recent 'histogram' data will be appended to any which were already present (e.g., for determining CPA). These data provide an estimate of porosity (0 - 40 range) inclusive of areas in the image beyond the endosteal or perisoteal margins, and the amount of bone (pixels) falling within each of the above steps defined in the LUT. If extracortical porosity is present in the image, use the AOI and histogram functions to define these areas and identify the number of pixels within them. Subtract these values from the initial porosity estimate to find the amount of intracortical porosity. If the image does not contain all of the bone between the periosteal and endosteal margins, unfreeze the current image and shift the field of view to include the remaining bone but excluding that already analysed, and repeat the above steps. Sum the tabled values. Determine % porosity as {(# pixels in 0-40 range) ÷ total number of pixels - extraneous porosity} x 100. For each of the nonporosity ranges, calculate the proportion for each cell (intensity range; e.g. 41-60; 61-80, etc.) of the tabie relative to the total number of pixels in the nonporosity range, e.g., {(# pixels 61-80 range) ÷ (total number of bone pixels) x 100}. Use the values arrived at in the preceding step to determine MR_A, from the formulae derived in chapter 3.

Appendix 6: Table A6. Male LMC SLCOMM data. (n = in () = 50 % location)

Variable	All	Cadaver	Y Cadaver	O Cadaver	Historic
n =	31 (29)	26 (25)	15	11 (10)	5
70% TA	19.15 (2.85)	19.29 (2.89)	19.02 (3.08)	19.66 (2.70)	18.39 (2.84)
CA	10.43 (1.84)	10.71 (1.81)	10.79 (1.87)	10.60 (1.80)	8.95 (1.27)
MA	8.72 (2.62)	8.58 (2.60)	8.23 (2.19)	9.06 (3.12)	9.45 (2.89)
Imin	21.18 (5.82)	21.97 (5.82)	21.74 (6.28)	22.28 (5.43)	17.05 (4.09)
Imax	27.30 (7.50)	27.89 (7.71)	27.68 (8.69)	28.17 (6.54)	24.20 (5.99)
J	48.47 (13.06)	49.86 (13.28)	49.42 (14.72)	50.46 (11.70)	41.25 (9.96)
Imin / Imax	0.78 (0.08)	0.79 (0.08)	0.79 (0.07)	0.79 (0.09)	0.71 (0.06)
60% TA	15.96 (2.05	16.07 (2.05)	15.73 (2.22)	16.53 (1.80)	15.37 (2.14)
CA	10.88 (1.87)	11.21 (1.78)	11.25 (1.85)	11.15 (1.76)	9.18 (1.45)
MA	5.08 (1.74)	4.86 (1.59)	4.48 (1.55)	5.38 (1.56)	6.19 (2.28)
Imin	15.88 (3.92)	16.34 (3.98)	15.88 (3.83)	16.96 (4.28)	13.51 (2.76)
Imax	21.96 (5.89)	22.58 (5.96)	22.00 (6.58)	23.38 (5.21)	18.74 (4.76)
J	37.85 (9.42)	38.92 (9.51)	37.87 (10.06)	40.35 (8.96)	32.25 (7.36)
Imin / Imax	0.74 (0.10)	0.74 (0.11)	0.74 (0.10)	0.73 (0.12)	0.74 (0.10)
50% TA	14.73 (1.82)	14.77 (1.75)	14.60 (1.95)	15.02 (1.46)	14.50 (2.48)
CA	11.24 (1.78)	11.51 (1.65)	11.67 (1.65)	11.27 (1.71)	9.58 (1.89)
MA	3.49 (1.50)	3.26 (1.40)	2.93 (1.33)	3.75 (1.43)	4.92 (1.47)
Imin	13.58 (3.32)	13.76 (3.20)	13.90 (3.66)	13.56 (2.53)	12.40 (4.34)
Imax	20.12 (5.10)	20.41 (5.06)	19.85 (5.31)	21.25 (4.82)	18.31 (5.74)
J	33.70 (8.04)	34.18 (7.82)	33.75 (8.49)	34.81 (7.08)	30.72 (9.99)
Imin / Imax	0.67 (0.11)	0.69 (0.11)	0.71 (0.11)	0.65 (0.10)	0.67 (0.07)
Age	65.97 (11.09)	66.77 (9.75)	60.07 (6.03)	75.91 (5.24)	61.80 (17.41)

Table A7. Male RMC SLCOMM data.

Variable	All	Cadaver	Y Cadaver	O Cadaver	Historic
n =	32	27	16	11	5
70% TA	20.26 (2.65)	20.41 (2.67)	20.26 (2.56)	20.63 (2.93)	19.44 (2.68)
CA	11.40 (2.30)	11.85 (2.17)	12.22 (1.87)	11.31 (2.56)	8.97 (1.16)
MA	8.86 (2.39)	8.56 (2.30)	8.03 (2.05)	9.32 (2.54)	10.47 (2.39)
Imin	24.55 (6.79)	25.53 (6.26)	25.62 (6.04)	25.40 (6.86)	19.24 (4.43)
Imax	31.01 (8.50)	32.08 (8.42)	32.32 (7.97)	31.72 (9.42)	25.25 (7.10)
J	55.56 (14.60)	57.61 (14.38)	57.94 (13.06)	57.12 (16.11)	44.49 (11.21)
Imin / Imax	0.80 (0.08)	0.80 (0.08)	0.80 (0.09)	0.81 (0.07)	0.77 (0.10)
60% TA	16.87 (2.23)	17.11 (2.22)	16.82 (1.88)	17.54 (2.68)	15.53 (1.97)
CA	11.87 (2.14)	12.33 (2.00)	12.59 (1.76)	11.94 (2.33)	9.43 (0.90)
MA	4.99 (1.75)	4.79 (1.64)	4.23 (1.27)	5.60 (1.83)	6.10 (2.13)
Imin	18.06 (4.81)	18.95 (4.66)	18.42 (4.15)	19.71 (5.44)	13.30 (2.13)
Imax	25.06 (6.83)	25.94 (6.83)	25.58 (5.81)	26.46 (8.37)	20.33 (5.04)
J	43.12 (11.30)	44.88 (11.17)	44.00 (9.58)	46.17 (13.55)	33.63 (6.77)
Imin / Imax	0.73 (0.10)	0.74 (0.09)	0.73 (0.09)	0.76 (0.10)	0.67 (0.12)
50% TA	15.63 (1.85)	15.87 (1.77)	15.59 (1.44)	16.28 (2.18)	14.35 (1.92)
CA	11.91 (2.19)	12.47 (1.84)	12.73 (1.53)	12.10 (2.25)	8.84 (1.13)
MA	3.73 (1.84)	3.40 (1.66)	2.86 (1.14)	4.18 (2.03)	5.51 (1.89)
Imin	15.16 (3.82)	15.90 (3.56)	15.43 (3.40)	16.59 (3.84)	11.15 (2.66)
Imax	22.65 (5.30)	23.58 (5.05)	23.43 (4.58)	23.79 (5.89)	17.62 (3.86)
J	37.81 (8.64)	39.48 (8.00)	38.86 (6.97)	40.38 (9.59)	28.77 (6.43)
Imin / Imax	0.68 (0.11)	0.69 (0.12)	0.67 (0.14)	0.71 (0.09)	0.63 (0.05)
Age	66.62 (10.44)	67.52 (8.84)	61.62 (4.95)	76.09 (5.47)	61.80 (17.41)

Table A8. Male MT SLOMM data. (n = in () = 50 % location)

Variable	All	Cadaver	Y Cadaver	O Cadaver	Historic
n =	26 (24)	22 (21)	13 (12)	9	4 (3)
70% TA	8.40 (1.48)	8.10 (1.09)	7.95 (0.84)	8.32 (1.40)	10.01 (2.40)
CA	5.18 (0.84)	5.19 (0.79)	5.21 (0.69)	5.16 (0.96)	5.13 (1.19)
MA	3.21 (1.19)	2.91 (0.78)	2.74 (0.66)	3.16 (0.90)	4.87 (1.81)
Imin	3.63 (1.23)	3.46 (0.94)	3.37 (0.73)	3.58 (1.21)	4.56 (2.24)
Imax	6.42 (2.11)	6.10 (1.66)	5.86 (1.40)	6.45 (2.01)	8.18 (3.59)
J	10.05 (3.23)	9.56 (2.45)	9.23 (2.04)	10.03 (3.01)	12.74 (5.79)
Imin / Imax	0.57 (0.09)	0.57 (0.10)	0.58 (0.09)	0.56 (0.12)	0.56 (0.08)
60% TA	8.94 (1.56)	8.57 (1.13)	8.35 (0.82)	8.90 (1.46)	10.92 (2.28)
CA	5.92 (0.91)	5.90 (0.95)	5.91 (0.74)	5.88 (1.25)	6.03 (0.72)
MA	3.02 (1.35)	2.68 (0.93)	2.44 (0.84)	3.02 (0.99)	4.89 (1.88)
Imin	4.52 (1.32)	4.31 (1.23)	4.03 (0.70)	4.72 (1.71)	5.65 (1.36)
Imax	7.35 (2.79)	6.73 (1.64)	6.52 (1.53)	7.03 (1.84)	10.79 (5.23)
J	11.87 (3.87)	11.04 (2.68)	10.55 (2.09)	11.75 (3.37)	16.44 (6.45)
Imin / Imax	0.63 (0.12)	0.64 (0.12)	0.63 (0.10)	0.66 (0.15)	0.57 (0.15)
50% TA	10.07 (1.69)	9.68 (1.18)	9.37 (0.84)	10.09 (1.47)	12.82 (2.49)
CA	7.13 (1.13)	7.08 (1.12)	6.95 (0.97)	7.25 (1.34)	7.50 (1.33)
MA	2.94 (1.28)	2.60 (0.85)	2.43 (0.96)	2.84 (0.65)	5.32 (1.41)
Imin	6.22 (1.83)	5.86 (1.58)	5.38 (0.90)	6.50 (2.09)	8.71 (1.64)
Imax	9.25 (3.59)	8.51 (2.08)	8.07 (1.94)	9.10 (2.24)	14.38 (7.73)
J	15.46 (5.17)	14.38 (3.47)	13.46 (2.61)	15.60 (4.22)	23.08 (9.37)
Imin / Imax	0.69 (0.12)	0.69 (0.11)	0.68 (0.12)	0.70 (0.11)	0.68 (0.20)
Age	66.81 (8.45)	66.32 (9.06)	60.46 (5.62)	74.78 (5.65)	69.50 (3.00)

Table A9. Female LMC SLCOMM data.

Variable	All (n=7)	Cadaver (n=5)	Historic (n=2)
70% TA	16.22 (1.23)	16.21 (1.51)	16.24 (0.13)
CA	8.57 (1.54)	8.25 (1.52)	9.36 (1.81)
MA	7.65 (2.13)	7.95 (2.34)	6.88 (1.94)
Imin	14.86 (2.15)	14.22 (2.16)	16.48 (1.34)
Imax	18.14 (2.74)	17.92 (3.14)	18.68 (2.18)
J	33.00 (4.34)	32.13 (4.68)	35.16 (3.52)
Imin/Imax	0.83 (0.11)	0.80 (0.12)	0.88 (0.03)
60% TA	13.42 (0.92)	13.39 (1.11)	13.48 (0.35)
CA	8.75 (1.41)	8.53 (1.47)	9.28 (1.60)
MA	4.67 (1.84)	4.86 (1.99)	4.19 (1.94)
Imin	11.38 (1.32)	11.16 (1.54)	11.95 (0.19)
Imax	13.98 (1.54)	13.83 (1.81)	14.38 (0.81)
J	25.37 (2.71)	24.98 (3.18)	26.33 (0.99)
Imin/Imax	0.82 (0.06)	0.81 (0.07)	0.83 (0.03)
50% TA	12.48 (1.01)	12.48 (1.19)	12.48 (0.62)
CA	8.57 (1.72)	8.08 (1.69)	9.78 (1.47)
MA	3.91 (2.20)	4.40 (2.27)	2.70 (2.09)
Imin	9.71 (1.14)	9.46 (1.29)	10.35 (0.16)
Imax	12.40 (1.78)	12.06 (2.06)	13.24 (0.30)
J	22.12 (2.86)	21.53 (3.27)	23.59 (0.46)
Imin/Imax	0.79 (0.05)	0.79 (0.07)	0.78 (0.01)
Age	71.29 (21.81)	74.00 (10.95)	64.5 (47.38)

Table A10. Female RMC SLCOMM data.

Variable	All (n=8)	Cadaver (n=6)	Historic (n=2)
70% TA	17.49 (2.30)	17.21 (2.63)	18.35 (0.81)
CA	8.92 (1.61)	8.59 (1.36)	9.92 (2.49)
MA	8.57 (2.34)	8.61 (2.66)	8.43 (1.68)
Imin	16.88 (4.19)	15.91 (4.02)	19.81 (4.39)
Imax	21.07 (4.91)	20.25 (5.17)	23.51 (4.38)
J	37.95 (9.00)	36.16 (9.09)	43.32 (8.77)
Imin/Imax	0.80 (0.06)	0.79 (0.07)	0.84 (0.03)
60% TA	14.27 (1.37)	14.08 (1.47)	14.84 (1.18)
CA	8.78 (1.20)	8.55 (1.26)	9.49 (0.95)
MA	5.49 (1.97)	5.54 (2.12)	5.35 (2.13)
Imin	12.47 (2.35)	12.20 (2.11)	13.30 (0.71)
Imax	15.43 (2.35)	14.79 (2.00)	17.37 (2.96)
J	27.91 (3.94)	26.99 (4.07)	30.67 (2.25)
Imin/Imax	0.81 (0.08)	0.82 (0.05)	0.78 (0.17)
50% TA	13.44 (1.57)	12.94 (0.59)	14.95 (3.10)
CA	9.68 (1.97)	9.00 (1.66)	11.74 (1.42)
MA	3.76 (1.80)	3.94 (1.95)	3.21 (1.68)
Imin	11.76 (3.68)	10.40 (1.31)	15.86 (6.43)
Imax	15.15 (3.76)	13.85 (1.56)	19.05 (6.80)
J	26.91 (7.29)	24.25 (2.30)	34.91 (13.23)
Imin/Imax	0.77 (0.09)	0.76 (0.10)	0.83 (0.04)
Age	72.25 (20.87)	74.83 (11.36)	64.50 (47.38)

Table A11. Female MT SLCOMM data.

Variable	All (n=6)	Cadaver (n=4)	Historic (n=2)
70% TA	9.53 (1.26)	9.94 (1.21)	8.71 (1.24)
CA	5.31 (1.01)	4.89 (0.70)	6.15 (1.25)
MA	4.22 (1.81)	5.05 (1.64)	2.56 (0.01)
Imin	4.52 (0.99)	4.51 (0.73)	4.53 (1.80)
Imax	7.10 (1.23)	7.21 (1.17)	6.87 (1.82)
J	11.62 (2.17)	11.72 (1.85)	11.40 (3.62)
Imin/Imax	0.63 (0.06)	0.63 (0.05)	0.65 (0.09)
60% TA	10.38 (1.30)	10.83 (1.04)	9.47 (1.67)
CA	6.74 (1.52)	6.37 (1.36)	7.48 (2.08)
MA	3.64 (1.53)	4.46 (1.07)	1.99 (0.42)
Imin	6.18 (1.77)	6.05 (1.29)	6.44 (3.24)
Imax	9.14 (2.57)	9.87 (2.68)	7.68 (2.24)
J	15.32 (4.04)	15.92 (3.97)	14.12 (5.48)
Imin/Imax	0.68 (0.13)	0.62 (0.04)	0.81 (0.19)
50% TA	11.88 (1.60)	12.60 (1.10)	10.44 (1.71)
CA	8.03 (1.58)	7.81 (1.69)	8.49 (1.82)
MA	3.85 (1.76)	4.80 (1.24)	1.95 (0.11)
Imin	8.50 (2.07)	8.86 (1.86)	7.80 (3.07)
Imax	12.15 (3.67)	13.50 (3.6)	9.44 (2.54)
J	20.65 (5.41)	22.36 (5.15)	17.24 (5.61)
Imin/Imax	0.72 (0.13)	0.67 (0.13)	0.81 (0.11)
Age	72.00 (23.42)	75.75 (10.47)	64.50 (47.38)

Table A12. LMC (JAVA), Male Cadaver data only.

Variable	50 %	60 %	70 %
n =	6	7	2
DJ IP	19.59 (4.27)	17.76 (5.25)	16.27 (0.38)
CPA	2.55 (2.83)	3.01 (4.21)	2.71 (3.83)
MBA	6.33 (0.33)	6.76 (0.29)	6.69 (0.09)
Z	82.69 (16.04)	90.34 (25.07)	101.38 (13.30)
CT	2.58 (0.32)	2.38 (0.71)	1.65 (0.35)
PJ IP	18.37 (8.31)	17.70 (7.84)	14.62 (1.50)
CPA	3.35 (3.83)	2.25 (3.95)	1.93 (2.72)
MBA	5.95 (0.70)	6.73 (0.26)	7.32 (0.03)
Z	80.02 (13.91)	85.92 (18.57)	82.16 (7.68)
CT	2.50 (0.46)	2.30 (0.54)	2.42 (0.32)
DN IP	18.09 (8.97)	22.20 (5.87)	14.59 (7.77)
CPA	1.09 (2.67)	4.47 (4.74)	0.00 (0.00)
MBA	6.04 (0.84)	6.22 (0.55)	7.12 (0.34)
Z	66.58 (15.44)	74.28 (21.26)	78.78 (7.53)
CT	2.33 (0.50)	2.38 (0.37)	1.68 (0.37)
PN IP	16.72 (4.59)	14.28 (6.02)	12.40 (1.64)
CPA	3.73 (4.20)	3.19 (3.12)	6.89 (2.86)
MBA	6.30 (0.35)	6.49 (0.20)	6.95 (0.63)
Z	71.39 (15.13)	82.90 (19.52)	84.35 (19.72)
CT	2.04 (0.43)	1.85 (0.47)	1.55 (0.48)
AGE	66.17 (6.05)	68.71 (8.04)	64.00 (5.66)

Table A13. RMC (JAVA), Male Cadaver data only.

Variable	50 %	60 %	70 %
n =	7	6	1
DJ IP	17.81 (3.34)	18.56 (6.61)	14.77
CPA	4.54 (3.57)	5.65 (4.99)	7.49
MBA	6.78 (0.22)	6.69 (0.58)	7.39
Z	93.68 (13.50)	111.95 (19.47)	98.33
CT	3.06 (0.59)	2.85 (0.52)	2.40
PJ IP	17.68 (5.11)	18.10 (6.91)	10.14
CPA	4.33 (4.48)	0.00 (0.00)	0.00
MBA	6.70 (0.46)	6.42 (0.87)	6.99
Z	91.85 (11.76)	108.62 (18.86)	138.44
CT	2.86 (0.18)	2.55 (0.60)	1.75
DN IP	15.68 (6.39)	17.00 (7.28)	13.69
CPA	4.04 (5.07)	2.42 (3.96)	14.42
MBA	6.71 (0.51)	6.61 (0.37)	7.56
Z	70.99 (9.53)	83.04 (8.80)	101.16
CT	2.47 (0.26)	2.14 (0.43)	2.53
PN IP	17.57 (3.36)	16.15 (6.93)	8.53
CPA	4.15 (4.15)	3.71 (4.39)	0.00
MBA	6.40 (0.37)	6.62 (0.73)	7.41
Z	74.67 (12.09)	96.52 (13.59)	108.58
CT	2.41 (0.25)	2.01 (0.27)	1.92
AGE	63.71 (7.95)	64.17 (8.45)	68.00

Table A14. MT (JAVA), Male Cadaver data only.

Variable	50 %	60 %	70 %
n =	6	7	4
DJ IP	21.01 (5.41)	19.37 (1.59)	19.42 (4.94)
CPA	6.18 (5.01)	5.95 (4.14)	4.38 (5.13)
MBA	6.08 (1.01)	6.61 (0.39)	6.38 (0.53)
Z	53.29 (15.40)	48.05 (9.28)	42.45 (9.75)
CT	2.15 (0.52)	2.02 (0.32)	1.83 (0.82)
PJ IP	17.52 (2.60)	15.30 (3.23)	14.13 (2.09)
CPA	3.89 (3.08)	7.31 (3.88)	4.50 (5.20)
MBA	6.07 (0.82)	6.66 (0.42)	6.75 (0.18)
Z	54.04 (10.89)	53.89 (6.65)	44.02 (8.49)
CT	2.12 (0.59)	2.00 (0.42)	1.54 (0.41)
DN IP	20.70 (5.36	15.30 (2.18)	15.11 (0.41)
CPA	1.32 (3.23)	7.28 (5.00)	8.17 (5.95)
MBA	6.38 (0.62)	6.71 (0.45)	6.52 (0.46)
Z	47.12 (11.53)	41.27 (7.72)	32.73 (8.21)
CT	1.72 (0.30)	1.70 (0.07)	1.25 (0.25)
PN IP	19.10 (3.99)	14.12 (2.78)	14.20 (0.40)
CPA	7.38 (4.36)	7.55 (2.06)	10.12 (4.27)
MBA	6.13 (1.06)	6.83 (0.53)	6.93 (0.45)
Z	44.89 (10.87)	40.04 (6.93)	29.90 (7.00)
CT	2.26 (0.52)	2.14 (0.40)	1.82 (0.41)
AGE	61.33 (5.13)	61.86 (6.39)	60.25 (5.56)

BIBLIOGRAPHY

Adams P, Davies GT, and Sweetnam P (1970) Osteoporosis and the effects of ageing on bone mass in elderly men and women. Quart. J. Med. 39: 601-615.

Aksharanugraha K, Harris EF, and Behrents RG (1987) Normal length changes in hand bones during adulthood. Am. J. Phys. Anthropol. 72: 173-174 (A).

Anderson C (1982) Manual for the Examination of Bone. Boca Raton: CRC Press.

Armelagos GJ, Carlson DS, and Van Gerven DP (1982) The theoretical foundations and development of skeletal biology. In F Spencer (ed.): A History of American Physical Anthropology. New York: Academic Press. pp. 305-328.

Ascenzi A (1980) Contribution of biomechanics to bone research. Cal. Tiss. Int. 31:1-3.

Ascenzi A, Boyde A, Portigliatti Barbos M, and Carando S (1987) Micro-biomechanics vs. macro-biomechanics in cortical bone. A mechanical investigation of femurs deformed by bending. J. Biomech. 20: 1045-1053.

Baer MJ (1956) Dimensional change in the human head and face in the third decade of life. Am. J. Phys. Anthropol.14: 557-575.

Bassett EJ, Keith MS, Armelagos GJ, Martin DL, and Villanueva AR (1980) Tetracycline-labeled human bone from ancient Sudanese Nubia (A.D. 350). Science 209: 1532-1534.

Behrents RG (1985) The biological basis for understanding craniofacial growth. Pp. 307-319 in AD Dixon and BG Sarnat (eds.): Normal and Abnormal Bone Growth: Basic and Clinical Research. New York: AR Liss.

Behrents RG, and Harris EF (1987) Normal length changes in hand bones during adulthood: exploratory study of ray two. Ann. Hum. Biol. 14: 277-283.

Bertram JEA, and Biewener AA (1988) Bone curvature: sacrificing strength for load predictability? J. Theor. Biol. 131: 75-92.

Bohatirchuk F (1954) Some microradiographical data on bone ageing. Br. J. Radiol. 27: 177-182.

Boivin G, and Baud C-A (1984) Microradiographic methods for calcified tissues. In GR Dickson (ed.): Methods of Calcified Tissue Preparation. Amsterdam: Elsevier, pp. 391-412.

Bouvier M (1985) Application of in vivo bone strain measurement techniques to problems of skeletal adaptation. Yearbk. Phys. Anthropol. 28: 237-248.

Bowes DN, and Dunn EJ (1975) A simple vacuum cassette for microradiography. Stain Technol. 50: 355-357.

Bridges P (1989a) Changes in activities with the shift to agriculature in the southeastern United States. Curr. Anthropol. 30: 385-394.

Bridges P (1989b) Bone cortical area in the evaluation of nutrition and activity levels. Am. J. Hum. Biol. 1: 785-792.

Bromage T (1982) Mapping remodeling reversals with the aid of the scanning electron microscope. Am. J. Orthod. 81: 314-321.

Browthwell DR (1963) Dental Anthropology. Oxford: Pergamon Press.

Buikstra J (1975) Healed fractures in *Macaca mulatta*: age, sex and symmetry. Folia Primat. 23: 140-148.

Burr DB, and Martin RB (1983) The effects of composition, structure and age on the torsional properties of the human radius. J. Biomech. 16: 603-608.

Burr DB, and Martin RB (1989) Errors in bone remodeling: towards a unified theory of metabolic bone disease. Am. J. Anat. 186: 186-216.

Burr DB, Martin RB, Scaffler MB, and Radin EL (1985) Bone remodeling in response to in vivo fatigue microdamage. J. Biomech. 18: 189-200.

Burr DB, Ruff CB, and Johnson C (1989a) Structural adaptations of the femur and humerus to arboreal and terrestrial environments in three species of macaque. Am. J. Phys. Anthropol. 79: 357-367.

Burr DB, Schaffler MB, Yang KH, Wu DD, Lukoschek M, Kandzari D, Sivaneri N, Blaha JD, and Radin EL (1989b) The effects of altered strain environments on bone tissue kinetics. Bone 10: 215-221.

Cadien JD, Harris EF, Jones WP, and Mandarino LJ (1974) Biological lineages, skeletal populations and microevolution. Yearbk. Phys. Anthropol. 20: 194-201.

Carlson DS, Armelagos GJ, and Van Gerven DP (1976) Patterns of age-related cortical bone loss (osteoporosis) within the femoral diaphysis. Hum. Biol. 48: 295-314.

Carter DR (1983) The relationship between in vivo strains and cortical bone remodeling. CRC Crit. Rev. Biomed. Engr. 8: 1-28.

Carter DR (1984) Mechanical loading histories and cortical bone remodeling. Calcif. Tiss. Int. 36: S19-S24.

Carter DR, Caler WE, Spengler DM, and Frankel VH (1981) Uniaxial fatigue of human cortical bone. The influence of tissue physical properties. J. Biomech. 14: 461-470.

Carter DR, Fyhrie DP, and Whalen RT (1987) Trabecular bone density and loading history: regulation of connective tissue biology by mechanical energy. J. Biomech. 20: 785-794.

Carter DR, and Hayes WC (1977) The compressive behavior of bone as a two-phase porous structure. J. Bone Jt. Surg. 59A: 954-962.

Carter DR, Orr TE, and Fyhrie DP (1989) Relationships between loading history and femoral cancellous bone architecture. J. Biomech. 22: 231-244.

Carter DR, and Spengler DM (1978) Mechanical properties and composition of cortical bone. Clin. Orthop. Rel. Res. 135: 192-217.

Cohen J (1977) Statistical Power Analysis for the Behavioral Sciences. New York: Academic Press.

Compston J, Vedi S, and Stellon A (1986) Interobserver and intraobserver variation in bone histomorphometry. Calcif. Tiss. Int. 38: 67-70.

Conover WJ, and Iman RL (1981) Rank transformations as a bridge between parametric and nonparametric statistics. The Amer. Statistician 35: 124-129.

Coupron P (1981) Bone tissue mechanisms underlying osteoporoses. Orthop. Clin. N. Amer. 12: 513-545.

Cowin SC (1984) The mechanical and stress adaptive properties of bone. Ann. Biomed. Engnr. 11: 263-295.

Cowin SC (1987) Bone remodeling of diaphyseal surfaces by torsional loads: theoretical predictions. J. Biomech. 20: 1111-1120.

Cowin SC (ed.) (1989a) Bone Mechanics. Boca Raton: CRC Press.

Cowin SC (1989b) The mechanical properties of cortical bone tissue. Pp. 97-127 in SC Cowin (ed.) (1989) Bone Mechanics. Boca Raton: CRC Press.

Cowin SC, Hart RT, Balser JR, and Kohn DH (1985) Functional adaptation in long bones: establishing in vivo values for surface remodeling rate coefficients. J. Biomech. 18: 665-684.

Currey JD (1962) Stress concentrations in bone. Quart. J. Micro. Sci. 103: 111-133.

Currey JD (1969a) The mechanical consequences of variation in the mineral content of bone. J. Biomech. 2: 1-11.

Currey JD (1969b) The relationship between the stiffness and the mineral content of bone. J. Biomech. 2: 477-480.

Currey JD (1975) The effects of strain rate, reconstruction and mineral content on some mechanical properties of bovine bone. J. Biomech. 8: 81-86.

Currey JD (1979) Mechanical properties of bone with greatly differing functions. J. Biomech. 12: 313-319.

Currey JD (1984a) Effects of differences in mineralization on the mechanical properties of bone. Phil. Trans. R. Soc. Lond. B 304: 509-518.

Currey JD (1984b) The Mechanical Adaptations of Bones. Princeton: Princeton University Press.

Currey JD (1984c) Comparative mechanical properties and histology of bone. Am. Zool. 24: 5-12.

Currey JD (1984d) What should bones be designed to do? Calcif. Tiss. Int. 36: S7-S10.

Currey JD (1988) The effect of porosity and mineral content on the Young's modulus of elasticity of compact bone. J. Biomech. 21: 131-139.

Currey JD (1990) Physical characteristics affecting the tensile failure properties of compact bone. J. Biomech. 23: 837-844.

Currey JD, and Alexander RMcN (1985) The thickness of the walls of tubular bones. J. Zool 206(A): 453-468.

Dahlberg AA, Cederquist R, Mayhall JT, and Owen D (1978) Eskimo craniofacial studies. In PL Jamison, SL Zegura and FA Milan, (eds.): Eskimos of Northwestern Alaska: A Biological Perspective. Stroudsburg, PA: Dowden, Hutchison and Ross, pp. 94-113.

Dunn EJ, Bowes DN, Rothert SW, and Greer III RB (1974) An inexpensive x-ray source for the microradiography of bone. Calcif. Tiss. Res. 15: 329-332.

Enlow DH (1982) Handbook of Facial Growth, 3rd Ed. Philadelphia: WB Saunders.

Epker BN, and Frost HM (1966) Periosteal appositional bone growth from age two to age seventy in man. Anat. Rec. 154: 573-578.

Ericksen MF (1976) Cortical bone loss with age in three native American populations. Amer. J. Phys. Anthropol. 45: 443-452.

Ericksen MF (1982) How 'representative' is the Terry collection? Evidence from the proximal femur. Amer. J. Phys. Anthropol. 59: 345-350.

Eschman P (1990) SLCOMM: A User Supported Real-Time Digitizing Package. Eschman Archaeological Services, Alberquerque, NM.

Facchini G, and Gualdi-Russo E (1982) Secular anthropometric changes in a sample of Italian adults. J. Hum. Evol. 11: 703-714.

Fleagle JG (1985) Size and adaptation in primates. In WL Jungers (ed.): Size and Scaling in Primate Biology. New York: Plenum Press, pp. 1-19.

Forsberg CM (1979) Facial morphology and ageing: a longitudinal cephalometric investigation of young adults. Eur. J. Orthod. 1: 15-23.

Forwood MR, and Parker AW (1989) Microdamage in response to repetitive torsional loading in the rat tibia. Calcif. Tiss. Int. 45: 47-53.

Fox KM, JD Tobin, and Plato CC (1986) Longitudinal study of bone loss in the second metacarpal. Calcif. Tiss. Int. 39: 218-225.

Frost HM (1969) Tetracycline-based histological analysis of bone remodeling. Calcif. Tiss. Res. 3: 211-237.

Frost HM (1980) Skeletal physiology and bone remodeling. In MR Urist (ed.): Fundamental and Clinical Bone Physiology. Philadelphia: JP Lippencott, pp. 208-241.

Frost HM (1981) Coherence treatment of osteoporoses. Orthop. Clin. N. Am. 12: 649- 669.

Frost HM (1982) Mechanical determinants of bone remodeling. Metab. Bone Dis. Rel. Res. 4: 217-229.

Frost HM (1983) A determinant of bone architecture. The minimum effective strain. Clin. Orthop. Rel. Res. 175: 286-292.

Frost HM (1985) The 'new bone': some anthropological potentials. Yearbk. Phys. Anthropol. 28: 211-226.

Frost HM (1987a) Secondary osteon populations: an algorithm for determining mean bone tissue age. Yearbk. Phys. Anthropol. 30: 221-238.

Frost HM (1987b) Secondary osteon population densities: an algorithm for estimating the missing osteons. Yearbk. Phys. Anthropol. 30: 239-254.

Frost HM (1987c) The mechanostat: a proposed pathogenic mechanism of osteoporoses and the bone mass effects of mechanical and nonmechanical agents. Bone and Mineral 2:73-85.

Frost HM (1988a) Vital biomechanics: proposed general concepts for skeletal adaptations to mechanical usage. Calcif. Tiss. Int. 42: 145-156.

Frost HM (1988b) Structural adaptations to mechanical usage. A proposed "three-way rule" for bone modeling. Part I. V.C.O.T. 1: 7-17.

Frost HM (1988c) Structural adaptations to mechanical usage. A proposed "three-way rule" for bone modeling. Part II. V. C. O. T. 2: 80-85.

Frost HM (1989a) Some ABCs of skeletal pathophysiology I: introduction to the series. Calcif. Tiss. Int. 45: 1-3.

Frost HM (1989b) Some ABCs of skeletal pathophysiology II: general mediator mechanism properties. Calcif. Tiss. Int. 45: 68-70.

Frost HM (1989c) Some ABCs of skeletal pathophysiology III: bone balance and the ΔB.BMU. Calcif. Tiss. Int. 45: 131-133.

Frost HM (1989d) Some ABCs of skeletal pathophysiology IV: the transient / steady state distinction. Calcif. Tiss. Int. 45: 134-136.

Gardner WD, and Osburn WA (1978) Anatomy of the Human Body, 3rd Ed. Philadelphia: WB Saunders Co.

Garn SM (1970) The Earlier Gain and Later Loss of Cortical Bone. Springfield: C. C. Thomas.

Garn SM (1975) Bone loss and aging. In R Goldman and M Rockstein (eds.): The Physiology and Pathology of Human Aging. New York: Academic Press, pp. 39-57.

Garn SM (1981) Contributions of the radiographic image to our knowledge of human growth. Am. J. Radiol. 137: 231-239.

Garn SM, Frisancho AR, Sandusky ST, and McCann MB (1972) Confirmation of the sex difference in continuing subperiosteal apposition. Am. J. Phys. Anth. 36: 377- 380.

Garn SM, Poznanski AK, and Larson K (1976) Metacarpal lengths, cortical diameters and areas from the 10-state nutrition survey, including: estimated skeletal weights, weight, and stature for whites, blacks, and Mexican-Americans. In ZFG Jaworski (ed.): Proceedings of the First Workshop on Bone Morphometry. Ottawa: University of Ottawa Press, pp. 367-391.

Garn SM, Rohrmann CG, Wagner B, and Ascoli W (1967) Continuing bone growth throughout life: a general phenomenon. Am. J. Phys. Anthropol. 26: 313-318.

Garn SM, Sullivan TV, Decker SA, and Hawthorne VM (1990) Continuing bone expansion and increasing bone loss over a 2 decade period in 745 men and women from a total community sample. Am. J. Phys. Anthropol. 81: 226 (A).

Garn SM, Wagner B, Rohmann CG, and Ascoli W (1968) Further evidence for continuing bone expansion. Am. J. Phys. Anthropol. 28: 219-222.

Hanson DB, and Buikstra JE (1987) Histomorphological alteration in buried human bone from the Lower Illinois Valley: implications for paleodietary research. J. Arch. Sci. 14: 549-563.

Harper AB, Laughlin WS, and Mazess RB (1984) Bone mineral content in St. Lawrence Island Eskimos. Hum. Biol. 56: 63-77.

Hart RT (1989) Computational techniques for bone remodeling. In SC Cowin (ed.): Bone Mechanics. Boca Raton: CRC Press, pp. 279-304.

Hart RT (1990) A theoretical study of the influence of bone maturation rate on surface remodeling predictions: idealized models. J. Biomech. 23: 241-257.

Hart RT, and Davy DT (1989) Theories of bone modeling and remodeling. In SC Cowin (ed.): Bone Mechanics. Boca Raton: CRC Press, pp. 253-277.

Hart RT Davy DT, and Heiple KG (1984) Mathematical modeling and numerical solutions dependent bone remodeling. Cacif. Tiss. Int. 36 (S): 104-109.

Hattner R, and Frost HM (1963) Mean skeletal age: it's calculation, and theoretical effects on skeletal tracer physiology and on the physical characteristics of bone. Henry Ford Hosp. Med. Bull. 11: 201-216.

Heathcote GM (1986) Exploratory Human Craniometry of Recent Eskaleutian Regional Groups From the Western Arctic and Subarctic of North America. BAR Int. Series, 301.

Hodges DC, and Schell LM (1988) Power analysis in biological anthropology. Am. J. Phys. Anthropol. 77: 175-181.

Horsman A, and Kirby PA (1972) Geometric properties of the second metacarpal. Calcif. Tiss. Res. 10: 289-301.

Inoué S (1986) Video Microscopy. New York: Plenum Press.

Israel H (1967) Loss of bone and remodeling-redistribution in the craniofacial skeleton with age. Fed. Proc. 26: 1723-1728.

Israel H (1968) Continuing growth in the human cranial skeleton. Arch. Oral Biol. 13:133-137.

Israel H (1970) Continuing growth in sella turcica with age. Am. J. Roent. 108:516-527.

Israel H (1973a) Age factor and the pattern of change in the craniofacial skeleton. Am. J. Phys. Anthropol. 39: 111-128.

Israel H (1973b) Progressive enlargement of the vertebral body as part of the process of human skeletal aging. Age Ageing 2: 71-79.

Israel H (1977) The dichotomous pattern of craniofacial expansion during aging. Am. J. Phys. Anthropol. 47: 47-52.

Israel H (1979) Evidence for continued apposition of adult mandibular bone. J. Prosthet. Dent. 41: 101-104.

Jaworski ZFG (1984a) Coupling of bone formation and bone resorption: a broader view. Calcif. Tiss. Int. 36: 531-535.

Jaworski ZFG (1984b) Lamellar bone turnover system and its effector organ. Calcif. Tiss. Int. 36: S46-55.

Jaworski ZFG (1987) Does the mechanical usage (MU) inhibit bone "remodeling"? Cal. Tiss. Int. 41: 239-248.

Jee WSS, LI XJ, and Schaffler MB (1991) Adaptation of diaphyseal structure with aging and increased mechanical usage in the adult rat: a histomorphometrical and biomechanical study. Anat. Rec. 230: 332-338.

Jowsey, J (1960) Age changes in human bone. Clin. Orthop. 17: 210-217.

Jowsey, J (1968) Age and species differences in bone. Cornell Vet. 58: 74-94.

Jungers WL (1984) Aspects of size and scaling in primate biology with special reference to the locomotor skeleton. Yrbk. Phys. Anthropol. 27: 73-97.

Keller TS, Lovin JD, Spengler DM, and Carter DR (1985) Fatigue of immature baboon cortical bone. J. Biomech. 18: 297-304.

Keller TS, Mao, Z, and Spengler, DM (1990) Young's modulus, bending strength, and tissue physical properties of human compact bone. J. Orthopaed. Res. 8: 592-603.

Kelsey JL (1987) Epidemiology of osteoporosis and associated factors. Pp. 409-444 In W. Peck (ed.): Bone and Mineral Research, Vol. 5. Amsterdam: Elsevier.

Kendrick GS, and Risinger HL (1967) Changes in the anteroposterior dimensions of the human male skull during the third and fourth decades of life. Anat. Rec. 159: 77-82.

Kimura K (1990a) Bilateral asymmetry of cross-sectional radiogrametric and microdensitometric measurements of the second metacarpal. Okaj. Folia Anat. Jap. 67: 39-45.

Kimura K (1990b) Age and sex differences in bone density of the second metacarpal in its midshaft cross-section. Ann. Hum. Biol. 17: 399-406.

Kirkwood BR (1988) Essentials of Medical Statistics. Oxford: Blackwell Scientific Publ.

Kokich VG (1976) Age changes in the human frontozygomatic suture from 20 to 90 years. Am. J. Orthodont. 69: 411-430.

Krogman WM, and Iscan MY (1986) The Human Skeleton in Forensic Medicine, 2nd Ed. Springfield: C. C. Thomas.

Lampe EW (1989) Surgical Anatomy of the Hand. Clinical Symposia.

Lanyon LE (1987) Functional strain in bone tissue as an objective, and controlling stimulus for adaptive bone remodelling. J. Biomech. 20: 1083-1093.

Laval-Jeantet A-M, Bergot C, Carroll R, and Garcia-Schaefer F (1983) Cortical bone senescence and mineral bone density of the humerus. Calcif. Tiss. Int. 35: 268-272.

Lazenby R (1986a) The Interaction of Bone Porosity and Cross-Sectional Geometry for the Conservation of Bone Strength. MA Thesis, Dept. of Archaeology, Simon Fraser U.

Lazenby R (1986b) Porosity-geometry interaction in the conservation of bone strength. J. Biomech. 19(3): 257-258.

Lazenby R, Oliver L, and Saunders SR (1989) The use of rib histomorphometry as an aid in the personal identification of unknown skeletons. Can. Soc. Forens. Sci. J. 22: 261-271.

Lazenby R, Saunders SR, Southern R, Rogers T, and Gibbs L (1991) Descriptive Osteology. Pp. 21-28 in Saunders SR, and Lazenby R (eds.) The Links That Bind: The Harvie Family Nineteeth Century Burying Ground. Copetown Press: Copetown.

Lewis OJ (1989) Functional Morphology of the Evolving Hand and Foot. Clarendon Pres: Oxford.

Li XJ, and Jee WSS (1991) Adaptation of diaphyseal structure to aging and decreased mechanical loading in the adult rat: a densitometric and histomorphometric study. Anat. Rec. 229: 291-297.

Lieber RL (1990) Statistical significance and statistical power in hypothesis testing. J. Orthopaed. Res. 8: 304-309.

Lindsay RA (1987) Prevention of osteoporosis. Clin. Orthop. 222: 44-59.

Lips P, van Ginkel FC, Netelenbos JC, Wiersinga A, and van der Vijgh WJF (1990) Lower mobility and markers of bone resorption in the elderly. Bone and Mineral 9: 49-57.

Lloyd E, and Hodges D (1971) Quantitative characterization of bone: a computer analysis of microradiographs. Clin. Orthop. 78: 230-250.

Lovell, NC (1990) Skeletal and dental pathology of free-ranging mountain gorillas. Am. J. Phys. Anthropol. 81: 399-412.

Macho GA (1986) Cephalometric and craniometric age changes in adult humans. Ann. Hum. Biol. 3: 49-61.

Marotti G (1976) Maps of bone formation rate values recorded throughout the skeleton of the dog. In ZFG Jaworski (ed.): Proceedings of the First Workshop on Bone Morphometry. Ottawa: University of Ottawa Press, pp. 202-207.

Martin DL (1984) Spatial distribution of osteons in femoral bone cross-sections. Paper presented at the 53rd Ann. Meeting of the Am. Assoc. Phys. Anthrop., Philadelphia, PA.

Martin DL, Goodman AH, and Armelagos GJ (1985) Skeletal pathologies as indicators of quality and quantity of diet. In RI Gilbert, Jr and JH Mielke (eds.): The Analysis of Prehistoric Diets. New York: Academic Press, pp. 227-279.

Martin RB (1972) The effects of geometric feedback in the development of osteoporosis. J. Biomech. 5: 447-455.

Martin R (1984) Porosity and specific surface of bone. Crit. Rev. Biomed. Eng. 10:179-222.

Martin RB, and Atkinson PJ (1977) Age and sex-related changes in the structure and strength of the human femoral shaft. J. Biomech. 10: 223-231.

Martin RB, and Burr DB (1982) A hypothetical mechanism for the stimulation of osteonal remodeling by fatigue damage. J. Biomech. 15: 137-139.

Martin RB, and Burr DB (1984) Mechanical implications of porosity distribution in bones of the appendicular skeleton. Orthop. Trans. 8: 342-343 (A).

Martin RB, and Burr DB (1989) Structure, Function, and Adaptation of Compact Bone. New York: Raven Press.

Martin RB, Papamichos T, and Dannucci GA (1990) Linear calibration of radiographic mineral density using video-digitizing methods. Calcif. Tiss. Int. 47: 82-91.

Martin RB, Pickett JC, and Zinaich S (1980) Studies of skeletal remodeling in aging men. Clin. Orthop. 149: 268-282.

Martin RB Burr DB, and Schaffler MB (1985) Effects of age and sex on the amount and distribution of mineral in Eskimo tibiae. Amer. J. Phys. Anthropol. 67: 371-380.

Mazess RB (1982) On aging bone loss. Clin. Orthop. 165: 239-252.

McCulloch RG, Bailey DA, Houston CS, and Dodd BL (1990) Effects of physical activity dietary calcium intake and selected lifestyle factors on bone density in young women. Can. Med. Assoc. J. 142: 221-227.

McCutchen CW (1975) Do mineral crystals stiffen bone by straightjacketing its collagen? J. Theor. Biol. 51: 51-58.

McQueen CM, Monk IB, Horton PW, and Smith DA (1972) Preparation of undecalcified bone sections for auto- and microradiography. Calcif. Tiss. Res. 10: 23-30.

Meade J (1989) The adaptation of bone to mechanical stress: experimentation and current concepts. In SC Cowin (ed.): Bone Mechanics. Boca Raton: CRC Press, pp. 211-251.

Mjör I (1963) Microradiography of partially decalcified bone tissue. Acta Anat. 53:259-267.

Mooney MP, Kraus EM, Bardach J, and Snodgrass JI (1982) Skull preparation using the enzyme-active detergent technique. Anat. Rec. 202: 125-129.

Morita S, and F Ohtsuki (1973) Secular changes of the main head dimensions in Japanese. Hum. Biol. 45: 151-165.

Mosekilde L, and Mosekilde L (1990) Sex differences in age-related changes in vertebral body size, density and biomechanical competence in normal individuals. Bone 11: 67-73.

Muvdi BB, and McNabb JW (1984) Engineering Mechanics of Materials, 2nd Ed. New York: Macmillan.

Nagurka ML, and WC Hayes (1980) An interactive graphics package for calculating cross-sectional properties of complex shapes. J. Biomech. 17: 203-213.

Niemcryk, SJ, Kraus, TJ and Mallory, TH (1990) Empirical considerations in orthopaedic research design and data analysis. Part I: strategies in research design. J. Arthroplasty 5:99-103.

Norman GR, and Streiner DL (1986) PDQ Statistics. Toronto: BC Decker, Inc.

Ortner DJ (1975) Aging effects on osteon remodeling. Calcif. Tiss. Res. 18: 27-36.

Parfitt AM (1984a) Age-related structural changes in trabecular and cortical bone: cellular mechanisms and biomechanical consequences. Calcif. Tiss. Int. 36:S123-128.

Parfitt AM (1984b) The cellular basis of bone remodeling: the quantum concept re-examined in light of recent advances in the cell biology of bone. Cal. Tiss. Int. 36:S37-45.

Perzigian AJ (1973) Osteoporotic bone loss in two prehistoric Indian populations. Am. J. Phys. Anthropol. 39: 87-96.

Pfeiffer S (1980) Age changes in the external dimensions of adult bone. Am. J. Phys. Anthropol. 52: 529-532.

Phillips HB, Owen-Jones S, and Chandler B (1978) Quantitative histology of bone: a computerized method of measuring the total mineral content of bone. Calcif. Tiss. Res. 26: 85-89.

Plato CC, and Norris AH (1980) Bone measurements of the second metacarpal and grip strength. Hum. Biol. 52: 131-149.

Plato CC, and Purifoy FE (1982) Age, sex and bilateral variability in cortical bone loss and measurements of the second metacarpal. Growth 46: 100-112.

Plato CC, Fox KM, and Garruto RM (1984) Measures of lateral functional dominance: hand dominance. Hum. Biol. 56: 259-275.

Polig E, and WSS Jee (1987) Bone age and remodeling: a mathematical treatise. Calcif. Tiss. Int. 41: 130-136.

Pugliese LR, and C Anderson (1986) A method for the determination of the relative distribution and relative quantity of mineral in bone sections. J. Histotech. 9: 91-93.

Raab DM, TD Crenshaw, DB Kimmel and EL Smith (1991) A histomorphometric study of cortical bone activity during increased weight-bearing exercise. J. Bone Miner. Res. 6:741-750.

Rangel RD, Oyen OJ, and Russell MD (1985) Changes in masticatory biomechanics and stress magnitude that affect growth and development of the facial skeleton. In AD Dixon

and BG Sarnat (eds.): Normal and Abnormal Bone Growth: Basic and Clinical Research. New York: AR Liss, pp. 281-293.

Recker RR (ed.) (1983) Bone Histomorphometry: Techniques and Interpretations. Boca Raton: CRC Press.

Reilly DT, and Burstein AH (1974) The mechanical properties of cortical bone. J. Bone Jt. Surg. 56(A): 1001-1022.

Resnick N, and Greenspan S (1989) "Senile" osteoporosis reconsidered. J. Amer. Med. Assoc. 261: 1025-1029.

Richman EA, Ortner DJ, and Schulter-Ellis FP (1979) Differences in intracortical remodeling in three aboriginal populations: possible dietary factors. Calcif. Tiss. Int. 28: 209-214.

Roesler H (1987) The history of some fundamental concepts in bone biomechanics. J. Biomech. 20: 1025-1034.

Roy TA, Ruff CB, and Plato CC (1991) Handedness and bilateral asymmetry in the geometry of the second metacarpal. Amer. J. Phys. Anthropol. Supp. 12: 154-155 (A).

Rubin CT, Bain SD, and McLeod KJ (1990a) The inability of the aging skeleton to respond to osteogenic stimuli: the origins of type II osteopenia? Orthop. Res. Soc. 14(2): 330-331.

Rubin CT, and Lanyon LE (1984) Regulation of bone formation by applied dynamic loads. J. Bone Jt. Surg. 66A: 397-402.

Rubin CT, and Lanyon LE (1987) Osteoregulatory nature of mechanical stimuli: function as a determinant for adaptive remodeling in bone. J. Orthop. Res. 5: 300-310.

Rubin CT, McLeod KJ, and Bain SD (1990b) Functional strains and cortical bone adaptation: epigenetic assurance of skeletal integrity. J. Biomech. 23, Supp. 1: 43-54.

Ruff CB (1980) Age differences in craniofacial dimensions among adults from Indian Knoll, Kentucky. Am. J. Phys. Anthropol. 53: 101-108.

Ruff CB (1984) Allometry between length and cross-sectional dimensions of the femur and tibia in *Homo sapiens sapiens*. Am. J. Phys. Anthropol. 65: 347-358.

Ruff CB (1987a) Postcranial adaptation to subsistence changes on the Georgia coast. Am. J. Phys. Anthropol. 72: 248 (A).

Ruff CB (1987b) Structural allometry of the femur and tibia in hominoidea and *Macaca*. Folia Primatol. 48: 9-49.

Ruff CB (1987c) Sexual dimorphism in human lower limb bone structure: relationship to subsistence strategy and sexual division of labor. J. Hum. Evol. 16: 391-416.

Ruff CB (1989) New approaches to structural evolution of limb bones in primates. Folia Primatol. 52: 142-159.

Ruff CB, and Jones HH (1981) Bilateral asymmetry in cortical bone of the humerus and tibia - sex and age factors. Hum. Biol. 53: 69-86.

Ruff CB, and Hayes WC (1982) Subperiosteal expansion and cortical remodeling of the human femur and tibia with aging. Science 217: 945-947.

Ruff CB, and Hayes WC (1983a) Cross-sectional geometry of Pecos Pueblo femora and tibiae - a biomechanical investigation I. Method and general patterns of variation. Am. J. Phys. Anthropol. 60: 359-381.

Ruff CB, and Hayes WC (1983b) Cross-sectional geometry of Pecos Pueblo femora and tibiae - a biomechanical investigation II. Sex, age and side differences. Am. J. Phys. Anthropol. 60: 383-400.

Ruff CB, and Hayes WC (1984a) Bone mineral content in the lower limb. J. Bone Jt. Surg. 66A: 1024-1031.

Ruff CB, and Hayes WC (1984b) Age changes in geometry and mineral content in the lower limb bones. Ann. Biomed. Engr. 12: 573-584.

Ruff CB, and Hayes WC (1988) Sex differences in age-related remodeling of the femur and tibia. J. Orthop. Res. 6: 886-896.

Ruff CB, Larsen CS, and Hayes WC (1984) Structural changes in the femur with the transition to agriculture on the Georgia coast. Am. J. Phys. Anthropol. 64: 125-136.

Rybicki EF, Simonen FA, and Weis Jr. EB (1972) On the mathematical analysis of stress in the human femur. J. Biomech. 5: 203-215.

Salathé EP Jr., Arangio GA, and Salathé EP (1986) A biomechanical model of the foot. J. Biomech. 19: 989-1001.

Saunders SR (1985) Surface and cross-sectional comparisons of bone growth remodeling. Growth 49: 105-130.

Saunders SR, and Lazenby R (eds.) (1991) The Links That Bind: The Harvie Family Nineteeth Century Burying Ground. Copetown Press: Copetown.

Schaffler MB, and Burr DB (1988) Stiffness of compact bone: effects of porosity and density. J. Biomech. 21: 13-16.

Schaffler MB, Radin EL, and Burr DB (1989) Mechanical and morphological effects of strain rate on fatigue of compact bone. Bone 10: 207-214.

Schaffler MB, Radin EL, and Burr DB (1990) Long-term fatigue behavior of compact bone at low strain magnitude and rate. Bone 11: 321-326.

Schaffler MB, Burr DB, Jungers WL, and Ruff CB (1985) Structural and mechanical indicators of limb specialization in primates. FoliaPrimatol. 45: 61-75.

Schoutens A, Laurent E, and Poortmans JR (1989) Effects of inactivity and exercise on bone. Sports Med. 7: 71-81.

Simmons ED, Grynpas MD, and Pritzker KPH (1985) Bone mineral changes in aging human cortical bone. Orthopaed. Trans. 9: 222 (A).

Singh I (1960) Variations in the metatarsal bones. J. Anat. 94: 345-350.

Skerry TM, Bitensky L, Chayen J, and Lanyon LE (1988) Loading-related reorientation of bone proteoglycan in vivo. Strain memeory in bone tissue? J. Orthop. Res. 6: 547- 551.

Skerry TM, Suswillo R, El Haj AJ, Ali NN, Dodds RA, and Lanyon LE (1990) Load- induced proteoglycan orientation in bone tissue in vivo and in vitro. Cal. Tiss. Int. 46: 318-326.

Smith BH, Garn SM, and Cole PE (1982) Problems of sampling and inference in the study of fluctuating dental asymmetry. Am. J. Phys. Anthropol. 58: 281-289.

Smith EL, and Gilligan C (1989) Mechanical forces and bone. In WA Peck (ed.): Bone and Mineral Research, Vol. 6. Amsterdam: Elsevier, pp. 139-173.

Smith EL, and Raab DM (1986) Osteoporosis and physical activity. Acta Med. Scand. (S). 711: 149-156.

Smith RW Jr., and Walker RR (1964) Femoral expansion in aging women: implications for osteoporosis and fractures. Science 145: 156-157.

Snow CE (1948) Indian Knoll Skeletons. Reports in Anthropology IV, No. 3, Part 2. U. Kentucky.

Sokal RR, and Rohlf FJ (1969) Biometry. San Francisco: WH Freeman.

Steele DJ, and Bramblett CA (1988) The Anatomy and Biology of the Human Skeleton. College Station: Texas A&M University Press.

Stini WA (1990) "Osteoporoses": Etiologies, Prevention and Treatment. Yearbk. Phys. Anthropol. 33: 151-194.

Stout SD (1986) The use of bone histomorphometry in skeletal identification: the case of Francisco Pizarro. J. Foren. Sci. 31: 296-300.

Stout SD, and Teitelbaum SL (1976) Histomorphometric determination of formation rates of archaeological bone. Calcif. Tiss. Res. 21: 163-169.

Sumner DR (1984a) Size, Shape and Bone Mineral Content of the Human Femur in Growth and Aging. Ph.D. Dissertation, University of Arizona.

Sumner DR (1984b) Postembryonic dimensional allometry of the human femur. Amer. J. Phys. Anthropol. 64: 69-74.

Sumner DR, Morbeck ME, and Lobick J (1989) Apparent age-related bone loss among adult female Gombe chimpanzees. Amer. J. Phys. Anthropol. 79: 225-234.

Takahashi, H, Epker, B, and Frost, H (1965) Relation between age and size of osteons in man. Henry Ford Hosp. Med. Bull. 13:25-31.

Tallgren A (1974) Neurocranial morphology and ageing - a longitudinal roentgen cephalometric study of adult Finnish women. Amer. J. Phys. Anthropol. 41: 285-294.

Tappen NC (1977) Three dimensional studies of resorption spaces and developing osteons. Am. J. Anat. 149: 301-332.

Tappen NC (1983) The development of the vermiculate pattern in the brow region of crania from Indian Knoll, Kentucky. Amer. J. Phys. Anthropol. 60: 523-537.

Thomas CL (ed.) (1985) Taber's Cyclopaedic Medical Dictionary. 15th Ed. Philadelphia: FA Davis.

Thompson JL, and Kendrick GS (1964) Changes in the vertical dimensions of the human male skull during the third and fourth decades of life. Anat. Rec. 150: 209-214.

Tideiksaar R, and A Kay (1987) Explaining falls: a logical prodcedure. Geriat. Med. Aug: 25-30.

Trotter M, and Peterson RR (1967) Transverse diameter of the femur: on roentgenograms and on bones. Clin. Orthop. 52: 233-239.

Trotter M, Peterson RR, and Wette R (1968) The secular trend in the diameter of the femur of American whites and negroes. Amer. J. Phys. Anthropol. 28: 65-74.

Turner CH (1991) Homeostatic control of bone structure: an application of feedback theory. Bone 12: 203-217.

Vaughan J (1975) The Physiology of Bone, 2nd Ed. Oxford: Clarendon Press.

Viceconti M, and Seireg A (1990) A generalized procedure for predicting bone mass regulation by mechanical strain. Calcif. Tiss. Int. 47: 296-301.

Vincentelli R, and Grigorov M (1985) The effect of Haversian remodeling on the tensile properties of human cortical bone. J. Biomech. 18: 201-207.

Wainwright SA, Biggs WD, Currey JD, and Gosline JM (1981) Mechanical Design in Organisms, 2nd Ed. Princeton: Princeton University Press.

Warwick R, and Williams PL (eds) (1973) Gray's Anatomy, 35th Ed. Great Britain: Longman.

Whalen RT, Carter DR, and Steele CR (1988) Influence of physical activity on the regulation of bone density. J. Biomech. 21: 825-837.

Whittaker DK (1985) The effect of continuing eruption on bone growth at the alveolar margin. In AD Dixon and BG Sarnat (eds.): Normal and Abnormal Bone Growth: Basic and Clinical Research. New York: AR Liss, pp. 259-267.

Wu K, Schubeck KE, Frost HM, and Villaneuva AR (1970) Haversian bone formation rates determined by a new method in a mastodon and in human diabetes mellitus and osteoporosis. Calcif. Tiss. Res. 6: 204-219.

Young JZ (1971) An Introduction to the Study of Man. New York: Oxford University Press.